PROCEEDINGS OF THE

THIRD INTERNATIONAL CONFERENCE ON

ADVANCED SCIENCE & TECHNOLOGY

TRANSFER TO THAILAND

.....

JULY 23 - 25, 1993

AMBASSADOR HOTEL

BANGKOK, THAILAND

Editors :

Supachai Lorlowhakorn

The National Science and Technology Development Agency, Thailand

Nongnuch Inpanbutr

The Ohio State University, U.S.A.

PREFACE
From Thai Professional Abroad

•••••••••••••••

The Third International Conference on Advanced Science and Technology Transfer to Thailand to be held at the Ambassador Hotel in Bangkok, Thailand, July 23-25, 1993. Approximately sixty five Thai professionals from abroad are invited and are expected to join this Conference. There are two main goals we wish to achieve from this conference. The first goal is to promote the advancement and transfer of scientific knowledge, technology and education to Thailand. The second goal is to establish and to promote collaboration between the scientists, educators, corporations and related organizations in Thailand, United States, Canada, Japan, Europe and other countries.

The fact that these meetings are held annually and that their attendance increases annually, signifies the continuing and increasing interest in helping the development of Thailand. The first Conference was started in 1991 with 19 Thai professionals from the United States and was organized by Dr. Kamchad Mongkolkul, from the Damrong Lathapipat Foundation, and Mr. Sirithan Pairoj-Boriboon (Ministry of Science, Technology and Environment, MOSTE). The second Conference was held in Bangkok and Pattaya, Thailand in August of 1992 with 45 participants of Thai professionals from abroad. The format of the Conference has evolved to this third Conference which is designed to achieve and surpass the previous conference goals.

This third Conference is expanded to include panel discussions, poster presentations, workshops and a consortium. We hope that this year's format will prove to be the most beneficial to the professionals from Thailand and abroad in exchanging ideas and promoting science and technology transfer. The success and progress of the Conference can be judged not only by the number of participants from abroad, but more importantly, by the number of high level officials, professional, and participants from Thailand as well as the number of papers and communications submitted. Four areas of interests identified at the third Conference are as follows: Biomedical Technology, Electronics and Computer, Manufacturing Technology & Industrial Engineering, and Natural Resources and Environment. At present, there are 55 abstracts and 26 manuscripts submitted for this conference. The success of this Conference will lie equally on the acceptance and participation of Thai professionals from abroad and in Thailand. We hope that the Conference will evolve into it's best format yet in achieving our goals and objectives to continue to grow at a sufficient rate and in time to help with the scientific and technological development of Thailand. It is hoped that the Conference will continue it's success by helping the science and technology development in Thailand, and we, the Thai professionals, everywhere in the world, will contribute, participate and make the mission a great success.

A special tribute is due to the tireless efforts of Dr. Kamchad Mongkolkul, the Organizing Committee and the support from the Damrong Lathapipat Foundation, The Ministry of Science, Technology and Environment, and The National Science and Technology Development Agency (NSTDA).

Nongnuch Inpanbutr
The Ohio State University

คำปรารภจากประธานโครงการจัดการประชุม
The Third International Conference on
Advanced Science and Technology Transfer To Thailand

•••••••••••••••

ปัจจัยสำคัญของการถ่ายทอดเทคโนโลยีสู่ประเทศไทย

เมื่อเดือนสิงหาคม 2534 มีนักวิทยาศาสตร์และวิศวกรชาวไทย 18 ท่านที่ประกอบอาชีพอยู่ในสหรัฐ-อเมริกา (และอีก 1 ท่านที่เหลือตัดสินใจกลับมาทำงานในประเทศไทย) ได้รับเชิญจากมูลนิธิดำรง ลัทธพิพัฒน์ ให้มาร่วมสัมมนา เรื่อง "ความร่วมมือระหว่างนักวิทยาศาสตร์และเทคโนโลยีไทยที่ทำงานในสหรัฐอเมริกากับผู้เกี่ยวข้องในประเทศไทย" โดยผู้มาจากต่างประเทศออกค่าใช้จ่ายเองทั้งหมด และมูลนิธิดำรงลัทธพิพัฒน์ได้อนุมัติงบประมาณสองแสนบาทเพื่อจัดประชุมที่ศูนย์สารนิเทศ จุฬาลงกรณ์มหาวิทยาลัย เป็น เวลา 3 วัน ในการประชุมครั้งนั้น ผู้มาจากต่างประเทศทุกท่านมีโอกาสเสนอผลงานด้านวิทยาศาสตร์และเทคโนโลยีของตนเองต่อที่ประชุม ท่านละ 15 นาที เพื่อจะให้ผู้เข้าประชุมจากประเทศไทยทั้งจากภาครัฐและภาคเอกชนได้ทราบว่า แต่ละท่านที่มามีความชำนาญในเทคโนโลยีด้านใด เพื่อผู้ที่ทำงานใกล้ชิดกันในประเทศไทยจะได้ทราบ ปรากฏว่าเวลา 15 นาทีค่อนข้างน้อย ที่จะทำให้ผู้ฟังทราบลึกซึ้งเกี่ยวกับผู้บรรยาย

ในการประชุมในปีต่อมาจึงตั้งชื่อใหม่ว่า "Second International Workshop on Advanced Science and Technology Transfer To Thailand" ในเดือนสิงหาคม 2535 ซึ่งมีนักวิทยาศาสตร์และเทคโนโลยีไทยจากสหรัฐอเมริกา 33 คน ญี่ปุ่น 8 คน และยุโรป 5 คน รวม 46 คน มาร่วมประชุมด้วย แม้ว่าส่วนใหญ่ของผู้มาประชุมจะมีโอกาสเสนอผลงานของตนเอง แต่เพื่อให้ได้เนื้อหาลึกซึ้งและกว้างขวางยิ่งขึ้น จึงมีความพยายามจัดพิมพ์ Proceedings มาแจกในที่ประชุม และส่งไปยังห้องสมุดคณะวิทยาศาสตร์ และวิศวกรรมศาสตร์ ในมหาวิทยาลัยและหน่วยงานต่าง ๆ ทั่วประเทศ ใน Proceedings ดังกล่าว มีผู้เขียนบทความรวม 43 เรื่อง มาจากสหรัฐอเมริกา 31 เรื่อง ญี่ปุ่น 9 เรื่อง คานาดา เยอรมัน และไทย แห่งละ 1 เรื่อง การจัดพิมพ์ Proceedings ครั้งนี้ แม้จะมีเวลาน้อยแต่สำเร็จลงได้ด้วยความมุ่งมั่นของบรรณาธิการ 2 ท่าน คือ ดร. เมธี เวชารัตนา และ ดร. ลือศักดิ์ นันทวานิช ในนามของ Association of Thai Professionals in America and Canada (ATPAC) และได้รับความช่วยเหลืออย่างดียิ่งจาก คุณศุภชัย หล่อโลหการ สำนักงานพัฒนา-วิทยาศาสตร์และเทคโนโลยีแห่งชาติ ในการจัดพิมพ์ และได้รับเงินสนับสนุนค่าจัดพิมพ์ 120,000 บาท จากเครือเจริญโภคภัณฑ์ Proceedings เล่มนี้ จึงนับเป็นถาวรวัตถุที่เกิดขึ้นจากนักวิทยาศาสตร์และเทคโนโลยีไทยในต่างประเทศทั่วโลก ที่ใคร่จะมีส่วนในการนำเทคโนโลยีใหม่ ๆ ที่ตนเองได้สร้างกันขึ้นในระยะเวลานานปีกลับมาช่วยถ่ายทอดให้แก่หน่วยงานต่าง ๆ ในบ้านเกิดเมืองนอนของตนที่อยู่ในสาขาใกล้เคียงกัน

สำหรับปี 2536 นี้ การประชุมนี้ยังคงใช้ชื่อคล้ายกับที่เคยใช้เดิมว่า "The Third International Conference on Advanced Science and Technology Transfer to Thailand" ซึ่งจะจัดที่โรงแรมแอมบาสซาเดอร์ซิตี้ ระหว่างวันที่ 23-25 กรกฎาคม 2536 โดยถึงขณะนี้ (9 ก.ค. 36) มีผู้แสดงความจำนงมาร่วมประชุมจากสหรัฐอเมริกา 29 คน ยุโรป 12 คน ญี่ปุ่น 7 คน และคานาดา 2 คน รวม 50 คน โดยการประชุมจะมีกิจกรรมหลากหลายไปกว่าปีที่แล้ว เช่น มีการบรรยายพิเศษ อภิปรายกลุ่ม Tutorials และ Poster Sessions และเป็นสิ่งน่ายินดีว่า คุณศุภชัย หล่อโลหการ จากสำนักงานพัฒนาวิทยาศาสตร์และเทคโนโลยีแห่งชาติ และ ดร. นงนุช อินปันบุตร จาก ATPAC ได้กรุณาเป็นบรรณาธิการจัดพิมพ์ Proceedings สำหรับการประชุมครั้งนี้อีก โดยได้รับเงินสนับสนุนการจัดพิมพ์จากสำนักงานพัฒนา-วิทยาศาสตร์และเทคโนโลยีแห่งชาติ จำนวน 50,000 บาท และค่าใช้จ่ายอื่น ๆ จากมูลนิธิดำรง สิทธิพิพัฒน์ ซึ่งบริจาคเงินเพื่อการจัดประชุมครั้งนี้รวม 200,000 บาท

ในนามของประธานโครงการจัดการประชุม The Third International Conference on Advanced Science and Technology Transfer To Thailand กระผมใคร่ขอขอบคุณ บรรณาธิการ ผู้เสนอ บทความวิชาการ ผู้จัดพิมพ์ ตลอดจนผู้สนับสนุนด้านการเงินทั้งหลายที่มีส่วนให้ Proceedings เล่มนี้สำเร็จลงได้ เอกสารเล่มนี้ซึ่งนอกจากจะรวบรวมความรู้ทางวิชาการวิทยาศาสตร์และเทคโนโลยี ที่พี่น้องชาวไทยของเรามีความสามารถเป็นที่ประจักษ์แจ้งชัดแล้ว ยังเป็นที่รวมน้ำใจของคนไทยจากทุกทวีปของโลก ซึ่งมุ่งมั่นจะนำความรู้ที่ตนมีอยู่มาช่วยพัฒนาประเทศให้เจริญสถาพรยิ่งขึ้นไป กระผมเชื่อว่าเอกสารเล่มนี้ คงจะเป็นประโยชน์อย่างยิ่งต่อบรรดานักวิทยาศาสตร์และเทคโนโลยีในหน่วยงานต่าง ๆ ไม่เฉพาะแต่ได้พบเนื้อหาวิชาอันทันสมัย แต่จะได้ติดต่อขอความร่วมมือช่วยเหลือกันต่อไปอีกยาวนานในอนาคต

รองศาสตราจารย์ ดร.กำจัด มงคลกุล

ประธานโครงการจัดการประชุมฯ

TABLE OF CONTENTS

Papers of the Third International Conference on Advanced Science and Technology Transfer to Thailand

Session I BIOTECHNOLOGY

Session II ELECTRONICS AND COMPUTER

Session III ENVIRONMENT & TRANSPORTATIONS

Session IV MANUFACTURING & INDUSTRIAL ENGINEERING

THE THIRD INTERNATIONAL CONFERENCE ON ADVANVED SCIENCE AND TECHNOLOGY TRANSFER TO THAILAND
JULY 23-25, 1993, BANGKOK, THAILAND

FULL NAME: (First) Apinya (Last) Ngam-ek
OCCUPATION Medical Research Technician
ADDRESS: 14 Cambridge Center
Cambridge, MA 02142
PHONE: (617) 252-9311 FAX: (617) 252-9616 E-MAIL:
FORUM: Biogen, Inc.

FIRST AUTHOR STATUS: Yes MEMBER OF ATPAC: _____ NON-MEMBER OF ATPAC

LYMPHOTOXIN-ß: A NEW MEMBER OF THE TNF FAMILY THAT FORMS A HETEROMERIC COMPLEX WITH LYMPHOTOXIN ON THE CELL SURFACE

Apinya Ngam-ek*, Pornsri Lawton*, Jeffrey L. Browning*, Richard Tizard*, Janice DeMarinis*, E. Pingchang Chow*, Catherine Hession*, Betsy Greco*, Susan Foley* and Carl F. Ware# Biogen* Cambridge Ma. and University of California, Riverside Ca.#

The lymphokine TNF has a well-defined role as an inducer of inflammatory responses; however, the function of the structurally related molecule, lymphotoxin (LT-α), is essentially unknown. Previously, we had noted that LT-α is present on the surface of activated T-, B- and LAK cells as a complex with a 33 kDa glycosylated integral membrane protein. Cloning of the cDNA encoding the associated protein, now called lymphotoxin-ß (LT-ß), revealled it to be a type II membrane protein with significant homology to TNF, LT-α and the ligand for the CD-40 receptor. The nature of the homology regions suggests that the LT-α/ß complex also retains a TNF-like trimeric structure. In transient expression experiments, LT-α is normally secreted, but when co-transfected with LT-ß, surface LT-α forms were detected. The addition of LT-ß to the family of TNF-related ligands indicates that the TNF family is more extensive than previously realized and raises the possibility that the surface LT-α/ß complex may have a specific role in immune regulation distinct from the functions ascribed to TNF.

THE THIRD INTERNATIONAL CONFERENCE ON ADVANCED SCIENCE AND TECHNOLOGY TRANSFER TO THAILAND
JULY 23-25,BANGKOK,THAILAND

FULL NAME: ARTNARONG THANSANDOTE
OCCUPATION: RESEARCH SCIENTIST
ADDRESS: BUREAU OF RADIATION AND MEDICAL DEVICES, HEALTH AND WELFARE CANADA
775 BROOKFIELD ROAD, OTTAWA, ONTARIO K1A 1C1, CANADA
PHONE: (613) 954-0306 FAX: (613) 993-0281
FORUM: POSTER PRESENTATION UNDER THE TOPIC OF ENVIRONMENT OR BIOTECHNOLOGY
FIRST AUTHOR STATUS: MEMBER OF ATPAC

ACTIVITIES OF HEALTH AND WELFARE CANADA IN PROTECTION FROM NON-IONIZING RADIATION

Artnarong Thansandote, David W. Lecuyer, J.D. Yvon Deslauriers, Wayne Gorman, Stephen H.P. Bly, Robert G. Hussey and Pavel Dvorak. Bureau of Radiation and Medical Devices, Health and Welfare Canada, 775 Brookfield Road, Ottawa, Ontario K1A 1C1, Canada.

In this paper, we present a broad overview of Health and Welfare Canada's program in the protection of the general public from non-ionizing radiation (NIR) such as power line fields, radiofrequency fields, laser emissions, ultraviolet, ultrasound and noise. The major objectives of the program are (1) to identify potential health hazards and assess health risks associated with devices which emit NIR, and (2) to minimize unnecessary exposure to these radiations where potentially hazardous. The program covers a wide range of activities in three main areas: electromagnetics, lasers and electro-optics, and acoustics. Health criteria have been developed for a number of types and frequencies of radiation and, where necessary, controls have been applied by implementing regulations under the Radiation Emitting Devices Act of Canada. Regulations for microwave ovens, laser scanners, demonstration laser devices, sunlamps, mercury lamps, and ultrasound therapy devices are now in force. In addition, a number of safety codes and safe use guidelines relating to the installation and use of various devices have been developed. Safety codes for active metal detectors, radiofrequency exposure, ultrasound devices, short-wave diathermy devices and magnetic resonance clinical systems have been published and distributed. In the area of electromagnetics, the assessment of risks of electric and magnetic fields at extremely low frequencies (1-300 Hz) is a major activity. The work includes in-house animal tumor co-promotion studies to determine the potential health risks from 60-Hz magnetic field exposure. The major activities in lasers and electro-optics include the development of laser light show safety assessment procedures and laser regulations, as well as the provision of information and education on the health effects of and the protection from ultraviolet exposure. In the area of acoustics, guidelines for assessment and control of the health effects of aircraft noise and machinery noise are being developed.

THE THIRD INTERNATIONAL CONFERENCE ON ADVANVED SCIENCE AND TECHNOLOGY TRANSFER TO THAILAND
JULY 23-25, 1993, BANGKOK, THAILAND

FULL NAME: (First) Buncha (Last) Ooraikul
OCCUPATION Professor
ADDRESS: Dept. of Food Science, Univ. of Alberta
Edmonton, Alberta, Canada T6G 2P5
PHONE: (403) 492-3268 FAX: (403) 492-8914 E-MAIL: ZZfood sc. @vm.ucs.
FORUM: Manufacturing Technology and Industrial Engineering

FIRST AUTHOR STATUS: X MEMBER OF ATPAC; _____ NON-MEMBER OF ATPAC

EDIBLE CONTAINERS

ABSTRACT

As a result of environmental concerns with food containers based on plastics (styrofoam) or paper products, an alternative food container has been developed from edible materials. Edible container is not a new concept, the forerunner being ice cream cones and artificial "potato skin". The major problem preventing these containers from being more universally used is the fact that they cannot hold liquid products without leaking or disintegrating. Numerous patents have been issued in the past 20 years on the development of sealants or sealing processes to make edible containers water resistant. However, so far none have achieved commercial success.

We have recently developed an edible sealant and a practical method to apply it to baked containers. The product appears to have very strong commercial potential and would solve problems associated with plastic or paper containers. The technology may be applied to a wide range of food containers from ice cream cones, to cups or containers for yoghurt, chilli concarne, coffee or tea, softdrinks or alcoholic beverages to containers for hamburgers or french fries. The containers have the following properties:

1. They are made of approved food ingredients, the major components being potato starch and wheat flour.
2. They can hold hot or cold liquid for at least two hours.
3. They may be colored or flavored as desired and may be embossed or labeled.
4. The containers may be eaten as a snack after the content has been consumed. The dry containers are crisp, similar to potato chips or puffed products; the softened containers are chewable, similar to fruit leather.
5. Uneaten containers may be collected for animal feed, or if thrown away will biodegrade quickly.

Further research and development is being planned to design and construct prototype production equipment.

THE THIRD INTERNATIONAL CONFERENCE ON ADVANVED SCIENCE AND TECHNOLOGY TRANSFER TO THAILAND
JULY 23-25, 1993, BANGKOK, THAILAND

FULL NAME: (First) GRIANGSAK (Last) CHAIROTE
OCCUPATION: Assoc.Prof.of Chemistry
ADDRESS: Department of Chemistry, Faculty of Science
Chiang Mai University, Chiang Mai 50002, Thailand
PHONE: (053)221699 ext 3331 FAX:66-53-222268 E-MAIL: -
FORUM: Analysis of Volatile Aroma Compounds from "Reow Hom"

FIRST AUTHOR STATUS:_____MEMBER OF ATPAC; _____ NON-MEMBER OF ATPAC

Essential oil of "Reow" was studied using separation by column chromatography,gas chromatography and mass spectrometry, We found that the main compound before and after separation by column chromatography was anethole. The compositions in both case were sligthly different. Almost all of the components obtained after applying to column chromatography was anethole while the original sample composed of other subbstances such as santalol, copaene, etc. However, almost all of the components was anethole.

THE THIRD INTERNATIONAL CONFERENCE ON ADVANVED SCIENCE AND TECHNOLOGY TRANSFER TO THAILAND
JULY 23-25, 1993, BANGKOK, THAILAND

FULL NAME: (First) Kukiat (Last) Tanteeratarm
OCCUPATION Food Technologist
ADDRESS: 110 Mumford Hall, University of Illinois
1301 W. Gregory Drive, Urbana, IL 61801, USA
PHONE: 217/244-5417 FAX: 217/333-5838 E-MAIL: AXINSOY@UICVMC.BITNET
FORUM: Soybean Processing & Technology (Food Science/Biotechnology)

FIRST AUTHOR STATUS: X MEMBER OF ATPAC; _____ NON-MEMBER OF ATPAC

MANUFACTURING OF BLAND SOYMILK

Kukiat Tanteeratarm, Alvin I. Nelson and Lun S. Wei

Soymilk is conventionally made in the Orient by soaking whole raw soybeans, grinding in water, filtering to remove sediment and then heating the extract. Although this process is simple, the resulting beverage has a strong painty, beany off-flavor and odor. Thus, it is not suitable as a base for preparing dairy analogs such as beverage, yogurt, ice cream and coffee creamer. Numerous modifications of this traditional Oriental process have been reported to partially improve the off-flavor and odor defects. Some of these modifications include: hot water extraction, acid grinding, alkali soaking, vacuum deodorization, fermentation and enzyme treatment. Certain modifications gave some flavor improvement but generally are only partially effective in reducing off-flavor.

Recent processing method for preparing high quality soymilk has been developed by food scientists and engineers at the University of Illinois. This is an improved process over the patented Illinois soymilk process. The soymilk is very smooth and bland, therefore, it is suitable for preparing a wide varieties of dairy analogs. Moreover, powders from this soymilk and tofu impart no off-flavors in the secondary generation products. The basic steps for preparing the soymilk involve cleaning and dehulling of soybeans, blanching of cotyledons, grinding, extracting of soymilk, pasteurizing, formulating, homogenizing, cooling, packaging and refrigeration. Existing soymilk equipment has generally proved to be suitable for this soymilk process. Manufacturing steps, processing conditions, and equipment used in this process are discussed in detail in the review paper. Composition of soymilk can be developed during processing to have a desired level of total solids, protein and oil. This soymilk process has been successfully adopted by a number of soymilk and dairy analog manufacturers in the US as well as worldwide.

The market of this bland soymilk and its derived products is expanding in many countries in North America, Western Europe, Eastern Europe, Africa and Indian subcontinent. A Hong Kong soymilk company has recently entered the US market. Exporting plays a significant role in Thailand's marketing development. Soymilk companies in Thailand can also have a share in the world market by adjusting their process and adding certain necessary equipment to the existing plant.

THE THIRD INTERNATIONAL CONFERENCE ON ADVANCED SCIENCE AND TECHNOLOGY TRANSFER TO THAILAND
JULY 23-25, 1993, BANGKOK, THAILAND

FULL NAME: (First) Nongnuch (last) Inpanbutr
OCCUPATION:Assistant Professor
ADDRESS:Dept. of Veterinary Anatomy & Cellular Biology A100 Sisson Hall, 1900 Coffey Road Columbus, OH 43210-1092
PHONE:614-292-2091 FAX:614-292-7599 E-MAIL:ninpanbu@magnus.acs.ohio-state.edu
FORUM:
FIRST AUTHOR STATUS: X MEMBER OF ATPAC: __ NON-MEMBER OF ATPAC

Calbindin-D_{9K} Gene Expression throughout the Bovine Estrous Cycle.

N. Inpanbutr, B.K. Petroff, T.M. Franklin, E.K. Miller, X.F. Zhuang and A.M. Iacopino

Recent studies have established CaBP as a mediator of transepithelial calcium transport. The current study was designed to characterize uterine CaBP expression throughout the bovine estrous cycle using immunohistochemical techniques, RIA, and Northern blot analysis. Uterine samples were collected at an abattoir and snap-frozen. Uteri were designated as luteal phase (d5-d17; n=11) or non-luteal phase (d18-d4; n=7) using morphology of ovarian structures and uterine tissue progesterone (P) and 17ß-estradiol (E) levels. Samples for microscopy were fixed by freeze-substitution and CaBP was immunohistochemically localized using the PAP method. Immunostainable CaBP was seen in the uterine glandular epithelium of all specimens with staining intensity increasing deeper toward the myometrium. CaBP appeared to localize both within the cytosol and nucleus of immunopositive cells. Staining appeared most intense in luteal phase uterine glands. Uterine E was greatest ($p<.01$) in the non-luteal phase (312.7 ± 40.2 pg/g) vs. luteal phase tissue (187.4 ± 32.1). Luteal phase samples had higher ($p<.01$) P (5.5 ± 0.5pg/mg) than non-luteal phase tissue (1.0 ± 0.6). CaBP levels were nearly thre-fold higher ($p<.01$) in luteal phase uterine samples ($8.9\pm0.3\mu$g/mg totsl protein) than in non-luteal phase samples (3.3 ± 0.3). Likewise, CaBP mRNA expression was increased ($p<.01$) in the luteal phase uterus ($16{,}383.8\pm1214.0$ arbitrary units) compared to the non-luteal phase uterus (5325.9 ± 409.0). To our knowledge, this study is the first to demonstrate the presence of CaBP within the bovine uterus. These results suggest that factors associated with the presence of a fuctional corpus luteum may increase uterine expression of CaBP in the non-pregnant cow.

THE THIRD INTERNATIONAL CONFERENCE ON ADVANVED SCIENCE AND TECHNOLOGY TRANSFER TO THAILAND
JULY 23-25, 1993, BANGKOK, THAILAND

FULL NAME: (First) Porn (Last) Israngkun na Ayudthaya
OCCUPATION Clinical Pathologist
ADDRESS: University Reference Labs, Inc. 1214 Kinnear Road
Columbus, Ohio 43212
PHONE: (614) 487-9222 FAX:(614) 487-1502 E-MAIL:
FORUM: Biomedical Science

FIRST AUTHOR STATUS:_____MEMBER OF ATPAC; X NON-MEMBER OF ATPAC

DETERMINATION OF SERTRALINE AND NORSERTRALINE BY HIGH-PRESSURE LIQUID CHROMATOGRAPHY

Porn P. Israngkun, Cheryl M. Hamon, Carleen M. Taylor and Ickbok K. Juhng, University Reference Labs., Columbus, Ohio 43212

Sertraline is a selective serotonin reuptake inhibitor having little or no effect on dopamine and noradrenaline uptake. It possesses tolerability advantage over tricyclic antidepressants and is essentially devoid of cardiovascular effects. Since sertraline will undoubtedly become an important option in the treatment of depression and because there is no assay available for this drug in the literature, a high-pressure liquid chromatographic method for sertraline and its metabolite, norsertraline, was developed.

Sertraline and norsertraline were isolated by solid-phase extraction employing a Bond-Elut C18 column. The extracts were injected into a 5 u, 4.6 mm x 150 mm reverse-phase CN column with phosphate, methanol, and acetonitrile as the mobile phase; flow rate 1.5 mL/min; ambient temperature;sample volume 25 uL; and detection wavelength 215 nm at 1.0 AUFS. Analysis time was about 8 min. and trimipramine was used as internal standard.

Peak heights ratio were linearly correlated to concentration ranges of 20 to 1000 ug/L. Recoveries for sertraline and norsertraline were 83 and 97%. Acceptable coefficients of variation were demonstrated for both within-run and day-to-day studies. Selected drugs were checked for interference. The assay has been verified in serum samples of patients treated with sertraline. Serum concentrations of sertraline and norsertraline ranged from 50 to 700 ug/L and 30 to 400 ug/L respectively.

THE THIRD INTERNATIONAL CONFERENCE ON ADVANCED SCIENCE AND TECHNOLOGY TRANSFER TO THAILAND
JULY 23-25, 1993, BANGKOK, THAILAND

FULL NAME: (First)Thunyasinth (last) Nimittherapharp
OCCUPATION: Physician and Surgeon in Opthalmology
ADDRESS:Hochdahler Strabe 32 D-4000 Dusseldorf 12 Germany

PHONE:0211/297727 FAX: E-MAIL:
FORUM: Biotechnology and Medicine
FIRST AUTHOR STATUS: __ MEMBER OF ATPAC: __ NON-MEMBER OF ATPAC
X MEMBER OF ATPER: __ NON-MEMBER OF ATPER

Myopic Photorefractive Keratectomy with the Eximer Laser

Since the first study demonstration of precise removing a fraction of a micron of corneal tissue with the eximer laser by Trokel et al. in 1983, many people recognized its enormous surgical potential for both therapeutic and refractive applications. During its first 4 years of clinical use the eximer laser is an incremental achievement that has substantially improved any alternative technology for refractive keratectomy. This article will review briefly about the history of the eximer laser and demonstrate the current state of the art in detail. Some new directions in eximer laser technology will be presented and discussed for the potential standard clinical treatment.

THE THIRD INTERNATIONAL CONFERENCE ON ADVANCED SCIENCE AND TECHNOLOGY TRANSFER TO THAILAND
JULY 23-25, 1993, BANGKOK, THAILAND

FULL NAME: (First) Wichai (last) Ekataksin
OCCUPATION:
ADDRESS:Univ. of Arizona 1501 N Campbell Ave. Tucson, AZ 85724 USA

PHONE:602-626-6086 FAX:602-626-2097 E-MAIL:
FORUM: Biotechnology: Medical Science
FIRST AUTHOR STATUS: __ MEMBER OF ATPAC: __ NON-MEMBER OF ATPAC

Intravital Observations of the Dynamic Distribution of Blood-Borne Substances: A Study of Hepatic Microcirculatory Events with A Combined Technology of In Vivo Microscopy, Fluorescent Dye Infusion and Video Microdensitometric Image Analysis.

Examining of structure as related to function is mandatory to a comprehensive understanding of the organ in health and disease. The living tissue with extensive vascularity, such as the liver, is particularly dynamic, in terms of circualtion, and due to its subdiaphragmic location is amply subject to respiratory movements. These conditions, however, do not preclude its intravital observation. Based on the established method of high-resolution in vivo microscopy (McCuskey, 1986), the surgically exposed liver of experimental animals was infused through a mesenteric vein with bolus of Fluorescent dye (fluoroisothiocyanate-dextran and sodium fluorescein) and the intralobular perfusion and clearance and accumulation of dye was visualized under epiilumination. Continous changes of the microcirculatory events were recorded through a high-sensitivity, image-intensified Newvicon camera which enabled repeated infusions to be observed with adjustable background fluorescence. The video cassette records were analyzed by microdensitometry, using the BioQuant System IV. Quantification in pseudocolors made possible ther real-time visualization of the microcirculatory heterogeneity and metabolic zones, and facilitated recognition of the hepatic microcirculatory subunit (HMS). Application of the combined techniques to study of other organs is implied.

THE THIRD INTERNATIONAL CONFERENCE ON ADVANCED SCIENCE AND TECHNOLOGY TRANSFER TO THAILAND
JULY 23-25, 1993, BANGKOK, THAILAND

FULL NAME: (First)Wichai (last)Ekataksin
OCCUPATION:
ADDRESS:Univ. of Arizona 1501 N Campbell Ave., Tucson,AZ 85724 USA

PHONE: 602-626-6086 FAX: 602-626-2097 E-MAIL:
FORUM:
FIRST AUTHOR STATUS: __ MEMBER OF ATPAC: __ NON-MEMBER OF ATPAC

The Spatial Third Dimension of Organ Microcirculation: A study of Hepatic Microvascularization with a Combined Technology of Perfusion Marker Injection, Histologic Serial Sections and Computer-Aided Three-Dimensional Reconstruction

The study by in vivo microscopy of fluorescent solutes provides an excellent tool for observing dynamic events related to the circulation of the organ. This advantage is especially effective when changes are to be considered as a function of time, so to say, the temperal (third) dimension of the live organ. However, spatial changes in the hidden third dimension remains unresolved, as in the case encountered by most techniques in light microscopy. To cope with this limitation, we have designed a combination of a histologic serial sectioning technique, a microscopic densitometry, and a computer-assisted tridimensional imaging. Circualtory effect was marked on the lobules by injecting the liver tissue through a portal vessel, with a small amount of 1% osmium tetroxide solution containing 1000 ppm ruthenium red (modified after Oda et al., 1983). In the tissue section, the injection medium created redish brown areas stained to various degrees. the apparances of perfusion pattern were closely comparably with the results obtained from in vivo microscopy of fluorescent dye. Densitometric quantification of sections in a complete series followed by serial reconstruction, appreciably visualized the space-occupying nature of the microcirculatory zonation. This methodology enabled us to delineate the configuration in three dimensions of the hepatic microcirculatory subunits that occured seperately or in cluster. Application of the combined techniques to study of other organs is implied.

THE THIRD INTERNATIONAL CONFERENCE ON ADVANCED SCIENCE AND TECHNOLOGY TRANSFER TO THAILAND
JULY 23-25, 1993, BANGKOK, THAILAND

FULL NAME: (First) Yuth (last) Nimit
OCCUPATION:Director, Off. of Prog coor and Re, NIH
ADDRESS:5600 Fishers Lane Rockwell II Bldg., Suite 630
Rockville, MD 20857
PHONE: 301-443-8455 FAX:301-443-3355: E-MAIL
FORUM: Biomedical Technology
FIRST AUTHOR STATUS: X HONORARY MEMBER OF ATPAC

The presentation will focus on the recent advancement and frontiers of biotechnology in the United States during my twenty six years of experience related to the biomedical and biotechnology fields. An overview based on my research, teaching and administrative management experience as a medical scientist at the National Institute of Health, as neuropsychopharmacologist at the Veteran Administration Hospital, as Professor at Baylor College of Medicine and Henan Medical University, Supervisory Health Scientist Administrator and currently, Director of the Office of Program Coordination and Review in the US Department of Helath and Human Servises. The theme will focus on the use of biotechnological methods, such as, drug receptor concepts of the development of medicinal, genetic engineering technology in new drug and vaccines designs. It will also cover development of new biotechnological and medical devices, diagnostic kits for biomedical research, medical diagnostic, treatment, and vaccine delivery systems as well as gene therapy. The later is directed toward future health care treatment and goals, and the principal of using genes to alter the immune system to fight infections and diseases. These techniques are used to build products for and toward the achievement of human environmental well being, health and longevity. The discussion will steer toward concerns regarding Thai health care and preaparation to deal with the epidemic of AIDS, which is predicted by experts to take place in Thailand by the year 2000.

A transferring of other knowledge and technology will not be possible if the country has to deal with the impending major AIDS crisis and disaster, and is not ready to accept them. Therefore, immediate attention to the highest priority using all resources for building up an infrastructure for prevention and treatment of HIV/AIDS infection is recommended.

THE THIRD INTERNATIONAL CONFERENCE ON ADVANCED SCIENCE AND TECHNOLOGY TRANSFER TO THAILAND
JULY 23-25, 1993, BANGKOK, THAILAND

FULL NAME: (First) Apisak (last) Ittipiboon
OCCUPATION: Engineer
ADDRESS:Communication Research Center 3701 Carling Ave.
Ottawa, ON. K2H 8S2 Canada
PHONE: 613-998-2400 FAX:613-990-8369 E-MAIL:ittipia.dgcd.doc.ca
FORUM: Electronics, Telecommunication
FIRST AUTHOR STATUS: __ MEMBER OF ATPAC: X_ NON-MEMBER OF ATPAC

General Method for the Computation of Electromagnetic Scattering Problems

A method has been developed for solving electromagnetic scattering problems. It has been realized by applying an eigenfunction expansion, together with the Lorentz reciprocity and Poynting theorems. The proposed technique is an alternative way of solving scattering problems without using the rather complicated Green's function method. The technique, however, can also be applied to derive the Green's function for such problems. One of the most atractive features of this technique is its simplicity and elegance in deriving an equivalent circuit of the structure being investigated. This technique leads directly to a stationary expression of the circuit parameters, including impedance or admittance. It is not necessary to determine explicitly the input voltage, current, and reflection and transmission coefficients which generally are required by other techniques. The proposed method has been successfully applied to solve the problems of aperture coupled microstrip patch antennas, aperture coupled microstrip lines and non-radiating dielectric waveguide fed slot antennas.

THE THIRD INTERNATIONAL CONFERENCE ON ADVANCED SCIENCE AND TECHNOLOGY TRANSFER TO THAILAND
JULY 23-25, 1993, BANGKOK, THAILAND

FULL NAME: (First)Chidchanok (last)Lursinsap
(first)Thitipong (last)Tanprasert
OCCUPATION: Professor
ADDRESS:The Center for Advanced Computer Studies P.O. Box 44330, USL, Lafayette, LA 70504
PHONE:318-231-6305 FAX:318-231-5791 E-MAIL:
FORUM:Electronic and Computer
FIRST AUTHOR STATUS: X MEMBER OF ATPAC: __ NON-MEMBER OF ATPAC

An Analytical Model for 3-D Placement of Rectangular Modules

T. Tanprasert and C. Lursinsap

The Center for Advanced Computer Studies
University of Southwestern Louisiana
Lafayette, LA 70504

Abstract

The technology trend in IC fabrication is moving towards the three dimensional fabrication process. Along this trend, many new design automation problems have been generated including the 3-dimensional layout generation. One of the critical problems in the analysis and design of layout generation is placement where the locations and orientations of components are determined. The proposed research concerns the placement of rectangularly approximated 3-dimensional modules. We formally state the problem and derive an analytical model of the problem in 3-D Euclidean space that takes into account of the total routing length and routability. The model is constructed based on solid analytical geometry in such a way that exact pin positions for estimating interconnection lengths, overlap constraints among all irregularly shaped rectangle modules, and approximated routing space requirement can be optimized simultaneously. Our 3-D placement model is optimized by a highly successful technique for constrained optimization, namely Multiplier Penalty Function. The placement layouts generated by our experimental program have been successfully global routed to verify good routability. Exceptional results have also been clearly evidenced for well-structured configurations such as 27-module cubic, 6-module clique, etc.

THE THIRD INTERNATIONAL CONFERENCE ON ADVANCED SCIENCE AND TECHNOLOGY TRANSFER TO THAILAND
JULY 23-25, 1993, BANGKOK, THAILAND

FULL NAME: (First) Chidchanok (last)Lursinsap
(First) Chularat (last)Khunasaraphan
OCCUPATION: Professor
ADDRESS:the Center for Advanced Computer Studies P.O. Box 44330, USL, Lafayette, LA 70504
PHONE:318-231-6305 FAX: 318-231-5791 E-MAIL:
FORUM:Electric and Computer
FIRST AUTHOR STATUS: _X MEMBER OF ATPAC: __ NON-MEMBER OF ATPAC

Simulated Light Sensitive Model for Thai Handwritten Alphabets Recognition[1]

A new technique for Thai handwritten alphabet recognition based on our simulated light sensitive model combined with the classical back-propagation network is proposed. It is much simple and more natural than the existing techniques. The concept is to transform and map a deformed Thai handwritten letter into a domain that is easy to manipulate because the preprocessing is the the important step of handwrittern alphabet recognition. We treat the input image as a visual image stimulated by the light. The light from the visual image will stimulate the receptor neurons. Then these receptor neurons excite and inhibit each other until they are in the stable state. Next they transmit signals to the back-propagation network. The primary objective is to overcome the space and time complexities of the problem, to recognize all 44 handwritten Thai letters, and to implement the recognition technique on a VLSI chip. The experiments confirm that this technique substantially reduces the time and space complexities of the neural network and recognizes all 44 soft error Thai letters.

THE THIRD INTERNATIONAL CONFERENCE ON ADVANCED SCIENCE AND TECHNOLOGY TRANSFER TO THAILAND
JULY 23-25, 1993, BANGKOK, THAILAND

FULL NAME: (First)Chokchai (last)Leangsuksun
OCCUPATION:Instructor (G.A)
ADDRESS:215 Bowman Dr. Kent, Ohio 44242 USA

PHONE:(216) 672-4004 ext. 215 FAX:672-7824 E-MAIL:chokchai@mcs.kent.edu
FORUM:Computer and Electronic
FIRST AUTHOR STATUS: X MEMBER OF ATPAC: __ NON-MEMBER OF ATPAC

PDC: A Parallel Distributed C Language for Distributed Computing Systems

The needs for high-speed computation have surged and never ended since the invention of the first computer. Computation-intensive applications require high performance computers that typically are parallel computing systems. The obvious solution is to divide the application into several subtasks, then execute them in different well-coordinated parallel processors. These such systems range from a network of workstations (LAN), to a multiple-processor system. LAN can be used as a *Distributed Computing System* that is certainly the most economical and best suited parallel system for Thailand.

In the past, the distributed systems were programmed in traditional languages with some library calls. This ad-hoc approach is uneasy to implement distributed applications, too restricted and unlikely that the code can be portable for other networks without massive modifications. Hence, our motivation in this research is to design a high level parallel language that is highly expressive and effortless in programming on distributed system. In this paper, we present supported parallel computational models and constructs extension to C language. This yields a new parallel language that we call Parallel Distributed C (PDC).

PDC methods of computation can be viewed as hierarchical task model. There are two primary methods of parallel execution within PDC; "data parallelism" and "functional parallelism". The language supports both asynchronous and synchronous communication among subtasks. The asynchronous fashion is accomplished via an assignment statement on special *asynchronous common* data structures. The PDC synchronous communication scheme allows an implicit way to enforce data integrity (i.e. a mutual exclusion based on the status of an updated variable). This is accomplished by a special *synchronous common* data declaration, called "*sync*". Explicit synchronization and mutual exclusion are supported in PDC via conditional barrier and conditional critical section respectively.

At the current status, the front-end of PDC, which is lexical and syntax analysis implemented in UNIX LEX-YACC, is completed and can be obtained by contacting the author.

THE THIRD INTERNATIONAL CONFERENCE ON ADVANCED SCIENCE AND TECHNOLOGY TRANSFER TO THAILAND
JULY 23-25, 1993, BANGKOK, THAILAND

FULL NAME: **(First)** Cholthanee **(Last)** Koerojna
OCCUPATION: Executive Director for the Computer Software Initiative
ADDRESS: 50 Oakland Street
Wellesley Hills, Massachusetts 02182
PHONE: (617) 237-1100 Ext 137 **E-MAIL:** CKOEROJNA@ECN.MA.EDU
FORUM: Electronic and Computer

FIRST AUTHOR STATUS: X MEMBER OF ATPAC _____NON-MEMBER OF ATPAC

Information Technology of the 90's: Multimedia Application Development for Training

Multimedia has become the computer industry's hottest information technology for the 90's. It is receiving so much attention. Many people are exploring the use of multimedia. The development is still under cost effective consideration but many industries are ready to use multimedia in educational and business applications. Some examples of multimedia applications are training, Just-in-Time guidance, Education, Business desktop, Point-of-Information and Merchandising.

At Massachusetts Bay Community College, the automated Advising, Degree Audit and Graduation Approval was developed for use by approximately 3,000 students and 400 faculty and staff members. It has become an increasing problem to train users. Currently students are trained to use this application through a Computer Literacy class. Additional training can be obtained from the Learning Center. Monthly ongoing training classes have been offered to faculty and staff. Nevertheless, many users still need a "private" lesson and special attention for training. If users seldom use the application, they forget it. To make training available to users at their finger tips, multimedia for training is necessary. This paper describes the concept of multimedia applications, tools, the development process and a design of an application for training.

THE THIRD INTERNATIONAL CONFERENCE ON ADVANVED SCIENCE AND
TECHNOLOGY TRANSFER TO THAILAND
JULY 23-25, 1993, BANGKOK, THAILAND

FULL NAME: (First) Kavee (Last) Techapichetvanich
OCCUPATION Faculty member in Engineering (English) Program, Thammasart Univer
ADDRESS: 344 Worachak Road, Bangkok 10100, Thailand sity

PHONE: 222-5544 FAX: E-MAIL: u32pth@chulkn.chula.ac.th
FORUM:

FIRST AUTHOR STATUS: YES MEMBER OF ATPAC: NON-MEMBER OF ATPAC X

INVESTIGATION OF LAGRANGIAN HEURISTICS FOR SET COVERING PROBLEMS

By : *Techapichetvanich, Kavee* and *Bricker, Dennis*
Department of Industrial Engineering, The University of Iowa,
Iowa City, IA 52242, USA

ABSTRACT

In this paper, we study and present Lagrangian heuristics for the set covering problem (SCP) which is a well-known problem in the literature. The SCP models numerous real world situations and is used world-wide especially for airline crew scheduling. It also has applications in fields such as location of emergency facilities, routing problems, truck deliveries, bus driver scheduling, assembly line balancing, and information retrieval. A number of optimal algorithms have been described in the literature. However, to date, no algorithm has been discovered that will find an optimal solution in polynomial time. Given the current situation with respect to optimal algorithms, there is a place for a computationally effective heuristic algorithm capable of producing good-quality (near-optimal) solutions with considerably less effort than that required by an optimal algorithm. The Lagrangian heuristic algorithm demonstrated in Beasley (1990) looked very promising and outperformed a number of other existing heuristic algorithms. However, there is still room for improvement in Beasley's heuristic. Furthermore, his heuristic algorithm worked well only for random-cost problems which may not resemble many real world applications. Thus, the purpose of this research is to investigate his algorithm and develop new improved ones which could also work well for classes of problems which more adequately model real world problems, i.e., unicost and correlated-cost problems, which appear to be much harder to solve than his random-cost problems. Computational results, based on problems involving 200 rows and 1000 columns, indicate that our Lagrangian heuristics produce good-quality solutions and outperform Beasley's heuristic significantly for unicost and correlated-cost problems.

THE THIRD INTERNATIONAL CONFERENCE ON ADVANCED SCIENCE AND TECHNOLOGY TRANSFER TO THAILAND
JULY 23-25, 1993, BANGKOK, THAILAND

FULL NAME: (First) Porponth (last) Sichanugrist
OCCUPATION:
ADDRESS:Fuji Electric Corp. R&D Ltd. 2-2-2 Nagasaka, Yokosuka-shi, Kanagawa-ken 240-01, Japan

PHONE: 0468-55-1241 FAX: 0468-55-1241 E-MAIL:
FORUM:
FIRST AUTHOR STATUS: X MEMBER OF ATPAC: __ NON-MEMBER OF ATPAC

HIGH PERFORMANCE AMORPHOUS SILICON SOLAR CELLS

Porponth Sichanugrist

Fuji Electric Corp. R&D, Ltd.,
2-2-2 Nagasaka, Yokosuka-shi,
Kanagawa-ken 240-01, JAPAN

Amorphous silicon (a-Si) has become one of the most promising materials for mass production of low-cost solar cells. Material cost a-Si solar cell is about 1/200 times cheaper than the one for crystalline silicon (c-Si) type solar cells since just thin film is needed. Manufacturing processing is much easier since it can be fabricated by plasma CVD at relatively low temperature as low as 200 C and simple processes which can be automatically controlled such as laser patterning, screen printing are utilized. Furthermore, it is the most promising solar cell to be used in the tropical country such as THAILAND since its power drop at high operating temperature is about half of the one for c-Si and absorbs more light in the short wavelength region.

R&D on a-Si solar cell has been carried out under the Sunshine Project[1]. High efficiency of more that 13% have been achieved on 1 cm^2 area cell and more than 10% on 30cm x 40cm area module.

In the past few years a-Si solar cells have been used in customer products in Japan. They have been used in calculators or battery charger and recently, they have been used as the power source for air-conditioning and for car ventilation system.

THE THIRD INTERNATIONAL CONFERENCE ON ADVANCED SCIENCE AND TECHNOLOGY TRANSFER TO THAILAND
JULY 23-25, 1993, BANGKOK, THAILAND

FULL NAME: (First)Suriya (last) Suntrarachun
OCCUPATION:
ADDRESS:Fujikura Ltd. 1440 Mutsuzaki

PHONE:043-484-3967 FAX:043-484-3989 E-MAIL:
FORUM:
FIRST AUTHOR STATUS: X MEMBER OF ATPAC: __ NON-MEMBER OF ATPAC

Local Area Network Management System using SNMP

Because of information exchanging need is growing up, more and more businesses or organizations are linking their computers into local area networks (LANs). Even smallest LANs should be managed to get network running with good performance and solve preventable problems by periodically monitoring network devices.

In late 1990, a large number of venders were providing SNMP (simple network management protocol) products. This standardization efforts result from recommendations of the Internal Activities Board, SNMP maintain images of the network in a database called management information base (MIB). The consistency between the image and the network is maintained by exchanging messages. When a management application modifies attributes of an object in the database, messages are sent to the physical device represented by the object to modify its corresponding attributes. Conversely, the database can learn the attributes of the physical devices by polling the devices periodically or by having the devices send relevant information about selected events.

In SNMP, A management application sends the commands get, set, and get next to objects in the MIBs of managed devices. These commands are formatted in ASN.1 and are sent using UDP/IP. This connectionless exchange of commands and responses is used to set and read attributes of managed objects. The managed objects can also signal events to the management application.

THE THIRD INTERNATIONAL CONFERENCE ON ADVANCED SCIENCE AND TECHNOLOGY TRANSFER TO THAILAND
JULY 23-25, 1993, BANGKOK, THAILAND

FULL NAME: (First) Suwanchai (last) Sangsuk-Iam
OCCUPATION:Professor
ADDRESS:Engineering (English) Program, Thammasat Univ. Klong Luang, Patumtani 12121, Thailand
PHONE:(66-2)5164357-8 FAX:(66-2)5164359 E-MAIL:
FORUM: Electronic and Computer
FIRST AUTHOR STATUS: __ MEMBER OF ATPAC: X_ NON-MEMBER OF ATPAC

DETECTION OF SENSOR FAILURES

Unexpected changes often occur in dynamical systems. These changes may degrade the system performance. Such changes are often referred to as failures. To improve the performance of systems under failures, the failures must be promptly detected, isolated, and accommodated.

Sensor failures are one of failures which commonly occur. These failures can occur in several forms. For example, sensors may become completely non-operational or unsatisfactorily operational. In the former case, sensors simply stop operating. While in the latter case the measurements provided by sensors contain unexpected disturbances. The degradation in sensor performance caused by these disturbances is usually in the form of increased inaccuracies.

In this paper, we present a theory for detection of sensor failures in the form of increased inaccuracies. A residual-based detection scheme is developed. The test statistic used in the detection scheme is rigorously derived by utilizing the Roy's union-intersection principle. The detection scheme presented in the paper has many areas of applications.

THE THIRD INTERNATIONAL CONFERENCE ON ADVANCED SCIENCE AND TECHNOLOGY TRANSFER TO THAILAND
JULY 23-25, 1993, BANGKOK, THAILAND

FULL NAME: (First)Viroj (last)Junlowjiraya
OCCUPATION:Management Information System Engineer
ADDRESS:Commonwealth Edison Company, Byron Nuclear Power Station, Byron, Illinios, 61010 USA
PHONE:815-234-5441ext.2186FAX:815-234-5441ext.22270 E-MAIL:
FORUM: Electronics and Computer
FIRST AUTHOR STATUS: __ MEMBER OF ATPAC: X_ NON-MEMBER OF ATPAC

Managing Information System in a Nuclear Power Plant in the 90's

Viroj Junlowjiraya, Commonwealth Edison Company, Byron Nuclear Power Station, Byron, Illinois, 61010 USA.

Using nuclear energy to produce electricity is an environmental sounded option. However the major concern is safety to general public and plant workers. State-of-the-Art plant equipments, well designed safety feathers, well emergency and security plans, well trained personnel, and well designed information system are essential components. These components are important to safe and reliable plant operations.

Today computer technology is changing very rapidly. A demand of computer utilization is also increases. Planning and managing of information system play an essential role in successful plant operations.

This presentation will focus on the management of information system in a nuclear power plant. The author will discuss three major types of data in the nuclear power plant operations, i.e. plant operation parameters, administration, and security data. The author will also discuss current and future computer technology both hardware and software.

THE THIRD INTERNATIONAL CONFERENCE ON ADVANCED SCIENCE AND TECHNOLOGY TRANSFER TO THAILAND
JULY 23-25, 1993, BANGKOK, THAILAND

FULL NAME: (First) Woraphon (last)Watunyuta
OCCUPATION: Student
ADDRESS:USL Box No. 43189 Lafayette, LA 70504

PHONE: 318-231-3639 FAX: E-MAIL:ww@cacs.usl.edu
FORUM: Electronics and Computer
FIRST AUTHOR STATUS: __ MEMBER OF ATPAC: __ NON-MEMBER OF ATPAC

Contour Shape Matching by a Constraint Satisfaction Network

W. Watunyuta and C. H. Chu

CENTER FOR ADVANCED COMPUTER STUDIES
THE UNIVERSITY OF SOUTHWESTERN LOUISIANA
LAFAYETTE, LOUISIANA, U.S.A.

Abstract

The matching of contours based on their shape attributes is an important task in computer vision. This contour shape matching task is formulated as a constraint satisfaction problem. The Hopfield net is a coorperative algorithm useful for solving optimization and constraint satisfaction problems. The stable states of the network corresponds to near–optimal solutions of the shape matching task. Constraints that are intrinsic to the shape matching task are coded in the network interconnection weights. Direct evidence obtained from the observed data, as guaged by a local shape measure, are provided as the external input to the network. The local shape measure used is developed based on an affine transformation model, which is a general class of mappings that includes the rigid body motion. Another constraint for this local shape measure is that it must be bounded to avoid overloading any of the input nodes. Empirical results are used to demonstrate the performance of this network when applied to match a contour with another that has undergone rotation, or scale–change, or translation, or combinations of these transformations. The network is capable of handling noisy data, as well as a reasonable amount of deformation. The deformation model is based on the perspective transformation of rotation in the three–dimensional space. The applications of contour shape matching are in image motion analysis, stereo vision computation, and multi–sensor data fusion problems. The network's ability to handle shape deformation due to three–dimensional rotation facilitates its use for tracking objects in an image sequence and for recovering structures of objects in a three–dimensional scene.

THE THIRD INTERNATIONAL CONFERENCE ON ADVANCED SCIENCE AND TECHNOLOGY TRANSFER TO THAILAND
JULY 23-25, 1993, BANGKOK, THAILAND

FULL NAME: (First)Sawat (last)Tantiphanwadi
OCCUPATION: Senior Electrical Engineer
ADDRESS:Orbital Sciences Corp. 21700 Atlantic Blvd., Sterling ,VA 20166-6801
PHONE:703-802-8228 FAX:703-802-8255 E-MAIL:
FORUM:Computer and Electronics
FIRST AUTHOR STATUS: __ MEMBER OF ATPAC: X_ NON-MEMBER OF ATPAC

Seastar Spacecraft Computer

Seastar is a remote sensing satellite to provide ocean color data for both scientific and commercial applications. The information is in the form of daily multispectral images which define photoplankton and chlorophyll levels as well as deduce the distribution of marine life, map detailed surface currents, and measure various aerosol levels above the ocean.

Ther are two main spacecraft computers of which only one computer will be active at a given time. The two spacecraft computers are cross-strapping to each other. Each unit consists of three computer slices and a power supply slice. The three computer slices are identical in hardware, but different in functionality and software. The three main functions are payload service, spacecraft maintenance and ground interface.

The specifications of each computer slice are, 16 MHz operation, three Motorola MC 68302, nine serial communication channels capable of synchronous data transfer rate up to 2 MBps, 2MBytes of EDAC SRAM, 512 KBytes of EEPROM, 64 KBytes of EPROM, hardware/software watchdog timers, non-volatine real-time clock, seven levels of interrupt, 12 constant-current outputs, and 16 TTL level inputs/outputs.

Major considerations were given to the radiation, thermal and EMI problems so that the computers would last the mission lifetime of ten years.

THE THIRD INTERNATIONAL CONFERENCE ON ADVANCED SCIENCE AND TECHNOLOGY TRANSFER TO THAILAND
JULY 23-25, 1993, BANGKOK, THAILAND

FULL NAME: (First) Charussri (last) Lorprayoon
OCCUPATION:Government Officer
ADDRESS:Dept. material Science Chulalongkorn Univeristy Bangkok 10330 Thailand

PHONE: 251-1954 FAX:252-4966 E-MAIL:
FORUM: 5
FIRST AUTHOR STATUS: __ MEMBER OF ATPAC: X_ NON-MEMBER OF ATPAC

Influence of Calcination Upon the Sintering Behaviour of Hydroxyapatite

As an attempt to improve the property of the hydroxy-apatite compact, calcination prior to sintering was carefully performed. Hydroxyapatite powder prepared by precipitation from aqueous solutions was divided into two portions. One portion was calcined before passing through the conventional processes and its property was studied in comparasion to those of the second portion which was uncalcined. Both powders were isostatically pressed into cylindrical shaped specimens and sintered in a flow of steam at 1100, 1200 and 1250^{0}C. As a direct measurement, the compact density was used to study the sintering behaviour. The results from this study suggested that calcination prior to sintering process was essential in obtaining stronger sintering products. Moreover, the SEM micrograph of the sintered compact revealed all characteristics needed in better products.

THE THIRD INTERNATIONAL CONFERENCE ON ADVANCED SCIENCE AND TECHNOLOGY TRANSFER TO THAILAND
JULY 23-25, 1993, BANGKOK, THAILAND

FULL NAME: (First)Dusit (last)Kruangam
OCCUPATION:Assistant Professor, DR.
ADDRESS: Dept. of Electrical Engineering, Faculty of Engineering Chulalongkorn University, Bangkok 10330 Thailand
PHONE: 662-252-5001 ext. 265 FAX:662251-8991 E-MAIL:-
FORUM:
FIRST AUTHOR STATUS: MEMBER OF ATPAC: NON-MEMBER OF ATPAC X

World's First Thin Film LED Made of Amorphous Silicon Nitride
-Possibility of New Type of Flat Panel Display-

Displays are optoelectronic devices that produce the ultimate output of an information system. They are interface between man and machine. In a highly informationalized society, the potential needs of flat-panel displays are increased day by day. LCDS, ELS, LEDS are well-known flat-panel displays. But the drawbacks of LCDs are that the viewing angle is limited and the contrast is band and LCDs need external light source. EL (electroluminescence) can emit light, but it need and operation voltage higher than 150 voltages. LEDs (Light Emitting Diodes) are made of high cost crystalline material, E.G., GaA1As, GaP, InP and have small areas. Therefore, a new type of flat-panel display that can overcome these drawbacks is required.

In this work, a novel flat panel display made of amorphous silicon nitride (a-SiN:H) thin film LED has been developed for the first time in the world. The basic structure of the Thin Film LED is shown in Fig. 1. The amorphous p-i-n layers were prepared by a glow discharge plasma CVD system constructed by the authors. The total thickness of the amorphous layers is as thin as 1000 Å. The a-SiN:H thin film LED has various attractive advantages, e.eg., low-cost and large area flat-panel display. It is operated at a low voltage ($< 10V$). Various emission colors from red, yellow, green to white-blue can be emitted.

The success in this work has given a big impact to both worlwide amorphous semiconductor technologies and flat-panel display industries.

In the full paper, recent R&D on amorphous silicon based optoelectronic devices including thin film solar cell in Thailand are presented. A series of technical data of basic characteristics of a-SiN:H thin film LED is described and discussed. Fiigure 2 shows and example of a white-blue thin film LED. The height of the emission pattern is 6 nm.

THE THIRD INTERNATIONAL CONFERENCE ON ADVANCED SCIENCE AND TECHNOLOGY TRANSFER TO THAILAND
JULY 23-25, 1993, BANGKOK, THAILAND

FULL NAME: (First)Kasemsan (last)Siri
OCCUPATION:Electrical Engineer
ADDRESS: Rockwell International Corp. Rocketdyne Division(FB67) 6633 Canoga Ave., Canoga Park, CA 91309-7922
PHONE: 818-586-2802 FAX:818-772-9223 E-MAIL:
FORUM:
FIRST AUTHOR STATUS: MEMBER OF ATPAC: NON-MEMBER OF ATPAC

Current Distribution Control of Converters Connected in Parallel

This paper presents two schemes of current distribution control in a parallel connected converter system; master-slave and central-limit controls. In these techniques, we introduce inner control loops to the converters connected in parallel to achieve output current equalization. We use the current distribution error as a criterion for the system performance. Using these control schemes, the current distribution error can be much improved even with non-identical converters in the system. The central-limit technique provides much less transient current overshoot as compared to the response due to the master-slave approach. These distribution techniques are refined so that only a necessary number of converters are active for each condition.

THE THIRD INTERNATIONAL CONFERENCE ON ADVANCED SCIENCE AND TECHNOLOGY TRANSFER TO THAILAND
JULY 23-25, 1993, BANGKOK, THAILAND

FULL NAME: (First) Mana (last)Sriyudthsak
OCCUPATION: Government Service
ADDRESS: Dept. of Electrical Eng. Faculty of Eng. Chulalongkorn University Bangkok 10330, Thailand
PHONE: 662-252-5001 FAX: 662-2518991 E-MAIL:fengmsy@chulkn.chula.ac.th
FORUM:
FIRST AUTHOR STATUS: MEMBER OF ATPAC: NON-MEMBER OF ATPAC X

Development of Glucose Analysing System

Mana Sriyudthsak, Narameth Nananukul

Semiconductor Device Research Laboratory (SDRL), Department of Electrical Engineering Chulalongkorn University, cooperated with the Institute of Biotechnology and Genetic Engineering (IBGE), Chulalongkorn University has developed glucose analyzing system. The system consists of glucose biosensor, flow injection analysis (FIA) system with data processing unit. The measure principle is based on the reaction of the enzyme glucose oxidase with the glucose in the samples which produce electron that be transfered to platinum electrode, which is made by thin film technology. By measuring the current, glucose concentration in the samples can be determined. With the system, more than 60 samples per hour can be analyzed for glucose at carrier flow rate of 3.0 ml/min. Very small amount of the sample is required in the measurement (20 μl). The linear measuring range is 50-400 mg/dl with a coefficient of variation of 3.0 percent without any interference from sucrose, lactose, maltose, uric acid and ascorbic acid. The glucose biosensor is stable up to 3 months. The system can be applied to determine glucose concentration in biotechnology research, food industry process control and medical service in hospitals.

THE THIRD INTERNATIONAL CONFERENCE ON ADVANVED SCIENCE AND TECHNOLOGY TRANSFER TO THAILAND
JULY 23-25, 1993, BANGKOK, THAILAND

FULL NAME: (First) Methi (Last) Wecharatana
OCCUPATION Professor of Civil Engineering
ADDRESS: Dept. of Civil and Environmental Engineering
New Jersey Institute of Technology, Newark, NJ 07102
PHONE: (201) 596-2474 FAX:(201)242-1823 E-MAIL: WECHARATANA@TESLA.NJIT.EDU
FORUM:

FIRST AUTHOR STATUS:_____MEMBER OF ATPAC; __X__ NON-MEMBER OF ATPAC

EFFECT OF FRACTIONATED FLY ASH AND SILICA FUME ON HIGH STRENGTH CONCRETE

Chai Jaturapitakkul and Methi Wecharatana

ABSTRACT

Fly ash is fractionated into different small ranges of particle size distribution which have a much smaller particle size than the original fly ash. A very fine particle size of fractionated fly ash (smaller than 5 microns) was employed to produce high strength fly ash concrete. Fifteen and twenty five percent of fly ash by weight of cementitious materials were used in the concrete mix as a replacement of cement. Silica fume in the powder form was also used in the same proportion as fly ash. The compressive strength of fly ash and silica fume concrete was determined and compared to the control high strength concrete.

The results show that the compressive strength of fly ash and silica fume concrete achieves a strength of 6000 psi (42 MPa) after 7 days of curing. The rate of strength gain of concrete made from silica fume is very fast at early age but seems to slow down after 7 days. Its strength is almost the same as the control strength at 28 days. High strength concrete made from fractionated fly ash behaves differently that at the early age, the strength of fly ash concrete is lower than those of control and of silica fume concrete. After 14 days, the use of fractionated fly ash in concrete produces the same strength as the control concrete. While at 28 days, the strengths of fly ash concrete are higher than the control and silica fume concrete. The strengths of these fly ash concretes are in the order of about 8500 psi (58 MPa) whereas the strength for the control and silica fume concretes are about 8000 psi (55 MPa). The compressive strengths of fly ash concrete are in the range of 107% to 115% of the control concrete at the age of 90 days. The results obtained here suggest that fractionated fly ash is a suitable material to produce high strength concrete. The use of fly ash in concrete not only eliminates the cost incurred for the disposal of fly ash but also reduces the cost of high strength concrete.

THE THIRD INTERNATIONAL CONFERENCE ON ADVANVED SCIENCE AND
TECHNOLOGY TRANSFER TO THAILAND
JULY 23-25, 1993, BANGKOK, THAILAND

FULL NAME: (First) Pavadee (Last) Aungkavattana
OCCUPATION Graduate Student
ADDRESS: 626 S. Pugh St. #16
State College, PA 16801
PHONE: (814)-8672326 FAX: - E-MAIL: June@ecl.psu.edu
FORUM: Electronic Ceramic

FIRST AUTHOR STATUS: X MEMBER OF ATPAC; _____ NON-MEMBER OF ATPAC

MIXED-CONDUCTING OXIDE ELECTRODE FOR SOLID OXIDE FUEL CELL

P. AUNGKAVATTANA AND V. S. STUBICAN

THE PENNSYLVANIA STATE UNIVERSITY
CERAMIC SCIENCE PROGRAM
DEPARTMENT OF MATERIALS SCIENCE AND ENGINEERING
UNIVERSITY PARK, PA 16802

ABSTRACT

The purpose of this research was to study and develop new cathode materials for solid oxide fuel cell. The presently used cathode material $La_{1-x}Sr_xMnO_3$ reacts with YSZ (electrolyte) to form a poorly conductive compound such as $La_2Zr_2O_7$. Materials proposed as the new cathodes were Ca-doped $YFeO_3$ perovskite materials which do not form $La_2Zr_2O_7$ and which were expected to have high electrical conductivity and good thermal expansion match with YSZ.

Fine, uniform, dense and crack-free microstructures were developed with $Y_{1-x}Ca_xFeO_3$ (x = 0 to 0.2). Samples were prepared conventionally, from mixed oxides and carbonates or by Pechini process and sintered at 1350°C or 1400°C for 8-16 hours. All specimens were found to be single phase orthorhombic. Thermal expansion coefficients were measured on the samples with x=0, 0.10 and 0.20. The values for all samples were near 10×10^{-6} /°C in the temperature range 200° to 900°C. A value of 10.8×10^{-6} /°C was measured for the YSZ specimen, indicating an excellent match. The electrical conductivity of doped specimens (except x=0.025) in air was 10^3 S/m at temperature above 500°C, with negligible variations as a function of dopant concentration. This value compares favorably with other perovskites.

second experiment extends that to a two camera system. The third experiement adds mobility to the two camera system which increases the range of asembly tasks that can be performed. The visions systems are uncalibrated and work without having to rely on any central world model.

30

THE THIRD INTERNATIONAL CONFERENCE ON ADVANCED SCIENCE AND TECHNOLOGY TRANSFER TO THAILAND
JULY 23-25, 1993, BANGKOK, THAILAND

FULL NAME: (First)Pongpan (last)Chindaudom
OCCUPATION: Scientist
ADDRESS: C10 Prof.K. Vedam, 276 MLR, The Pennsylvania State Univ.
University Park, PA 16802
PHONE:814-863-1880 FAX:- E-MAIL:ET@PSUVM.EDU
FORUM:Manufacturing Technology and Industrial Engineering
FIRST AUTHOR STATUS: __ MEMBER OF ATPAC: X NON-MEMBER OF ATPAC

32

THE THIRD INTERNATIONAL CONFERENCE ON ADVANCED SCIENCE AND TECHNOLOGY TRANSFER TO THAILAND
JULY 23-25, 1993, BANGKOK, THAILAND

FULL NAME: (First)Schitt (last)Laowattana
OCCUPATION: Engineering Instructor
ADDRESS: Center of Operation for Field Robotics Development(FBO) King Mongkul's Institute of Technology Thonburi
PHONE: 412-268-8880 FAX:268-3348 E-MAIL:srk@andrew.cmu.edu
FORUM: 5

FIRST AUTHOR STATUS: X MEMBER OF ATPAC: NON-MEMBER OF ATPAC

A Voice-Actuated, Tendon-Controlled Device for Endoscopy

Dept. of Mechanical Engineering
Carnegie Mellon University
Pittsburgh, Pennsylvania 15213

The high level of skill required to maneuver present-day, flexible endoscopes that are utilized in esophagoscopy and colonoscopy has prompted us to propose a new class of safer, more easily controlled devices. The primary issues in control include command system design to free the hands of the endoscopist and sequencing techniques to assure reliable motion of the stem. These devices are mechanical releoperators with few degrees of freedom based on the familiar bead chain with internal control cables. The study of the physics associated with the flexiblecontrol devices is carried out with respect to the design parameters of both the practical system and its environment. We introduce the "Slide Motion" scheme, which provides a smooth movement of the endoscope stem with only three continuously controlled degrees of freedom. Such movement is acomplished by implementing a series of relative motions between an outer tube and intermittently stiff spines inside. The strength and stability of the locking menchanism, which exhibits intermittent stifness, is also discussed.

THE THIRD INTERNATIONAL CONFERENCE ON ADVANCED SCIENCE AND TECHNOLOGY TRANSFER TO THAILAND
JULY 23-25, 1993, BANGKOK, THAILAND

FULL NAME: (First)Schitt (last)Laowattana
OCCUPATION:Engineering Instructor
ADDRESS: Center of Operation for Field Robotics Development(FIBO) King Mongkul's Institute of Technology Thonburi
PHONE: 4120268-8880 FAX:268-3348 E-MAIL:s12k@andrew.cmu.edu
FORUM: 5

FIRST AUTHOR STATUS: X MEMBER OF ATPAC: NON-MEMBER OF ATPAC

Representation of Relative Freedom Derived from Geometric Models

Dept. of Mechanical Engineering
Carnegie Mellon University
Pittsburgh, Pennsylvania 15213

Multi-contact constraints representing the assembled state of polygonal solid objects can be represented by screw systems which provide a complete description of rotational and translational freedom. In most cases, the computation of relative freedom does not require consideration of all constraints. We have developed an algorithm to identify redundant constraints, therefore minimizing the complexity of assembly/disassembly planning. We also employ the method to determine relative stability which identifies unstabe configurations of assembled parts.

THE THIRD INTERNATIONAL CONFERENCE ON ADVANCED SCIENCE AND TECHNOLOGY TRANSFER TO THAILAND
JULY 23-25, 1993, BANGKOK, THAILAND

FULL NAME: (First)Schitt (last)Laowattana
OCCUPATION:Engineering Instructor
ADDRESS: Center of Operation for Field Robotics Development(FIBO) King Mongkul's Institute of Technology Thorburi
PHONE: 412-268-8880 FAX:268-3348 E-MAIL:s12k@andrew.cmu.edu
FORUM: 5

FIRST AUTHOR STATUS: X MEMBER OF ATPAC: NON-MEMBER OF ATPAC

Virtual Wedging in Three Dimensional Peg Insertion Tasks

Dept. of Mechanical Engineering
Carnegie Mellon University
Pittsburgh, Pennsylvania 15213

Quasi-static wedging of three point contacts is investigated, wherein the concepts of virtual and redundant wedging due to a resultant force falling into a friction cone are proposed. We consider the fully started case of a square peg and hole consisting of two point-surface contacts and one line-line contact. An analysis of the wedging diagram for this highly constrained configuration is carried out and compared to the two dimensional case. An approximate wedging diagram is constructed which shows that wedging of square pegs into square hole is more likely than cylindrical pegs and holes of similar sizes.

THE THIRD INTERNATIONAL CONFERENCE ON ADVANCED SCIENCE AND TECHNOLOGY TRANSFER TO THAILAND
JULY 23-25, 1993, BANGKOK, THAILAND

FULL NAME: (First)Somchai (last)Ratanathamnaphan
OCCUPATION:Gover. Officer
ADDRESS: Dept. of Electrical Engineering, Faculty of Engineering Chulalongkorn University, Bangkok 10330, Thailand
PHONE: 252-5001 ex.265FAX: 251-8991 E-MAIL:fengsrt@chulkn.chula.ac.th
FORUM:
FIRST AUTHOR STATUS: MEMBER OF ATPAC: NON-MEMBER OF ATPAC X

A Novel Phase Epitaxy Technique for GaAs-GaA1As Single Quantum Well Lasers Fabrication

Somchai Ratanathammaphan, Choompol Antarasena, Somsak Panyakeow

The GaAs-GaA1As quatum well structure with a well layer of GaAs has been successfully fabricated by liquid phase epitaxy (LPE). By combination of the two-phase solution to grow very thin layers and the supercoolong technique to grow the thick layers with fast growth rate for minimizing the diffusion problem. The GaAa well thickness less than 300 Å can be obtained by LPE at 795^{0}C. These lasers showed quatum size effects as the lasing peak wavelength shorter than this obtained from the conventional bulk type. The broadening spectrum of spontaneous emission was also detected. In addition to the blue shift hopping of using wavelength occurs when increasing the injection. A room temperature threshold current density as low as 500 A/cm^2 was obtained from the broad area structure laser under pulse condition.

THE THIRD INTERNATIONAL CONFERENCE ON ADVANCED SCIENCE AND TECHNOLOGY TRANSFER TO THAILAND
JULY 23-25, 1993, BANGKOK, THAILAND

FULL NAME: (First)Somnuk (last) Tangtermsirikul
OCCUPATION:Asistant Professor
ADDRESS: Engineering(english)Program, Thammasat University Klong Luang, Patumtani 12121, Thailand Rangsit Campus
PHONE: 66-2-516-4357-8 FAX: 66-2-516-4359 E-MAIL: -
FORUM:
FIRST AUTHOR STATUS: MEMBER OF ATPAC: X NON-MEMBER OF ATPAC

A Simulation of Chloride Condensation in Concrete

A mathematical model for simulating chloride movement in hardened concrete has been proposed by the authors. The model was proved to be effective for computing chloride content in hardened concrete in a chloride environment, with many kinds of boundary and environmental conditions. The model also takes into account the effect of arbonation which was found to have effect on the amount of free chloride in the carbonated concrete.

Many researchers including the authors reported that free chloride concentration in the concrete,especialy at the surface portion,can be higher than that of the environemnt when the specimens were submerged in salt water or uderwent cyclic wetting and drying with salt water. The phenomenon is called chloride condensation in this paper. There has been no model which is able to deal with the chloride condensation. This paper proposed a model and an idea to account for the chloride condensation in both submerged and cyclic wetting and drying cases. Chloride condensation in the submerged case was modeled by integrating the idea of influx of chloride ion onto the concrete due to ion adsorption with the theory of diffusion. Chloride condensation in the case of cyclic wetting and drying was modeled by taking the following occurences into account. In drying state, only water evaporates from the conrete surface, leaving salt at the drying portion. In wetting state, salt water enter the concrete in a very short period mainly by capillary action. Therefore, chloride condensation occurs when the specimen undergoes cyclic wetting and drying for a long period.

Experiment was conducted for verification and it was found that the proposed model and idea are effective for simulating chloride condensation.

THE THIRD INTERNATIONAL CONFERENCE ON ADVANVED SCIENCE AND TECHNOLOGY TRANSFER TO THAILAND
JULY 23-25, 1993, BANGKOK, THAILAND

FULL NAME: (First) SUANG (Last) KHUWATSAMRIT
OCCUPATION
ADDRESS:

PHONE: FAX: E-MAIL:
FORUM:

FIRST AUTHOR STATUS: ✓ MEMBER OF ATPAC; _____ NON-MEMBER OF ATPAC

ELECTRIC VEHICLES DEVELOPMENT PROGRAM

GENERAL STATEMENT

Electric Vehicles (EVs) do not burn gasoline. EVs also do not use energy when they are caught in the traffic jam in Bangkok. Air quality in Bangkok is beyond crisis proportion. We must electrify our buses, the major source of air pollution. Why should we start with buses? There are several reason behind this selection. First of all, EV is not suitable for long distance traveling, usually less than 150 km which is well within the distance of any bus routes but beyond the vacation traveling in a passenger car. Secondly, passenger cars require both reliability and low cost while public-service buses need reliability over absolute minimum cost. We should start with one goal, making it work good. Then, we can make it inexpensive. The third reason is that Electric bus is the niche product that giant auto manufacturers ignore. But the large size of the traction drive is strategically important for our country to electrify our public transportation system, Electric commuter train and eventually implementing our own intelligent highway Program. Recharging Stations for passenger EV's are considered one of the infrastructure that requires wide-spread political stimulation and huge business investment while they are relatively easy to facilitate for Electric Bus at bus depots. Last but not least, It is impossible to compete with giant auto manufacturers on competitive passenger car market. But, it is quite possible to outdo those giants in this niche market.

Next question is whether we have the technological know how's to do it. There are three technically challenging fields that need real-world design expertise and world-class manufacturing skill. They are human comfort controller which is likely to involve Fuzzy logic, Energy storage and management techniques and high-power PWM Inverter Drive System, likely in the 200-300 kW range. All these are by no mean state of the art technologies. Nor they require multi-million dollar development tools. This product is well within our technical expertise and capital strength to develop. Although, there are a few know-how's to be explored in this program that are not publicly known at this moment. Decades of research in the West and Japan does not translate into decade of catching up for us. Luckily the key technology in this field, namely Static Converter Drive System, changes rapidly in this past five years, most of the old studies need to be re-evaluated in the context of new micro-controller based control strategies, new power semiconductor devices and circuit topologies. We are not that far behind after all.

THE THIRD INTERNATIONAL CONFERENCE ON ADVANVED SCIENCE AND TECHNOLOGY TRANSFER TO THAILAND
JULY 23-25, 1993, BANGKOK, THAILAND

FULL NAME: (First) SUANG (Last) KHUWATSAMRIT
OCCUPATION Electrical Engineer & Engineering Management
ADDRESS: 197 Honey Tree Drive
Athens, GA 30605
PHONE: (706) 548-4105 FAX: (706) 354-8056 E-MAIL:
FORUM:

FIRST AUTHOR STATUS: ✓ MEMBER OF ATPAC; _____ NON-MEMBER OF ATPAC

GENERAL STATEMENT (cont.)

Now that the technical aspect of the project has been discussed. It is appropriate to address political business issues. What is the return of this investment? The most immediate return will be one less major sources of air pollution. This project also serves as a stepping stone into World-Class Manufacturing and Global OEM Business. Export of Electric Buses from Thailand is quite realistic if we intend to carry this development through second phase and commit to World-Class Manufacturing. The long term benefit will be basis to stimulate the growth of Electronic Manufacturing Industries. This might well be the only mechanism that will transform our industries from agriculture product base to equipment manufacturing base. The know-how's from this project may serve as basis for reverse-engineering of the Light Rail Commuter train system that we are building as part of our infrastructure development in the third phase of this plan.

In summary this plan will directly produce:
- two prototypes of full-size electric bus in three and a half years;
- world-class production of full-size electric bus in five and a half years;
- three prototypes of medium speed commuter trains in seven years.

indirectly, this development plan will support:
- surface-mount contract manufacturing;
- Hybrid electronic component manufacturing;
- Distributed control system design and manufacturing;
- Adjustable speed drive design and manufacturing;
- high efficiency motor manufacturing;
- Industrial process system integrators;
- Industrial Equipment OEM's.

DEVELOPMENT PLAN

PHASE 1 : ELECTRIC BUS DEVELOPMENT

PHASE 2 : ELECTRIC BUS MANUFACTURING

PHASE 3 : ELECTRIC COMMUTER TRAIN REVERSE ENGINEERING

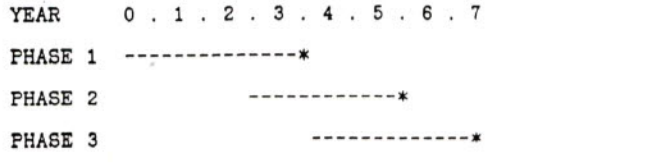

THE THIRD INTERNATIONAL CONFERENCE ON ADVANVED SCIENCE AND TECHNOLOGY TRANSFER TO THAILAND
JULY 23-25, 1993, BANGKOK, THAILAND

FULL NAME: (First) Suebsak (Last) Nanthavanij
OCCUPATION: Associate Professor in Industrial Engineering
ADDRESS: Engineering (English) Program, Thammasat University
Klongluang, Patumtanee 12121, Thailand
PHONE: (66-2) 516-4357 FAX: (66-2) 516-4356 E-MAIL:
FORUM: Technical Presentation - Industrial Engineering

FIRST AUTHOR STATUS: x MEMBER OF ATPAC; _____ NON-MEMBER OF ATPAC

Recently, a large number of computer users suffering from carpal tunnel syndrome (CTS) has been reported in U.S.A. Some of the job-related factors contributing to this cumulative trauma disorder in the computer users are the use of poorly designed workstation and improper body posture while operating a computer keyboard. During the past few years, many business and industrial corporations in Thailand have intensively utilized microcomputers in their day-to-day operations and on continuous basis. Thus it is of great concern that some percentage of Thai computer users will be soon affected by CTS if they are not promptly warned of and protected. Fortunately, it has been found that by ergonomically designing workstation and adjusting it properly, the risk of developing CTS can be greatly reduced.

An intelligent adjustment (**IntelAd**) system is a computerized tool developed to help a computer user adjust a workstation according to ergonomic principles. Its purpose is to recommend near-optimal computer workstation settings that help the user maintain correct body posture; thus reducing the risk of developing CTS. **IntelAd** utilizes an algorithm specifically designed to position the computer user and certain hardware units (keyboard and monitor) so that the recommended body posture is obtained. From the user's standing height and sex, **IntelAd** calculates relevant measures such as seat height and depth, lengths of upper and lower arms, eye height, etc. These measures are mapped into the Cartesian coordinate system along with other reference points such as a home row of a keyboard and the center of monitor screen. The resulting set of workstation settings is then compared to ANSI/HFS-100 Standards for Computer Workstations to verify the feasibility of the recommended solution. If one or more conflicts exist, **IntelAd** will search for alternate settings and suggest the best compromise. It is also capable of recommending appropriate settings for workstations with limited adjustment capability (e.g., fixed table height, fixed chair height, etc.)

This paper is organized as follows. Firstly, the design and theoretical framework of **IntelAd** is discussed in detail. The flowchart showing approximation and verification routines are also given to provide an insight to the system's architecture. Then, in a step-by-step manner, assumptions and mathematical formulas used in determining ergonomic settings are explained. Finally, a realistic example is given to demonstrate **IntelAd**'s application.

THE THIRD INTERNATIONAL CONFERENCE ON ADVANVED SCIENCE AND TECHNOLOGY TRANSFER TO THAILAND
JULY 23-25, 1993, BANGKOK, THAILAND

FULL NAME: (First) Suebsak (Last) Nanthavanij
OCCUPATION Associate Professor in Industrial Engineering
ADDRESS: Engineering (English) Program, Thammasat University
Klongluang, Patumtanee 12121, Thailand
PHONE: (66-2) 516-4357 FAX: (66-2) 516-4359 E-MAIL
FORUM: Technical Presentation - Industrial Engineering

FIRST AUTHOR STATUS: x MEMBER OF ATPAC NON-MEMBER OF ATPAC

Theoretical Framework of Intelligent Adjustment (IntelAd) System

by

Suebsak Nanthavanij, Ph.D.
Department of Industrial Engineering
Engineering (English) Program
Thammasat University
Klongluang, Patumtanee 12121, Thailand

ABSTRACT

An intelligent adjustment (IntelAd) system is a computerized tool developed to help a computer user adjust a workstation according to ergonomic principles. Its purpose is to recommend near-optimal computer workstation settings that help the user maintain correct body posture; thus reducing the risk of developing carpal tunnel syndrome (CTS). IntelAd utilizes an algorithm specifically designed to position the computer user and certain hardware units so that the recommended body posture is obtained. IntelAd calculates relevant body measures such as seat height and depth, lengths of upper and lower arms, etc. and maps them into the Cartesian coordinate system along with other reference points such as a home row of a keyboard, etc. The resulting set of workstation settings is then compared to ANSI/HFS-100 Standards for Computer Workstations to verify the feasibility of the recommended solution. If one or more conflicts exist, IntelAd will search for alternate settings and suggest the best compromise. It is also capable of recommending appropriate settings for workstations with limited adjustment capability (e.g., fixed table height, fixed chair height, etc.)

This paper is organized as follows. Firstly, the design and theoretical framework of IntelAd is discussed in detail. The flowchart showing approximation and verification routines are also given to provide an insight to the system's architecture. Then in a step-by-step manner, assumptions and mathematical formulas used in determining ergonomic settings are explained. Finally, a realistic example is given to demonstrate IntelAd's application.

THE THIRD INTERNATIONAL CONFERENCE ON ADVANVED SCIENCE AND TECHNOLOGY TRANSFER TO THAILAND
JULY 23-25, 1993, BANGKOK, THAILAND

FULL NAME: (First) Taweep (Last) Chaisomphob
OCCUPATION Assistant Professor
ADDRESS: Engineering (English) Program, Thammasat University Rangsit Campus
Klong Luang, Patumtani 12121, Thailand
PHONE: (662)5164356-8 FAX: (662)5164359 E-MAIL:
FORUM: Structural Engineering and Construction Technology

FIRST AUTHOR STATUS: __/__ MEMBER OF ATPAC; ____ NON-MEMBER OF ATPAC

Development of the Design Method of Steel-Concrete Sandwich Composite Structures

Chaisomphob Taweep*, Tamon Ueda**

Among the new types of composite structures applied to both inland and offshore structures, steel-concrete sandwich composite structures seem to be one of the best choice due to its higher toughness and strength compared with conventional reinforced concrete structures, and short period of construction. Hence, the sandwich composite structures are expected to be applied widely in the near future.

Considering the needs of the design method for this structure, the Japan Society of Civil Engineers (JSCE) established the Committee on Research of Steel-Concrete Sandwich Composite Structures, which aimed to propose design recommendations especially applied to a submerged tunnel.

In this paper, the content of proposed design recommendations is introduced. Due to significant differences between the shear resisting capacity of sandwich composite structures and reinforced concrete structures, the proposed shear design method is emphasized here, and the results of full-scale model tests are presented to verify the reliability of proposed ultimate shear strength formula.

---

* Assistant Professor, Engineering (English) Program, Thammasat University.
** Associate Professor, Department of Civil Engineering, Hokkaido University.

THE THIRD INTERNATIONAL CONFERENCE ON ADVANVED SCIENCE AND TECHNOLOGY TRANSFER TO THAILAND
JULY 23-25, 1993, BANGKOK, THAILAND

FULL NAME: (First) Thamrong (Last) Prempridi
OCCUPATION Professor of Civil Engineering
ADDRESS: Faculty of Engineering Rangsit University
Lakhok , Muang, Pathumthani 12000 THAILAND
PHONE: 5339020-4Ex 1522 FAX: 5339472 E-MAIL:
FORUM:

FIRST AUTHOR STATUS:_____MEMBER OF ATPAC; _____ NON-MEMBER OF ATPAC

Transfer of Process Pumps Technology from Japan

This paper describes the joint efforts between the Faculty of Engineering Chulalongkorn University and Rangsit University and EBARA Corporation (TOKYO) to transfer the technology of design, construction, operation and maintenance of Pumps used in industrial processes. The transfer includes training workshop, visit to pump manufacturers in Thailand and field operation and maintenance of precess pumps

Instruction manuals in English for the training workshop were translated into Thai. Some of these manuals and work examples were also modified into text books published by the Engineering Institute of Thailand to be used as references for practiced engineers and engineering undergraduates. The joint effort was started in 1985 and is still going strong.

THE THIRD INTERNATIONAL CONFERENCE ON ADVANCED SCIENCE AND TECHNOLOGY TRANSFER TO THAILAND
JULY 23-25, 1993, BANGKOK, THAILAND

FULL NAME: (First)Vira (last)Chankong
OCCUPATION: Principal Investigator/Project Director
ADDRESS: Dept. of Systems Engineering, Case Western Reserve University, Cleveland, Ohio 44106-7070
PHONE: FAX: E-MAIL:
FORUM:
FIRST AUTHOR STATUS: MEMBER OF ATPAC: NON-MEMBER OF ATPAC

A Multiobjective Optimal Design Method For Magnetic Resonance Imaging Gradient Waveforms

Vira Chankong and Jeffrey L. Duerk

In this research, we propose a new strategy for designing gradient waveforms for magnetic resonance imaging (MRI) that (i) provides optimal image contrasts, and (ii) eliminates artificial constraints on the wavefrom imposed by the traditional multi-lobe design procedures. The stradegy describes a gradient wavefrom as a set of discrete amplitudes and selects such amplitudes and other key design parameters (such as echo time (TE), repetion time (TR), sampling time (TS), and resolution levels to optimize several design criteria subject to restrictions defined by imaging conditions and hardware requirements. The design criteria are selected to achieve diagnostically optimal images in terms of contrasst, resolution, slice selection, field of view, chemical shift, and motion sensitivity while minimizing imaging time.

There are three principal tasks to be performed in this research. First, a careful modeling exercise will be performed to ensure that the essence of gradient wavefrom design for MRI is fully captured and that its output is practical and usable. Second, the resulting gradient wavefrom design model will be a mathematical program with multiple objective functions characterized by high nonlinearity due to complicating variables (such as TE, TR, and TS). It is believed that such a problem is best solved using a multilevel aproach where the portion of the model involving primarily the complicating variables (i.e. image contrast) is handled in the top level, and the rest of the model (i.e. gradient wavefrom) is solved in the lower level. An effective multilevel procedure for solving such multiobjective optimization problems will be developed. Also it is anticipated that the problem in the lower level will be of the quadratically constrained quadratic program (QCQP) variety. A good optimizer for solving QCQP will also have to be explored and developed. A prototype of the proposed design support system that integrates all the pieces combined with and easy-to-use user-interface will then be biult. Finally, the third and final task will involve a testing and demonstration of the developed design procedure using an MRI facility at MetroHealth.

An advantage of this new design approach is that it allows all relevant design criteria and real constraints imposed by imaging requirements and hardware restrictions to be considered

together in a single framework without imposing artificial approximations. The waveform designers and radiologists would thus be able to make explicit trade-offs among various design criteria to achieve the best possible image for a given set of image specifications and imaging goals. From the algorithmic viewpoint, contributions will be made in terms of a new efficient optimizer for quadratically constrained quadratic programs (QCQPs), and an effective procedure for dealing with a class of multiobjective optimization problems using multilevel optimization.

THE THIRD INTERNATIONAL CONFERENCE ON ADVANCED SCIENCE AND TECHNOLOGY TRANSFER TO THAILAND
JULY 23-25, 1993, BANGKOK, THAILAND

FULL NAME: (First)Wannee (last)Chinsirikul
OCCUPATION:Grad Student
ADDRESS: 626 S. Pugh St. #16 State College, PA 16801 USA
PHONE: 814-867-2326 FAX: - E-MAIL: Wannee@ecl.psu.edu
FORUM:
FIRST AUTHOR STATUS: X MEMBER OF ATPAC: NON-MEMBER OF ATPAC

Property Improvement in Polypropylene/Aluminum Laminates by Surface Modification

by
Wannee Chinsirikul and Ian. R. Harrison

Adhesion of polyolefins to metals, such as polypropylene(PP) and aluminum(Al), is a particularly difficlut problem. To address this problem, a new method of surface modifaction utilizing a recently-developed copolymer of polypropylene (Polypropylene Cohexanol (PP-OH) has been developed. Comparing this copolymer bonding method and a common oxidative treatment involving an acid etching process, PP/Al laminates utilizing the PP-OH copolymer show an extraordinary 7-10 fold increase in peel strength over acid etched samples.

Based on fractographic and wettability studies of peeled PP/PP-OH/Al laminates, the fracture path propagates within bulk P film representing primary cohesive failure. Extemely high peel strengths of $\approx$1200 N/m and $\approx$700 N/m were found for high modulus oriented PP/Al and unoriented PP/Al laminates, respectively. These results indicate excellent bonding between polypropylene and aluminum. In addition to adhesion, we observe improvement in the laminates' tensile strength, modulus and impact properties. Recently, tests on multilayer composites (i.e. cross-ply laminates) have shown attractive impact properties form which a comparison can be made between PP/Al composite properties and those of the other available materials.

THE THIRD INTERNATIONAL CONFERENCE ON ADVANCED SCIENCE AND TECHNOLOGY TRANSFER TO THAILAND
JULY 23-25, 1993, BANGKOK, THAILAND

FULL NAME: (First)Abhisak (last)Chulya
OCCUPATION: Research Scientist
ADDRESS: NASA Lewis Research Center, 21,000 Brookpark Rd. MS 6-1 Cleveland, OH 444135;
PHONE: (216)433-8523 FAX:(216)433-8300 E-MAIL:Smartc@ariel.Lerc.NASA.GOV
FORUM: Transportation Technology
FIRST AUTHOR STATUS: X MEMBER OF ATPAC: NON-MEMBER OF ATPAC

THE ROLE OF HIGH TEMPERATURE MATERIAlS IN THE NEXT GENERATION SUPERSONIC CIVIL TRANSPORT

There is a growing, worldwide interest in a second generation supersonic transport aircraft. The booming market for transpacific flights is expected to help create a lucrative new market for a plane that can shrink long distances. By the end of the decade, transpacific travel is expected to reach 315,000 passengers a day. A plane flying at Mach 2.5 could more than halve the duration of a Los Angeles-Toyko flight to just 4.5 hours. The Concorde has always been a money loser for its operators. It carries too small a passenger load, guzzles too much fuel, and makes so much noise that 30 countries have restricted its use. In order to become a reality, the next generation of supersonic civil transport (SSCT) must be both enviromentally acceptable and economically competitive with future subsonic aircraft.

Current research is now focused on advanced high temperature materials which is expected to have a major impact on the overall economic viability of SSCT. The use of these materials inpropulsion systems of the SSCT can reduce the block fuel burn through increased effeciency via higher operating temperatures and smaller size via increased specific thrust of the engines. Advanced materials also lowers the weight of the airplane. A reduction of 1 pound of total propulsion system weight reduces the aircraft weight by 24 pounds for a 4-engine SSCT. Analysis has clearly indicated the importance of utilizing these materials as engine components: Ceramic Matrix Composites (CMC) and Intermatallic Matrix Composites (IMC) in the combuster and exhaust nozzle, Polymeric Matrix Composites (PMC) and Metal Matrix Composites (MMC) in the front end of the engine for ducting, casings, and fan blisks. Advancements in materials technology is the key. This paper provides an insight into NASA's ongoing research and highlights the propulsion system's influence on the viability of the next generation SSCT.

THE THIRD INTERNATIONAL CONFERENCE ON ADVANCED SCIENCE AND TECHNOLOGY TRANSFER TO THAILAND
JULY 23-25, 1993, BANGKOK, THAILAND

FULL NAME: (First) B (last) Emaruchi
OCCUPATION: PhD Student
ADDRESS: Royal Forest Dept. of Thailand Faculty of Engineering, University of Regina, SK, S4S 0A2, Canada
PHONE: FAX:306-585-4855 E-MAIL:
FORUM:
FIRST AUTHOR STATUS: __ MEMBER OF ATPAC: __ NON-MEMBER OF ATPAC

Water Resources Using Passive Microwave Remote Sensing

by
Emaruchi, B.;Jin, Y.;and Kite, G.W.

Water shortage has become a critical problem of Thailand and is likely to occur every year during the dry season due to the heavy deforestation. Recently, droughts have been spreading in many parts of the country destroying a large amount of crops. Before solutions to the drought problem can be devised, it is necessary to carry out large scale water resources survey. Passive microwave remote sensing is considered to be the most effective method for the large scale water resources survey because it can provide us with information covering large areas almost once every 14 days. Advantages of the passive microwave remote sensing include: the sensitivity to detect moisture; the ability to operate in all kinds of weather, days and nights; low resolution which reduces CPU time and costs to analyze the data.

In this investigation, the passive microwave remote sensing has been used to detect the large scale soil moisture content. By measuring soil moisture contents of sampled points and relating them to the spectral reflectance of the passive microwave remote sensing data, a model to estimate soil moisture content for the whole area of interest may be developed. Soil moisture content is a useful tool to locate potential areas for effective water resources development such as construction of wells and ponds for collecting water. Moisture zones, obtained by using the passive microwave remote sensing, can be used to locate potential seepage zones where ground water can be found.

THE THIRD INTERNATIONAL CONFERENCE ON ADVANCED SCIENCE AND TECHNOLOGY TRANSFER TO THAILAND
JULY 23-25, 1993, BANGKOK, THAILAND

FULL NAME: (First) Fuangfoo (last) Jugravee
OCCUPATION: Instrumentation Engineering, STRR Div. city of LA
ADDRESS:1235 Glenclaire Dr. Diamondbar, California 91789

PHONE: 909-594-7339 (res)FAX: - E-MAIL: - 310-524-1144(bus)
FORUM:
FIRST AUTHOR STATUS: _X_ MEMBER OF ATPAC: __ NON-MEMBER OF ATPAC

STRR Division (SOLID TECHNOLOGY RESOURCE RECOVERY)
HYPERION TREATMENT PLANT is one of the largest municiple wastewater processing facilities in the United States. Daily flow range from 320 million to 420 million gallons.

Raw Biosolids (sludge) from the city of Los Angeles to Primary treatment flow to effluent pumping sludge settles to the bottom. Sludge is collected and directed to sumps from where it is pumped to sludge digester. Three fourths of effluent from the primary tanks were pumps to the sea 5 miles long ocean outfall. Four 2500 horsepower motors discharging 200 million gallons per day. From digseter tanks which it enclosed odor gas (biogas) blow to gas turbines to burn gas produces electricity about 12,000 kilowatts.

From the bottom of digester tanks pump to centrifuge dewatering and uses steam to heat the mechanically dewatered sludge in order to drive off all the remaining water. The process called MEE (MULTIPLE EFFECT EVAPORATION) to drive off the water with very little outside energy input. MEE is used in several of industrial plants. For example, in making concentrated orange juice and powdered milk products, because of the low energy requirement to drive off water. When sludge is drying to be mixed with oil and go to centrifuge to dry again and burn sludge to boilers make steam turbines produce about another 8,000 kilowatts called combined cycle power generation. The sludge that results from dehydation looks like a fluffy gray-brown powder, and collected by truck load to landfill (dump site).

The project in construction now is steam dryer to add on uses rotary-disc dryer utilize steam-fed disc which rotate within a large vessel containing dewatered biosolids cake. Heat is conducted from the disces to the cake (sludge); raising its temperature to the boiling point of water thereby evaporating much of the moisture. This operation currently operating in Germany.

From Jugravee Fuangfoo instrumentation & control dept.
STRR Division city of Los Angeles.

THE THIRD INTERNATIONAL CONFERENCE ON ADVANCED SCIENCE AND TECHNOLOGY TRANSFER TO THAILAND
JULY 23-25, 1993, BANGKOK, THAILAND

FULL NAME: (First) Kate (last) Grudpan
OCCUPATION:
ADDRESS:Dept. of Chemistry, Faculty of Science, Chiang Mai University
Chiang Mai 50002, Thailand
PHONE: FAX:6653-222268 E-MAIL:
FORUM:
FIRST AUTHOR STATUS: __ MEMBER OF ATPAC: __ NON-MEMBER OF ATPAC

A Novel continuous/automatic Analytical System for the Environment Analyses : An Example of the Appropriate Science and Technology Transfer to Thailand.

Environmental awareness has gained much more interests in Thailand. Environmental studies including the monitoring and assessment have been emphasized. Analyses as an important part of such the studies are to be realized in the aspects of reliability (precision and accuracy) and performance (cost and time consuming) and the capability of operation and maintanance. Flow injection analysis (FIA) as a novel continuous/automatic analysis being introduced in 1976 has now been accepted internationally including in the US-EPA procedures, due to its many advantages. In Thailand, FIA was first studied in 1983. Since then FIA has been investigated in various aspects. As an example of the appropriate science and technology transfer to Thailand, development, investigation and application of FIA for environmental analyses in Thailand with emphasis on the analysis for water-quality parameters using low cost FIA instrumentation. The discussion will be based on the investigation at Chiang Mai University yielding the real industrial uses.

THE THIRD INTERNATIONAL CONFERENCE ON ADVANVED SCIENCE AND TECHNOLOGY TRANSFER TO THAILAND
JULY 23-25, 1993, BANGKOK, THAILAND

FULL NAME: (First) Dr. Kris T. (Last) Rugsaken
OCCUPATION: Associate Professor/Academic Advisor
ADDRESS: Ball State University, NQ 324
Muncie, Indiana 47306
PHONE: (317) 285-1162 FAX: E-MAIL: 00KTRUGSAKEN@BUSVAX1
FORUM: Natural Resources and Environment

FIRST AUTHOR STATUS: X MEMBER OF ATPAC; _____ NON-MEMBER OF ATPAC

CHARACTERISTICS OF GLOBAL LABOR FORCE IN THE YEAR 200

ABSTRACT

The primary goal of this session is to present projected characteristics of the labor force of Thailand as well as other developing and industrialized nations in the year 2000. Focuses will be placed on the labor force of Thailand, compared to that of other developed and developing countries, including Japan, Korea, the United States, Brazil, and some industrialized countries in Europe. Other countries surrounding and affecting the economic growth of Thailand will also be examined.

The development of the next decade is rooted in today's demographics, particularly those having to do with the size and character of various countries' work force. In some areas of the world, for instance, women have not been absorbed in large number of labor force, elsewhere the absorption process is nearly complete. In some countries, the majority of today's labor force have less than high school education whereas in other countries high school education is a prerequisite for entering the work force. Such national differences are a good starting point for understanding what the future global labor force will look like and how it will affect individual nations and companies.

The paper will discuss changes in women's participation, levels of workers' education, ages of workers, the growing rate of individual nation's labor force, and the globalization of the world's labor force by the year 2000.

THE THIRD INTERNATIONAL CONFERENCE ON ADVANVED SCIENCE AND TECHNOLOGY TRANSFER TO THAILAND
JULY 23-25, 1993, BANGKOK, THAILAND

FULL NAME: (First) NOPHADOL (Last) IN-NA
OCCUPATION FACULTY MEMBER
ADDRESS: ENGINEERING (ENGLISH) PROGRAM
THAMMASAT UNIVERSITY, RANGSIT CAMPUS, PATHUMTANEE 12121
PHONE: 5164356 FAX 5164359 E-MAIL
FORUM:

FIRST AUTHOR STATUS: DR. MEMBER OF ATPAC NON MEMBER OF ATPAC

GLOBAL WARMING EFFECT ON RIVER BASINS IN SRI LANKA

Nophadol In-na[1] and E.J. Hemantha[2]

ABSTRACT

A global climatic change is likely to occur due to an increase of Carbon Dioxide(CO_2) and other trace gasses in the atmosphere. This climatic change is expected to affect hydrological processes in river basins.

For this paper, a river basin in tropical Sri Lanka was considered for analyzing the sensitivity of hydrological variables due to climatic change. Thirty-six years of historical daily mean monthly temperatures of the year and mean annual temperatures of the river basin were analyzed. Climatic conditions projected by three General Circulation Models(GCM) at double CO_2 conditions were considered as future climatic scenarios for analyzing the sensitivity of Potential Evapotranspiration(ETO), rainfall, and runoff due to the climatic change. Modified ETO and rainfall, according to the GCM's projections at double CO_2 conditions were input into the selected rainfall runoff model for the river basin to obtain runoff projections for future climatic scenarios.

The results concluded the mean temperature of each month of the year and the mean annual temperature were gradually increased during the past thirty-six years. At double CO_2 conditions, the rainfall pattern changed and the high rainy season shifted toward the end of the year. Increased peaks of rainfall and runoff projected the possibility of high floods at double CO_2 conditions. Reduction of rainfall and runoff in dry seasons projected severe droughts.

THE THIRD INTERNATIONAL CONFERENCE ON ADVANCED SCIENCE AND TECHNOLOGY TRANSFER TO THAILAND
JULY 23-25, 1993, BANGKOK, THAILAND

FULL NAME: (First) Osoth (last) Jamjun
OCCUPATION: Environmental Engineer
ADDRESS:6545 N. Kilpatrick, Lincolnwood, IL 60646, USA

PHONE:708-222-4008 FAX: 708-222-4067 E-MAIL:
FORUM:
FIRST AUTHOR STATUS: X MEMBER OF ATPAC: __ NON-MEMBER OF ATPAC

Preservation of Kawn Payao Water Resource Project

Kawn Payao is a fresh water lagoon in the heart of Payao Province, an ancient city in the north of Thailand. The Kawn is an ecomonic security for Payao Province and her half a million population.

The algae and other water born vegatative in the Kawn Payao indicates eutrophication and if no action is taken to remedy the situation, it will be a tragedy for the Payao Province and her population.

The objective of the project is to preserve the Kawn Payao and prevent it from further deterioration. The project envisions three strategies to accomplish the objective. The three strategies are:

1. Protecting the Kawn Payao through polution prevention.
2. Empowering all sectors, central and local government agencies, leaders of the community such as members of the House of Representatives, and private citizens,to get involved with the project
3. Planning and managing the Kawn Payao water quality and water quantity for both short term and long term plans.

It is anticipated that the project will succeed through the cooperation from the central government and local government agencies, members of the house of representatives, private citizens, and ATPAC.

The success of this project will be an example for the remedy of other pollution problems in Thailand.

THE THIRD INTERNATIONAL CONFERENCE ON ADVANCED SCIENCE AND TECHNOLOGY TRANSFER TO THAILAND
JULY 23-25, 1993, BANGKOK, THAILAND

FULL NAME: (First) Sarakorn (last) Gerjarusak
OCCUPATION: Student
ADDRESS: MIT 66-053, 77 Massachusetts Ave. Cambridge, MA 02139

PHONE: 617-225-9816 FAX:617-253-9695 E-MAIL:
FORUM: Natural Resoueces and Environment
FIRST AUTHOR STATUS: __ MEMBER OF ATPAC: _X_ NON-MEMBER OF ATPAC

Plasticity Kinetics of Different Coal Types

Plastic coals are important feedstocks in coke manufacture, coal liquefaction, gasification, and combustion. During these processes, the thermoplastic behavior of these coals is also important since it may contribute to desirable or undesirable characteristics. For example, during liquefaction, the plastic behavior is desired since it leads to liquid-liquid reactions which is faster than solid-liquid reactions. During gasification, the plastic behavior is undesired since it leads to caking and agglomeration of coal particles which result in bed bogging in fixed or fluidized bed gasifiers.

The plastic behavior of different coals are being studied using a fast-response plastometer. The plastometer measures the torque required to turn at constant angular speed a cone-shaped disk embedded in a thin layer of coal. The coal particles are packed between two metal plates which are heated electrically. Heating rates, final temperatures, and durations of experiment range from 200-800 K/s, 700-1300 K, and 0-40 s respectively. The torque is translated into the molten coal's apparent viscosity by the governing equation of the cone-and-plate viscometer. Using a concentrated suspension model, the molten coal's apparent viscosity is related to the quantity of the liquid metaplast present during the pyrolysis. A multiple independent parallel reaction (MIPR) kinetics model is used to describe the metaplast generation and depletion and thus the magnitude and duration of plasticity of different coals. In addition, coal plasticity is correlated to simple indices of coal type, such as its elemental composition.

Seven coals from Argonne National Laboratory Premium Coal Sample Bank are being studied. Five bituminous coals, from high-volatile to low-volatile bituminous, have been found to have very good plastic behavior. Effects of pressure, temperature, and coal type on coal plasticity were investigated. Elevated pressures up to 49 atm of helium above atmosphere, did not affect coal plasticity, but reducing pressure from atmosphere to vacuum resulted in diminished plasticity, i.e. a shorter plastic period and a higher minimum apparent viscosity. It is hypothesized that high pressure inhibits mass transport of metaplast to tar vapors, but also favors metaplast repolymerization into coke and char. Higher holding temperature decreased the coal plastic period. It is hypothesized that higher temperature increases mass transport of liquid metaplast to tar vapors and metaplast repolymerization to coke and tar. Heating rate had essentially no effect on the individual softening temperatures of five different plastic coals. A possible explanation is that, depending on coal type, metaplast generation, by chemical bond breaking or physical melting, or both, is not strongly affected by heating rate. Increasing the heating rate, however, decreased the plastic period of each coal. It is hypothesized that higher heating rate enhances mass transport and reaction kinetics, speeding the global mechanism of metaplast generation and thus the depletion.

THE THIRD INTERNATIONAL CONFERENCE ON ADVANVED SCIENCE AND TECHNOLOGY TRANSFER TO THAILAND
JULY 23-25, 1993, BANGKOK, THAILAND

FULL NAME: (First) Somkiat (Last) Pongkanta
OCCUPATION Engineer
ADDRESS: 33045 Korbel Street
Union City,CA.94587
PHONE: (510) 471-6196 FAX:(510) 464- 6539 E-MAIL:
FORUM: Transportation or (510) 464-6818

FIRST AUTHOR STATUS: X MEMBER OF ATPAC; _____ NON-MEMBER OF ATPAC

MANAGING PUBLIC TRANSPORTATION

Abstract

We are facing a transportation crisis, the one that becomes more critical as time goes on, a crisis which threatens to overwhelm us while we are standing around seeking solutions. Concurrently, we are facing a land usage crisis as we face the task of accommodatng more population increase in the limited space that has also been shaped to suit additional transportation requirements. One of the critical issues facing us today is traffic congestion. The congestion will get worst during the next 20 years. Billions of hours are wasted each year in the traffic jams. They do not only impede our mobility but also pollute air, waste fuel, and hamper economic growth. The paper describes general problems and an approach to solve the problems of transportation in the United States. Balance of transportation between supply and demand is presented including short term and long term solutions. As one of the long term solutions, rail transit systems are described.

Electric Trolley Bus is presented as a mass transit that can help achieving clean air. And finally, the advantages of the Turn Key public transportation project are examined.

THE THIRD INTERNATIONAL CONFERENCE ON ADVANCED SCIENCE AND TECHNOLOGY TRANSFER TO THAILAND
JULY 23-25, 1993, BANGKOK, THAILAND

FULL NAME: (First)Soonthon (last)Lupkitaro
OCCUPATION: Senior Lecturer
ADDRESS: Civil Engineering Dept. Kasetsart Univ. Bangkok 10903 Thailand

PHONE: 579-0730 FAX: E-MAIL:
FORUM:
FIRST AUTHOR STATUS: __ MEMBER OF ATPAC: __ NON-MEMBER OF ATPAC

Hierarchical Evaluation of Water Resource

It is realized that the problem of water resource in development scheme is composed of multiple factors and objectives. Therefore, a systematic evaluation of water resource is essential for the comprehensive plan of any region. This paper will extend social analysis in the systems approach. First of all, scale, hierarchy, trade-off and feedback of the regional system are conceptually, structurally and qauntitatively discussed. Next, compatable evaluation procedures are adopted to recognize the water resource within a region with use of a large number of data. At the final stage the problem is solved by considering an interactive process to compare with decision making criteria.

In brief, conceptual model, structural model and quantitative model are applied to certain water basin to express factors related to the environmental control and use of water. Cause and effect diagram, directional diagram (digraph) and interaction of water use in agricultural as well as industrial sectors are expirically presented. In order to quantify extents of water use, a set of objective functions is derived.

The functions are simulated with the system dynamic method under empirical data. As a consequence, they are concluded to be significantly affected with social and technological measures. That is, heirachical evaluation of water resource can reflect regional economic and social demand as well as the role of technology being exploited within the whole system.

THE THIRD INTERNATIONAL CONFERENCE ON ADVANCED SCIENCE AND TECHNOLOGY TRANSFER TO THAILAND
JULY 23-25, 1993, BANGKOK, THAILAND

FULL NAME: (First) Viroj (last) Isaradharm
OCCUPATION: Engineer
ADDRESS:MESA Engineering, Inc. 207 E. Pomona Blvd., Suite A
Montery Park, CA 91754
PHONE:213-722-1236 FAX: 213-722-0109 E-MAIL:
FORUM: Natural Resource and Environment
FIRST AUTHOR STATUS: X MEMBER OF ATPAC: __ NON-MEMBER OF ATPAC

Hazardous/Flammable Waste Storage Facilities

This paper is to present the problems of hazardous/flammable wastes that effect the environment. Improper disposal and storage of the hazardous waste can lead t contamination of soil, contamination of ground and surface water, and air pollution. Discussion of storage facilities for both old and new systems in the U.S.A. with a case study of the Edwards Air Force Base in California will be presented in this paper. A superior and more suitable system will be suggested for use in Thailand. Proper and applicable codes and enforcement shall be the major consideration for the Thai governing authority.

THE THIRD INTERNATIONAL CONFERENCE ON ADVANCED SCIENCE AND TECHNOLOGY TRANSFER TO THAILAND
JULY 23-25, 1993, BANGKOK, THAILAND

FULL NAME: (First)Richard F. (last) Doner
OCCUPATION:
ADDRESS:Dept. of Political Science,Emory University
Atlanta, Georgia 30322 USA
PHONE: 404-727-7914 FAX:404-727-4586 E-MAIL:
FORUM: Social Science
FIRST AUTHOR STATUS: __ MEMBER OF ATPAC: X_ NON-MEMBER OF ATPAC

Learning from Alliances with Japanese Firms in High Tech

How do non-Japanese firms learn managerial and technological skills from Japanese partners? This paper examines this question from the perspective of US firms involved in joint ventures or other types of alliances with Japanese frims. However, the paper may hold lessons for non US firms as well. The paper begins by tracing the reasons for and results of joint ventures with Japanese firms. It then explores the Japanese capacity to cooperate with and learn from joint venture partners. In the third section it identifies some problems emerging in joint ventures with Japanese firms, and in the final section it offers three suggestions for non-Japanese firms partnering with Japanese: The importance of knowing what you want to share with your Japanese partner and what you don't what to share; the need to learn how to learn from your partner; and the importance of getting experience in partnering from alliances with other non-Japanese firms.

ACTIVITIES OF HEALTH AND WELFARE CANADA IN PROTECTION FROM NON-IONIZING RADIATION

Artnarong Thansandote, J.D. Yvon Deslauriers, Stephen H.P. Bly, David W. Lecuyer, Wayne Gorman, Robert G. Hussey, Jack R.N. McLean and Pavel Dvorak

Bureau of Radiation and Medical Devices
Health and Welfare Canada
775 Brookfield Road, Ottawa, Ontario K1A 1C1, Canada.

Abstract---In this paper, we present a broad overview of Health and Welfare Canada's program in the protection of the general public from non-ionizing radiation (NIR) such as power line fields, radiofrequency fields, laser emissions, ultraviolet, ultrasound and noise. The major objectives of the program are to identify potential health hazards and assess health risks associated with devices which emit NIR, and to minimize unnecessary exposure to these radiations where potentially hazardous. The program covers a wide range of activities in three main areas: electromagnetics, lasers and electro-optics, and acoustics. The major activities in each of these areas are discussed.

I. INTRODUCTION

Electromagnetic radiation is energy that travels through space and exists throughout our entire environment. It can be natural, such as light from the sun, or it can be man-made, such as microwaves in the kitchen oven. Electromagnetic radiation is somewhat arbitrarily divided into two major types: ionizing and non-ionizing. Ionizing radiation usually refers to all radiation having individual photon energies greater than 12.4 eV, which is sufficient to ionize most atoms. Non-ionizing radiation (NIR) is known as a group of radiations which have longer wavelengths and less photon energy, as shown in Figure 1. Except for the narrow spectrum of visible radiation, electromagnetic NIR is imperceptible to any of the human senses unless it is absorbed by specific skin pigments - as in tanning or in specific skin diseases, e.g. lupus, or unless its intensity becomes so great that it is felt as heat. The term NIR also includes all acoustical radiation from infrasound (less than 20 Hz) to sound (20 Hz to 20 kHz) to ultrasound (greater than 20 kHz).

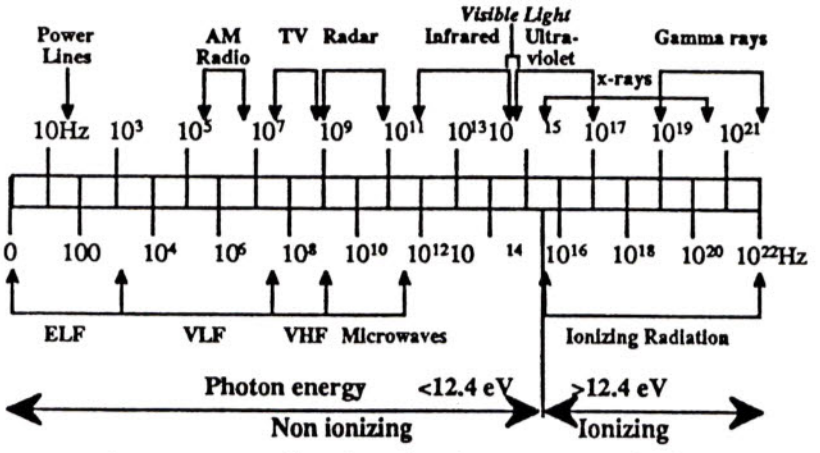

Figure 1. Electromagnetic spectrum showing the frequency and photon energy distinction between ionizing and non-ionizing radiations (Repacholi, 1992).

Except for exposure to ultraviolet (UV) radiation from the sun, it does not appear that humans have been exposed in the past to high levels of natural NIR. However, UV radiation, lasers and ultrasound are increasingly used in research, industry, medicine and even in consumer products. Also, the use of electrical devices that generate electromagnetic fields have increased considerably in the past few decades. Increased mechanization in industry and transportation has also led to a significant increase in acoustical noise. These man-made NIR sources not only lead to occupational exposure but also to exposure of the general public that is several orders of magnitude above the natural background. Scientific data have shown that exposure to excessive levels of NIR over a prolonged period of time can cause adverse health effects (Duchêne et al., 1991).

Like the populations in other industrialized countries, Canadians are becoming increasingly aware and concerned about the potentially harmful effects of NIR. The public awareness and concern has been reflected in Canadian media coverage and increased scientific research about these effects over the years. Health and Welfare Canada has developed a program to protect workers and the general public from NIR. The major objectives of the program are: (1) to identify potential health hazards and assess health risks associated with devices which emit NIR, and (2) to minimize unnecessary exposure to these radiations where potentially hazardous. The program covers a wide range of activities in three main areas: electromagnetics, lasers and electro-optics, and acoustics. Health criteria have been developed for a number of types and frequencies of radiation and, where necessary, controls have been applied by implementing regulations under the Radiation Emitting Devices (RED) Act of Canada. Regulations for microwave ovens, laser scanners, demonstration laser devices, sunlamps, mercury lamps, and ultrasound therapy devices are now in force. In addition, a number of safety codes and safe use guidelines relating to the installation and use of various devices have been developed. Safety codes for active metal detectors, radiofrequency exposure, ultrasound devices, short-wave diathermy devices and magnetic resonance clinical systems have been published and distributed.

A brief overview on the major activities in NIR of Health and Welfare Canada is given below.

II. ELECTROMAGNETICS

In this area, the assessment of risks of electric and magnetic fields at extremely low frequencies (1-300 Hz) has been a major activity in the past 4 years. The work includes in-house animal studies to determine the potential health risks from 60-Hz magnetic field exposure with emphasis on an investigation of tumor co-promotion in mouse skin. Experiments were carried out with SENCAR mice, one group of which was sham exposed and the other exposed to a 2 mT, 60 Hz magnetic field. The dorsal skin of all animals was initiated with a tumor-causing chemical (dimethylbenz[a]anthracene) and treated weekly with a tumor-promoting chemical (phorbol-12 myristate-13 acetate). In a 52-week study completed in early 1992, we found that the magnetic field appeared to increase the rate of tumor development but did not affect the yield of tumors (McLean et al., 1992). However, a recent replication of this study did not support the previous findings. We are now in the process of studying the feasibility of using an alternative to the SENCAR mouse in the investigation of tumorigenic potential of magnetic fields. The most promising model at the present time is planaria (flatworms). The response of this model to chemical promoters or co-promoters

similar to the mouse response but the results can be obtained in only a few weeks.

There have been concerns about possible health effects among industrial workers who are chronically exposed to transient electric and magnetic fields in the course of their jobs. Examples of industrial transient field sources are power company switching yards, spark plugs in motor vehicles, arc-welding devices, and radiofrequency heaters and dielectric sealers. In collaboration with the University of Ottawa and National Research Council, several broadband active and electro-optic sensors have been developed (Kopola et al., 1990; Stuchly et al., 1991; Thansandote et al., 1991). Measurements of transient fields have been carried out for a number of industrial and domestic electrical devices (Thansandote et al., 1993). The results show that these devices generate high-intensity transient magnetic fields and relatively low-intensity transient electric fields as compared to ambient fields. For most devices, the frequencies of the measured fields are below 1 kHz, with 60-Hz components predominating.

Recently, the general public has expressed concern about potential health effects of electromagnetic field exposure from high-voltage power lines and common devices such as hand-held cellular phones, police radars and video display terminals (VDTs). Short information sheets on cellular phones and VDTs were prepared and distributed by the Bureau of Radiation and Medical Devices in response to these concerns. Information materials on the other two issues are under preparation. Evaluation of radiofrequency fields from portable cellular phones is underway in order to assess the safe use of the device and to determine whether the device interferes with the performance of critical medical devices in a hospital environment.

III. LASERS AND ELECTRO-OPTICS

The major present activities in the lasers and electro-optics program include the development of laser regulations and laser light show safety guidelines as well as the provision of information and education on the health effects of and the protection from natural ultraviolet exposure.

There are many applications of lasers in the medical, industrial and research fields. The proposed laser regulations establish standards of design, construction and function, as well as labelling requirements, for all laser equipment. The proposal is intended to reduce health hazards such as skin burns, retinal burns, visual receptor damage and corneal burns associated with many types of laser equipment. The industry has assisted in the development of this proposal.

Laser light shows are the application where the number of individuals from the public to be exposed at once is likely to be the largest. For this reason laser light show safety guidelines will soon be published to help companies set and provide laser light shows in a safe manner.

Because of continuous reported stratospheric ozone depletion and the particular geographical position of Canada near the north pole, the media and the Canadian public at large have been extensively enquiring about the dangers of natural UV. In accordance with the program's mandate, it was proposed very early in the ozone crisis that the ozone problems be kept separate from over-exposure to ultraviolet radiation. Special resources were allotted to the program to cover the public demand. In partnership with private publishing industry and the Canadian Dermatology Association, the program has produced a booklet entitled "The Sun, Your Baby and You." One million four hundred thousand copies have been distributed

to health professionals, hospitals, public health units, prenatal classes, educational conferences, and the public. A supplementary poster was also distributed. It has also produced and distributed two Health Protection Branch Issues publications entitled: (1) Thinning of the Ozone Layer - The Health Effects, and (2) Preventing Skin Cancer - It's Up To You. These publications discuss increased exposure to UV radiation caused by ozone depletion, and ways in which people can reduce exposure. The goal of the electro-optics program is to reduce short-term and long-term UV effects in the Canadian population by modifying mainly the attitudes of people toward sunbathing and sun over-exposure, whether or not ozone depletion is significant. This would help reduce the extra burden on our health care systems as well as reduce the present mortality due to skin cancer. Health and Welfare Canada, in partnership with Environment Canada, the Canadian Cancer Society, the Canadian Dermatology Association and the Canadian Ophthalmology Society, is ensuring that the public receives credible, consistent and positive messages about preventing UV-related diseases. In the available documents, advice to the public is provided along the following lines:

- Prudent avoidance is the appropriate response. Unprotected skin exposure to strong sunlight should be discouraged.

- The use of adequate clothing is recommended along with natural or artificial shade on bright sunny days.

- The use of a sun block having a Sun Protection Factor (SPF) value of 15 or higher is recommended on skin exposed to bright sunlight for extended periods of time. Eyes also need to be protected.

- The above advice also applies to children.

- It is noted that some exposure to UV-B radiation is necessary to facilitate the Vitamin D_3 metabolism.

- Suntanning should be avoided especially between 10 A.M. and 4 P.M. during the summer months.

Another target of the program is to increase our knowledge of UV effects on living cells. The Health Protection Branch has sponsored a Symposium on Ultraviolet Radiation-Related Diseases held in Ottawa on March 24-26,1992, bringing together Canadian and world experts in fields such as ophthalmology and dermatology. As a result, various research projects have been set in motion to further investigate the health effects of UV exposure and to measure UV levels more precisely and on a broader scale. The long term goals of research within the Lasers and Electro-Optics program is to develop standard methods for the testing of the efficiency of sunscreens and other means of personal protection, and to develop methods to identify individuals and groups requiring specific considerations in UV protection.

Health and Welfare is also regulating sun screens, and the Lasers and Electro-Optics program is looking into the possibilities of regulating sunglasses, with the cooperation of other organizations, to provide adequate labelling information on the UV filtration characteristics of sunglasses.

There are also regulations under RED Act to establish standards of design, construction and functioning, as well as labelling requirements, for sunlamps and mercury vapour lamps. The purpose of these regulations is to reduce health hazards such as skin burns and corneal burns associated with ultraviolet radiation over-exposure.

IV. ACOUSTICS

In the area of acoustics, major activities have been in the fields of noise and medical ultrasound. In the area of medical ultrasound, a compliance program has been developed and successfully implemented for the ultrasound physical therapy devices standard (Environmental Health Directorate, 1989). Another major activity has been the assessment of the risk of ultrasound exposure during fetal Doppler ultrasound blood flow examinations. Given the current voluntary limits on output from diagnostic ultrasound devices, it appears that the risk to the fetus is negligible, except for a small number of devices in rare circumstances where the following conditions would have to occur simultaneously: fetal bone is exposed, the attenuation of the ultrasonic exposure by maternal tissues is well below average, and the distance from the maternal abdomen to the fetus exceeds about 8 cm (Bly et al., 1992). The major undertaking at present is the development of a noise control program. Its major outcomes will be the completion of guidelines for the assessment and control of the health effects of aircraft noise and machinery noise. In addition, in collaboration with the Canadian Standards Association, American National Standards Institute, and the International Standards Organization, voluntary national standards will be developed for the disclosure of the sound output power from noisy machinery. These voluntary standards can serve as the basis for regulatory standards, if necessary. An international standard for the measurement of sound power using the scanning intensity technique is now being developed in collaboration with the Institute for Machinery Research at the National Research Council of Canada.

Over the past two years a major review has been undertaken of the health effects of aircraft noise (Bly, Goddard and McLean, 1993). A presentation on the health effects of aircraft noise was given at the public hearings of the Environmental Assessment and Review Panel on the runway expansion at Toronto's Lester B. Pearson International Airport (Health and Welfare Canada, 1992). A pamphlet was also published to provide information to the public on the health effects of aircraft noise on residents living in the vicinity of airports (Health Protection Branch, 1993). Research is now being undertaken into the possibility of aircraft noise being a risk factor for stress related diseases such as hypertension.

The scientific research support for these standards and guidelines will be done in a dedicated anechoic chamber. It will provide an environment in which surveys and uncertainty assessments can be performed for the measurement of sound power on noisy machinery. It will also provide a laboratory for exposure to simulated aircraft noise. This chamber is one of the largest in the world with wall wedges large enough to provide free field conditions down to 50 Hz. The chamber's isolation is sufficient to obtain a background of -5 to -10 dB re 20 μPa from 500 Hz to 8 kHz. Finally, the size of the chamber, 12.7 x 8.7 x 7.6 m between wedge tips on opposite walls, provides for measurements requiring considerable space. Characterization of the chamber is now in progress (Bly, Lightstone, Hewlings and Lourador, 1993) and upon its completion, the chamber will be available for acoustics research not feasible elsewhere in Canada.

V. CONCLUDING REMARKS

Canadians, as well as populations in many other countries, live in an environment of NIR varying from natural UV radiation to microwaves used in communications, electric and magnetic fields produced by power lines, as well as aircraft and machinery noise. The increased use of devices which emit NIR not only leads to occupational exposure but also to exposure of the general public. The levels of these exposures may be several orders of magnitude above the natural background. In view of this fact, there exists a necessity of risk assessment and exposure controls.

Health and Welfare Canada has developed a health protection program on NIR which covers a wide range of activities in three main areas: electromagnetics, lasers and electro-optics, and acoustics. Regulations for devices such as microwave ovens, laser scanners, sunlamps, mercury lamps, and ultrasound therapy devices are now in force. Safety codes for radiofrequency exposure, ultrasound devices, magnetic resonance clinical systems and other devices have been published and distributed. In the area of electromagnetics, the assessment of risks of electric and magnetic fields at extremely low frequencies (1-300 Hz) is a major activity. The work includes in-house animal tumor co-promotion studies to determine the potential health risks from 60-Hz magnetic field exposure. The major activities in lasers and electro-optics include the development of laser light show safety assessment procedures and laser regulations, as well as the provision of information and education on the health effects of and the protection from ultraviolet exposure. In the area of acoustics, guidelines for assessment and control of the health effects of aircraft noise and machinery noise are being developed.

At present, health protection programs on NIR may not be available in many of the developing countries where NIRs are not considered as a major public concern. However, for countries with rapid industrial development, there may be a need for these programs in the near future.

REFERENCES

1. Bly, S., Goddard, M., and Mclean, J., A Review of the Effects of Noise on the Immune System. Proceedings of the 6th International Congress on Noise as a Public Health Problem, Nice, France, July 6-9, 1993.

2. Bly, S.H.P., Lightstone, A.D., Hewlings, T.G. and Lourador, J-L., Performance of a Large New Anechoic Chamber at the Canadian Bureau of Radiation and Medical Devices. The Journal of the Acoustical Society of America. 93: Pt. 2, p. 2344, 1993

3. Bly, S.H.P., Vlahovich, S., Mabee, P.R. and Hussey, R.G.(1992)Computed Estimates of Maximum Temperature Elevations in Fetal Tissues During Transabdominal Pulsed Doppler Examinations. Ultrasound in Medicine and Biology. 18: 389-397, 1992

4. Duchêne, A.S., Lakey, J.R.A., Repacholi, M.H., (eds), IRPA Guidelines on Protection Against Non-Ionizing Radiation (Pergamon Press, 1991)

5. Environmental Health Directorate, Safety Code 23 - Guidelines for the Safe Use of Ultrasound, Part 1, Medical and Paramedical Applications. Canadian Government Publishing Centre, Ottawa, Canada,1989

6. Health and Welfare Canada, The Effects of Aircraft Noise on the Health of Residents Living in the Neighbourhood of Lester B. Pearson International Airport (LBPIA). Public Hearings of the Environmental Assessment Panel on Air Traffic Management in Southern Ontario, January 14, 1992 - evening. Federal Environmental Assessment Review Office, Ottawa, Canada, 1992

7. Health Protection Branch, Issues, Aircraft Noise in the Vicinity of Airports - Implications for Human Health. Health and Welfare Canada, Publications, Ottawa, Canada, 1993

8. Kopola, H., Thansandote, A., Chrostowski, J., Stuchly, S.S., An Optical E-Field Sensor. Proceedings of the Conference on Precision Electromagnetic Measurements, Ottawa, Ontario, Canada, June 11-14, 1990, pp 196-197

9. McLean, J.R.N., Thansandote, A., Stuchly, M.A., Goddard, M., Burnett, Lecuyer, D.W., Mitchel, R.E.J., Repetition of a Study Using a 60-Hz Magnetic Field as a Tumor Co-Promotor in Mouse Skin. Program and Abstracts Book of the First World Congress for Electricity and Magnetism in Biology and Medicine, Lake Buena Vista, Florida, U.S.A., June 14-19, 1992, p. 107

10. Repacholi, M.H., Non-Ionizing Radiation, in M.W. Greene (ed), Non-Ionizing Radiation, Proceedings of the 2nd International Non-ionizing Radiation Workshop (University of British Columbia Press, 1992) pp 3-13

11. Stuchly, M.A., LePocher, H., Gibbons, D.T., Thansandote, A., Active Magnetic Field Sensor for Measurements of Transients. IEEE Transactions on Electromagnetic Compatibility. 33: 275-280, 1991

12. Thansandote, A., Stuchly, S.S., Stuchly, M.A., Barski, M., Broadband Active E-Field Sensors for Measurement of Transients. IEEE Transactions on Instrumentation and Measurements. 40:465-468, 1991

13. Thansandote, A., Lecuyer, D.W., Stuchly, M.A., Stuchly, S.S., Measurements of Transient Electric and Magnetic Fields from Industrial and Home Devices. In M. Blank (ed), Electricity and Magnetism in Biology and Medicine (San Francisco Press, 1993) pp 1-3

14. Thansandote, A., Health Protection from Exposure to Environmental Electromagnetic Fields. Proceedings of the Second International Conference on Advanced Science and Technology Transfer to Thailand, Bangkok, Thailand, August 21-23, 1992, pp 437-455

15. United Nations Environment Programme, Environmental Effects of Ozone Depletion: 1991 Update. Panel Report Pursuant to Article 6 of the Montreal Protocol on Substances that Deplete the Ozone Layer, Nairobi, Kenya, November, 1991.

MANUFACTURING OF BLAND SOYMILK

Kuklat Tanteeratarm, Alvin I. Nelson and Lun S. Wei[1]

Introduction

Soymilk is conventionally made in the Orient by soaking whole raw soybeans, grinding in water, filtering to remove okara (soy residue) and then heating the extract. Although this process is simple, the resulting beverage has a strong painty, beany off-flavor and odor. Thus, it is not suitable, in most areas outside the Orient, as a base for preparing dairy analogs such as beverage, yogurt, ice cream and coffee creamer. Numerous modifications of this traditional Oriental process have been reported to somewhat reduce the off-flavor and odor defects. Some of these modifications include: hot water extraction, acid grinding, alkali soaking, vacuum deodorization, fermentation and enzyme treatment. Certain modifications gave some flavor improvement but generally are only partially effective in reducing off-flavor.

A recent processing method for preparing high quality soymilk has been developed by food scientists and engineers at the University of Illinois. This is an improved process over the patented Illinois soymilk process. The present soymilk is very smooth and bland, and is suitable for preparing a number of dairy analogs. Moreover, powders from this soymilk and tofu impart no off-flavors in the secondary generation products. The basic steps for preparing the soymilk include cleaning and dehulling of soybeans, blanching of cotyledons, grinding, extracting of soymilk, pasteurizing, formulating, homogenizing, cooling, packaging and refrigeration. Existing soymilk equipment has generally proved to be suitable for this soymilk process. Manufacturing steps, processing conditions, and equipment for this process are discussed in this paper. Composition of soymilk can be altered during processing to develop a desired level of total solids, protein and oil contents. The soymilk process has been successfully adapted by a number of soymilk and dairy analog manufacturers in the US as well as worldwide.

Development of Illinois Soymilk Process

Illinois process is a premier method of preparing bland soymilk with no beany off-flavor from whole soybeans developed by food scientists, A.I. Nelson, M.P. Steinberg and L.S. Wei at the University of Illinois in the early 1970's. It was first patented in 1975 (Nelson et al.. 1975). Later, several variation in processing procedures have also been published and patented (Nelson et al., 1976 and 1977). The Illinois process has been widely applied in the current day soymilk industry. A summary of the Illinois process is shown in Table 1. The key for producing a bland soymilk with this process is to eliminate the lipoxygenase enzymes responsible for developing beany off-flavor in soymilk either by alkaline soak followed by alkaline blanch or alkaline blanch without soaking. With this process, no filtering or desludging is used; therefore, protein and solids recoveries are extremely high. However, the soy beverage prepared using the Illinois process is high in viscosity, was sometimes chalky and required two high pressure homogenization treatments.

---

[1] *Drs. Tanteeratarm, Nelson and Wei are with International Soybean Program (INTSOY) and Department of Food Science, University of Illinois, 110 Mumford Hall, W. Gregory Drive, Urbana, IL 61801, USA; Phone: 217-244-5417; Fax: 217-333-5838*

Table 1. Traditional, Illinois and INTSOY/Food Science Soymilk Process

	Traditional	Illinois	Illinois	INTSOY/Food Science
Method	Cold Water Grind	Blanch (Nelson et al., 1975)	Direct Blanch (Nelson et al., 1977)	Direct Blanch (Tanteeratarm et al., 1989)
Process	WSB | Soak | Cold Water Grind | Cook/Filter or Filter/Cook	WSB | Alkaline Soak | Alkaline Blanch | Cold Water Grind | Cook | Homogenize	DSB or WSB | Alkaline Blanch | Cold Water Grind | Cook | Homogenize	DSB or WSB | Alkaline Double Blanch | Hot Water Grind with Steam | Filter | Cook | Homogenize
Solids & Protein Recoveries	High	Very High	Very High	Medium to High
Beany Off-Flavor	Very Strong	None	None	None
Mouth-feel	Smooth	Often Chalky	Often Chalky	Smooth
Remaining Oligosaccharides	High	Reduced	Reduced	Low

INTSOY/Food Science: International Soybean Program and Department of Food Science, University of Illinois;
WSB = Whole soybeans; DSB = Dehulled soybeans

An improved soymilk process for home use was developed in the late 1970 at the University of Illinois (Kanthamani et al., 1978). With this method, raw whole soybeans are blanched for 10 min, ground into slurry and then filtered. The filtrate is simmered for 20 min and the flavoring ingredients are added. The resulting soymilk is very good in flavor and mouthfeel. Later, this home process has been further developed and scaled up to a commercial level which is called INTSOY/Food Science soymilk process (Tanteeratarm et al., 1992). The soymilk is bland and very smooth. It is excellent as a base for preparing soy beverage and dairy analogs.

INTSOY/FOOD SCIENCE Soymilk Process

Processing Operation

The basic steps for preparation of non-beany flavor, high quality soymilk involves cleaning and dehulling of soybeans, blanching cotyledons in a low percentage of sodium bicarbonate (baking soda), grinding, extracting of soymilk, cooking and formulating, homogenizing, cooling, packaging and refrigeration. A flow diagram which shows the step by step process and the flow chart which illustrates the equipment used in this process are shown in Figures 1 and 2.

1. Selection of soybean varieties

Damaged seeds results in lipid oxidation which produces off-flavor in the end products. Thus, only sound soybean seeds should be used for producing high quality soymilk. However, some characteristics of soybeans are preferred over others. Some preferred factors are a). high protein, b). large seed size, c). light color hilum and seed coat, d). high protein dispersibility

index, and e). low flatulence factor (raffinose and stachyose). Using the quality soybeans and methods described in Figures 1 and 2, the final soymilk tends to have higher protein and solids recoveries with a whiter color and a lower flatulence problem.

Figure 1. Flow diagram for soymilk preparation

2. Cleaning of soybeans

Cleaning is one of the most important step in preparing soymilk of excellent sensory properties. Soybeans often contains foreign materials such as stones, straw, grass seeds, dirt, dust and metals such as small nuts or bolts. Thus, removing these unwanted materials is necessary in terms of eliminating foreign flavor and color or seriously damaging equipment. In addition, cleaning also reduces the microorganisms associated with the foreign materials.

3. Dehulling of soybeans

Dehulling refers to removal of the outer seed coat or hull. Soybean seeds contain about 9 % seed coat on dry basis. The seed coat is mainly composed of cellulosic type materials, but it also contains about 9 % protein. The soymilk prepared from whole soybeans is very viscous due to the fibrous materials in the hull. Seed coats also contain unwanted compounds including subtle bitter components which impart off-flavors to the soymilk.

Seed coat and hilum vary greatly in color and these, especially the hilum, also affect the color of the soymilk. Soymilk as well as okara prepared from the dehulled soybeans is whiter in color. Dehulled soybeans used for preparing soymilk can be selected from larger soybean varieties which are available in the market. Dehulling also aids the cleaning step in reducing the foreign material and the numbers of microorganisms. Thus, elimination of the soybean hull improves soymilk quality by improving flavor, color and shelf-life of the product. Dehulling shortens the blanching time which tends to reduce the denaturation of the protein and improve soymilk quality. Dehulling reduces the volume of okara considerably.

The soybean dehulling process includes three steps. First, the soybeans are heated in a through-flow air drier (at 200°F for 15 min) to a moisture content of 12-14 %. The function of this treatment is to break the bonds which loosens the hulls from the cotyledons. After the heated beans are passed through a roller and stationary concave plate, the hulls which are very brittle are broken while the cotyledons, which are resilient, are still intact. The hulls are finally separated from the cotyledons by air aspiration. Dehulling efficiencies of this operation will yield up to 88 % cotyledons. However, soybeans can be dehulled by other means such as using abrasive type dehullers similar to those for rice and sorghum with some modifications.

Although dehulling is one of the significant steps in developing quality soymilk, it may be omitted if high quality soybeans are available. In this case, soybeans of light seed coat and hilum color should be used.

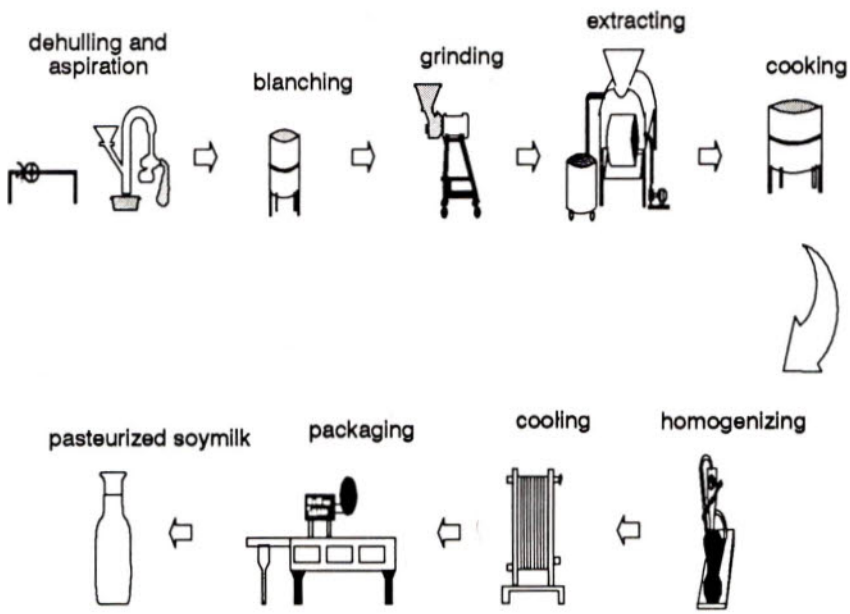

Figure 2. Flow chart of soymilk operation at the University of Illinois, Urbana

4. Blanching of cotyledons

Substantial amounts of soymilk available on the world market today are often inferior in quality. Poor sensory quality, such as beany and grassy odors and taste are often associated with the product. Traditionally, soymilk is prepared by soaking the raw soybeans overnight in cold water followed by grinding and filtering. The resulting soymilk has a strong painty, beany off-flavor and odor due to the reactions of enzymes, lipids, oxygen and water. Thus, it is not suitable as a base for preparing high quality soymilk and dairy analogs such as yogurt, ice cream and coffee creamer. Inactivation of the enzymes at the beginning prevent the formation of the off-flavors.

Blanching has two important functions, i.e. hydration of cotyledons (or whole soybeans) and inactivation of enzymes. Lipoxygenase enzymes are responsible for beany off-flavor in soymilk. Beany off-flavor develops when the beans are damaged, and the lipoxygenase is available for oxidizing the lipids in the presence of water and air (oxygen). Besides lipoxygenases, other enzymes and components may be responsible for developing anti-nutritional factors that can be inactivated by blanching. Trypsin inhibitors which reduce protein nutrition are adequately decreased by blanching and cooking of the soymilk.

To prevent the beany off-flavor from developing, lipoxygenase must be inactivated. It can be accomplished by heat treatment such as water blanching the soybean cotyledons in a steam jacketed kettle. The blanching of soybean consists of two steps. First, the cotyledons are placed directly into boiling water (five times the weight of the dry cotyledons) containing 0.25 % baking soda and blanched for 5 min. After draining and rinsing with very hot water (>200°F), the cotyledons are reblanched in boiling water (five times the weight of the dry cotyledons) containing 0.05 % baking soda for another 5 min. From the practical standpoint, one-ten minute blanching can also be used. It is important to note here that the size of soybeans or cotyledons from different varieties is often varied. Thus, the blanching time may need to be adjusted for this factor.

Besides inactivating enzymes, blanching aids in further cleaning the cotyledons, and reducing number of microorganisms and water soluble oligosaccharides such as raffinose and stachyose which cause flatulence. Baking soda serves several functions during the blanching process. It tenderizes the cotyledons to allow shorter blanching time and aids in a reduction of trypsin inhibitor activity. Baking soda also increases protein recovery due to increasing pH of soy slurry before extracting. Soymilk obtained from this process has a pH of 7.1; therefore, the protein in the soymilk is highly soluble and the overall flavor is definitely improved. Although baking soda slightly darkens the blanched cotyledons, most of this color is removed during the blanching step which includes draining and rinsing. Thus, the baking soda has no significant effect on the color of soymilk but does improve the flavor of the soymilk.

5. Grinding of blanched cotyledons

Grinding results in breaking down the cellular structure of the soybean cotyledons and releases cellular components. In this process, blanched cotyledons are ground twice with a predetermined amount of very hot water into a soy slurry using a Bean Machine disintegrator equipped with 0.02 inch opening screen. Steam is injected into the disintegrator during the grinding process which limits the availability of oxygen and thus reduces oxidized flavor in the

milk. The amount of hot water used in the grinding steps range from 5 to 10 times of the dry cotyledon weight, and this concentration affects the richness and total solids and protein recoveries. Reducing water addition increases the richness of the soymilk which yields higher solids and protein in the product.

Several types of disintegrators can be used for grinding soybeans into slurry. In some grinders, crushing parts are made of stone; therefore, they are an ideal place for microbial and fine stone particle contamination. These are serious problems and can be avoided when using stainless steel mills.

6. Extracting and filtering of soymilk

Soymilk can be extracted from the soy slurry by removing the insoluble materials which are known as soy residue or okara. This can be accomplished by passing the soy slurry through a roller soymilk extractor (Takai) and vibrating screen separator (Kason). The soymilk obtained from the roller extractor (80 mesh screen) still contains very fine insoluble materials or so-called sludge which may result in poor mouth-feel or chalkiness in soymilk and increase settling tendency in the product. These fine materials are essentially removed by the vibrating screen separator (150 mesh screen). The okara or sludge still contains protein which can be extracted by mixing in hot water and followed by a second extraction and filtration. The okara obtained from the second extraction is much drier than that from the first operation.

Soymilk may also be separated from okara using several different types of equipment. These include decanter, press filter, curd (cheese) remover and other similar type machines. Effectiveness of these units varies considerably. In general, okara with the moisture content of 80% or lower is considered desirable. Higher moisture content in okara is usually obtained from an improperly designed system.

7. Cooking of soymilk

After the extracting and filtering process, the soymilk is simmered at 190-200^{o}F in a steam jacketed kettle for 20 min. The purposes of the cooking are to further inactivate trypsin inhibitors as well as some proteolytic enzymes and to destroy microorganisms and improve flavor of soymilk. Using the treatment mentioned, the soymilk is considered as a pasteurized product. Soymilk can be formulated as needed during the cooking step. Other methods can also be used for extending the shelf-life of soymilk. Similar to cows' milk, soymilk can be pasteurized using plate heat exchanger. With this system, soymilk may be first homogenized which is followed by heating and cooling in the plate heat exchanger. Methods of preservation and types of packaging are very important and will be discussed later.

8. Homogenizing of soymilk

Homogenization is a process which ruptures and dramatically reduces size of fat globules and remaining insoluble materials into very fine and uniform particles by forcing them under high pressure through very small openings. Without homogenization, the fat globules tend to form clumps and gradually rise to the top of the storage container while the remaining insoluble particles tend to settle to the bottom.

Homogenization gives soymilk a smoother, creamier and whiter appearance. In addition, it also improves uniformity of the product when formulating ingredients are added to soymilk. In this process, homogenization can be accomplished by passing the soymilk at cooking temperature through a two stage homogenizer (first stage, 3500 psi and second stage, 500 psi).

9. Cooling of soymilk

Since soymilk is an ideal medium for microbial growth, it must be adequately heated. In this process, the soymilk is heated at 190-200°F in a steam jacketed kettle for a period of 20 minutes and cooled from 200°F to 35°F within 15 seconds through a series of cooler plates using chilled water (35°F) as the cooling medium. With this practice, the shelf-life of the product is about 7-10 days at 35°F refrigeration temperature. This shelf-life is very comparable to pasteurized cows' milk under similar conditions.

Table 2. Heat treatment, equipment, packaging materials and shelf-life for fluid soymilk

Treatment	Equipment	Packaging Materials	Shelf-life
Vat Pasteurization (145°F, 30 min.)	Steam jacketed kettle	Plastic bag (Pouch) Glass or Plastic bottle	7-10 days (refri. temp., 35°F)
HTST Pasteurization (161°F, 15 sec.)	Heat Exchanger	Carton (Pure-Pak) Plastic bag (Pouch) Glass or Plastic bottle	7-10 days (refri. temp., 35° F)
Ultra-high Temperature (280°F, 2 sec.)	UHT/Aseptic packaging system	Carton (Tetra Bricks, Combiblok) Plastic bag (Pouch) Plastic bottle	Up to 6 mths. (room temp.)
Sterilization	Retort or Autoclave	Can Bottle	Up to 2 years (room temp.)
Spray Drying	Spray drier	Plastic bag (Pouch) Plastic bottle	Up to 1 year (room temp.)

10. Packaging of soymilk

After cooling, soymilk is filled in pre-sanitized bottles or containers and refrigerated immediately to control microbial growth. In fact, the types of packaging materials depend very much on the methods of heat treatments such as pasteurization, ultrapasteurization or ultra high temperature (UHT) and sterilization. Overall quality and shelf-life of the product also depend on the heat treatment and type of packaging materials used. Table 2 illustrates the heat treatments, equipment, packaging materials and shelf-life of the finished fluid soymilk products.

Composition and recovery of soymilk and okara

As mentioned earlier, the ratio of cotyledon to water used in the soymilk process can be varied, and this affects the quality and composition of soymilk. The percentages of total solids, protein, oil, carbohydrate and ash contents (WB) present in soymilk prepared from the cotyledon:water ratio ranging from 1:5 to 1:10 are summarized in Table 3. In this case, the Sherman variety of soybeans were processed. In general, the soymilk constituents increase with decreasing the cotyledon to water ratio from 1:10 to 1:5. Thus, richer soymilk can be prepared by lowering the soybean to water ratio. Okara obtained at lower ratio contains higher protein and fat. The chemical composition of soymilk varies and depends upon the type of equipment and processing conditions. For example, soymilk constituents are greatly affected by the size of screen mesh used in the filtration step. Varieties and the quality of soybeans also affects the soymilk composition.

Table 3. Composition of soymilk at various ratios of dry cotyledon to water (No. 150 screen mesh equipped with vibrating shaker)

Dehulled Soybean: Water	Total Solids (%)	Protein (%, WB)	Oil (%, WB)	Carbohydrate (%, WB)	Ash (%, WB)
1:5	9.2	4.5	2.4	1.8	0.48
1:6	8.7	4.2	2.2	1.9	0.44
1:7	7.9	3.8	1.9	1.8	0.39
1:8	7.2	3.4	1.7	1.7	0.35
1:9	6.3	2.9	1.5	1.6	0.30
1:10	5.6	2.6	1.4	1.3	0.27

Rate of soymilk production is very much dependent upon the equipment type and the amount of soybeans and water used. The production rate can be significantly increased by simply using more water. If too much water is used in preparing soymilk, protein content and other constituents in the soymilk may be unacceptably low. Thus, the production rate of a given soymilk system should be reported as a production rate of soymilk of specified protein or solid content e.g. 1000 liters of soymilk at 3 % protein.

A summary on the production of soymilk and okara from soybeans is shown in Table 4. As mentioned, the INTSOY/Food Science processing operation may be scaled down or up to several production levels. With the example shown in Table 4, soymilk of 500 liters at various protein contents may be produced from 144, 95 and 65 kg dehulled soybeans using a dehulled soybeans (DSB) to water ratio of 1:6, 1:8 and 1:10, respectively. Soymilk production can be doubled by increasing the DSB:water ratios from 1:6 to 1:10. It is significant to note that soymilk at higher DSB:water ratio is lower in protein and other important soybean constituents. The amount of the hydrated okara is generally more than that of original whole soybeans used in the process, and it increases with decreasing DSB:water ratio.

Table 4. A production of soymilk and okara from whole soybeans or dehulled soybeans

Soymilk (liter)	DSB:Water ratio	DSB (WSB) (kg)	Okara (kg)	Okara:WSB ratio	Soymilk:okara (liter/kg)	Soymilk recovery (%, compared to WSB)	Protein in soymilk (%, WB)
500	1:6	144 (166)	274	1.7:1	1.8:1	301	4.2
	1:8	95 (109)	152	1.4:1	3.3:1	459	3.4
	1:10	65 (76)	98	1.3:1	5.1:1	667	2.6

WSB = Whole soybeans, DSB = Dehulled soybeans
Dehulling efficiency = 85 %

Formulation of soymilk

Most soymilks in the market are formulated soymilks. Examples of formulated soymilks that can be prepared from this soymilk are listed in Table 5. Consumers in Europe, North America and many regions of the world who are used to regular cows's milk tend to compare soymilk with dairy milk. Thus, the soymilk in these regions is formulated to have flavor which resembles cows' milk. However, consumers in East Asia consider soymilk as a healthy beverage. Formulated soymilk in the Far East is somewhat sweeter and that in Southeast Asia which is very sweet. Up to 9% sugar is used in soymilk in Southeast Asia. Thus, the information in Table 5 should be considered as a guideline for further development of formulated soymilks suitable or acceptable for a specific target market.

Table 5. Soymilk formulation

Type of Soymilks	Added Ingredients (% of ingredients based on the weight of soymilk)
Plain Soymilk	3% cane sugar, 3% CSS (10 DE), and 0.2% salt
Cream Flavored Soymilk	3% cane sugar, 3% CSS (10 DE), 0.2% salt, and 0.01% cream flavor
Vanilla Flavored Soymilk	3% cane sugar, 3% CSS (10 DE), 0.2% salt, 0.05% vanilla extract, and 0.01% cream flavor
Chocolate Flavored Soymilk	6% cane sugar, 1.5% CSS (10 DE), 0.65% cocoa powder, 0.2% salt, 0.03% vanilla extract, and 0.01% cream flavor

(CSS = corn syrup solids, DE = Dextrose equivalent)

In most cases, sugars are used as ingredients in soymilk. Corn syrup solids (CSS) can also be used as an ingredient to increase solid content and improve smoothness of finished products. The CSS of 10 dextrose equivalent (DE) or higher is found to be suitable. Cane sugar or sucrose is used as a sweetener. Several manufacturers in the US also use high fructose syrup or brown rice syrup or honey for improving solids and contributing sweetness and flavors. A small amount of added salt tends to improve flavor.

Plain soymilk contains about 15 % as much calcium as cows' milk (15 and 100 mg Ca/per 100 ml soymilk and cows' milk, respectively). Calcium in the forms of tricalcium phosphate, calcium lactate, calcium citrate or calcium carbonate can be added to soymilk to the

level found in cows' milk. Besides minerals, highly nutritious soymilk can be fortified with vitamins (A, D, B_2 and/or B_{12}) and essential amino acid (methionine).

Normally, soymilk in North America and Europe contains no added oil. Light soymilk which is low in fat is also marketed along with regular soymilk. Most manufacturers produce the low fat soymilk by simply adding more water to the product. By doing this, protein from soybean in the soymilk is also significantly diluted. Low fat soymilk, high in protein can be prepared using the INTSOY/Food Science soymilk process. The fat in soymilk from this process separates easily on the top after extracting. The unwanted fat can be significantly reduced from soymilk before homogenization by centrifugal force without lowering the original protein. Commonly, soymilk in Japan and Korea contains added oil (1.5-3.0 %). Added oil contributes to smoothness, creaminess, whiteness, flavors as well as calories in soymilk. Refined oil in the forms of corn, soybean, canola, sunflower or rapeseed oils are reported to be used. Stabilizers and emulsifiers are also added to some of the formulated soymilk to improve physical and sensory properties.

Since the soymilk prepared from the INTSOY/Food Science process is bland, it is also an ideal base for preparing high quality dairy analogs such as soy ice cream, yogurt and coffee creamer. These soybased products have been successfully developed at the university of Illinois.

Processing Equipment

The soymilk process can be designed to be either a semi-continuous or fully continuous system in which equipment from several companies may be used in this process. The capacity of each unit has to be carefully selected and matched to the rest of the system. It can also be done by adding certain necessary equipment to an existing plant and applying the soymilk procedure as discussed in this manuscript. This soymilk process has been adopted by a number of soymilk and dairy analog manufacturers at various scales in the US as well as worldwide. Some manufacturers and/or agencies for the soymilk equipment used at the University of Illinois are listed as follows:

Aspirator for hull removal and Dehuller: Custom designed by Nelson et al. (1980), the University of Illinois, Urbana, IL, USA.
Disintegrator: Bean Machines Inc., San Francisco, California, USA.
Forced-air heater: Proctor & Schwartz, Inc., Philadelphia, PA, USA.
Homogenizer: APV Gaulin, Inc., Wilmington, Massachusetts, USA.
Ice builder: Girton Manufacturing Co., Inc., Millville, PA, USA.
Plate heat exchanger: Groen, A Dover Industries Co., Elk Grove Village, IL, USA.
Refrigerator: Bally Engineered Structures, Inc., Bally, PA, USA.
Roller extractor: Takai Tofu & Soymilk Equipment Co., Nonoichi-machi, Ishikawa-ken, Japan.
Seed cleaner: Seedburo Equipment Co., Chicago, IL, USA.
Steam generator: Clayton Industries, El Monte, CA, USA.
Steam jacketed kettle: Groen, A Dover Industries Co., Elk Grove Village, IL, USA.
Storage tanks: APV Crepaco Inc., Chicago, IL, USA.
Vibrating screen separator: Kason Corp., Paramus, NJ, USA.

References

Nelson, A.I., M.P. Steinberg and L.S. Wei. 1975. Soybean Beverage Base. U.S. Patent 3,901,978.

Nelson, A.I., M.P. Steinberg and L.S. Wei. 1976. Illinois process for preparation of soymilk. J. Food Sci. 41:57.

Nelson, A.I., M.P. Steinberg and L.S. Wei. 1978. Soymilk Beverage and Process. U.S. Patent 4,041,187.

Nelson, A.I., B.J. Shyeh and E.D. Rodda. 1980. Evaluation of new soybean dehuller. Amer. Soc. Agri. Eng. 23(2):523-528.

Nelson, A.I. 1989-1992. Hull separator. In. "Soybean Processing for Food Uses". Tanteeratarm, K. (Eds). International Soybean Program (INTSOY), University of Illinois, Urbana.

Kanthamani, S., A.I. Nelson and M.P. Steinberg. 1978. Home preparation of soymilk: A new concept. In "Whole Soybean Foods for Home and Village Use" ed. A.I. Nelson et al. International Agricultural Publications, INTSOY Series No. 14. University of Illinois.

Tanteeratarm, K., A.I. Nelson and L.S. Wei. 1989-1992. INTSOY/FOOD SCIENCE soymilk process. In. "Soybean Processing for Food Uses". Tanteeratarm, K. (Eds). International Soybean Program (INTSOY), University of Illinois, Urbana.

Intravital Observations of the Dynamic Distribution of Blood-Borne Substances: A Study of Hepatic Microcirculatory Events with A Combined Technology of In Vivo Microscopy, Fluorescent Dye Infusion, and Video Microdensitometric Image Analysis

WICHAI EKATAKSIN[1], NISHIDA JIRO[1], AND ROBERT S. MCCUSKEY[1,2]
Departments of Anatomy[1] and Physiology[2], College of Medicine
University of Arizona Health Sciences Center, Tucson, AZ, USA

ABSTRACT

Taking advantages of the optical and electronic microscopy, combined with computerized densitometry, we examined in vivo the livers of three mammalian species with fluorescent tracers. As a result, the dynamic formation of the hepatic microcirculatory subunits (HMSs) were clearly demonstrated. A new look into the elementary unity of the liver is discussed.

INTRODUCTION

Literature reveals that microscopic examination of living tissues dates back 327 years, having been pioneered by Marcello Malpighi in 1666, followed by a number of great investigators like William Harvey (1651) and Johannes Müller (1844). However, it was not until the first few decades of the present century that the technique of observing intravitally live organs became established (Basler,1917; Löffler and Nordman,1925; Krogh,1929; Knisely,1936; among others). Improvements achieved during the past several decades in optical microscopic methods have resulted in a better understanding of their morphology as related to function in health and disease (for recent reviews, see McCuskey,1986; McCuskey,1993). Although the development and versatile use of fluorescent tracers (see review in Poenie and Chen,1993), and the advents of electronic light microscopy and digital image processing (see reviews in Shotton,1993a,b) have added significant impetus to the rigorous growth in this multidisciplinary technology. However, most research interests have been shifted towards the study of living cells *in vitro*, leaving the *in situ* topographic relationships inadequately explored. We, from the anatomist viewpoint, took advantages of the cutting-edge techniques, using the *in vivo* microscopic methods (McCuskey,1986) to observe the dynamic circulation of livers perfused with fluorescent molecules. By implementation of video microdensitometry we could demonstrate the liver lobules as being composed of numerous elementary units referred to as the hepatic microcirculatory subunits, HMSs (Ekataksin et al.,1992,1993).

MATERIALS AND METHODS

By the *in vivo* microscopic method (McCuskey,1986), the surgically exposed livers of anesthesized animals, including 3 mice, 3 rats, and 3 hamsters, were examined for intralobular distribution of fluorescein-labeled substances imported in bolus through mesenteric venous infusion. Real-time changes of fluorescence intensity were observed live under the oculars and through digital image processing were simultaneously visualized on the video monitors. The video cassette recordings were analyzed and processed in microdensitometric pseudocolors by BioQuant System IV.

Infusion Preparation

Among the many fluorescent substances available we used dextrans, labeled with fluorescein isothiocyanate (FITC-dextrans, MW 9,000 and 40,500; Sigma Chemical Co., St.Louis, MO). FITC-dextrans are considered inert fluid-phase markers of endocytosis (Lake et al.,1985), rendering the solutes useful for quantitatively evaluating transport at the anatomical sites where blood-hepatocyte exchange occurs. A 10% solution (Stock et al.,1989) was prepared freshly before use in endotoxin-free physiologic saline. Alternately, sodium fluorescein (MW 371) prepared 1:1000 in saline was also used. We have evaluated in preliminary study and found that under our experimental conditions both fluorescent molecules yielded qualitatively similar results. Typically a bolus of 0.1~0.3 ml was injected; increasing amounts were required on repeated infusions.

Surgical Procedure

To obtain adequate duration of anesthesia and optimal control over respiratory movement for animals to be observed under the in vivo microscopy, 20% urethane (0.5 ml/100 g bw; for mice) and sodium pentobarbital (7 mg/100 g bw; for rats and hamsters) was injected intraperitoneally. Through abdominal incision the mesenteric vein was cannulated by a polyethylene tubing (Intramedic PE-10, ID 0.28mm, OD 0.61mm, Becton Dickinson & Co.) with a 27g needle. Having the xyphoid process excised and falciform ligament released, the concave (visceral) surface of the left lobe was reflected and laid on the mica window of the purpose-built tray, the animal being positioned on its left side. A small piece of Saran film was placed to cover the exposed lobe to help secure the liver and prevent it from drying.

In Vivo Microscopy

Details of in vivo microscopic equipment are described elsewhere (McCuskey,1986). For descriptive purposes, the construction is outlined here briefly. A compound trinocular microscope (Leitz Wetzlar) equipped with transillumination and epiillumination was modified to hold the specially designed animal tray. The tray had provision for drainage of irrigating fluid (Ringer's solution). By constant suffusion of the fluid, which was maintained thermostatically at rectal temperature ($\pm$ 0.3°c), this ensured homeostasis over the exteriorized organ. When mounted on the stage, the tray overlay a long working distance condenser, having the mica window aligned with the light path (Fig.1).

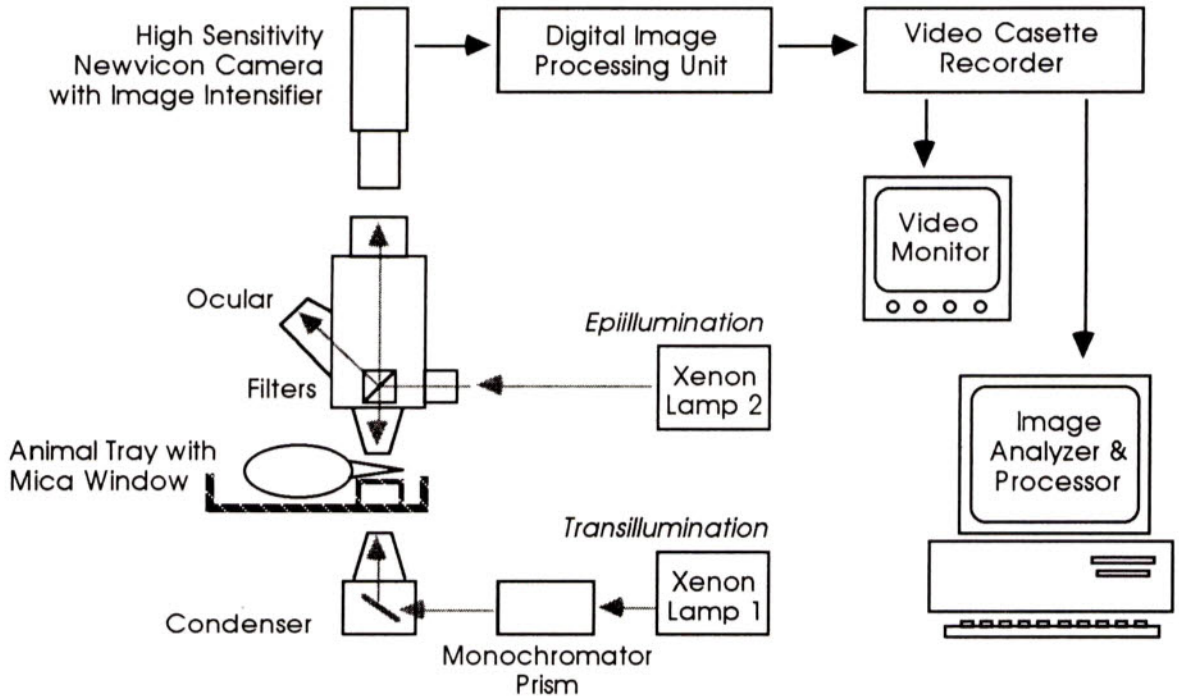

Fig.1. Diagram of optical and electronic equipment.

Transillumination light was obtained from a xenon lamp with a monochromator prism allowing a selectible spectrum of light at wavelengths between 400~800 nm. For studying highly vascularized organs, such as liver and spleen, wavelengths between 575~750 nm are appropriate to avoid light absorbtion by hemoglobin, resulting in sufficient light transmitting through the organs, and hence the enhanced definition of different tissue components. Epiillumination was supplied by another xenon lamp, coupled with specific excitation and barrier filters. In the present investigation, because observations were mostly done with the epiillumination, the excitaion filter with peak at wavelenth 490 nm and a barrier filter at 530 nm were used for visualizing both FITC and sodium fluorescein. The transillumination was useful to first scan and localize the area to be studied.

The optical image was studied directly and televised and video recorded through a projection ocular by a high-sensitivity, image-intensified Newvicon camera (KS 1381; Videoscope International Ltd., Washington DC, VA) which had the relative sensitivity spetrum peaked at 500 nm. Without this adjustible highly sensitive camera, the dye infusion study would have been difficult, since the increased background

fluorescent intensity would interfere with the observation field. By lowering the camera sensitivity, one animal sample could be studied for several boli with reproducible results. As camera sensitivity was reduced, definition of the television images became degraded. This was readily corrected by the digital image processing unit (Model 794 Image Σ; Hughes Aircraft Co., Carlsbad, CA) which averaged a selected number of frames and optimized the contrast and brigntness in various modalities.

Observation

Since the dynamic circulation that prevailed the microscopic fields was full of very rapidly changing events, we paid, in actual practice, more attention to video imaging and recording than to direct viewing through the oculars (10X). Specimens were examined (objective 4X) with focus on the periportal region, the pericentral region, and the midseptal region, either with the principal vessel appearing in cross or lengthwise profiles. Each field was studied with at least three repeated dye infusions. Date and time were digitally generated.

Image Analyzing and Processing

Quantification measurements, concerning such as extraction, uptake, diffusion, transport, retention, and excretion of the fluorescent compounds have been variously reported (e.g., Gumucio et al.,1981; Sherman and Fisher,1986; Stock et al.,1989; Schmidt and Busher,1991). With this in mind it is our main interest to compensate the qualitative observations that so far have been overlooked. Based on the previous study that fluorescent light intensities are proportional to the solute concentration (Stock et al.,1989), we analyzed our observations from the recordings, processed the images by videomicrodensitometry using BioQuant System IV, and played back the digitized results in pseudocolors as compared with the pre-processed original tape. Densitometric criteria were set up for each recorded scene individually. This was accomplished by selecting, frame by frame, the moment which the fluorescent inflow showed highest intensity at the periportal region while the spreading front was just filling the pericentral region. The range of gray levels, i.e. fluorescent intensities, at this very moment was divided digitally into three segments, each being imparted with red, yellow, and green, from high to low, respectively, and the background level imparted as blue, so as to visually create three comparable zones in the lobules. It should be noted that two categories of background levels were distinguished, the tissue areas and the blank areas; the tissue background would appear as blue, and the non-tissue (like the empty spaces in vessels and sinusoids) would appear as black.

RESULTS

Transillumination and epiillumination of the concave surface of the left lobe revealed some species differences. In rats, portal veins sent branches towards the hepatic capsule but usually terminated before being visible; most of the superficial vessels were central venules, either in longitudinal or in transverse profiles. Mice were similar to rats, but occasionally a superficial portal venule could be encountered at the liver edge in caudal half of the left lobe. In contrast, most of the superficial vessels in hamsters were portal venules; central venules were less numerous. Despite the different superficial dominancy, the observed findings from fluorescent infusions were alike in all three species. The sinusoidal beds, although, were highly interconnected in three dimensions, they showed strong tendency to be discerned as smaller divisions, referred to as *hepatic microcirculatory subunits*, HMSs (Fig.2). Appearance of HMSs was easily recognized in pseudocolor motion video which showed array of long slender wedge-shaped areas with three colors. Each formed a pyramidal sector with a base on the lobule's perimeter and a pointed end converging on the central venule. Two or three HMSs when occurred close together would present a pie-shaped sector. If all HMSs were synchronized, the lobular field was fully brightened with fluorescence which in densitometric display produced beautiful concentric zones around the central venule. HMSs were observed as lobule-dependent, i.e., the flow direction of an HMS in one lobule would not curve back into another HMS of the adjacent lobule.

At the periportal region where circulation was very active, individual HMSs usually were not delineated. In stead, the corners of those adjoining lobules were observed with fluorescent dye spreading into the lobule as a concave front, reminiscent of the primary lobule (Matsumoto et al.,1979). The fluorescent intensities perfused the corner of the lobule as a wave which faded likewise as a concave contour away from the corner into the central venule. We have recorded the occasion which the inflow front appeared as a convex outline; in this lobule the central venule was found to be in longitudinal profile having a curvature in accord with the observed convex (Fig.3, lobule 3).

The midseptal region often was not readily perfused by the infusion, appearing as a cruciate watershed,

reminiscent of the *nodal point* of Mall (1906, his Figure 46). Sometimes, when the midseptal region was seen well perfused, the pattern resembled the 'liver acinus' (Rappaport et al.,1954).

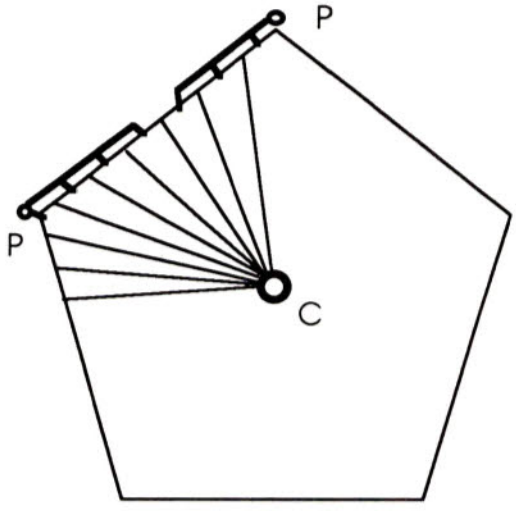

Fig.2. Division of a hepatic lobule into the microcirculatory sectors; each represents an HMS. P, portal venule in portal tract at the angle; C, central venule.

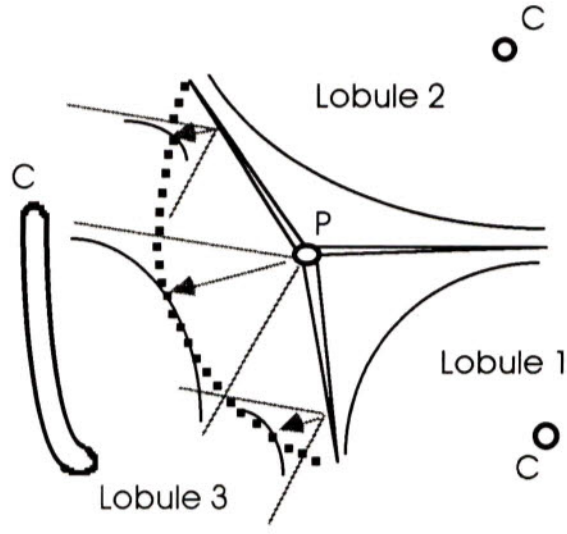

Fig.3. The heavy broken line in lobule 3 shows how this apparent convex curvature actually reflects the same concave contours as in lobule 1 and 2. Note that lobule 3 is viewed at a lateral profile with a longitudinal central venule.

DISCUSSION

By using in vivo microscopy to observe dynamic distribution of fluorescent substances, combined with videomicrodensitometric image analysis, we have demonstrated the subunits of the liver. The concept of HMS supports the concept that the hepatic lobules are the structural and functional units in the liver. It is also in agreement with the *primary lobule* concept proposed by Matsumoto and coworkers (1979), and the *compound hepatic lobule* concept by Ekataksin and Wake (1991). However, this contrasts strongly with the liver acinus concept (Rappaport et al.,1954). Acinar model defines zones on the assumption that the *whole length* of a side of the lobule is spanned by one portal venule (with an arteriole and a bile ductule), and it considers the periportal region partly as of the 'zone 3.' Our observations that the midseptal region contained a cruciate watershed suggests that a side of the lobule is supplied by two sources coming from opposite direction, and that the periportal region was dominated by concave (or convex) inflow front indicates that it is this very corner region which primarily admits the portal influx. It is understandable that a group of HMSs can mimic the appearance of an 'acinus' at any side of a lobule. The smooth merging of HMSs at the corner results in forming the primary lobule. The spreading wave of fluorescent intensities is comparable to the *equipotential continuous inflow front* of the primary lobule (compare our Fig.3 with Figure 12 of Matsumoto et al.,1979). That occasion which showed this wave as a convex outline actually represents a lateral view of the same structure, integrating the vertex of each concave contour.

The findings of the present study have shed new light to the centuries-long controversy against the hepatic lobules. There is little doubt that the combination of techniques used in the present investigation facilitated recognition of the HMS, although its hidden spatial third dimension remains to be resolved (in the following report of this issue). Many observers of intravital microscopy studied the liver with fluorescent technique but without videomicrodensitometric pseudocolor processing (Gumucio et al.,1981; Sherman and Fisher,1986; Stock et al.,1989; Schmidt and Busher,1991), did not recognized the liver lobules as being perfused in smaller subdivisions that are demonstrable. It is implied that elementary division of other organs may be similarly defined in terms of microciculatory zonation. The possibilities of obtaining new information using these tools are exciting and challenging.

ACKNOWLEDGEMENT

The present study is supported in part by grants from NIH (AA-08037 and HD-26013).

LITERATURE CITED

Adelmann, H.B., ed. 1966 Marcello Malpighi and the Evolution of Embryology. Cornell Univesity Press, Ithaca, New York, vols. I-V.

Ekataksin, W., and K. Wake 1991 Liver units in three dimensions: I. Organization of argyrophilic connective tissue skeleton in porcine liver with particular reference to the "compound hepatic lobule." Am. J. Anat.,191:113~153.

Ekataksin, W., K. Wake, and R.S. McCuskey 1992 Liver units in three dimensions: In vivo microscopy and computer-aided reconstruction of microvascular zonation in mammalian livers. Hepatology, 16: 135 [Abstract].

Ekataksin, W., K. Wake, J. Nishida, and R. McCuskey 1993 Mammalian liver units as revealed by temporal and spatial reconstructions: Recognition of the hepatic microcirculatory subunits. Anat. Rec., Sppl.1:48 [Abstract].

Basler, A. 1917 Über eine neue Methode zur mikroskopischen Untersuchung inere Organe des lebenden Tieres im durchfallenden Licht nebst dem Versuch einer Theorie der das Licht leitenden Glasstabe. Pflügers Arch. f.d. ges. Physiol., vol.167:228~244.

Gumucio, J.J., D.L. Miller, M.D. Krauss, and C.C. Zanolli 1981 Transport of fluorescent compounds into hepatocytes and the resultant zonal labeling of the hepatic acinus in the rat. Gastroenterology, 80:639~646.

Harvey, W. 1651 Exercitationes de Generatione animalium Quibus Accedunt Quaedam de partu; de membranis ac humoribus ureri, de conceptione, Londini, Typis Du Gardianis; Impensis O. Pulleyn.

Knisely, M.H. 1936 A method of illuminating living structures for microscopic study. Anat. Rec., 64:499~523.

Krogh, A., ed. 1929 The Anatomy and Physiology of Capillaries. Yale University Press, New Haven.

Lake,J.R., V. Licko, R.W. Van Dyke, et al. 1985 Biliary secretion of fluid-phase markers by the isolated perfused rat liver: Role of transcellular vesicular transport. J. Clin. Invest.,76:676~684.

Löffler, L., and M. Nordman 1925 Leberstudien. Virch. Arch. Pathol. Anat. Physiol., 257:119~181.

Mall, F.P. 1906 A study of the structural unit of the liver. Am. J. Anat., 5:227~308.

Malpighi, M. 1666 De viscerum structura exercitatio anatomica. Bononiae [An annotated translation is available; see Adelmann,1966].

Matsumoto, T., R. Komori, T. Magara, T. Ui, M. Kawakami, T. Tokuda, S. Takasaki, H. Hayashi, K. Jo, H. Hano, H. Fujino, and H. Tanaka 1979 A study on the normal structure of the human liver with special reference to its angioarchitecture. Jikeikai Med. J., 26:1~40.

McCuskey, R.S. 1986 Microscopic methods for studying the microvasculature of internal organs. In: Physical Techniques in Biology and Medicine: Microcirculatory Technology. C.H. Baker, and W.F. Nastuk, eds. Academic Press, NewYork, pp.247~264.

McCuskey, R.S. 1993 Intravital microscopy. In: Optical Microscopy: Emerging Methods and Applications. B. Herman and J.J. Lemasters, eds. Academic Press, San Diego, pp.355~372.

Poenie, M., and C.S. Chen 1993 New fluorescent probes for cell biology. In: Optical Microscopy: Emerging Methods and Applications. B. Herman and J.J. Lemasters, eds. Academic Press, San Diego, pp.1~25.

Rappaport, A.M., Z.J. Borowy, W.M. Lougheed, and W.N. Lotto 1954 Subdivision of hexagonal liver lobules into a structural and functional unit: Role in hepatic physiology and pathology. Anat. Rec.,119:11~33.

Schmidt, R., and H.P. Buscher 1991 Hepatic uptake of fluorescein, investigated by video fluorescence microscopy and digital image analysis. J. Hepatol.,13:208~212.

Sherman, I.A., and M.M. Fisher 1986 Hepatic transport of fluorescent molecules: In vivo studies using intravital TV microscopy. Hepatology, 6:444~449.

Shotton, D. 1993a An introduction to the electronic acquisition of light microscope images. In: Electronic Light Microscopy: Techniques in Modern Biomedical Microscopy. D. Shotton, ed. Wiley-Liss, New York, pp.1~38.

Shotton, D. 1993b An introduction to digital image processing and image display in electronic light microscopy. In: Electronic Light Microscopy: Techniques in Modern Biomedical Microscopy. D. Shotton, ed. Wiley-Liss, New York, pp.39~70.

Stock, R.J., E.G. Cilento, and R.S. McCuskey 1989 A quantitative study of fluorescein Isothiocyanate-Dextran transport in the microcirculation of the isolated perfused rat liver. Hepatology,9:75~82.

The Spatial Third Dimension of Organ Microcirculation: A Study of Hepatic Microvascularization with A Combined Technology of Injection Marker, Histologic Serial Sections, and Computer-Aided Three-Dimensional Reconstruction

WICHAI EKATAKSIN[1,2 (present address)] AND KENJIRO WAKE[1]
[1]Department of Anatomy, Faculty of Medicine, Tokyo Medical and Dental University Tokyo, Japan; and [2]Department of Anatomy, College of Medicine University of Arizona Health Sciences Center, Tucson, AZ, USA.

ABSTRACT

To provide documentation of the *hepatic microcirculatory subunit,* the HMS (Ekataksin et al.,1992,1993), in spatial three dimensions, a combination of techniques have been employed to study pig and rat livers. The injection marker, osmium-ruthenium red, created perfusion effect at one time point in the tissue which was fixed and examined in microscopic serial sections. By reconstruction of microdensitometrically digitized images we could demonstrate the space-occupying nature of the HMS. The results obtained were compatible with that reported by the study in temporal dimesion, *in vivo* microscopy, of the HMS (Ekataksin et al., this issue). As a result, a scientific demand to amend the prevailing knowledge derived from the acinar concept (Rappaport et al.,1954) is substantiated.

INTRODUCTION

We have reported (the previous paper in this issue) the use of *in vivo* microscopy to demonstrate in mammalian livers, the *hepatic microcirculatory subunits*, or the HMSs (Ekataksin et al.,1992,1993), visualized by infusion of fluorescent substances. Although there have been many investigators (Gumucio et al.,1981; Sherman and Fisher,1986; Stock et al.,1989; Schmidt and Busher,1991) who studied intravital fluorescent microscopy, they failed to observe that the liver lobules are perfused by small quantums, i.e., as a slender pyramidal sector, or the HMS. The formation of HMSs was dynamic as shown in the microdensitometric pseudocolor video. However, as a matter of fact, the spatial depth resolution was not enabled by the limited capacity of the equipment. Since the sinusoidal beds are, in other words, the 'syncytial' continuum of these subunits, we were tempted to clarify the hidden third dimension of the HMSs. This is ably accomplished by using an appropriate perfusion marker to generate a perfused, fixed tissue to be prepared in histologic serial sections, followed by a microscopic densitomeric process and a re-constructing of the serial image data in three dimensions.

MATERIALS AND METHODS

Since His pioneered the method of tissue restructuring in 1868, the technique had been accepted as a valuable investigative tool by microscopic morphological scientists, many of whom had contributed to the improvements that revolutionized it into a modern version of methodology (see a comprehensive review in Guant and Gaunt,1979; see also Rieder,1981). However, the advent of computer science technology has resulted in a new approach (reviewed in Ware and LoPresti,1975; Turner,1981) which in regards to routine adoption has placed an enormous impact to the classical method. For all that, we recently have developed a novel technique for solid reconstruction (Ekataksin and Wake,1991) which produces both positive and negative models in one operation, that so far had not been considered practicable. In addition to the physical reconstruction, we have also conducted the computer-assisted three-dimensional reconstruction based on serial sections which, due to its practicality, can demonstrate only the positive model type (Ekataksin and Wake,1991). We scrutinized the hand-made and the computer-aided techniques in a careful comparative study (Ekataksin and Wake,1992) and concluded that either technique has inherent scientific values that cannot be substituted by the other. For the present investigation we would not have adopted the computer imaging technique, if a 'transparent' color Styrenepaper could have been available to us.

Experimental Protocol

Since pig's liver lobules are suitable for reconstruction work (Mall,1906; Debeyre,1910; Johnson,1919; Braus,1921,1924; Pfuhl,1921; Tamura,1952; Ekataksin and Wake,1991), we are justified to use this non-laboratory mammal. However, to ensure the results obtained are universal, we performed likewise in the routine experimental animal. As a result, two pig livers were acquired freshly and the injection of perfusion marker was done at the slaughter house while the livers were still warm. The injection medium was prepared of 1% osmium tetroxide solution containing 1,000 ppm ruthenium red (modified after Oda et al.,1983). This was injected manually but gently into the portal vein identified on the cut surface of a lobe by a 5 ml plastic syringe with a polyethylene cannula. Immediately the liver surface appeared with dark spots of irregular patterns; care was taken not to do overinjection, otherwise individual lobules would turn totally dark. For comparison purposes, some pieces of the liver were injected into the sublobular vein. The samples were cut into smaller blocks and immersed in 3.7% formaldehyde fixative with two changes for at least two weeks. In the rat, the liver was injected *in situ* and removed from the abdominal cavity, followed by immersion fixation.

Histological Preparation

By preliminary experiment we have determined the section thickness of 40~50 μm as appropriate for serial image processing and reconstuction purposes. Since it is known that superficial lobules at convex surface are uniformly oriented perpendicular to the Glisson's capsule (Mall,1906; Johnson,1919; Elwyn and Strong,1932; Ekataksin and Wake,1991), cutting parallel to the hepatic capsule is helpful in referring to the orientation of the lobules in histologic sections.

After dehydration in ascending ethanol, tissue blocks were prepared for microtome serial sectioning which was accomplished by embedding in celloidin as described elsewhere (Ekataksin and Wake, 1991). As an alternate to the plastic embedment, which takes approximately three months, we cut some blocks unembedded. The ethanol-hardened block was mounted on the wooden stage and the block's perimeter was reinforced by paraffin, so that the tissue block became burried in the wax. This was then cut as previously described with a sliding microtome (Thoma-Jung type, Yamato, Tokyo). While cutting, the side exposed to the blade was suffused with ethanol to prevent it from drying. By the latterg method we could save up to 70~80% of the time required in celloidin procedure. Since the tissue was never embedded but only burried in paraffin, the outcome sections were free from the unpredictable (uneven) shrinkage effect of the paraffin. This advantage was reflected in the subsequent vertical alignment. Sections were stained with aniline blue for the connective tissue, cleared in xylol, and mounted in balsam. Non-serial sections were also prepared for general histologic examination.

Image Processing and Analyzing

Specimens were examined carefully under the light microscope from which typically interesting fields were selected for microdensitometric image processing by Luzex II (Nireco, Tokyo) and some of the photographic series thereof were further analyzed and hand-processed to be tridimensionally reconstructed by Cosmozone 2SA (Nikon, Tokyo). The overall system construction is schematically depicted in Figure 1. We have preliminarily tested the effects obtained from two different inputs, a color print specimen through the monochrome TV camera, and a microscopic specimen through the color TV camera; with aids of physical illumination and digital filtering and smoothing, both yielded essentially identical results. Single field images were not difficult to work with under the microscopic densitometry. However, when the same field had to be pursued trans-sectionally to create serial digitized images, we came to encounter the inconsistency of background density which was inherent to the serial histologic stained preparations. To cope with this problem, we segmented the gray scale into several divisions (up to 7 levels), allowing the highest end and the lowest end to cover wider ranges of gray level. Doing so facilitated us in determining zonation in a natural looking pseudocolor images.

For those serial specimens, the color monitor images were reproduced in color photographs from which the three zones with the interlobular connective tissue septa and portal and central venules were transferred onto the tracing paper. The traced materials were superimposed sequentially in the manner that outlines of major structures visually best fit the underlying ones. By penetrating the registered stack of tracing paper with a slender awl at two or three sites we established fiducial points for use as references to be inputted on the digitizer tablet (Graphtec KD-5050) in vertical alignment by the Cosmozone 2SA. For details of operation at the workstation, readers are referred to the user manual available with the application software package. The recontructed three dimensional images were rendered with 16.777 million colors visualized in Gouraud shading. The subtle shades of computer-generated color gradation were beautifully reproduced by the hard copier (Hitachi HC-1500) on 35 mm positive slides.

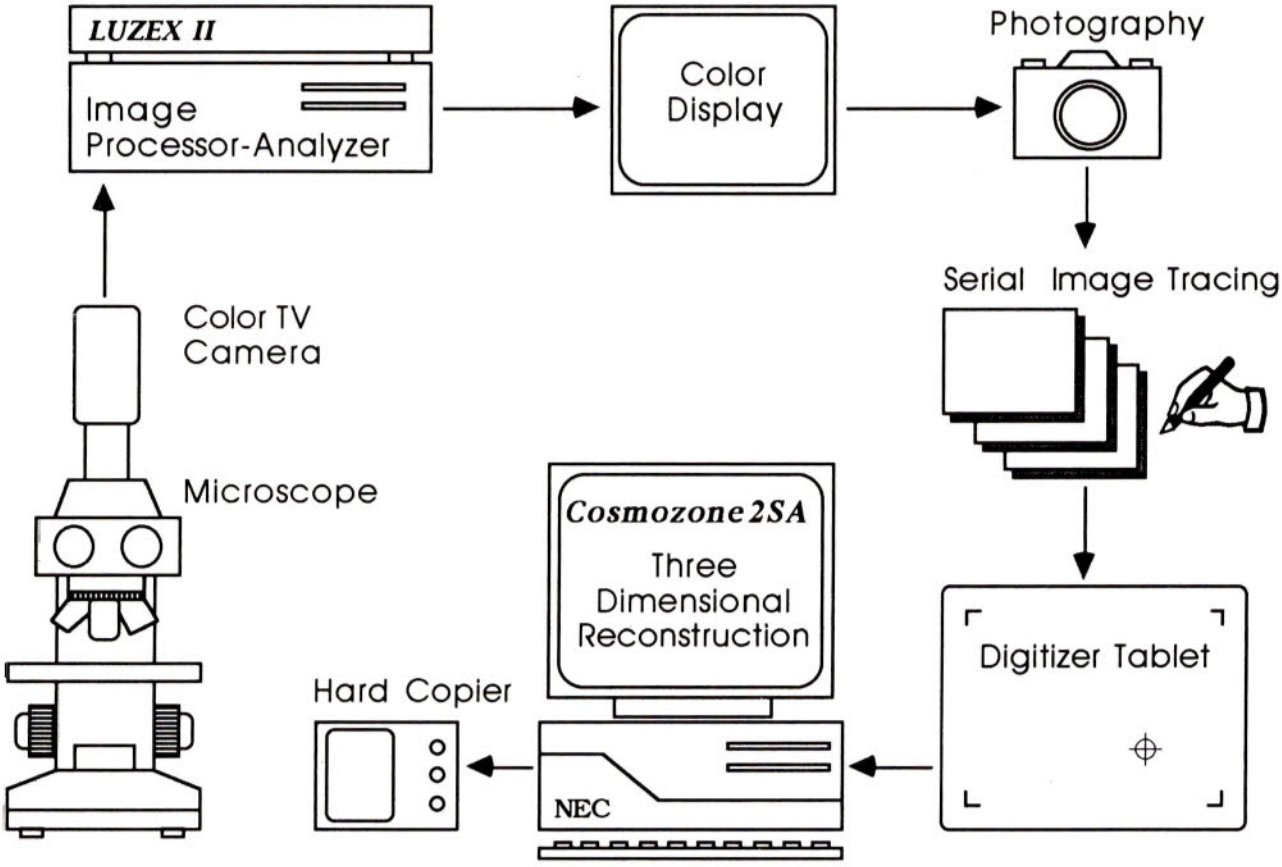

Fig.1. Diagram of image processing and analyzing system.

RESULTS

Where the perfusion marker, osmium-ruthenium red, was perfused, the liver tissue appeared reddish brown or dark brown against the clear background in sections of 40 and 50 μm thickness. The connective tissue septa stained brilliant blue, enhancing the contrast with other elements. The perfused areas were recognized with various patterns, large or small, in many lobules cut through different planes (judged by the appearance of central venules). However, the smallest amount of perfused tissue was obvious. It formed a slender wedge-shaped area, hereafter referred to as HMS. An HMS had a wider base, darker in color and starting on the peripheral side of the lobule, and had a tapering end, lighter in color and terminating centrilobularly. When cut transversely the HMS was rather rounded which in densitometric analysis showed concentric layers with the highest density located innermost. Where the HMS base was cut tangentially so that part of the septal substances were included, we found a portal inlet venule at the center of the highest density zone. Sometimes, two HMSs occurred close together, the concentric layers from each HMS, merged homogenously, resulting in an '8-shaped' area. In most cases the HMSs were clustered at the corners of adjoining lobules, being originated from the same portal tract. Where HMSs radiated into three lobules equally, they created a large triangular area, reminiscent of the 'triangular lobule of Mall' (Ham,1953, his Figure 356); if spreading into only one corner (i.e., one lobule), the perfused area resembled the kite-shaped *primary lobule* (Matsumoto et al.,1979) Likewise, when this occurred bilaterally on a side of two facing lobules, we saw a rugby-shaped area, reminiscent of the 'liver acinus' of Rappaport et al (1954). The midseptal region was not readily perfused. The septal and nearby area sandwiched by two portal tracts that were aligned and located at two adjacent corners of a lobule, sometimes created a clearcut perfusing borderline, forming a watershed midseptally. In three dimensional imaging reconstructed of a corner of a lobule, a preterminal portal venule coursed upright at the portal tract, branching out the terminal portal venules upon both lateral sides of the lobule, all being embedded in the connective tissue septa. At the lobule's center was standing a central venule with its tributaries. In the space between these two vessels, we observed that HMSs were densely packed along the corner horizontally and vertically. The high density zone of each HMS was erected on the connective tissue septum where it was found associated with an inlet venule. At the base they were

likely to fuse with the neighboring, whereas at the centrilobular end they tended to remain separated. Viewing only the high density zone we could appreciate a concave curvature being about to spread over the intralobular space, from the corner into the lobule.
In the rat liver injected with osmium-ruthenium red, we found similar patterns that the periportal regions were heavily perfused and the midseptal regions were consistently interrupted. Individual HMSs, arising from inlet venules, formed pyramidal sectors pointed centrilobularly, and were likely to fuse near base.
On the other hand, in the experiment which sublobular veins of pig liver were injected, the perfused areas formed a regular cuff around the central venules. The immediate perimeter of sublobular veins were also darkened. There was no HMS-like structure as observed in the portal perfusion.

DISCUSSION

By injecting perfusion marker into the portal vein of the liver, we created a microcirculation effect fixed at one time point. This was examined through serial sections to clarify the structures hidden in the depth not resolved by *in vivo* microscopy (McCuskey,1986), and was corroborated in computer-based three dimensional reconstruction that rendered multiple elements seen through the depth. Combining the results obtained from both studies, we therefore have established the documentation of the time-space dimensions of the HMS. The previous study (of this issue) explored the *temporal* dimension of the HMS visible without the depth perception. Complementarily the present study surveyed the *spatial* third dimension of the the HMS which was carried out at one point of time. It should be noted, however, that the histologic (serial) sections actually provide observors with structures that are related to different time points, as evidenced many findings we found both in the temporal study and in the spatial study. Johnson (1919) in studying the development of the lobule of the pig's liver observed that there are lobules at many stages of development in any single specimen. We similarly in studying the formation of connective tissue septum found that there are septa at many stages of development in any single specimen (Ekataksin and Wake,1991). Most investigators could confirm the temporal dimension by studying the development in animals at several age groups (e.g., Johnson,1919; Ekataksin et al.,1986). That a particular structure is examined for its spatial third dimension and for its dynamic temporal dimension (at *in vivo* microscopic time scale) has never been reported, to the best of our knowledge, or if any must be very rare.
That the HMSs tended to merge near base and separate near center is understandable. The periportal sinusoids are tortuous (Matsumoto et al.,1979; Ekataksin and Wake,1991), thus facilitating mixture of flow. The straight course of centrilobular sinusoids, however freely interconnected, would be less effective for interchange among stream lines.
Computer-aided reconstruction confirmed that the corner of the lobule was heavily occupied by the HMSs. This finding cannot support the liver acinar concept (Rappaport et al.,1954) which assumes that 'zone 3' extends into the periportal region. We confirmed that the midseptal region formed a sharp perfusion boundary that bisected a side of the lobule. This finding supports the *corbicula portalis* concept (Wünsche and Preuss,1986), but contrasts strongly with the acinar model which defines a terminal portal venule as the axial vessel that occupies the entire length of a side of the lobule. In a 'bible' textbook, Ham's Histology (9th edition), it is stated by the current author (Cormack,1987) that "increased emphasis has been given to the acinar concept of liver structure in recognition of the fact that it is fast gaining almost universal acceptance." Doubtless we are demanded to correct the prevailing knowledge. This is implied also that by applying similar techniques to re-investigate microcirculation of other organs, it is possible to obtain new information that so far has been overlooked.

ACKNOWLEDGMENTS

One of the author (WE) has been supported by the Research Award (1991) of Medical Alumni Association (*Ochanomizu Ikadosokai* 御茶ノ水医科同窓会), Tokyo Medical and Dental University, and by the Research Award (1992) of Inoue Foundation for Science (井上科学財団).

LITERATURE CITED

Braus, H. 1921 Mitteilungen uber Lebermodelle. Anat. Anz., 54 (Erg.-Bd.): 119-124.
Braus, H. 1924 Anatomie des Menschen: Ein Lehrbuch fur Studierende und Arzte. Julius Springer, Berlin.

Cormack, D.H. 1987 Ham's Histology. Lippincott, Philadelphia.
Debeyre, A. 1910 Morphologie du lobule hépatique. Bibliogr. Anat., 19: 249~263.
Ekataksin, W., E. Bhunachet, and K. Wake 1986 An ontogentic study on the lobulation of pig liver. Acta Anat. Nippon., 61:391 [Abstract].
Ekataksin, W., and K. Wake 1991 Liver units in three dimensions: I. Organization of argyrophilic connective tissue skeleton in porcine liver with particular reference to the "compound hepatic lobule." Am. J. Anat.,191: 113~153.
Ekataksin, W., and K. Wake 1992 The use of computer science technology in biological structural research: The art of three-dimensional imaging as compared with hand-made physical modeling in microscopic anatomy. Proc. 2nd Inl. Work. Adv. Sci. Technol. Transfer to Thailand, Aug 21~23, 1992, Bangkok-Pattaya, Thailand. Damrong Lathapipat Fondation, p.456 [Abstract].
Ekataksin, W., K. Wake, and R.S. McCuskey 1992 Liver units in three dimensions: In vivo microscopy and computer-aided reconstruction of microvascular zonation in mammalian livers. Hepatology, 16: 135 [Abstract].
Ekataksin, W., K. Wake, J. Nishida, and R. McCuskey 1993 Mammalian liver units as revealed by temporal and spatial reconstructions: Recognition of the hepatic microcirculatory subunits. Anat. Rec., Sppl.1: 48 [Abstract].
Elwyn, A., and U.S. Strong, eds. 1932 Bailey's Text-book of Histology. Bailliere, Tindall, and Cox, London.
Gaunt, W.A., and P.N. Gaunt, eds. 1978 Three Dimensional Reconstruction in Biology. Pitman Medical, Kent, England.
Gumucio, J.J., D.L. Miller, M.D. Krauss, and C.C. Zanolli 1981 Transport of fluorescent compounds into hepatocytes and the resultant zonal labeling of the hepatic acinus in the rat. Gastroenterology, 80: 639~646.
Ham, A.W., ed. 1953 Histology, 2nd ed. Lippincott, Philadelphia.
His, W. 1868 (Cited in Gaunt and Gaunt,1978)
Johnson, F.P. 1919 The development of the lobule of the pig's liver. Am. J. Anat., 25: 299~331.
Mall, F.P. 1906 A study of the structural unit of the liver. Am. J. Anat., 5:227~308.
Matsumoto, T., R. Komori, T. Magara, T. Ui, M. Kawakami, T. Tokuda, S. Takasaki, H. Hayashi, K. Jo, H. Hano, H. Fujino, and H. Tanaka 1979 A study on the normal structure of the human liver with special reference to its angioarchitecture. Jikeikai Med. J., 26:1~40.
McCuskey, R.S. 1986 Microscopic methods for studying the microvasculature of internal organs. In: Physical Techniques in Biology and Medicine: Microcirculatory Technology. C.H. Baker, and W.F. Nastuk, eds. Academic Press, NewYork, pp.247~264.
Oda, M., M. Nakamura, N. Watanabe, Y. Ohya, E. Sekizuka, N. Tsukada, Y. Yonei, H. Komatsu, H. Nagata, and M. Tsuchiya 1983 Some dynamic aspects of the hepatic microcirculation: Demonstration of sinusoidal endothelial fenestrae as a possible regulatory factor. In: Intravital Observation of Organ Microcirculation. M. Tsuchiya, H. Wayland, M. Oda, and I. Okazaki, eds. Excerpta Medica, Amsterdam, pp.105~138.
Pfuhl, W. 1921 Über die Form und die Gefäßbeziehungen der Leberläppchen beim Schweine. Z. Anat., 62:153~170.
Rappaport, A.M., Z.J. Borowy, W.M. Lougheed, and W.N. Lotto 1954 Subdivision of hexagonal liver lobules into a structural and functional unit: Role in hepatic physiology and pathology. Anat. Rec., 119:11~33.
Rieder, C.L. 1981 Thick and thin serial sectioning for the three-dimensional reconstruction of biological structure. In: Methods in Cell Biology. J.N. Turner, ed. Academic Press, New York, pp.215~249.
Schmidt, R., and H.P. Buscher 1991 Hepatic uptake of fluorescein, investigated by video fluorescence microscopy and digital image analysis. J. Hepatol., 13:208~212.
Sherman, I.A., and M.M. Fisher 1986 Hepatic transport of fluorescent molecules: In vivo studies using intravital TV microscopy. Hepatology, 6:444~449.
Stock, R.J., E.G. Cilento, and R.S. McCuskey 1989 A quantitative study of fluorescein Isothiocyanate-Dextran transport in the microcirculation of the isolated perfused rat liver. Hepatology, 9:75~82.
Tamura, T. 1952 Form of hepatic lobules. Trans. Soc. Pathol. Jpn., 41:212~213 [in Japanese].
Turner, J.N., ed. 1981 Three-dimensional ultrastructure in biology. Method in Cell Biol., 22:xiii.
Ware, R.W., and V. LoPresti 1975 Three-dimensional reconstruction from serial sections. Int. Rev. Cytol., 40:325~440.
Wünsche, A., and F. Preuss 1986 Pfortaderkörbchen um Leberläppchen beweisen die Läppchengleiderung der Leber. Acta Anat., 125: 32-36.

ABSTRACT

Dr. Yuth Nimit

The presentation will focus on the recent advancement and frontiers of biotechnology in the United States during my twenty six years of experience related to the biomedical and biotechnology fields. An overview based on my research, teaching and administrative management experience as a medical scientist at the National Institute of Health, as neuropsychopharmacologist at the Veteran Administration Hospital, as professor at Baylor College of Medicine and Henan Medical University, Supervisory Health Scientist Administrator and currently, Director of the Office of Program Coordination and Review in the US Department of Health and Human Services. The theme will focus on the use of biotechnological methods, such as, drug receptor concepts of the development of medicinal, genetic engineering technology in new drug and vaccine designs. It will also cover development of new biotechnological and medical devices, diagnostic kits for biomedical research, medical diagnostic, treatment, and vaccine delivery systems as well as gene therapy. The later is directed toward future health care treatment and goals, and the principal of using genes to alter the immune system to fight infections and diseases. These techniques are used to build products for and toward the achievement of human environmental well being, health and longevity. The discussion will steer toward concerns regarding Thai health care and preparation to deal with the epidemic of AIDS, which is predicted by experts to take place in Thailand by the year 2000.

A transferring of other knowledge and technology will not be possible if the country has to deal with the impending major AIDS crisis and disaster, and is not ready to accept them. Therefore, immediate attention to the highest priority using all resources for building up an infrastructure for prevention and treatment of HIV/AIDS infection is recommended.

AIDS IN THE YEAR 2000

Dr. Yuth Nimit

Acquired Immune Deficiency Syndrome (AIDS) triggered by the Human Immune-deficiency Virus (HIV) destroys the body's immune system, leaving it exposed to other infections. In lay terms, the HIV disease begins with a slow controlled infection, kept in check by a cascade of helpful immune responses for a few years. Then, the virus shifts into high gear through destruction of the white blood cells, immunologic function and mutation to full blown AIDS. It has been estimated that there are about 14 million people in the world who have been infected with the HIV virus. Public Health experts predict that without a massive and intensified effort to prevent new infections, as well as medical breakthroughs for prevention and treatment, the number will rise to 33 millions by the end of the decade.

In the U.S., according to the most recent CDC reports, with the expanded definition, projections of the prevalence of persons infected with HIV who have CD4+ T-lymphocyte counts less than 200/uL, 160,000 people with HIV, which causes AIDS, would be added to the 230,180 already diagnosed. About 33 percent of all reported AIDS cases were attributed to intervenors injecting of abuse drugs (IVAD) or sexual contract with an injecting drug user. For women, abuse of drug abuse related cases of AIDS represented 76 percent of all reported AIDS cases.

In Thailand, a survey indicated that, by the year 2000, without proper prevention and treatment plans, 500,000 AIDS patients will occupy all the hospital beds (only approximately 90,000 in the country at this time) and a loss of 40 billion dollars of productivity in the nation. It is imperative to recognize that now is the time to use the knowledge and technology transfer regarding health care products and systems to build a health care personnel infrastructure on prevention and preparation to deal with the epidemic of AIDS. A country that has to deal with an immediate major AIDS crisis and disaster, may not be ready to accept any transferring of necessary knowledge and technology.

The news from the Ninth International Conference on AIDS that took place in Berlin Germany on June 8, 1993, is grim. Not only is the AIDS epidemic spreading with disastrous results in the developing world, but the effectiveness of the currently available drugs used for treatment of HIV/AIDS, such as AZT, has been called into question. The meeting provided very little reason to expect that a new breakthrough will come soon. AZT, ddI, ddC and other substances were discussed at the conference. One of the ideas that does not require better drugs, is "convergent combination therapy". The idea is to give several medicines that all target the same weak spot in the virus's replication cycle. If the microbe escapes one drug by mutating, it may remain susceptible to the others.

The conference offered some new data but no full understanding of the virus. There are five main families or "clades" of the AIDS virus, and evidence of a sixth was presented at the conference. It was indicated that AIDS clades tend to be geographically separate. In Thailand, there are two, one more common among prostitutes and another among intravenous drug users. There is now increasing evidence of mixing and drifting of these families, and it remains to be seen how well vaccines based on the American family will protect against the others.

At present, the major modes of prevention of virus transmissions remain the use condoms, treatment of STDs such as AIDS, HB, Venereal Disease, and the use of clean needles and stopping needle sharing by addicts. The need for an effective woman-controlled form of protection was a universal call at the conference. There is need for a closer look at long-term survivors as keys to a cure. People infected early in the epidemic but remaining healthy are subjects of intense scrutiny as scientists probe the secrets of their immune control systems. Now, a consensus is building that cell-mediated immunity (CMI) is crucial in protecting these people against the ravages of AIDS. The CMI arm of the immune system attacks already-infected cells. In contrast, the humoral arm produces antibodies that latch on to free floating viruses and prevent them from infecting cells in the first place. CD8+ T cells are the target sites of the CMI system. Dr. Jay Levy indicated that "the efforts directed at these cellular immune processes and attention to the CD8+ cell antiviral factor could lead to long-term survival for all HIV infected individuals". CD8+ cell not only can kill infected cells but they also secrete a soluble factor that suppresses replication of HIV in infected cells. The patients remain healthy for 15 years. They are protected by high level of CD8 or suppressor cells which should be exploited for clues to treatment. Studies of immune profiles of people who resist HIV despite exposure have also been carried out at the National Cancer Institute at NIH. A study that may be boosting of CD4 of CMI by the infusion of Interleukin-2, a messenger that is known to stimulate CMI, in two patients whose immune systems have been seriously damaged by HIV.

Healthy HIV carriers may hold the key to AIDS drugs for future treatment. The healthy immune system and absence of AIDS in survival of the repeated infected homosexual men in San Francisco, prostitutes in Kenya and hemophiliacs through sexual transmission and blood transfusion respectively, prompted a suggested study of the healthy that could lead to new approaches to preventing and treating infection with the HIV/AIDS virus. Discovery of a gene for HIV resistance is attracting wide attention because genetic-engineering technology is making it possible to use genes as medicine. It is noted that "gene therapy" for HIV infection and AIDS is moving closer to reality.

The epidemic will undoubtedly pose the greatest economic and health challenge to the nation, and we must be prepared. It is

recommended that:

- A massive education and media campaign on HIV/AIDS and IVAD prevention be made a national priority,

- A crack program to educate people on HIV/AIDS infection prevention, such as stopping needle sharing practices among addicts, safe sex practices, and treatment of other sexually transmitted diseases be begun,

- Physician and health care providers use the new HIV infection diagnostic such as quantitative competitive Polymerase Chain Reaction (PCR) analysis, which is 60,000 times more sensitive than the previous technique using culture-based plasma viremia assays. With this new diagnostic tool, scientists have found that there is far more HIV in infected people than was previously thought,

- Physician and health care providers keep abreast of advances in AIDS knowledge, current information about the mechanism, diagnosis, management and maintain proficiency as well as aid in the care of their AIDS patients. A combination of drug treatments is more beneficial,

- Research and services aimed at developing prevention, treatments, cures and vaccines must be continued and expanded, and

- Maintenance of a safe blood supply program is essential.

Prior to this meeting, a Third International Conference on Advanced Science and Technology Transfer to Thailand held in Chicago on June 11-13, 1993, was sponsored by the Minister-Counsellor of the Office of Science Technology (OST), the Royal Thai Embassy, Washington, D.C. I presented an overview of recent advancement and frontiers of biotechnology in the United States during my more than twenty years experience related to the biomedical and biotechnology fields. The presentation was based on my research and administrative management experience as a medical scientist at the National Institute of Health, as neuropsychopharmacologist at the Veteran Administration Hospital, as professor at Baylor College of Medicine and Henan Medical University, Supervisory Health Scientist Administrator and currently, Director of the Office of Program Coordination and Review in the US Department of Health and Human Services. The theme of the overview was focussed on the use of biotechnological methods for building products for and toward the achievement of human environmental well being, health and longevity. It was also steered toward concerns regarding Thai health care and preparing for the biotechnology topic "AIDS in the year 2000" for the meeting on July 23-25, 1993, which is the topic of discussion.

In the 1970's, preliminary biotechnology related biomedical research activities focussed on synthetic chemistry, neurochemistry, pharmacology and mechanism of action of alkaloids and drug receptor concepts of the development of medicinal.

In the 1980's, a surge of biotechnology activities addressed using genetic engineering technology in new drug designs, development of new biotechnological and medical devices as well as diagnostic kits for biomedical research, medical diagnostic, treatment, and vaccine for disease prevention.

In the 1990's, the most recent advancement of biotechnology in medical fields is centered around drugs and vaccine delivery systems as well as gene therapy, which is directed toward future health care treatment and goals, and the principal of using genes to alter the immune system to fight infections and diseases. The example of the success of first experiments on clinical trials of human project carried out at the US-NIH on a four year old girl with a Adenosine Deaminase Deficiency, a hereditary enzymatic problem that virtually wiped out her immune system and crippled her ability to fight infectious disease, is a commendable scientific achievement by biomedical and biotechnological scientist in this important field. There are many new advancements in using this technique in the combat of cancer, neural blood diseases, AIDS, Cystic Fibrosis and Gaucher Disease. The above biomedical research and technology have contributed to the current techniques for the diagnosis and treatment of HIV/AIDS.

The Biotechnology group, which I lead and Chaired in the afternoon meeting, had more than fifty participants composed of physicians, professors and senior scientists, as well as young scientists who are scholarship recipients working toward their doctoral degree. Each participant was asked to present a short summary of his or her expertise and availability of knowledge or technology to be transferred. I requested and recommended the presentations in a format of short, intermediate and long term visions as well as the role of the ATPAC's biotechnology members. Feasibility and potential contributions were discussed. The meeting lasted three hours and adjourned with the conclusion that each of the biotechnology members has a clear understanding, responsibility and commitment to his or her role.

In the group reporting session, I presented and made recommendations to the ATPAC, OST and other officials as follows:

1) members should definitely stress transferring the real knowledge and technology and <u>not</u> transferring turn-key products,

2) A licensing, registration and regulatory process and procedures such as quality control, product safety, good manufactured products and other procedures should be established to prevent future

dire liability and disaster loss,

3) A list of identified priorities, programmatic relevance and nationally significant unmet needs should be provided to ATPAC as guidance for recruiting future contributors,

4) Various reverse brain-drain pathways for members' actions based on person availabilities should be considered:

   a. a short term, two week to one month, technical consultation or teaching.

   b. one academic year of sabbatical leave.

   c. a "Thai trains Thai" concept:

      ATPAC members to take their positions and responsibilities as mediators for transferring their knowledge and technologies as well as acting as preceptors or indirect advisors for young scientists during their pre-doctoral and post-doctoral tenures in the US.

   d. permanent return to take a permanent position.

5) Biotechnology group now, with consent and agreement from Thai physicians, scientists and paramedics identified themselves as examples of experts who are ready to transfer their knowledge and medical technology for the agencies who are at need, and

6) ATPAC will set up a separate list of thousands of physician, biomedical and biotechnology members database and tracking system for accumulating and providing the name, expertise and availability of position, needs, time, knowledge and technology transfer. A member will be appointed as contact person to handle these public affairs.

A vision to use the knowledge and technology transfer of health care products and systems to build health care personnel infrastructure for promoting health care systems, particularly on prevention and preparation to deal with the epidemic of AIDS, which is predicted by many experts to take place in Thailand, is far more crucial a priority than others. A transferring of other knowledge and technology will not be possible if the country that has to deal with the immediate major AIDS crisis and disaster is not ready to accept them. Therefore, a call for immediate attention to the highest priority using the recommendations above for building up an infrastructure for prevention and treatment of HIV/AIDS infection is recommended.

Simulated Light Sensitive Model for Thai Handwritten Alphabets Recognition[1]

Chidchanok Lursinsap and Chularat Khunasaraphan
The Center for Advanced Computer Studies
University of Southwestern Louisiana
Lafayette, LA 70504

Abstract.

A new technique for Thai handwritten alphabet recognition based on our simulated light sensitive model combined with the classical back-propagation network is proposed. It is much simple and more natural than the existing techniques. The concept is to transform and map a deformed Thai handwritten letter into a domain that is easy to manipulate because the preprocessing is the most important step of handwrittern alphabet recognition. We treat the input image as a visual image stimulated by the light. The light from the visual image will stimulate the receptor neurons. Then these receptor neurons excite and inhibit each other until they are in the stable state. Next they transmit signals to the back-propagation network. The primary objective is to overcome the space and time complexities of the problem, to recognize all 44 handwritten Thai letters, and to implement the recognition technique on a VLSI chip. The experiments confirm that this technique substantially reduces the time and space complexities of the neural network, and recognizes all 44 soft error Thai alphabets.

1. Introduction

One of the major applications of a neural network is used by an optical character recognition program. There are several proposed techniques for recognizing handwritten alphabets obtained from an optical scanner. These techniques are grouped into two classes. The first class is by extracting the features of each character and training a neural network to memorize and recognize it. The neural networks can be a Hebbian-like model [4][6][7] or a neocognitron [9]. The second class is by letting the input images organize themselves by using a self-organizing model [5]. Although these approaches are quite successful in classifying and recognizing handwritten characters they are not efficient enough due to the time and space complexities of the algorithms. For examples, the feature extraction models require lots of neurons to extract and recognize the features.

We propose a new technique which is much simple and more natural than the existing techniques. It can be applied to any kind of handwritten recognition problem such as handwritten digits as we described in [1], or alphabets. In this paper, we have decided to apply our technique with Thai alphabets to confirm that our technique really works well even with the group of alphabets that look very similar to each other and compose of many classes. The primary objective is to overcome the space and time complexities of the problem, and to classify a large number of similar letters. But the ultimate goal is to implement the recognition technique on a VLSI chip. The paper is organized into seven sections. Section 2 discusses the recognition concept. Section 3 explains the light receptor model. The feature selection rules are presented in Section 4. Section 5 summarizes the back-propagation model used in our technique. Section 6 discusses how the experiments are performed and finally Section 7 concludes the paper.

2. Recognition Concepts and Structure

The important step of handwritten alphanumeric recognition is the preprocessing step. Then the recognition step can be performed by any supervised or unsupervised learning. Our approach is based on the study by Hubel and Wiesel [11] and Bruce, Desimone, and Gross [10]. In those studies they found that the visual area of the cerebrum responds selectively to some features of the visual patterns and the visual cortex responds selectively to some shapes such as circles, triangle, squares. What we apply from the studies is the simulated the visual cerebrum

[1] This work is partially supported by National Science Foundation under grant NSF-ADP-04 and Ministry of Science, Technology and Environment of Thailand under The Development and Promotion of Science and Technology Talents Project from Thailand.

and visual cortex models. We propose a simpler model used particularly for handwritten alphanumeric recognition application. We treat the input image as a visual image stimulated by the light. The light from the visual image will stimulate the receptor neurons. Then the feature selection will be applied to these receptor neurons for collecting only significant neurons for using in the next step. Next they transmit signals to the image recognition neurons to change their synaptic strength. Figure 1. illustrates the structure of our recognizer.

The concept is to transform and map a deformed handwritten letter into a domain that is easy to manipulate. Typically, the input handwritten letters are in the form of a $\{0, 1\}$ bit map which may or may not have any gray scale involved. We use noise injected inputs in our techniques becuase it has been shown that the recognized capability could remarkably be enhanced [2]. An input image is represented in a form of an $N \times N$ matrix. This $N \times N$ matrix is mapped to a $\{0, 1\}$ vector of size M, where $M < N \times N$. The mapping function must preserve the features or characteristics of the structure of each handwritten letter.

3. Light Receptor Model

The time complexity that we refer to in this paper is the training time as well as the recognizing time when operating the neural network. This complexity can be reduced by minimizing the number of bits in each training vector. Once the vector size is shorten we should be able to achieve the training convergence by using a smaller neural network.

The light receptor consists of an array of $N \times N$ cells. Each cell is sensitive and responsive to the different amount of intensity and grating orientations[1] of light falling on its surface. Not every receptor cells are sensitive to the light. All the receptor cells are located along the boundary, the middle horizontal area, the middle vertical area, and the forward and backward diagonals. These cells can be founded by mapping the input bit to the nearest receptor cell. Then we divide those boundaries into segments. Size of each segment depends on the intensity of light on each receptor cell. This structure is used to transform a deformed shape into a standard shape. The structure can be shrunk or expanded to fit any size of a receptor array.

The transformation of shape is controlled by two mechanisms, the sensitivity to the light intensity and the grating orientation. The grating orientation is measured in the degree of the grating angle. There are four grating orientations, 0 degree, 90 degree, 45 degree, and 135 degree that we consider. These four orientations are enough for detecting and transforming a deformed and irregular handwritten image to our standard pattern. Each pattern recognition problem may use different number of segments. With our statistical method, we have decided to use 28 segments for the Thai handwritten alphabet recognition as shown in Figure 3. When the light falls on the receptors, some may be on and some may be off depending upon the intensity of the light. The light intensity sensitivity (I_s) of any segment receptor s is defined by two parameters:

1. the distance ($d_{s,i}$) between the receptor cell $i \in s$ and the location of the light. Cell $i \in s$ is on when $d_{s,i} \leq \tau$, where τ is the sensitivity distance threshold.

2. the ratio (R_s) between the number of *on* receptor cells (O_s) of segment s and the total number of receptor cells (T_s) in segment s. Segment s is "on" when $\frac{O_s}{T_s}$

3.1. Analytical Model of Light Receptor

An input image can be viewed as a vector V in an n-dimensional binary space, B^n. The light receptor must perform a unique mapping function $f(V) : B^n \rightarrow B^m$, where m is the number of segments m is equal to 20 for handwritten digit case and equal to 28 for handwritten characters. The uniqueness means that given any inputs V_i and V_j, $f(V_i) \neq f(V_j)$. This uniqueness is defined by the sensitivity distance threshold (τ) and the segment sensitivity threshold (ζ). In order to find τ and ζ, we have derived the equation for this purpose as shown below. The idea is to compute the probability of each pixel of each alphanumeric that causes each segment to be "on".

---

[2]Naturally, the number of grating orientations can be infinite.

Let N_i be the number of pixels in segment i.

Let n_i be the number of pixels that causes segment i on.

Each training pattern is defined by each input vector or image $O_i = | \sum_{r \, \varepsilon \, on \; patterns} C_i^r |$.

where C_i^r is the rth pattern that turns on segment i.

Let S_i be the segment i.

Let a_{ki} is the kth pixel of segment i.

$$Prob(a_{ki} = on \mid S_i = on) = \frac{Prob(S_i = on \mid a_{ki} = on).\, Prob(a_{ki} = on)}{Prob(S_i = on)}$$

We would like to find $Prob(a_{ki} = on)$.

Consider $Prob(a_{ki} = on \mid S_i = on)$: the probability that if $S_i = on$, then $a_{ki} = on$ is the probability that $n_i - 1$ pixels of $N_i - 1$ pixels are on, plus the probability that n_i pixels of $N_i - 1$ pixels are on, plus through the probability that $N_i - 1$ pixels of $N_i - 1$ pixels are on, i.e.

$$Prob(a_{ki} = on \mid S_i = on) = \frac{C(N_i - 1, n_i - 1)}{\sum_{\alpha=n_i}^{N_i} C(N_i, \alpha)} + \frac{C(N_i - 1, n_i)}{\sum_{\alpha=n_i}^{N_i} C(N_i, \alpha)} + \ldots + \frac{C(N_i - 1, N_i - 1)}{\sum_{\alpha=n_i}^{N_i} C(N_i, \alpha)}$$

$$\text{where } C(a, b) = \frac{a!}{b! * (a - b)!}.$$

Consider $Prob(S_i = on \mid a_{ki} = on)$: it is the same as $Prob(a_{ki} = on \mid S_i = on)$ case. However, if $a_{ki} = on$, then the total numbers of remaining possible cases are 2^{N-1}, i.e.

$$Prob(S_i = on \mid a_{ki} = on) = \frac{C(N_i - 1, n_i - 1)}{2^{N-1}} + \frac{C(N_i - 1, n_i)}{2^{N-1}} + \ldots + \frac{C(N_i - 1, N_i - 1)}{2^{N-1}}$$

Let T_p be the total number of training patterns.

$$Prob(S_i = on) = | \sum_{r \, \varepsilon \, on \; patterns} \frac{C_i^r}{T_p} |$$

$$\text{So } Prob(a_{ki} = on) = \frac{\sum_{\beta=n_i-1}^{N_i-1} C(N_i - 1, \beta)}{\sum_{\alpha=n_i}^{N_i} C(N_i, \alpha)} . | \frac{\sum_{r \, \varepsilon \, on \; patterns} C_i^r}{T_p} | . \frac{2^{N_i-1}}{\sum_{\beta=n_i-1}^{N_i-1} C(N_i - 1, \beta)}$$

$$\text{Hence, } l_k = \sum_{\alpha=1}^{T_p} Prob(a_{ki} = on).\, l_k^{\alpha}$$

where l_k^{α} is a distance from kth pixel to segment ith of pattern α.

The experiment shows that the average distance of segment ith from the above equation is differed from the experimental average result only one pixel. So this result confirm our above equation. Since the O_i value is computed from C_i^r which depends on a set of input images, thus for the effective result, the input images should represent as many as characteristics of the alphabets. From this result, we are able to predict the suitable value of τ (the sensitivity distance threshold) and ζ (the segment sensitivity threshold).

4. Feature Selection

Although the output from the light receptor can be directly fed to the back-propagation network for training, it may not achieve a satisfactory result in terms of the number of neurons and training time. We need further reduce the size of each input vector by extracting only the relevant features or bits. It has been shown that all

$C(P_2, P_1)$ possible combinations has to be considered in order to find the best P_1 features from P_2 measurements [12]. We need some efficient method to avoid the exhaustive search for a practical problem. A number of techniques for determining the optimal sets of features are available. In our experiment, we consider to use "sequential forward selection" method [12]. It starts with the best single feature and then adds one measurement at a time which gives the maximum value of the criterion function in combination with the existing features. This technique can be adjusted to start and add p measurements at each time.

5. Back-Propagation Model

We use the classical 3-layered back-propagation network proposed by D.E. Rumelhart and J.L. McClelland to classify the output vectors from the receptor cells to get the roughly classes and to recognize them. During the learning period, we apply the technique of varying the number of hidden units proposed by Hirose, Yamashita and Hijiya [3] to speed up the learning. The concept of this algorithm is by gradually adding hidden neurons first until the network is converged and then gradually removing hidden neurons until the error increases beyond the threshold. The back-propagation neural network is applied for two steps. First, it is used to roughly classify the input from the light receptor model and the second step is for recognizing the input image.

6. Experiments

The proposed techniques are experimented with Thai alphabets. Thai characters have unique features and they are more complex than English characters as shown in Figure 2a. Most of the characters consist of curves and zigzag circles. Besides the curves and circles, different widths signify different characters. None of the neural recognition techniques have been applied to this language.

The input patterns are feeded into the statistical classifier to determine the roughly classes of them. For the precise accuracy, we apply the statistical technique with the raw input patterns which are arrays of size N x N. We create the representative pattern for each alphabet. It should be in the form that similar to the typed form. Then we compare all training patterns with each representative pattern by computing the variance of the distance between each training and the representative pattern. For the fixed level of acceptable variance, we will be able to roughly classify these patterns. The patterns which have the variance less than the fixed variance level will be put into the same group. In Thai handwritten recognition problem, we get the roughly classes by applying the above method which we divide all 44 alphabets into eight classes as shown in Figure 2b. The fixed variance level we decided to use is 1.0. It is much better to roughly classify the enormous groups of patterns because it make the learning process faster and easier. The result will be used by the first back-propagation network.

The size of the input array of Thai alphabet is 32 x 32. We have decided to divide all the receptor cells into 28 segments as shown in Figure 3. There are three different distance $d_{s,i}$ parameters. The first one (wh) is for all segments in the 0 grating orientation, the second one (wv) is for all segments in the 90 grating orientation, and the third one ($wdiag$) is for all segments in the diagonal grating orientation. Furthermore, there are three ratios R_s for the light intensity sensitivity. Each ratio is the real number less than 1. The first ratio (ph) is defined for segments {1,2,3,4,9,10,11,12,21,22,27,28}. The second ratio (pv) is defined for segments {5,6,7,8,13,14,15,16,18,19,24,25}. The third ratio ($pdiag$) is defined for segments {17,20,23,26}. From the equation in section 3.1, we determine to set the parameters as follow : $wh = 7$, $wv = 7$, $wdiag = 3$, and $ph = pv = pdiag = 0.625$. Figure 4. shows the partial Thai input image and the corresponding light receptor segments which are "on".

The feature selection is used to reduce the number of segments which are not important for the recognized process. The result will become the training vector for the back-propagation network. In Thai handwritten recognition, the segments {9,12,22,27} are selected out by the feature selector. These segments are not preserved the significant feature of Thai alphabets. The segments {9,12,22,27} have been shown from the experiments that most of the time they are not on.

The back-propagation network we used has three layers for both roughly classifier and output recognition process. All networks has 24 neurons for hidden layer. The first network is used for roughly classify all 44 alphabets into eight groups and the remaining network is created for recognizing the output codes. In the first network, there are 24 input neurons, and 3 output neurons, the output result is in binary code from 000 to 111. In the second step, the networks also has 24 input neurons but the number of output neurons is different for each group. All networks

are trained with the error level = 0.001.

For the training patterns, the model achieve 100% of correct output patterns. Then we test the recognition rates for more 77 untrained patterns which have been written by five people. The recognition rate for the final step is 70% and for the first network is 92%. The recognition rate of the final process is not quite high because all alphabets of each group look very similar as illustrated in Figure 2b. We will proceed the future experiment to improve this recognition rate by adding more training patterns of each group. Some of the difficult untrained patterns which can be recognized by our model can be seen in Figure 5. We have tried to train all raw training patterns with back-propagation network alone, without applying the light sensitive model. The result is shown that the network cannot be learned at all and the computation time is very slow.

Our technique is VLSI implementable. The light sensitive segments are possibly implemented by using some semiconductor cells [7]. We may use a ROM as a table lookup for recognizing the segment vectors instead of using a neural network, which is more difficult to implement. The actual size of the ROM is not known at this moment. We need to collect more data from the experiments.

7. Conclusion

A new efficient and VLSI implementable technique for handwritten alphanumeric recognition is proposed. The experiments confirm that our approach is much better than the current techniques in terms of time and space complexities. Especially, our technique gives the effective and efficient results for a large set of input images which form many different classes such as Thai language which could not be able to learn by the back propagation alone.

References

[1] Chidchanok Lursinsap and Chularat Khunasaraphan, "Simulated Light Sensitive Model for Handwritten Digit Recognition", *IJCNN'92*, Vol. IV, pp. IV-14 - IV-18.

[2] Kiyotoshi Matsuoka, "Noise Injection into Inputs in Back-Propagation Learning", *IEEE Transactions on Systems, Man, and Cybernetics*, Vol. 22, No. 3, May/June 1992.

[3] Y. Hirose, K. Yamashita, and S. Hijiya, "Back Propagation Algorithm Which Varies the Number of Hidden Units", *Neural Network*, Vol. 4, pp. 61-66, 1991.

[4] S. Knerr, L. Personnaz, and G. Dreyfus, "A New Approach to the Design of Neural Network Classifiers and Its Application to the Automatic Recognition of Handwritten Digits", *International Joint Conference on Neural Networks*. I.91-I.96, 1991.

[5] T. Shimada, K. Nishimura, and K. Haruki, "A New Self-Organizing Method and Its Application to Handwritten Digit Recognition", *International Joint Conference on Neural Networks*, I.275-I.281, 1991.

[6] T.P. Vogel, K. L. Blackwell, S. D. Hyman, G. S. Barbour, and D. L. Alkon, "Classification of Hand-Written Digits and Japanese Kanji", *International Joint Conference on Neural Networks*, I.97-I.102, 1991.

[7] Y. L. Cun, L. D. Jackel, B. Boser, J. S. Denker, H. P. Graf, I. Guyon, D. Henderson, R. E. Howard, and W. Hubbard, "Handwritten Digit Recognition: Application of Neural Network Chips and Automatic Learning", *IEEE Communication Magazine*, November, pp. 41-46, 1989.

[8] C. Mead, *Analog VLSI and Neural Systems*, Addison-Wesley Publishing Co., 1989.

[9] K. Fukushima, "Neocognitron: A Hierarchical Neural Network Capable of Visual Pattern Recognition", *Neural Networks*, Vol. 1, No. 2, pp. 119-130, 1988.

[10] C. Bruce, R. Desimore, and C. G. Gross, "Visual Properties of Neurons in a Polysensory Area in Superior Temporal Sulcus of the Macaque", *Journal of Neurophysiology*, 46(2), pp. 369-384, 1981.

[11] D. H. Hubel, and T. N. Wiesel, "Receptive Fields, Binocular Interaction and Functional Architecture in the Cat's Visual Cortex", *Journal de Physiologie*, 160(1), pp. 106-154, 1962.

[12] A. K. Jain, "statistical Pattern Recognition", *Lecture Note*, Department of Computer Science, Michigan State University, East Lansing, MI, 48824.

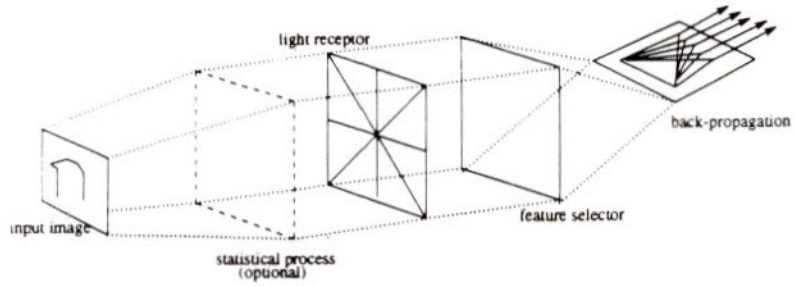

Figure 1. The structure of our organizer.

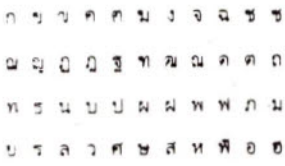

Figure 2a. 44 typed Thai alphabets.

Figure 2b. Eight groups of Thai letters from statistical process.

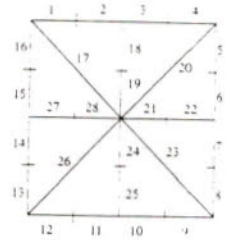

Figure 3. Receptor cell for Thai handwritten recognition.

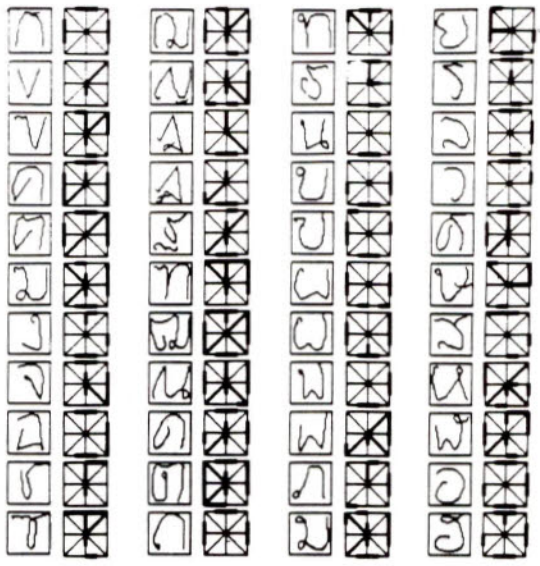

Figure 4. The input image and the corresponding light receptor segments which are "on" of Thai alphabets.

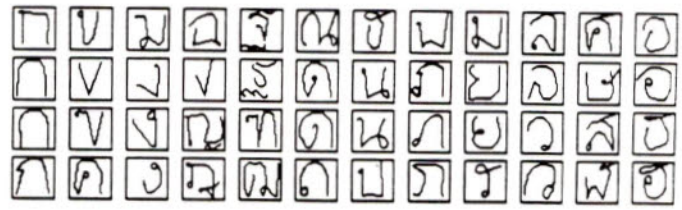

Figure 5. Examples of recognized Thai letters.

High Performance Amorphous Silicon Solar Cells

Porponth Sichanugrist
Fuji Electric Corp. R&D, Ltd.,
2-2-1 Nagasaka, Yokosuka-shi,
Kanagawa-ken 240-01, JAPAN

1. Introduction

Amorphous silicon (a-Si) has become one of the most promising materials for mass production of low-cost solar cells. Material cost a-Si solar cell is about 1/200 times cheaper than the one for crystalline silicon (c-Si) type solar cells since just thin film is needed. Manufacturing processing is much easier since it can be fabricated by plasma CVD at relatively low temperature as low as 200°C and simple processes which can be automatically controlled such as laser patterning, screen printing are utilized.

Recently, the technology for the a-Si solar cells has made remarkable progress in recent several years. In this paper, the present status of a-Si solar cell technology at Fuji Electric is presented and furthermore, the advantages of a-Si solar cells when it is applied to power use in Thailand is also discussed.

2. Device Structure

Fuji electric's a-Si solar cell has a tandem structure consisting of double p-i-n junctions. Its schematic diagram is shown in Fig.1. The top cell with thin i-layer is deposited first on the transparent electrode (tin oxide) coated on the glass by plasma CVD method. Then the bottom cell with thicker i-layer is deposited successively and finally the metal electrode is sputtered on a-Si as the back electrode. Up to now, high efficiency of 12.5 % was achieved with this device structure.

3. Large-area Submodules

The above-mentioned tandem structure is also applied to large-area submodules with a monolithic series connected structure shown in Fig.2. As seen from this figure, the submodule is divided into a number of unit cells, and the metal electrode of a unit cell is connected to the transparent of the next unit cell to make series connection. The size of

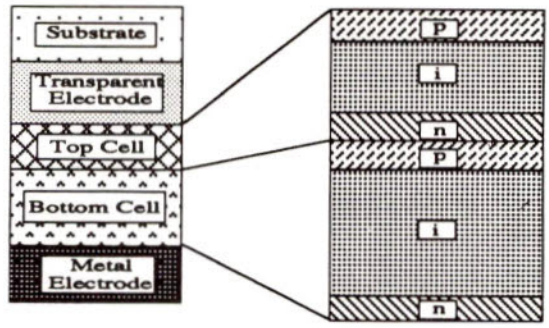

Fig.1 Schematic diagram of a-Si tandem cell

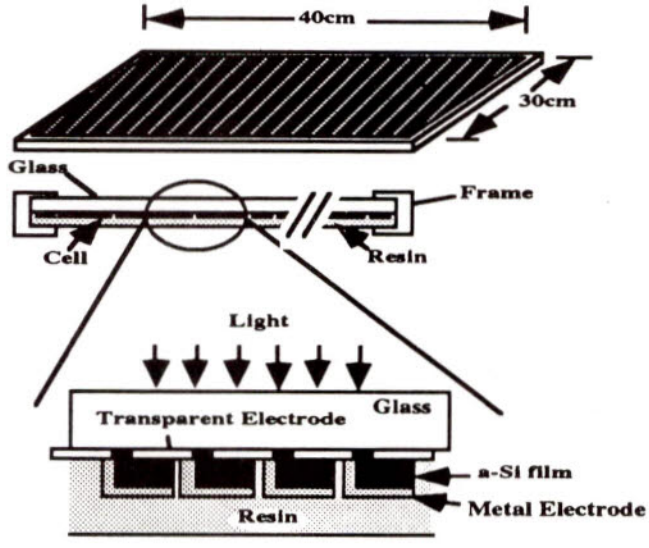

Fig.2 Structure of 30cm x 40cm a-Si tandem structure

submodule is 30cm x 40cm which can be scale up to 30cm x 120cm. A total-area efficiency of 10.5% (12.6Wp) was obtained so far on 30cm x 40cm area submodules.

4. Discussion

The technology of a-Si solar cell has made remarkable progress as described previously though the efficiency is still not so high compared with c-Si solar cells. However, it is important to note that a-Si solar cell has some advantages in the practical power application.

The drop in efficiency at higher temperature is much smaller than that of c-Si solar cells because of wider gap material. Figure 3 shows the efficiency of a-Si cell normalized by the value at 25 °C as a function of cell temperature. That of typical c-Si solar cell is also shown in the same figure. This feature is very important when the PV is used in summer or in tropical area such as Thailand since under such situations, the cell temperature easily increases up to 60-70 °C.

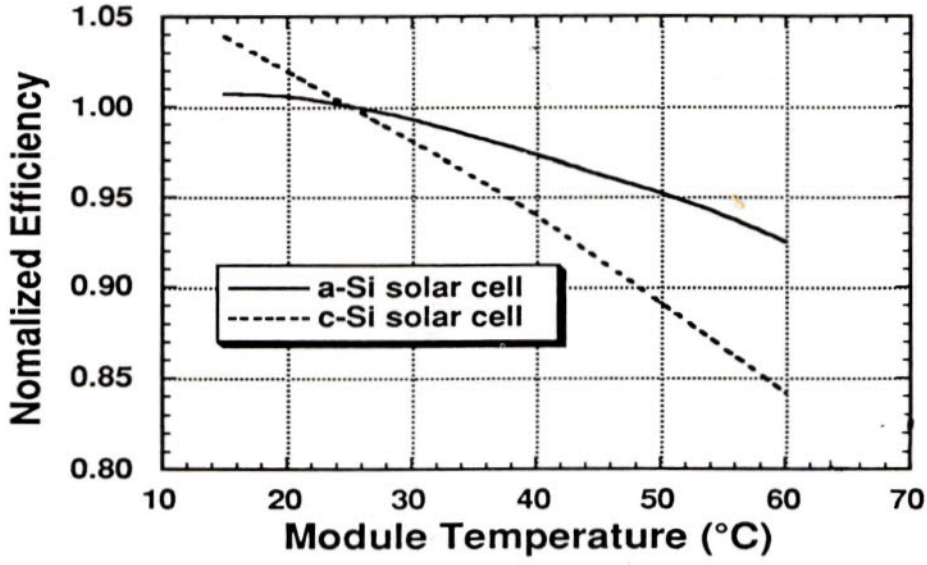

Fig.3 Temperature dependence of efficiency for a-Si and c-Si solar cells

ATPAC Information Systems for Advanced Science and Technology Transfer to Thailand

Voratas Kachitvichyanukul
Cholthanee Koerojna

Third International Conference for
Advanced Science and Technology
Transfer to Thailand

Bangkok, Thailand
July 23-25, 1993

Introduction

The Bulletin Board System (BBS) Committee and the Information Systems Committee were formed at the First Annual Seminar of Thai Professionals in North America during July 22-23, 1991 in Maryland. Their goal was to develop an information system to serve as a medium for Thai professionals in the U.S. and Canada to exchange expertise and provide professional support when the need arose.

Since that meeting in Maryland, a follow-up meeting was held in Washington DC in November 7-8, 1991 to review and approve the preliminary design of these systems. The first prototype of the information system was complete in late January 1992. The Clarion based ATPAC Database System was installed at the Office of the Science and Technology Counsellor (OSTC) in May 1992 and at the Siam Commercial Bank (SCB) in Nondhaburi, Thailand in August 1992. Because of the limitations, inflexibility, and lack of expertise in continuing support of a Clarion based system, the DBMS has been changed to FoxPro. The following sections describe the ATPAC information system as designed.

The ATPAC Information System

The ATPAC information system consists of the following components: the Bulletin Board System (BBS) and the ATPAC Database system. The system design of each component will

be described briefly as follows.

The ATPAC BBS

The ATPAC BBS has the same system design as many of the public access BBS's in the U.S. The major purpose of this system is to serve as a medium for the members to exchange mail-messages and news items electronically. The current design uses public domain software packages to handle the common BBS functions. The list of software packages utilized are shown in Figure 1.

Software	Function
Maximus 1.02	BBS System
Binkleyterm	Communication Program
Fossil	Communication Driver

Figure 1. Components of the ATPAC BBS.

The ATPAC BBS system was installed at the OSTC and access is available to all members. In Thailand, ManGroup has provided an option on ManNet to select the ATPAC BBS. Khun Wiroj Assawarungsi and Khun Rawich Poomrin from ManGroup are providing technical support and maintenance in Bangkok. Since the telephone number to use the BBS is a long distance Toll number, the cost will limit the number of people accessing through long distance. Allowing access to the BBS is the decision of the local site.

The ATPAC Database System

The ATPAC Database was designed to provide the following information:

1) Biographical and Expertise Information of Members
2) Company Biographical Information
3) Organization Needs and Areas of Interest
4) News and Articles

The member biographical section of the database stores the address, expertise, resumes and any research papers that members have written or published. The Company Biographical Information section contains information about the size, amount of sales, and computer system information of an organization. The Organization Need/Area of Interest section contains information about areas that companies in Thailand want to be involved in and expertise that they currently need. The news and articles section is self-explanatory.

The system is being re-developed using FoxPro, a relational database management development tool for the PC. FoxPro is a Microsoft product that contains one of the fastest DBMS's available on the PC platform. The new version has a good Graphical User Interface, an easy querying and reporting tool, and can incorporate images into

the data. At this time, the database specification is fairly stable but any suggestions or comments are welcome and should be directed to any of the members of the BBS and Computer Committee. Security will be implemented later in the development stage.

Hardware/Software Requirements

To develop and install the ATPAC database system the following is required:

1) A Personal Computer using a 386sx or higher Microprocessor
2) 4 MB of memory (8 Recommended)
3) a 5.25 high density or 3.5 high density disk drive
4) minimum hard disk of 40MB (100 recommended)
5) FoxPro 2.5
6) Windows 3.0 or higher if using FoxPro 2.5 for Windows
7) A pointing Device

Hardware/Software Requirements for Users

For access to the BBS or ATPAC database system remotely, a computer terminal or Personal Computer with communications software, modem and a phone line are required.

Maintenance of the ATPAC System

ATPAC Database and ATPAC Database Application

The ATPAC Information Systems Committee is responsible for maintaining the database and updating/enhancing the application. Any necessary enhancement or modification requests must be submitted to the ATPAC Information System Committee of ATPAC.

ATPAC Data

The biographical, expertise and resume information of Regular and Associate members will be entered and maintained at the ATPAC office in the U.S.

The U.S. and Canadian company biographic, organization needs, areas of interest, news and articles will be entered and maintained at the ATPAC office in the U.S.

The Thailand company biographic, organization needs, areas of interest, news and articles will be entered and maintained at the Siam Commercial Bank Information Technology Center.

The exchange of information between Thailand and the U.S. will be accomplished through file transfer via Internet, modem, or diskette.

Access to the ATPAC Systems - Policy and Procedures
Both systems can be accessed at the following locations:

1. Siam Commercial Bank
   Financial Information Technology Research Center
   SCB Information Technology Center
   111/178 M.5 Jangwattana Road
   Pakkred, Nondhaburi 10210, Thailand

   Contact Person: Ms. Pavadee Phongpana-ngam
   Phone: (662) 502-1058
   Fax: (662) 583-0155

2. Office of the Science and Technology Counsellor (OSTC)
   The Royal Thai Embassy
   4301 Connecticut Avenue, NW #429
   Washington, D.C. 20008 USA

   Contact Person: Science and Technology Minister
   Phone: (202) 364-2800/2801/2802
   Fax: (202) 362-2806

Once ATPAC has received the appropriate membership dues, a user-id and password will be assigned for access to the BBS and ATPAC database. At the time of the design, a general access policy has been established for the BBS. Once the user has an id and password, they can access the BBS at anytime.

Access to the ATPAC database system is handled a little differently. There are two types of access - Regular/Associate and Institutional Members. Once a Regular and Associate members have a user-id and password, they are able to access their own personal data as well as company biographic and interest/need information. Institutional members will have a designated person who will be responsible for either accessing the database directly or submitting written requests for the database searches. Institutional members may access Regular and Associate members' names and expertise information. Company biographic data can only be accessed by a companies own representatives. However, company interest/need information has public access. After a search is completed, the institution will have a list of ATPAC members who have expertise that match the search criteria. ATPAC will contact the individuals on the list to determine if he/she would like his/her resume to be given to the institution. Figure 2 displays a brief synopsis of information access.

Type of Data	Regular/Associate Member	Institutional Member
Regular/Associate Member Biographical and Expertise Information	Owner - All Colleagues - Name and Expertise Information Only	Name and Expertise Information Only
Regular/Associate Member Resume	Owner - All Colleagues - Per Request and By Permission of Member	Per Request and By Permission of Member
Organization Biographical Information	All	Owner - All
Organization Areas of Interest/Needs	All	All
News and Articles	All	All

Figure 2. Access to the ATPAC Database System.

Written requests for searches can be sent to:

1) ATPAC
Office of the Science and Technology Counsellor (OSTC)
The Royal Thai Embassy
4301 Connecticut Avenue, NW #429
Washington, D.C. 20008 USA

Phone: (202) 364-2800/2801/2802
Fax: (202) 362-2806

2) ATPAC
Siam Commercial Bank
Financial Information Technology Research Center
SCB Information Technology Center
111/178 M.5 Jangwattana Road
Pakkred, Nondhaburi 10210, Thailand

Phone: (662) 502-1058
Fax: (662) 583-0155

3) ATPAC c/o Ms. Cholthanee Koerojna
15 Given Drive
Burlington, MA 01803 USA

Phone: (617) 938-1967
Fax: (617) 932-3825

Online Access

Detailed access procedures will be announced in the ATPAC newsletter when they become available.

Summary

It has been a year since the current committee assumed the task of designing and implementing the ATPAC Information System. Many things have been accomplished and yet much more needs to be done. The system is being converted from Clarion to FoxPro. The design has been enhanced to meet changing user need and accommodate as much information as possible. More volunteers are needed in various areas, both technically and geographically, to feed the BBS system with news and information about science and technology regularly in order for the ATPAC BBS system to become the conduit of technology transfer. Anyone interested in helping can contact:

Dr. Voratas Kachitvichyanukul
Phone: (713) 469-9504
Fax: (713) 469-2570

Ms. Cholthanee Koerojna
Phone: (617) 938-1967
Fax: (617) 932-3825

Acknowledgments

The BBS and Computer Committee wish to express their sincere thanks to Khun Chaleo Souvannakitti, Vice Chairman, of Telecom Asia Corp. for the generous financial support, Khun Ong-Art Ithmon of ManGroup for volunteering his staff, Khun Wiroj Assawarungsi and Khun Rawich Poomrin who have assisted the committee on technical and local issues in Bangkok, and Dr. Pomthong Malakul for the coordinating work in Bangkok. The committees would also like to express their sincere appreciation to Khun Vichit Amonviratskul, Executive Vice President Technology Group of SCB, his staff, and the SCB for providing hardware, software, technical support and data entry. Many thanks to the OSTC staff for their help and encouragement on numerous occasions without which this project may not have been possible. Thanks, also, to Dr. Khokiat Kengskool and Dr. Methi Wecharatana, of ATPAC, and Dr. Kamchad Mongkolkul, of the Petroleum and Petrochemical College, for their tireless dedications to the cause of technology transfer. Finally, a heartfelt appreciation to the Damrong Lathapipat Foundation for the idea and effort that brought all of us together to work toward a common goal.

CONTOUR SHAPE MATCHING BY A CONSTRAINT SATISFACTION NETWORK

W. Watunyuta and C. H. Chu

CENTER FOR ADVANCED COMPUTER STUDIES
THE UNIVERSITY OF SOUTHWESTERN LOUISIANA
USL Box 44330
LAFAYETTE, LA 70504

Abstract

The matching of contours based on their shape attributes is an important task in computer vision. This contour shape matching task is formulated as a constraint satisfaction problem and solved using a Hopfield net. Constraints that are intrinsic to the shape matching task are coded in the network interconnection weights. Direct evidences obtained from the observed data, as gauged by a local shape measure, are provided as the external input to the network. The local shape measure used is developed based on an affine transformation model, which is a general class of mapping that includes the rigid body motion. Empirical results are used to demonstrate the performance of this network when applied to match contours that have undergone rotation, or scale–change, or translation, or combinations of these transformations. The network is capable of handling noisy data, as well as a reasonable amount of deformation resulting from object rotation in the three–dimensional space.

1 Introduction

The matching of contours in two-dimensional image planes based on their shape attributes is an important task in computer vision. This task is formulated as a constraint satisfaction problem, where the solution comprises a number of hypotheses, each of which corresponds to a local match between two contour segments. The problem is to be solved by an artificial neural network.

Hypothesis testing or classification problems in statistical pattern recognition can be implemented on an artificial neural network by associating the activation value of a neuron with the degree that the network accepts a certain hypothesis. A key aspect of using neural networks for problem solving is the distributed representation of the solutions [9]. A complex solution is typically represented by a large number of neurons, each representing a hypothesis. Different combinations of such hypotheses constitute alternate solutions to the problem. The neural network is then used to provide a collectively computed solution. A class of problems that maps well to this model is the constraint satisfaction problem, which requires a near–perfect solution with a large set of simultaneous constraints.

A scenario where such problems arises is in processing real world data that lack the precision necessary to allow a search for a perfect solution. Such problems are often encountered in computer vision research: to recover the three dimensional structure of the scene, multiple views obtained either by observing at different times, or from different angles, or by different sensors have to be employed. An underlying issue of all these methods is to extract the information from the redundant data by such processes as feature matching.

In this paper, a particular feature matching task, that of matching contour found in different images based on their shape, is considered. The approach described here is to use a neuron to represent how well a local part from one image matches another local part from another image, as measured by some local shape descriptors. A particular neural network model, the Hopfield network, will be used to solve the constraint satisfaction problem.

2 A Shape Matching Network

The Hopfield network is a constraint satisfaction network that has been used to solve optimization problems [7]. The constraints are to be encoded as the interconnection weights, and the weights are to be symmetric. There would be no network learning associated with this paradigm in that the weights must be set initially and are not to be changed. A connection weight can be determined by encoding a constraint between two different

hypotheses such that the sign of any particular weight depends on whether one hypothesis supports or refutes the other. Only the total input to each neuron will be changed over time which can be described by:

$$\frac{du_i}{dt} = -\frac{1}{\tau_i}u_i + \sum_j T_{i,j}V_j + I_i ,$$

where u_i is the total input to the ith neuron, $T_{i,j}$ represents the connection weight between the ith and the jth neurons, τ_i is a constant that controls the rate of change of u_i, V_j is the activation value of the jth neuron, and I_i is the external input to the ith neuron. The overall solution can be interpreted and analyzed by a minimizing criterion which depends on the weights. Since the activation of the entire network is continuous, the occurrence of the solution can be observed by the time the network reaches a *stable* state which corresponds to a minimum of the energy equation:

$$E = -\frac{1}{2}\sum_{i,j} T_{i,j}V_iV_j - \sum_j I_jV_j .$$

The Hopfield network is used to solve the matching problem, and the choice of the interconnection weights will be described below. Given two contours and a fixed point on each of them, the local shape change descriptor will make use of information local to each point to determine the difference in shape between the two contour segments. Since the matching is performed locally, each contour has to be initially partitioned and represented by a sequence of tokens. It is these two lists of tokens that will be matched. Specifically, the matching problem is that given a list of tokens find a match for each token from another list. A match between tokens A and B, where A is from the first list and B is from the second, therefore form one hypothesis.

Connection Weights

Suppose there are N_a and N_b tokens representing the two contours, respectively. Assuming $N_a \leq N_b$, a solution constitutes N_a hypotheses and they are to be selected from among the $N_a \times N_b$ possible hypotheses. There are therefore $N_a \times N_b$ nodes in the constraint satisfaction network to represent the hypotheses. The local shape change descriptor is used to provide direct input that are determined by the particular contours that being matched. The connections, on the other hand, are to be set according to the intrinsic properties of the shape matching task. The connection weights are thus providing the general constraints required for *any* contour shape matching problem, while the external input describes *which* contour shape matching problem is to be solved.

The $N_a \times N_b$ neurons can be organized as a two dimensional matrix. The (i,j)th neuron of this matrix, denoted as n_{ij}, will represent the hypothesis that the ith token from the first list is a match for the jth token from the second. Note that another neuron on the same column, n_{ik}, represents the hypothesis that the same ith token should match the kth token from the second list. These two hypotheses are in conflict with each other, thus the neurons n_{ij} and n_{ik} are mutually inhibitive. Similarly, the neurons n_{lj} for all values of l will be inhibitive to n_{ij}. Inhibitive weights are therefore set so that every node has an inhibitive connection to every other node on the same row and to every other node on the same column.

Some further assumptions are made about the problem. First, the tokens are to appear in the same order on both contours. With this assumption, a neuron will have an excitative connection to another neuron if that other neuron represents a hypothesis that would preserve the order of the match. For instance, the neuron n_{ij} matches the ith token from a list to the jth token of the other. This neuron would support a neuron n_{kl} provided both $k > i$ and $l > j$ or both $k < i$ and $l < j$. It will have the strongest support when $k = i + 1$ and $l = j + 1$ or when $k = i - 1$ and $l = j - 1$. In fact, if the two lists have the same number of tokens, e.g. N, the excitatory region of a neuron can simply be assigned to the neurons along the diagonals of the $N \times N$ matrix of neurons.

Direct Input

Thus far the nature of the tokens has not been restricted: the weights are set according to the geometry of the problem. The tokens could be any features on the image plane such as curve segments. The direct input is simply responsible for telling the network how well-matched a particular pair of tokens are based on local information.

Let (a_i, b_j) be a pair of tokens where a_i is from contour A and b_j is from contour B. The information *local* to the matching process for (a_i, b_j) is considered to be the segment of A from a_{i-1} to a_{i+1} and the segment of B from b_{j-1} to b_{j+1}. The nature of the matching tokens determines the choice of the shape measure. The matching token used in this paper is the set of curvature extremum points on the contour, which is known to capture the essential shape of contour [2].

A general method for describing the local shape change accurately is by using an affine transformation model, which has a linear and a translational part. The affine transformation of two dimensional data is given

by:

$$\begin{bmatrix} p_i \\ q_i \end{bmatrix} = \begin{bmatrix} a & b \\ c & d \end{bmatrix} \begin{bmatrix} x_i \\ y_i \end{bmatrix} + \begin{bmatrix} e \\ f \end{bmatrix}, \quad (1)$$

where (x, y) is in the domain and (p, q) is in the range. This transformation is characterized by six parameters: a, b, c, d, e, and f. Equation 1 can be solved by using at least three pairs of points. Only the first four parameters associated with the linear transformation are needed to measure the local shape change.

This linear transformation can be used to represent a wide class of deformation. The effect of a deformation by a linear transformation can best be seen through the mapping of a circle; i.e., consider the hypothetical case of the tokens in a list forming a circle. Clearly, a, b, c, and d can take on many values, corresponding to an infinite number of transformations. Among them, scale change and rotation are special cases. If $a = d = s\cos\theta$ and $c = -b = s\sin\theta$, the relation would be a scale change with factor s and a rotation of angle θ about an axis perpendicular to the image plane. There is no shape deformation in this case since a circle is mapped back to a circle after a scale change, or a rotation, or both. The transformation in this case is a unitary one, hence a unitary transformation indicates no deformation.

Any other linear transformation maps a circle into an ellipse; i.e., a linear transformation that is not unitary introduces a shape change. The amount of the elongation of the ellipse is a measure of the deformation. From matrix theory [5], the elongation of the ellipse can be measured by the condition number $\kappa(A)$ of the transformation matrix A: $\kappa(A) = \|A\|\|A^{-1}\|$, where $\|A\|$ is the norm of A. The larger the condition number, the more severely deformed the circle is; A is said to be "ill–conditioned" for large value of $\kappa(A)$. When the condition number is 1, A is "perfectly–conditioned" and the transformation is a unitary one. The 2–norm condition number is given by:

$$\kappa(A) = \frac{\sigma_1(A)}{\sigma_2(A)},$$

where $\sigma_1(A)$ and $\sigma_2(A)$ are the two singular values of A, and that $\sigma_1 > \sigma_2$. A dilatation measure δ defined in [1] [4] is given by:

$$\delta(A) = \frac{\lambda_1(A)}{\lambda_2(A)},$$

where $\lambda_1(A)$ and $\lambda_2(A)$ are the larger and the smaller eignevalues of A^TA, respectively. Since $\lambda_i(A) = \sigma_i{}^2(A)$ for i = 1, 2, $\delta(A) = \kappa^2(A)$. A geometrical interpretation of $\kappa(A)$ is that it is the ratio M/m, where M and m are the lengths of the major and the minor axis of the ellipse, respectively.

The ratio of M/m has values that range from 1 to ∞, which is undesirable because a good local match formed by accident might overwhelm the entire network. In [1], a *sphericity* measure, denoted γ, is defined in terms of λ_1 and λ_2:

$$\gamma = \frac{\sqrt{\lambda_1\lambda_2}}{(\lambda_1 + \lambda_2)/2}.$$

The sphericity measure is acceptable as an input function because it ranges from -1 to 1. The sphericity, in terms of a, b, c, and d, is given by:

$$\gamma = \frac{2(ad - bc)}{a^2 + b^2 + c^2 + d^2}. \quad (2)$$

After the transformation process, all the outcome direct evidences are to be used to search for the global matching result. In [1], a "hopping" dynamic programming procedure is used to search for a global match from among the sphericity values. Dynamic programming has been used to match local features decribed by Fourier descriptors [6]. A stochastic labelling procedure has also been used to solve the segment matching problem [3]. The constraint satisfaction network used here is an alternative optimization method.

3 Experiments

The shape matching network was tested experimentally for its tolerance of imprecise direct input and for its ability to handle rigid body motion both in a plane parallel to the image plane and in three–dimensional space. A network size of 10 × 10 is used for most of the experiments described here.

The first set of experiments was performed to determine the degree of noisy input that the network can tolerate. An ideal input pattern in the form of an $N \times N$ identity matrix was corrupted by a known amount of uniformly distributed random noise. Here, no token extracted from the image plane is considered, hence the affine transformation process is omitted. The input patterns are synthesized and are fed directly to the network. The results of presenting this input with various degrees of corruption are summarized in Table 1. The values of N used in these experiments are 5, 10, and 16. Note that the total number of neurons in the network is given by each value of N in column 1 times itself. The number of neurons to be corrupted is controlled by a parameter `falsenodes` listed on the fourth column of the table. If a neuron is to be corrupted and its original ideal input value is 1, the new input is reduced to be a value between a parameter `tnoise` and 1. On the other hand, if the neuron has an original ideal input value of 0, the

new input is between – **mnoise/2** and **mnoise/2**. The parameters **tnoise** and **mnoise**, both scaled by 1000, are listed on the second and third columns of the table, respectively. In the fifth column, **SF** is a parameter denoting the scaling factor for the interconnection weights in the network. Lastly, a unique solution is said to be *not found* if every neuron of more than one diagonal had the maximum activation value as listed on the sixth column of the table. The results show that the network can tolerate up to 33% of noisy input, with the noise level at up to 25% of the original input.

A second set of experiments was used to test the performance of the network for matching two lists of curvature extrema that have undergone rigid body motion in a plane parallel to the image plane. The two sets for a rotation of 30° are shown in Figure 1, where the first list is marked by asterisks and the second list is marked by diamonds. The direct input are computed and shown in Figure 2. The network found the correct match after 500 iterations (Figure 3). The results show that the network can handle all combinations of rotation, translation, and scale change that are confined to the plane parallel to the image plane.

For the last set of experiments, the network was tested for the performance of matching two lists of curvature extrema that have undergone rigid body motion in three dimensions. Specifically, the list is rotated about an axis that is parallel to the y–axis; i.e., the contour is rotated away from the image plane. Furthermore, a perspective transformation is used as the model for the imaging process. The rotation angles tested are: 10°, 20°, 25°, 30°, and 45°. The network found the correct solution for the case of 10°, 20°, and 25°. In the cases of 30° and 45° rotations, unique solutions are still found, but they do not correspond to the correct solutions. It should be noted that the object is assumed to be at a distance from the image plane equal to the focal length, hence the rotation angles used here result in gross deformation of the shapes of objects.

4 conclusions

A constraint satisfaction network was constructed to match two contours represented by their curvature extrema locations. The performance of the network was tested for its tolerance of noisy input, as well as for its ability to match contours that have undergone rigid body motion in three dimensions. It should be noted that the affine transformation can be generalized to match entire contour segments, hence the network is not confined to matching point patterns.

ACKNOWLEDGMENTS — The authors would like to thank Professor Nirwan Ansari of the Department of Electrical and Computer Engineering at the New Jersey Institute of Technology for his suggestions.

References

[1] N. Ansari and E. J. Delp, Patial shape recognition: A landmark based approach. *IEEE Trans. Pattern Analysis and Machine Intelligence*, vol. PAMI-12, no. 5, May 1990.

[2] P. J. Besl and R. C. Jain, Three–dimensional Object Recognition. *Computing Surveys*, vol. 17, pp. 75–145, March 1985.

[3] B. Bhanu and O. D. Faugeras, Shape Matching of Two–dimensional Objects. *IEEE Trans. Pattern Analysis and Machine Intelligence*, vol. PAMI-6, no. 2, pp. 137–155, March 1990.

[4] F. L. Bookstein, Tensor Biometrics for Changes in Cranial Shape. *Annals of Human Biology* vol. 11, no. 5, pp. 413–437, 1984.

[5] G. H. Golub and C. F. Van Loan, *Matrix Computations*. The Johns Hopkins University Press, second edition, Baltimore, MD., 1989.

[6] J. W. Gorman, O. R. Mitchell, and E. P. Kuhl, Partial Shape Recognition Using Dynamic Programming. *IEEE Trans. Pattern Analysis and Machine Intelligence*, vol. PAMI-10, no. 2, pp. 257–266, March 1990.

[7] J. J. Hopfield and D. W. Tank, 'Neural' Computation of Decisions in Optimization Problems. *Biological Cybernatics* vol. 52, pp. 141–152, 1985.

[8] R. P. Lippmann, An Introduction to Computing with Neural Nets. *IEEE Acoustics, Speech, and Signal Processing Magazine*. pp. 4–22, April 1987.

[9] D. E. Rumelhart, J. L. McClelland, and the PDP Research Group, *Parallel Distributed Processing*, volume 1. The MIT Press, Cambridge, Mass., 1986.

[10] V. Vemuri, *Artificial Neural Networks: Theoretical Concepts*. Computer Society Press Technology Series. IEEE Computer Society Press, Washington, D.C., 1988.

Table 1: Results of the experiments with noise added to the input of the shape matching network.

N	mnoise	tnoise	falsenodes	SF	Solution found	Number of iterations
5	100	900	9	1	Yes	5000
5	250	750	9	1	Yes	5000
10	100	900	33	1	Yes	5000
10	250	750	33	1	Yes	5000
10	250	750	33	10	No	2750
10	250	750	50	50	No	1000
10	250	750	33	100	No	680
16	100	900	85	1	Yes	4500
16	100	900	85	100	No	300

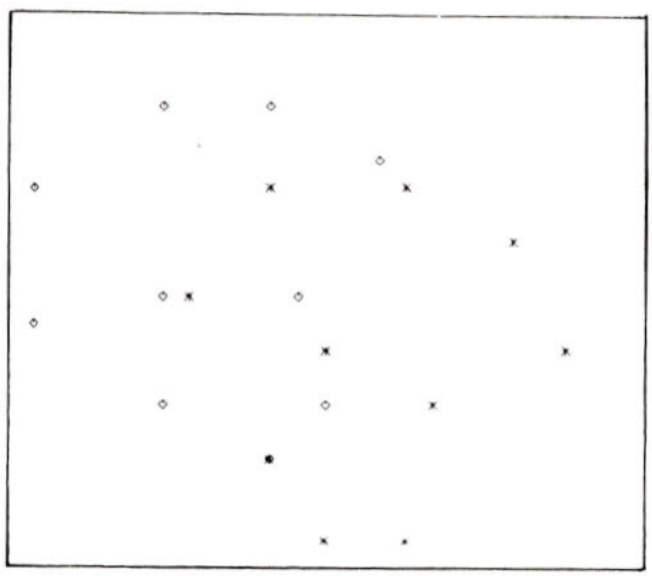

Figure 1: Two sets of curvature extrema to be matched. The first set is marked by asterisks, and the second set is marked by diamonds.

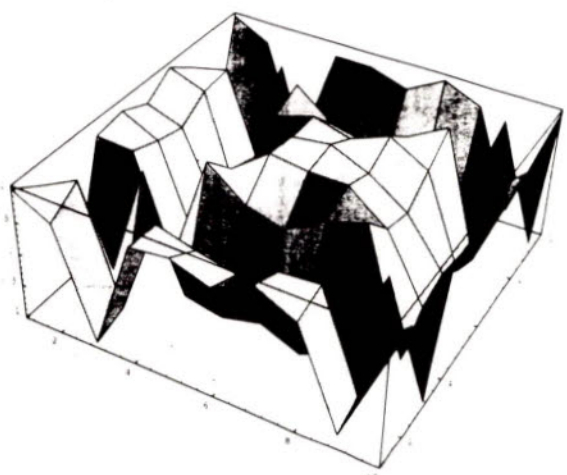

Figure 2: The direct input to the network for matching the two sets shown in Figure 1.

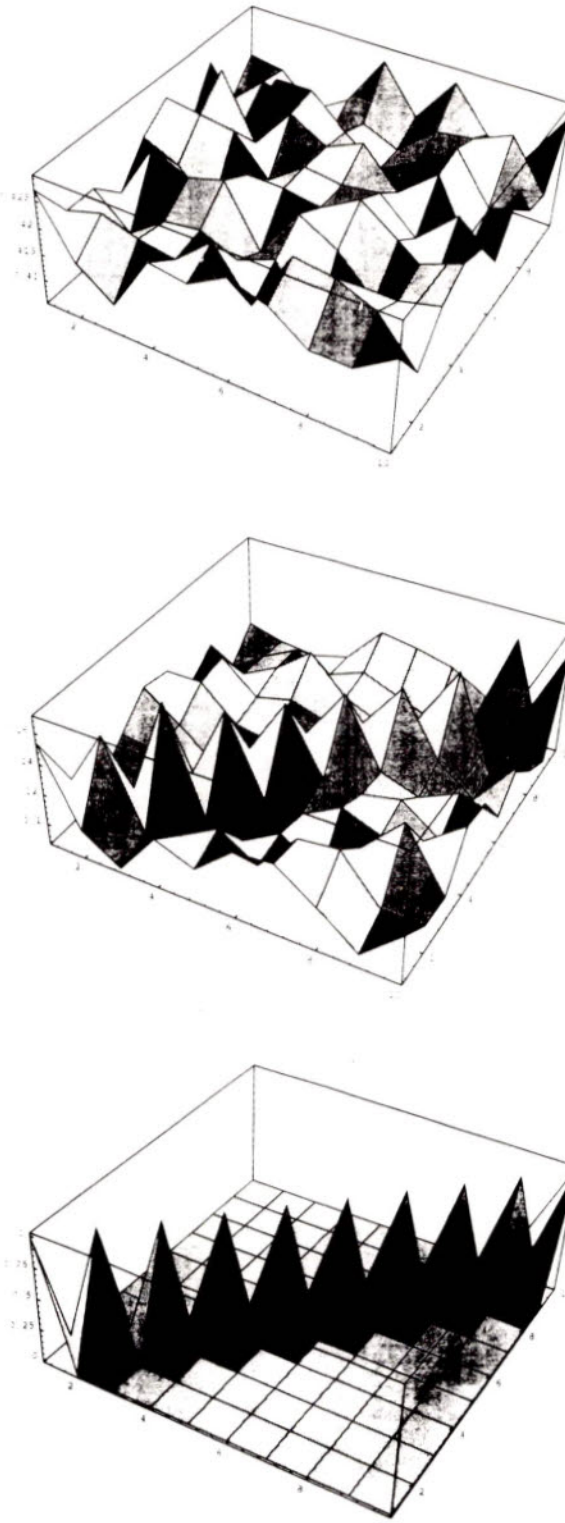

Figure 3: The activation levels of the network after 10, 120, and 600 iterations, respectively. Note that the scale along the z-axis changes with the maximum activation level.

CHARACTERISTICS OF GLOBAL LABOR FORCE IN THE YEAR 2000

Dr. Kris T. Rugsaken

Introduction

One of the most pressing issues of the world today is technological development which is the basis for economic and political development of the nation. The demographic composition of the world is changing much more rapidly than it is realized. In many respects, changes of one nation are driven by the developments of the larger society. The demographic trends in the nation are further complicated by the economic and political competitions. One nation cannot survive by its own without interrelating to and depending upon other nations. Among these many changes, the issue that is less realized but is equally important as other components is the human resources. Without this component, tasks cannot be completed to challenge the future goals of the world. Therefore, along with technological development, it is imperative to project and be prepared for the types of the labor force of the future. Just as managers speak of world markets for products, technology, and capital, they must now think in terms of a world market of labor.

This article examines trends of the global labor forces. Presented are projected characteristics of the labor force of Thailand as well as those of other industrialized and developing nations through the year 2000.

The Changing World Labor Forces

The developments of the next decade are rooted in today's demographics, particularly those having to do with the size and character of various countries's work forces. In some areas of the world, for instance, women have not yet been absorbed in large numbers and represent a huge untapped resource; elsewhere the absorption process is nearly complete. Such national differences are a good starting point for understanding what the globalization of labor will look like and how it will affect individual nations and companies.

Although looming labor shortages have dominated discussion in many industrialized nations, the world work force is growing fast. From 1993 to 2000, the work force is expected to grow by some 294 million people for the world and about 4 million people for Thailand where the total population is expected to grow by nearly 8 million. The global growth will take place unevenly. The vast majority of the workers will join the work forces of the developing countries. In countries like Pakistan and Mexico, for example, the work force will grow at about 3 percent a year whereas in Thailand the growth is projected at 1.7 percent a year. In contrast, growth rates in the United States, Canada, and Spain will be closer to 1 percent a year. Japan's work force will growth just .5 percent, and Germany's work force will actually decline.

The much greater growth in the developing world stems primarily from historical higher birth rates. But in many nations, the effects of higher fertility are magnified by the entrance of women into the work force. Not only will more young people enter the work force but also million of women in industrializing nations are beginning to leave home for paid jobs.

Moreover, the work force in the developing world is also better and better educated. The developing countries, including Thailand, are producing a growing share of the world's high school and college graduates.

When these demographic differences are combined with different rates of economic growth, they are likely to lead to major redefinitions of labor markets. Nations that have slow-growing work forces but rapid growth in service sector jobs such as Japan, Germany, and the United States, will become magnets for immigrants. Nations that produce prospective workers faster than their economies can absorb them will export people.

Beyond these differences in growth rates, the work forces of various nations differ enormously in make-up and capabilities. It is precisely differences like these in age, gender, and education that give us the best clues about what to expect in the year 2000.

More than half of all women between the ages of 15 and 64 now work outside the home, and women comprise one-third of the world's work force. In the 1990s, women will enter the work force in greater numbers and the average age of the world's work force will rise, especially in the developing countries. Based on the public figures of 1988, the population of Thailand was 54,589,000. Of these, 27,404,000 or 50.2% were men and 27,185,000 (49.8%) were women. Although the total population of women was slightly below that of men, the number of women caught up with men starting at age 40 and exceeded that of men starting at age 50. Between 1950 and 1990, the rates of women's participation in the work force increased by 28% for Brazil, 30% for Hong Kong, 29% for Mexico, 38% for Singapore, 27% for South Korea, and 32% for Thailand. In Japan, about 58% of women hold paid jobs. And for ideological reasons, China, with one of the lowest GNPs per capita of any nation, has female participation rates that are among the world's highest.

The degree of female labor force participation has tremendous implications for the economy. In many cases, rapid work force growth stimulates and reinforces economic growth. If other conditions are favorable, countries with women ready to join the work force can look forward to rapid economic expansion.

As a result of the slower birth rates and longer life spans, the world's population and labor forces are aging. The average age of the world's workers will climb by more than one year, to about 35, during the 1990s. But here again, it is important to distinguish between the developed and developing countries. The population of the industrialized nations is much older. Young people represent a small and shrinking fraction of the labor force, while the proportion of retirees over 65 is climbing. By 2000, fewer than 40% of workers in countries like the United States, Japan, Germany, and the United Kingdom will be under age 34, compared with 59% in Pakistan, 55% in Thailand, 59% in the Philippines, and 53% in China. The share of workers over age 65 will increase for most nations. Worldwide, over 6.8% of the labor force will be 65 years or older. For industrialized countries like the United States, Germany, Japan, and the United Kingdom, at least 13% of their labor forces will be over 65 years of age, compared with 7.3% for China, 4.2% for Indonesia, 3.9% for Pakistan, 4.9% for Mexico, 3.8% for the Philippines, and 5.2% for Thailand.

People worldwide will be increasingly well-educated. The developing countries will produce a growing share of the world's high school and college graduates. In the decade and a half between 1970 and 1986, world high school enrollments grew by some 120 million students, or more than 76 percent. College enrollments grew more than 100% during the same period, from 26 million to 58 million. This trend is likely to continue as nations and individuals increasingly recognize the economic value of

education. By the year 2000, it is likely that high school enrollments could grow by another 60%, reaching nearly 450 million, and college attendance could double again to top 115 million.

In 1990, higher percentages of children in industrialized nations attend high school and college. The United States, Japan, Canada, France, and Australia all have more than 95% of high school age children in schools. In some developing countries, however, high school education just started to catch on. Pakistan had 18% of high school age children in school. Elsewhere the figures were: 42% for China, 35% for India, 41% for Indonesia, 68% for the Philippines, 95% for South Korea, and 29% for Thailand. While 59% of people of college age in the United States were in college, 20% of the Thai people of the same age group attended college, compared with 2% for China, 38% for the Philippines, and 5% for Pakistan.

But an important shift is underway: the developing world is producing a rapidly increasing share of the world's skilled human capital. This trend has been underway for some time and will accelerate through the turn of the century. In the decade and a half from 1970 to 1986, the United States, Canada, Europe, Russia, and Japan saw their share of world high school enrollers shrink from 44% to 30%. If that trend continues, their share is expected to drop to 21% by the year 2000. U.S. high school students made up 9% of world enrollers in 1970 but only 5% in 1986. The developed world is also losing ground when it comes to higher education. Between 1970 and 1985, the share of the world's college students from the United States, Canada, Europe, Russia, and Japan dropped from 77% to 51%. The share of college students in the developing world, including Thailand, leaped from 23% to 49%, and these figures may be understatements because a great number of students in Western universities are from developing countries and will return home when they graduate. By the year 2000, students from developing nations will make up three-fifths of the world's college students.

It is true that in absolute numbers, the United States, Russia, and Japan are still the leading producers of college graduates of all kinds. However, a growing number of the world's college graduates are from outside of the traditionally highly- educated countries. Four of the next six greatest sources of college graduates are developing countries: Brazil, China, the Philippines, and South Korea. Differences in numbers of graduates are intriguing when sorted by discipline. China and Brazil rank third and fifth, respectively, in numbers of science graduates, following by Japan. For engineering graduates, Brazil, China, Mexico, Korea, and the Philippines all place ahead of France and the United Kingdom. For Thailand, although the numbers of graduates in the two areas have slightly improved during the last few years, it still lagging far behind other developing nations.
In 1992, the number of Thailand's graduates in Science and Engineering is expected to be around 3,520 and 5,452 respectively, compared with 19,900 and 23,600 for South Korea, 28,400 and 25,600 for the Philippines, and 38,500 and 76,500 for Japan.

What makes the rising levels of education in developing countries especially significant is the link between education and economic growth. Those developing nations that educate large proportions of their young have achieved above average rates of growth and higher standards of living.

Conclusion

By the turn of the century, tremendous changes will have taken place in technological and economic development around the globe. Along with these changes will be the world's supplies of labor
and the demands for it. While the supplies and demands for the labor forces occur unevenly and sporadically throughout the world, this will have several important implications for the 1990s: an increasing number of women will participate in the labor forces and the levels of education required for workers will be raised. It is projected that by the year 2000, one-half of the world's work forces will comprise women. Since education is the backbone of economic development, more young people will receive a better education than in the past, especially in developing countries.
The number of poorly educated workers is expected to decline due to the increasing demand for better educated workers. While the world is moving along fairly toward the new face of the new century, Thailand is slowly creeping behind. With its fragile political and economic infrastructures, its technological and economic development is somewhat far from certainty.

CHARACTERISTICS OF GLOBAL LABOR FORCE IN THE YEAR 2000

Dr. Kris T. Rugsaken

Introduction

One of the most pressing issues of the world today is technological development which is the basis for economic and political development of the nation. The demographic composition of the world is changing much more rapidly than it is realized. In many respects, changes of one nation are driven by the developments of the larger society. The demographic trends in the nation are further complicated by the economic and political competitions. One nation cannot survive by its own without interrelating to and depending upon other nations. Among these many changes, the issue that is less realized but is equally important as other components is the human resources. Without this component, tasks cannot be completed to challenge the future goals of the world. Therefore, along with technological development, it is imperative to project and be prepared for the types of the labor force of the future. Just as managers speak of world markets for products, technology, and capital, they must now think in terms of a world market of labor.

This article examines trends of the global labor forces. Presented are projected characteristics of the labor force of Thailand as well as those of other industrialized and developing nations through the year 2000.

The Changing World Labor Forces

The developments of the next decade are rooted in today's demographics, particularly those having to do with the size and character of various countries's work forces. In some areas of the world, for instance, women have not yet been absorbed in large numbers and represent a huge untapped resource; elsewhere the absorption process is nearly complete. Such national differences are a good starting point for understanding what the globalization of labor will look like and how it will affect individual nations and companies.

Although looming labor shortages have dominated discussion in many industrialized nations, the world work force is growing fast. From 1993 to 2000, the work force is expected to grow by some 294 million people for the world and about 4 million people for Thailand where the total population is expected to grow by nearly 8 million. The global growth will take place unevenly. The vast majority of the workers will join the work forces of the developing countries. In countries like Pakistan and Mexico, for example, the work force will grow at about 3 percent a year whereas in Thailand the growth is projected at 1.7 percent a year. In contrast, growth rates in the United States, Canada, and Spain will be closer to 1 percent a year. Japan's work force will growth just .5 percent, and Germany's work force will actually decline.

The much greater growth in the developing world stems primarily from historical higher birth rates. But in many nations, the effects of higher fertility are magnified by the entrance of women into the work force. Not only will more young people enter the work force but also million of women in industrializing nations are beginning to leave home for paid jobs.

Moreover, the work force in the developing world is also better and better educated. The developing countries, including Thailand, are producing a growing share of the world's high school and college graduates.

When these demographic differences are combined with different rates of economic growth, they are likely to lead to major redefinitions of labor markets. Nations that have slow-growing work forces but rapid growth in service sector jobs such as Japan, Germany, and the United States, will become magnets for immigrants. Nations that produce prospective workers faster than their economies can absorb them will export people.

Beyond these differences in growth rates, the work forces of various nations differ enormously in make-up and capabilities. It is precisely differences like these in age, gender, and education that give us the best clues about what to expect in the year 2000.

More than half of all women between the ages of 15 and 64 now work outside the home, and women comprise one-third of the world's work force. In the 1990s, women will enter the work force in greater numbers and the average age of the world's work force will rise, especially in the developing countries. Based on the public figures of 1988, the population of Thailand was 54,589,000. Of these, 27,404,000 or 50.2% were men and 27,185,000 (49.8%) were women. Although the total population of women was slightly below that of men, the number of women caught up with men starting at age 40 and exceeded that of men starting at age 50. Between 1950 and 1990, the rates of women's participation in the work force increased by 28% for Brazil, 30% for Hong Kong, 29% for Mexico, 38% for Singapore, 27% for South Korea, and 32% for Thailand. In Japan, about 58% of women hold paid jobs. And for ideological reasons, China, with one of the lowest GNPs per capita of any nation, has female participation rates that are among the world's highest.

The degree of female labor force participation has tremendous implications for the economy. In many cases, rapid work force growth stimulates and reinforces economic growth. If other conditions are favorable, countries with women ready to join the work force can look forward to rapid economic expansion.

As a result of the slower birth rates and longer life spans, the world's population and labor forces are aging. The average age of the world's workers will climb by more than one year, to about 35, during the 1990s. But here again, it is important to distinguish between the developed and developing countries. The population of the industrialized nations is much older. Young people represent a small and shrinking fraction of the labor force, while the proportion of retirees over 65 is climbing. By 2000, fewer than 40% of workers in countries like the United States, Japan, Germany, and the United Kingdom will be under age 34, compared with 59% in Pakistan, 55% in Thailand, 59% in the Philippines, and 53% in China. The share of workers over age 65 will increase for most nations. Worldwide, over 6.8% of the labor force will be 65 years or older. For industrialized countries like the United States, Germany, Japan, and the United Kingdom, at least 13% of their labor forces will be over 65 years of age, compared with 7.3% for China, 4.2% for Indonesia, 3.9% for Pakistan, 4.9% for Mexico, 3.8% for the Philippines, and 5.2% for Thailand.

People worldwide will be increasingly well-educated. The developing countries will produce a growing share of the world's high school and college graduates. In the decade and a half between 1970 and 1986, world high school enrollments grew by some 120 million students, or more than 76 percent. College enrollments grew more than 100% during the same period, from 26 million to 58 million. This trend is likely to continue as nations and individuals increasingly recognize the economic value of

education. By the year 2000, it is likely that high school enrollments could grow by another 60%, reaching nearly 450 million, and college attendance could double again to top 115 million.

In 1990, higher percentages of children in industrialized nations attend high school and college. The United States, Japan, Canada, France, and Australia all have more than 95% of high school age children in schools. In some developing countries, however, high school education just started to catch on. Pakistan had 18% of high school age children in school. Elsewhere the figures were: 42% for China, 35% for India, 41% for Indonesia, 68% for the Philippines, 95% for South Korea, and 29% for Thailand. While 59% of people of college age in the United States were in college, 20% of the Thai people of the same age group attended college, compared with 2% for China, 38% for the Philippines, and 5% for Pakistan.

But an important shift is underway: the developing world is producing a rapidly increasing share of the world's skilled human capital. This trend has been underway for some time and will accelerate through the turn of the century. In the decade and a half from 1970 to 1986, the United States, Canada, Europe, Russia, and Japan saw their share of world high school enrollers shrink from 44% to 30%. If that trend continues, their share is expected to drop to 21% by the year 2000. U.S. high school students made up 9% of world enrollers in 1970 but only 5% in 1986. The developed world is also losing ground when it comes to higher education. Between 1970 and 1985, the share of the world's college students from the United States, Canada, Europe, Russia, and Japan dropped from 77% to 51%. The share of college students in the developing world, including Thailand, leaped from 23% to 49%, and these figures may be understatements because a great number of students in Western universities are from developing countries and will return home when they graduate. By the year 2000, students from developing nations will make up three-fifths of the world's college students.

It is true that in absolute numbers, the United States, Russia, and Japan are still the leading producers of college graduates of all kinds. However, a growing number of the world's college graduates are from outside of the traditionally highly- educated countries. Four of the next six greatest sources of college graduates are developing countries: Brazil, China, the Philippines, and South Korea. Differences in numbers of graduates are intriguing when sorted by discipline. China and Brazil rank third and fifth, respectively, in numbers of science graduates, following by Japan. For engineering graduates, Brazil, China, Mexico, Korea, and the Philippines all place ahead of France and the United Kingdom. For Thailand, although the numbers of graduates in the two areas have slightly improved during the last few years, it still lagging far behind other developing nations.
In 1992, the number of Thailand's graduates in Science and Engineering is expected to be around 3,520 and 5,452 respectively, compared with 19,900 and 23,600 for South Korea, 28,400 and 25,600 for the Philippines, and 38,500 and 76,500 for Japan.

What makes the rising levels of education in developing countries especially significant is the link between education and economic growth. Those developing nations that educate large proportions of their young have achieved above average rates of growth and higher standards of living.

Conclusion

By the turn of the century, tremendous changes will have taken place in technological and economic development around the globe. Along with these changes will be the world's supplies of labor
and the demands for it. While the supplies and demands for the labor forces occur unevenly and sporadically throughout the world, this will have several important implications for the 1990s: an increasing number of women will participate in the labor forces and the levels of education required for workers will be raised. It is projected that by the year 2000, one-half of the world's work forces will comprise women. Since education is the backbone of economic development, more young people will receive a better education than in the past, especially in developing countries.
The number of poorly educated workers is expected to decline due to the increasing demand for better educated workers. While the world is moving along fairly toward the new face of the new century, Thailand is slowly creeping behind. With its fragile political and economic infrastructures, its technological and economic development is somewhat far from certainty.

GLOBAL WARMING EFFECT ON RIVER BASINS IN SRI LANKA

Nophadol In-na and E.J. Hemantha

Engineering (English) Program, Thammasat University
Rangsit Campus, Pathumathanee 12121, Thailand

ABSTRACT

In this paper, the global warming effect on evapotranspiration, rainfall, and runoff of a catchment in tropical Sri Lanka was analyzed according to GCM projections at double CO_2 conditions. Two future climatic scenarios were considered based on two selected GCM outputs and compared with other climatic scenarios which represented the present conditions. The global warming effect at double CO_2 conditions altered the timing and the magnitude of rainfall and runoff, and increased mean monthly evapotranspiration. Daily and monthly peaks of rainfall and runoff were likely to increase, projecting higher floods than present. Reduction in low flows in the dry seasons projected more severe droughts, but the changes in the mean annual precipitation and runoff were very small.

INTRODUCTION

A global climatic change is likely to occur within the next few decades due to these increases of CO_2 and other trace gasses in the atmosphere (Houghton et al, 1990). Scientist expect that by the middle of the next century the CO_2 concentration will be doubled if the present trend continues. There is some evidence detected, showing the climatic change; the average global temperature has been warmed by about 0.5 °C over the past 100 years (WMO, 1991).

Scenarios of future climate are mainly based on numerical models. Performances of the models predict that in the case of doubled CO_2 concentrations the global mean surface temperature rises from 2 °C to 5 °C, precipitation increases by 7-15%, and the mean sea level rises 10 cm to 100 cm (Waggoner, 1990).

This paper is based on a river basin in tropical Sri Lanka. The main objective is to analyze the global warming effect on potential evapotranspiration, rainfall, and runoff according to the future climatic scenarios projected by General Circulation Models (GCM) at double CO_2 ($2xCO_2$) conditions. GCM outputs are taken from the National Center for Atmospheric Research (NCAR), USA. At double CO_2 levels, peak rainfall is increased, projecting high floods. Reduction of low flows projects the possibility of severe droughts. The mean monthly maximum rainfall period is shifted.

CATCHMENT AREA

Historical data was collected from the "Ellagawa" catchment area in tropical Sri Lanka. The area of the catchment is 1393 km^2 and

its mean altitude is 34 m above mean sea level. The location is identified as about 6.7 °N and 80.3 °E. Historical data, monthly potential evapotranspiration (ETO) by the Modified Penman Method (Doorenbos and Pruitt, 1977) is available and is used in this study. Mean monthly rainfall and temperature values of the catchment are given in Table 1.

Table 1 Historical mean monthly rainfall and temperature

Month	Jan	Feb	Mar	Apr	May	Jun	Jul	Aug	Sep	Oct	Nov	Dec
RAIN (mm)	125	149	238	355	486	426	292	282	393	435	407	242
TEMP (°C)	27.1	27.8	28.3	28.4	27.9	27.2	27.1	27.1	27	27.1	27.1	27

RAIN: Rainfall TEMP: Temperature

GENERAL CIRCULATION MODELS (GCMs)

Three GCMs: Goddard Institute for Space Studies model (GISS) (Hansen et al, 1983), United Kingdom Meteorological Office model (UKMO) (Wilson and Mitchell, 1987), and Geophysical Fluid Dynamic Laboratory model (GFDL) (Manabe and Wetherald, 1987) are considered in this study to select future climatic scenarios.

Selection of GCMs for study area

It is important to know whether the considered GCMs follow climatic reality so that scenarios and their results are not misinterpreted (Kalktein, 1991). Therefore, the GCM projections of precipitation and temperature at present ($1xCO_2$) conditions are compared with historical precipitation and temperature. The non-parametric Kruskal-Wallis test (Walpole and Myers, 1978) is carried out to statistically compare each GCM projection with the historical data.

The Kruskal-Wallis test results show that the GISS model is best for temperature because the Kruskal-Wallis statistics are the lowest and below the critical region (for 0.05 significant level and one degree of freedom, the critical region $H > 3.84$). But for precipitation, UKMO is the best as it gives minimum statistics (Kruskal-Wallis statistics is below the critical region for 0.01 significant level). Therefore, considering the test results, both GISS and UKMO models are selected for future climate scenarios.

ESTIMATION OF GLOBAL WARMING EFFECT

Climatic Scenarios

Precipitation, temperature, and solar radiation are considered as key parameters. Three climatic scenarios are selected as listed below for comparison of present hydrological variables with variables at double CO_2 conditions in order to estimate the global

warming effect.

Scenario-0 : Based on historical climeteorological data
Scenario-1 : Historical key parameters are modified according to GISS projection at double CO_2 conditions.
Scenario-2 : Historical key parameters are modified according to UKMO projection at double CO_2 conditions.

Rainfall-Runoff Model

The rainfall-runoff model is used for simulation of runoff for each climatic scenario. The NAM model is selected for simulation of catchment runoff by comparing the performances of the NAM and Sacramento models. This model has been used successfully for some previous studies in Sri Lanka (DHI, 1989). Out of the available 29 years of daily historical runoff data, a 15 year period is used for calibration and the rest is used for verification. Simple statistical measures such as Efficiency (Nash and Sutcliffe, 1970) and Absolute Relative Error of the model are used to compare the simulated and the historical runoff series. Special consideration is given to the parameters which are used to estimate the global warming effect.

GLOBAL WARMING EFFECT ON EVAPOTRANSPIRATION

In this study, the Modified Penman Method (Doorenbos and Pruitt, 1977) is used to determine potential evapotranspiration (ETO) for climatic scenarios. Three sets of mean monthly ETO series are determined for three different scenarios. ETOs for scenario-0 are calculated using the historical meteorological data and for scenario-1 and scenario-2, temperature and solar radiation are modified according to GISS and UKMO model projections respectively. It is found from the study that both double CO_2 scenarios project increases in potential evapotranspiraton for each month of the year except October. A maximum increase of 15.2% is projected by scenario-1 in June and a minimum increase of 6.4% in March. The UKMO model projects a maximum increase of 20.8% in May and a small reduction of 2.2% in October. Both models project an almost equal increase of annual evapotranspiration.

GLOBAL WARMING EFFECT ON RAINFALL

Mean monthly and mean annual rainfall values of scenario-1 and scenario-2 are obtained by modifying the historical rainfall according to the GISS and UKMO models' outputs respectively. The GISS model projects a maximum increase of 48% in October and a maximum reduction of 55% in June. The UKMO model projects a 68% increase in October and a 51% reduction in July. When considering the annual rainfall values, GCM projects a negligible increase at $2xCO_2$ conditions. The maximum rainfall period from April to June is shifted to the period from September to November.

Thirty-six years of daily annual maximum rainfall and thirty days average annual minimum rainfall series for scenarios-0, 1, and 2

are obtained. To determine rainfall values for different return periods of the annual maximum and minimum series, Gumbel and General Extreme Value (GEV) distributions are fitted respectively. Parameters are estimated using Probability Weighted Moment method (PWM). The Kolmogorv-Smirnov (K-S) test (Haan, 1977) is carried out to test the assumed frequency distributions. K-S statistics are below the critical region for 0.05 significant level. The assumed frequency distributions are therefore accepted.

It is found from the study that both double CO_2 scenarios project almost the same magnitude of increase in all return period values for annual maximum series. But annual minimum series scenario-1 projects an increase in low rainfall while scenario-2 projects a reduction for all return periods. In this case, the projections of two GCMs are not compatible.

GLOBAL WARMING EFFECT ON RUNOFF

Both double CO_2 scenarios project a considerable reduction of runoff in July and August, and an increase in October and November. Scenario-1 projects a maximum increase of 39% in October and a maximum decrease of 61% in June. Scenario-2 projects a maximum increase of 53% in October and a maximum decrease of 51.5% in July. Both scenarios project little reduction in annual mean runoff i.e., 6.5% and 2.5% by scenario-1 and scenario-2 respectively.

Twenty-nine years average annual maximum of daily runoff and seven days average annual minimum runoff for scenarios-0, 1, and 2 are obtained. To determine the required return period values of annual maximum series and annual minimum series, Gumbel and GEV distributions are fitted respectively. Probability Weighted Moment (PWM) method is used for parameter estimation. Assumed frequency distributions are tested by K-S statistics as for precipitation and the test accepted.

Results show that both double CO_2 scenarios project an increase in all return periods for annual maximum series. Scenario-1 projects a reduction in low flows for all return periods for annual minimum series while scenario-2 projects a small increase in 100 years return period and small decreases in all other return periods.

CONCLUSION

The results conclude that the global warming effect would increase the potential evapotranspiration and alter the timing and magnitude of rainfall and runoff. Peak values of mean monthly and daily rainfall are increased. Meanwhile, the high rainy season from April to June is shifted to September to November, but mean annual rainfall is not significantly changed. Peak values of mean monthly and daily runoff are increased projecting high floods and increased return period values of annual maximum series, indicating the possibility of severe floods. Severity of droughts also are projected due to reduction of low flows. Reductions in the high runoff season, May to July and an increase in runoff in the period

October to November may affect water resources management. Annual mean runoff is not significantly changed.

REFERENCES

1. DHI (1989), NAM documentation, Short description and User's Guide, Danish Hydraulic Institute, Denmark.

2. Doorenbos, J. and Pruett W.O. (1977), Guidelines for Predicting Crop Water Requirement, FAO Irrigation and Drainage Paper 24.

3. Haan, C.T. (1977), Statistical Methods in Hydrology, The Iowa State University Press.

4. Hansen, J., Russel G., Rind D., Stone P., Lovis A., Lebedeff S., Ruedy R., and Travis L.(1983), Efficient Three Dimensional Global Model for Climate Studies: Model I and II, April Monthly Weather Review III, 609-662.

5. Houghton, J.T., Jenkins G.J., and Ephraums, J.J. (1990), Climate Change The IPCC Scientific Assessment.

6. Kalkstien, L.S. (1991), Global Comparison of Selected GCM Control Runs and Observed Climate Data. Report Prepared for United States Environmental Protection Agency.

7. Manabe S. and Wetherald R.T. (1987), Large-Scale Changes in Soil Wetness Induced by an Increase in Carbon Dioxide., April J. Atmos. Sci. 44. 1211-1235.

8. Nash, J.E. and Sutcliffe J.V. (1970), River Flow Forecasting Through Conceptual Models, J. of Hydrol., 10:282-290.

9. Waggoner, P.E. (1990), Climate Change And U.S. Water Resources, Report of the American Association of the Advancement of Sciences, Panel on Climatic Variability.

10. Walpole R.E. and Myers R.H.(1978), Probability and Statistics for Engineers and Scientists. Macmillan Publishing Co. Inc., New York.

11. Wilson C.A. and Mitchell J.F.B. (1987), A Double CO_2 Climate Sensitivity Experiments With a Global Climate Model Including a Simple Ocean, JGR, 92:D11-11/20, 13,316-13,343.

12. WMO (1991), World Meteorological Organization Bulletin, July, 1991.

WORKSHOP FOR PRESERVATION OF KAWN PAYAO WATER RESOURCE PROJECT

Osoth Jamjun, M.Sc. (ENVE), P.E.
Chairman of Natural Resources and Environmental Committee
The Association of Thai Professionals in America and Canada (ATPAC)

PRESERVATION OF KAWN PAYAO WATER RESOURCE PROJECT

Kawn Payao is a fresh water lagoon located in the heart of Payao Province, an ancient city in the north of Thailand. The Kawn is an economic security for Payao Province and her half a million population.

The algae and other water born vegetative in the Kawn Payao indicates eutrophication and if no action is taken to remedy the situation, it will be a tragedy for the Payao Province and her population.

The objective of the project is to preserve the Kawn Payao and prevent it from further deterioration. The project envisions three strategies to accomplish the objective. The three strategies are:

1. Protecting the Kawn Payao through pollution prevention.
2. Empowering all sectors , central and local government agencies, leaders of the community such as members of the House of Representatives, and private citizens, to get involve with the project.
3. Planning and managing the Kawn Payao water quality and water quantity for both short term and long term plans.

It is anticipated that the project will succeed through the cooperation from the central government and local government agencies, member of the house of representatives, private citizens, and ATPAC.

WORK SCHEDULE FROM JULY 19 TO 30, 1993 IN THAILAND

In the week of July 19, 1993, the work schedule includes attending a meeting and working together with officials from the Department of Pollution Control of the Ministry of Science, Technology, and Environment. The goal of this working session is to prepare a contract documents to be

advertised for a consultant service for a preliminary engineering for the Kawn Payao Preservation Project. The scope of the preliminary engineering includes:

a Provide report on the water quality of the Kawn Payao.
b. Provide surveying to identify existing and potential sources of pollution.
b. Making Topography of the areas around the Kawn Payao. This process is necessary for future detailed engineering design for the land runoff control, wastewater collection and possible wastewater treatment facilities.

Included in this week is to attend a meeting on July 23, 1993. The meeting will be held in Bangkok to discuss the Kawn Payao Preservation Project. Participants in the meeting will be from the central government and local government agencies, member of the house of representatives, private citizens, and ATPAC.

As indicated above, one of the strategies for the success of the project is to empower all the sectors. The July 23 meeting , the representatives from the following agencies will participate

1. Ministry of Science, Technology, and Environment, more specifically from the Department of Pollution Control
2. Interior Ministry - Provincial Governor and Provincial Chief Engineer Offices
3. Agriculture Ministry - Department of Irrigation
4. Public Health Ministry - Provincial Public Health Office
5. A member of the House of Representatives from Payao Province - Mrs. Ludawanya Wongsriwong
6. Payao Mayor Office
7. ATPAC - Natural Resources and Environmental Committee

In the week of July 26, 1993, the work will include site visit at Kawn Payao in Payao Province.

WORKSHOP FOR PRESERVATION OF KAWN PAYAO WATER RESOURCE PROJECT

Osoth Jamjun, M.Sc. (ENVE), P.E.
Chairman of Natural Resources and Environmental Committee
The Association of Thai Professionals in America and Canada (ATPAC)

PRESERVATION OF KAWN PAYAO WATER RESOURCE PROJECT

Kawn Payao is a fresh water lagoon located in the heart of Payao Province, an ancient city in the north of Thailand. The Kawn is an economic security for Payao Province and her half a million population.

The algae and other water born vegetative in the Kawn Payao indicates eutrophication and if no action is taken to remedy the situation, it will be a tragedy for the Payao Province and her population.

The objective of the project is to preserve the Kawn Payao and prevent it from further deterioration. The project envisions three strategies to accomplish the objective. The three strategies are:

1. Protecting the Kawn Payao through pollution prevention.
2. Empowering all sectors , central and local government agencies, leaders of the community such as members of the House of Representatives, and private citizens, to get involve with the project.
3. Planning and managing the Kawn Payao water quality and water quantity for both short term and long term plans.

It is anticipated that the project will succeed through the cooperation from the central government and local government agencies, member of the house of representatives, private citizens, and ATPAC.

WORK SCHEDULE FROM JULY 19 TO 30, 1993 IN THAILAND

In the week of July 19, 1993, the work schedule includes attending a meeting and working together with officials from the Department of Pollution Control of the Ministry of Science, Technology, and Environment. The goal of this working session is to prepare a contract documents to be

advertised for a consultant service for a preliminary engineering for the Kawn Payao Preservation Project. The scope of the preliminary engineering includes:

a Provide report on the water quality of the Kawn Payao.
b. Provide surveying to identify existing and potential sources of pollution.
b. Making Topography of the areas around the Kawn Payao. This process is necessary for future detailed engineering design for the land runoff control, wastewater collection and possible wastewater treatment facilities.

Included in this week is to attend a meeting on July 23, 1993. The meeting will be held in Bangkok to discuss the Kawn Payao Preservation Project. Participants in the meeting will be from the central government and local government agencies, member of the house of representatives, private citizens, and ATPAC.

As indicated above, one of the strategies for the success of the project is to empower all the sectors. The July 23 meeting , the representatives from the following agencies will participate

1. Ministry of Science, Technology, and Environment, more specifically from the Department of Pollution Control
2. Interior Ministry - Provincial Governor and Provincial Chief Engineer Offices
3. Agriculture Ministry - Department of Irrigation
4. Public Health Ministry - Provincial Public Health Office
5. A member of the House of Representatives from Payao Province - Mrs. Ludawanya Wongsriwong
6. Payao Mayor Office
7. ATPAC - Natural Resources and Environmental Committee

In the week of July 26, 1993, the work will include site visit at Kawn Payao in Payao Province.

THE THIRD INTERNATIONAL CONFERENCE ON SCIENCE
AND TECHNOLOGY TRANSFER TO THAILAND
JULY 23-25, 1993
BANGKOK, THAILAND

MANAGING PUBLIC TRANSPORTATION

Somkiat Pongkanta, P.E.
Senior Electrical Engineer
San Francisco Bay Area Rapid Transit District
800 Madison Street, Oakland, California

MANAGING PUBLIC TRANSPORTATION

INTRODUCTION

The development of civilization is directly connected with the development of transportation. Without proper transportation, life in this civilized society will be difficult and chaos.

We are facing a transportation crisis, the one that becomes more critical as time goes on, a crisis which threatens to overwhelm us while we are standing around seeking solutions. Concurrently, we are facing a land-usage crisis as we face the task of accommodating more population increase in the limited space that has to also be shaped to suit additional required transportation.

One of the most critical transportation issues facing us today is traffic congestion. This congestion will get worst during the next 10 years. Billions of hours are wasted each year in traffic jams. They do not only impede our mobility but also pollute air, waste fuel, and hamper economic growth.

Good public transportation is essential to economy. Whether the concern is job, business revenue, productivity, or global competitiveness, extensive public transportation provides critical connections. A strong commitment to national infrastructure by all levels of governments is necessary. Whether the commitment is direct or indirect, it contributes to an improved standard of living.

We need to develop comprehensive planning policies involving all the aspects of both transportation and land use.

The form and quality of any community is affected by many factors such as local administration, intergovernmental relations, municipal finance, private investment, water, sewer, safety, and other public facilities and basically by urban public transportation. The life of a city depends upon its public transportation system. Inefficient public transportation service increases the costs of local industry and commerce. They rob citizens of their time and comfort. They penalize members of community especially the poor and handicapped.

All levels of government should share responsibility of the transportation cost and benefit. Different systems of transportation should be fully integrated into the same network in order to achieve efficient connections. A master plan for transportation of each region as well as of the whole nation should be developed and implemented rigorously. Adjustment to the plan may be made whenever appropriate but should not be allowed to drastically deviate from its goal and milestones. Simulations should be performed to test each plan and to ensure accuracy.

Each master plan should include and coordinate each element of land, air and water transportation. A regional as well as a national organizations should be established with an authority to plan, coordinate and appropriately implement the transportation network.

PROBLEMS

Continued use of the automobiles to provide travel is causing severe impact problems in the urban areas. The problems are serious enough to warrant changes. Some of the problems leading to this conclusion are:

1. Congestion is increased to the level that automobiles are not practical means to travel in some high population density areas.

2. Increasing air pollution and noise.

3. The growing operating cost and future limit of fuel supply including uncontrollable imported oil price.

4. The social and economic price of facilities to accommodate automobiles, such as highways and parking structures.

These transportation problems are not beyond resolution. However, at this point in time, the solutions will not come cheap. The best course is to make a vast investment in the best selected systems and approach with a good coordinated plan on a scale that has never been attempted before in order to properly serve us as both a passenger and a resident of the environment.

In reviewing the past economic expansion of the United States. It has been found that the United States has been in the longest recession since the end of World War II. Despite the lengthy expansion of the 1980s, evidence of economic decline is apparent as follows;

- In the 1980s America's real Gross Domestic Product, GDP, grew by only 2.5% a year, compared with 4% in 1948-65 and 3.1% in 1965-79. The average growth in GDP per head slump from 2.3% a year in 1948-65 to 1.5% in the past decade. Productivity dropped from an annual growth rate of 1.8% in the 1960s to 0.8% in the 1970s and to 0.7% in the 1980s.

- Transportation delays in 1988 caused 1.4 billion gallons of wasted fuel and more than $9 billion in lost time.

- The estimated 2 billion hours of delay on urban freeways represented an economic loss of about $42 billion in the nation's top 25 cities in 1987 alone.

- Truck delays may add as much as $8 billion a year on to the cost of goods purchased in the United States.

The analyses show infrastructure investment is directly tied to the strength of the economy and to the levels of private investment. This connection is evident in the transportation sector.

The present United States economy demands immediate action. Economic growth and regional productivity require both short-term and long-term transportation solutions. Increased transportation investment as an essential part of the economic stimulus is being requested by the Clinton Administration to the Congress for an additional $750 million to create jobs as part of the total $4.5 billion fund of the Intermodal Surface Transportation Efficiency Act, ISTEA, for Fiscal Year 93-94.

AN APPROACH TO SOLUTIONS

The paramount transportation problem in urban areas is the emergence of congestion as a recurring characteristic of the network, particularly for the journey to work, social and recreational trips. Most planning dealing with the problem of congestion in the United States has been typically directed toward either the supply or demand side. Some of the solutions are as follows:

On the supply side, there is the possibility of:

1. Improving public transportation facilities and providing for increased capacity; such as mass transit system.

2. Facilitating the flow on the street network through traffic management and traffic control;

3. Adding to the supply of freeway and urban expressway facilities;

4. Increasing the utilization of automobiles through encouragement of car pools and increased car occupancy;

5. Improving utilization of public transit vehicles through priority lanes for buses or through the construction of busways.

6. Providing for separation of the movements of goods and persons.

7. Increasing mandatory utilization of the reduced emission vehicles, such as alternative fuel, and battery or electrically operated vehicles.

On the demand side, approaches to the reduction of congestion have

included the followings:

1. Use of staggered work hours;

2. Providing some restraints on motor vehicle use through direct or indirect pricing;

3. Prohibiting certain motor vehicle use in certain areas of the city and;

4. Designing urban activity systems and land use patterns that minimize or reduce the need to travel.

The actions to alleviate congestion that could be implemented in a short time are considered Short Term solutions while some others that would take a long time to implement are considered Long Term solutions.

Normally, one of the long term solutions would call for a mass transportation system, and usually a fixed guideway or a rail transit system would be specified.

RAIL TRANSIT SYSTEMS

There are two major types of modern rail transit services in the United States.

1. Heavy rail transit or rail rapid transit. This type should handle a heavy volume of passengers above 20,000 persons per hour per direction, multiple-car trains in exclusive right of way, high speed, normally between 60 and 80 MPH, fast acceleration and deceleration, at 2.5-3.0 MPH per second, automatic operation with sophisticated train control system, receiving power supply via third rail, normally called METRO or SUBWAY.

2. Light rail transit or LRT. This type of rail transit provides passenger capacity below 20,000 persons per hour per direction. It can operate on either grade separated or in mixed traffic on the city streets. The light rail transit receives direct current power from overhead trolley wires, and normally runs in pair of cars.

Recently, some LRT systems have been technologically improved to accommodate higher volume of passengers. The improved LRT systems are called Advanced LRT, or ALRT.

Another type of rail transportation that sometime classified as rail transit is the commuter train. The commuter train generally operates between a major downtown and suburban areas of a metropolitan region on main line railroad tracks, using high speed locomotives or self-propelled cars in multi-car trains.

HIGH SPEED TRAINS

A high speed train is normally defined as one that operates above 150 MPH. Few high speed train systems are being evaluated for various transportation corridors of the United States including the Triangle corridor between Houston and San Antonio and Dallas/Fort Worth in Texas. The technologies considered include French's TGV, Swedish's ABB X-2000, and German's ICE. The magnetically levitated vehicle system was also considered but believed to be premature for full commercialization.

THE SAN FRANCISCO BAY AREA CASE STUDY

The transportation network of San Francisco Bay Area is coordinated by the Metropolitan Transportation Commission, MTC. The MTC was created by the California State Legislature in 1970 to provide transportation planning for the nine county San Francisco Bay Area. It is responsible for planning and development of mass transit, highway, airport, seaport and railroad facilities. It administers funds received from the Federal, State, Regional and local governments including those provided by the Transportation Development Act. It oversees the efficiency and effectiveness of the region's transportation systems. It provides technical assistance and monitors transit operators' budgets, conducts performance audits and adopts yearly productivity and transit coordination improvement program.

The urban communities of San Francisco Bay Area Region are linked together by a trunk line, rapid transit rail system of San Francisco Bay Area Rapid Transit District, so called BART.

BART is a special District created by the California Legislature to design, construct and operate a regional rapid rail transit in counties of San Francisco, Alameda, Contra Costa, in San Francisco Bay Area region. It began operation in September 1972.

Its facilities generally consist of 75 miles of double-tracked 5-foot 6-inch gauge right of way, one-third of which is at grade, one-third on aerial structure, and one-third under ground in San Francisco, Oakland, and Berkeley subways, the Berkeley Hill Tunnel, and the under water Trans-Bay Tube. There are four yard facilities with control towers and maintenance shops at Hayward, Richmond, Concord, and Daly City, one separate maintenance shops and cash handling building in Oakland, 34 passenger stations, one with the administration building and a central control complex, and three major ventilation structures.

BART system is fully automated from fare collection to the train control system including traction power. Its trains are travelling up to 80 miles per hour connecting San Francisco to the East Bay communities at 3.5 minutes interval with train consists between 3 to 10 cars. The system was designed to operate as close as 90

seconds interval in the downtowns of San Francisco and Oakland. It is considered safe, reliable, economical, energy efficient, and fully accessible to disabled persons. On passenger-mile basis, BART's use of energy is three times as efficient as an automobile in its energy consumption and ten times as efficient during rush hours in the commute direction.

In April 1980 the first extension policy was adopted by the BART's Board of Directors to extend its service along four new corridors. The extension work actually began in 1991. It includes approximately 14 miles to Dublin/Pleasanton, 8 miles to Antioch/Pittsburgh, 6 miles to Warmspring and 1 mile to Colma with the routing planned for the service to San Francisco International Airport. The cost of extensions is estimated at $2.5 billion.

The major modes of the transportation systems are coordinated with an intermodal transfer from one to another. The modes of transportation system in the Bay Area include BART, commuter Cal-Train, interstate AMTRAK-Train, buses, ferry boat, cable car and light rail transit system.

The light rail transit connecting with BART is operated by the City and County of San Francisco, and called SF MUNI. Transfer between BART and SFMUNI is conveniently provided with coordinated fast pass that is acceptable by the automatic fare collection equipment of both properties. Four SF MUNI passenger stations have shared facilities with BART in San Francisco Downtown.

ELECTRIC TROLLEY BUS

One special mode of the transit systems in San Francisco that deserved to be mentioned herein is the Electric Trolley Bus, ETB. The ETB runs on rubber tires similar to normal bus except that it has an electric traction motor supplied by overhead electrical distribution trolley wires.

The ETB was called Trolley Coach when originally operated in Laurel Canyon of Hollywood, California in 1910. The ETB went through an expansion right after the World War II with more than 6500 units in operation in the United States, and then declining from 1950 to 1970. Bay early 1970's only 1800 units were still running in North American cities. Now, with the air pollution and noise problems of the regular internal combustion engine driven buses in our urban communities, the ETB is once again being looked at as part of the urban mobility solution. San Francisco, Seattle and Vancouver are upgrading the systems which have already been successful in their operations while Los Angeles and Sacramento just have finished their preliminary design for inclusion of the ETB on their major routes.

The standard size of ETB is 40 feet long. It can articulately be operated in a pair. Its traction power can be shared with the

light rail transit system nominally at 600 Vdc or 750 Vdc. Other voltages can also be made available. It can be furnished with an Off-Wire Capability, either with a battery-powered or engine driven auxiliary power unit (APU) to allow off wire movement to return to it maintenance yard.

One consultant team has analyzed both the capital and operation costs of implementing an ETB system for Sacramento, California, at $60 million for a four-line starter system. The cost includes engineering, vehicles, power distribution, aesthetic treatments, and contingencies. Of the total, capital costs for construction of the Overhead Contact system, with substations, engineering and contingency are estimated at $41 million, or approximately $1.47 million per mile. Beside the advantages of cleaner air quality, less noise, and higher reliability, it is estimated that the cost for repair and maintenance of the ETBs is half of the cost for similar work for the regular motor buses.

For Los Angeles Area, the initial 12-route, 184-mile of the ETB project is estimated to reduce 118 tons of particulate matter, 620 tons of carbon monoxide, and 2600 tons of nitrous oxides per year when fully operated.

MAKING A TRANSIT PROJECT

Traditionally, in the United States, the Transit Authority selects the type of transit technology recommended by its General Engineering Consultant, GEC, who has performed studies of applications of available technologies. The criteria may include service level, performance, efficiency, physical aesthetic, expendability and most important, costs. Most of the recent projects in the United States, except Honolulu Transit, are conventional rail transit technology which requires conventional approach to build. In Conventional Approach, with the assistance of GEC, the Transit Authority assumes all responsibility for management, finance, design, construction, start-up, integration, quality control, safety, and risk.

During the last twenty years, there have been unconventional transit technologies such as monorail, rubber tired, suspended guide-rail, Guided Light Rail (GLT), Personal Rapid Transit (PRT), Automatic Guideway Transit (AGT), Linear Induction Motor Vehicle (LIM), and Magnetically Levitated Vehicle system or maglev, where they are proprietary and can not be interchanged or integrated with others. Together with financial complication, the Traditional Approach may not be workable. A Turnkey Approach may be appropriate as such in the case of Honolulu Rapid Transit System.

Under the Turnkey Approach, the contract is awarded by the Transit Authority to a contractor to design, supply and build the transit system including all fixed facilities and the Operating System. The primary reasons are obvious as follows:

1. To maximize competition and select both technology and vendor on the basis of committed obligations and bid prices.

2. To reduce total project cost and avoid cost overrun.

3. To place technological and design risks on the vendor who benefits financially from the project.

4. To attract and facilitate private participation in funding the project.

5. To ensure specified performance in specified time.

However, it is not practical to assign all responsibility and risk to the Turnkey Contractor. In order to help implementation of the transit project, and besides the oversight function, the Transit Authority should assume certain responsibility and risk in following areas; funding, political, right of way and real estate, geotechnical, underground utility, regulations, inflation, liability insurance and finally, interface with public agencies and other transit services.

FINANCE

The transit projects in the United States are generally built with a conventional approach such as a case of the 1.6 billion dollars BART project. BART was financed from different sources in 1968 as follow; General Obligation Bond 48.4% California Bridge Toll 10.7%, Sales Tax 9.2%, Temporary Investment Earnings 6.8%, Transit Development Act 1.5%, Federal Government Grant 20.2%, and Miscellaneous 3.2%.

Beside special bonds or funds allocated by the Federal and State Governments, the following revenue sources are the most commonly utilized for the transportation improvements; Sales Tax, Payroll Tax, Motor Fuel Tax, Property Tax, Weight Tax, License Fee, Registration Fee, Charter Fee, Advertising Fee, Parking Fee, Special Assessment Fee, Right of Way Lease, and Bridge/Highway Tolls.

For Unconventional Approach, public and private partnership can be developed to provide funds for transportation improvements on highway expansion or construction and toll financing.

FINANCING A TURNKEY HONOLULU TRANSIT PROJECT

In the case of Honolulu Rapid Transit Project, the City of Honolulu has selected the Oahu Transit Group, a consortium of businesses led by Morrison Knudsen Corporation to design, construct the system and operate it for five years before turning it over to the City of Honolulu at a specified cost. The Federal Government will finance

approximately $500 million while the remainder will comE from 0.5 cent increase in the Oahu excise tax over the next 10 years.

COST

In the case of very high population density, the passenger demand for transportation is obvious and sometime is not a key parameter for analysis. The supply parameters play more significant role in selection of a transit system. These parameters are; capacity of service volume, speed, energy consumption, emission, noise, safety, operating costs, and capital costs. The capital costs normally include land, construction, structure, and vehicles. Price and cost change regularly with time, geography, labor wages, inflation, demand/supply, and the cost of money. They also change with special requirements and the degree of complication required to perform the work specified in the contract.

To accurately estimate cost of a transit project, the planners will have to rigorously perform analysis and collect a lot of data from reliable sources. Some of the published information sources are as follows:

- Survey of Current Business, by the Bureau of Economic Analysis of the US Department of Commerce, for source of price and income data.
- News by the United States Labor Department, for consumer price index.
- Economic Indicators, by the Joint Economic Committee of the United States Congress, for Economic and Price Indicators.
- Engineering News-Record, for construction price data.
- Cost Data, R. S. Means Co. Kingston, MA.
- National Urban Mass Transportation Statistics, by the Federal Transit Administration, US Department of Transportation, for data on transit revenues, expenses, services, safety, energy consumption, maintenance performance, mileage, employee counts, fleet size, and fleet age.

More accurate cost estimate could be obtained from industrial reviews of specifications by potential suppliers and construction industry.

As a study case, the cost of BART, a heavy rail transit system for 75 miles, 34 passenger stations was approximately $1.6 billion in 1973 with subsystem distribution as follows; Right of Way and Land 7%, Guideway 37%, Stations 20%, Trackwork 3%, Power 3%, Control &

Signalling 4%, Facilities 2%, Engineering/Management/Test 14%, Vehicles 12%.

The cost of San Diego Light Rail System for 16 miles was $116 million in 1981 with subsystem distribution as follows; Right of Way and Land 26%, Guideway 14%, Station 5%, Track 11%, Power 4%, Signal 5%, Facilities 2%, Management 19%, Vehicles 14%.

In 1992 the cost of Light Rail Transit system is estimated between $15 and $22 million per mile.

The cost of a vehicle in 1992 is estimated between $1 and $2 million depending on requirements. The difference between light rail and heavy rail transit vehicles are mainly performance, on-board train control equipment, acceleration rate, body width, loading and track gauge.

REFERENCES

1. Planning, Design and Operation of San Francisco Bay Area Rapid Transit Traction Power System, by Somkiat Pongkanta, BART. Presented at the Second International Conference on Science and Technology Transfer to Thailand, August 1992.

2. International Railway Journal, March 1993.

3. The Economist, December 26th 1992-January 8th 1993.

4. Transit California, March 1993.

5. Toward More Balanced Transportation, A Commission Report, Washington D. C. No. A-49, December 1974.

6. Beyond the Automobile, by Tabor R. Stone, Prentice-Hall.

7. Tomorrow's Transportation, Dept. of Housing and Urban Development, 1968.

8. Public Transportation, Planning, Operations and Management by G. E. Gray and L. A. Hoel, Prentice-Hall.

9. A Toolbox for alleviating Traffic Congestion, by the Institute of Transportation Engineers, 1989.

10. Comparison of the Super-Turnkey Procurement with the Traditional Approach for the Design and Construction of Fixed Guideway Transit Systems, by Charles P. Elms, Lea + Elliott, Inc. Washington D. C. Presented at Los Angeles APTA 1992 Conference.

11. Characteristic of Urban Transportation Systems, Report No. UMTA-MA-06-0173-85-1 United States Department of Transportation.

12. Financing Urban Transportation Improvements, Publication No. FHWA-HI-88-045, United States Department of Transportation.

13. Rebirth of the Trolley Bus, Something New for Los Angeles, by N. Tahir and M. Long, presented at Los Angeles 1992 APTA Conference.

AUTHOR'S BIOGRAPHY

Somkiat Pongkanta was born in Thailand in 1938. He received BS in Electrical Engineering from FEATI University, Philippines in 1968 and MS in Engineering from University of Santa Clara, California in 1982. After his graduation from a technical college in Bangkok in 1957 he worked as a mechanic with Express Transportation Organization in Bangkok for 3 years and then as an instructor at Northern Technical Institute, Chiangmai, Thailand, for 8 years.

He started his professional work as an electrical engineer with Air America Inc. in 1968 while serving as a consulting engineer to the US Embassy in Vientiane, Laos during the Vietnam War. He joined BART in 1969 and has been with BART since then.

His experience with BART has been varied. It has included design, specifications, research, development, project engineering, administration and other engineering activities to support the transit operations. He has specialized in traction power system and equipment. His current responsibility is reviewing engineering designs and support the construction of BART Extensions Program. He is a member of The Institute of Electrical and Electronics Engineers and a registered professional engineer in the State of California.

LEARNING FROM ALLIANCES WITH JAPANESE FIRMS IN HIGH TECH

Richard F. Doner
Dept. of Political Science, Emory University
Atlanta, Georgia 30322 USA
Tel. 404-727-7914 / Fax. 404-727-4586

Introduction

How do non-Japanese firms learn managerial and technological skills from Japanese partners? This paper examines this question from the perspective of US firms involved in joint ventures or other types of alliances with Japanese firms.[1] However, the paper may hold lessons for non US firms as well.

The question of learning and benefiting from alliances with Japanese firms in high tech is critical for two reasons. First, while one of our strengths in the U.S. is our independence and competitiveness, one of our weakness is our lack of experience in cooperation with other firms, whether they are competitors, suppliers, or primes. The Japanese have extensive experience in partnering. Indeed, one of the mytisfying features of the Japanese economy is how Japanese firms manage to combine competition and cooperation. Also, this is an important time to be discusing this issue because japanese firms are moving to internationalize to a greater degree than ever before. And they are doing so with an increasing emphasis on R and D in advanced manufacturing technologies. And they are supported by japanese government programs with labels such as "techno globalism" and intelligent manufacturing systems. This presents new opportunities as well as challenges.

Background

For the Japanese, international partnering of one form or another has quite a long history. You are all undoubtedly aware of the successful efforts by Japanese auto firms to learn from the US beginning in the early 1950s, whether by sending their people to the US, as Toyota did, or by learning from then unknown Prof. Demming. During the following decade, Japanese firms came to the US to help get their fledgling semiconductor industry off the ground. They succeeded so well because they were good at learning and American firms are so good at teaching.

It was thus only natural that in the 1980s, when US firms awakened to a competitiveness crisis in industries such as electronics, many firms turned to Japan for the same kind of help they once provided. The result has been an explosion of international joint ventures. A recent McKinsey study shows that the number of ventures established annuallly grew sixfold from 1976 to 1987 (Hladik and Linden 1991?). Even more significant is the structure of those ventures: Fortune 100 firms were the most active, but many smaller firms participated as well, some for the first time. In 1980, over a half of the players in international joint ventures were in high tech industries; by 1987 the proportion had grown to almost 3/4s, with computers, semiconductors and pharmaceuticals dominating. U.S. chip companies concluded almost a thousand partnerships in the 1980s in the form of joint ventures, manufacturing alliances and technology exchanges. Most of these were with Japanese

---

[1] This paper is very preliminary and not for publication. A list of references can be found at the end of the paper. An earlier version of this paper was presented to the "International Technology Alliances Seminar: Opportunities and Challenges in the Japanese Market." Sponsored by JETRO, Madison Country Commission International Trade Program, North Alabama International Trade Association and Technol. Transfer Society, Huntsville Chapter, Huntsville Ala., June 22, 1993.

firms (Rice 1991; Hladik and Linden 199?). Indeed, since 1976 the number of international JVs with R and D activity has more than tripled; these now account for almost 25% of recently formed joint ventures. This represents a real shift for US firms: traditionally US joint ventures were formed **at the end of the business chain** in marketing and sales. Later they moved to the middle of the chain and added a manufacturing facility, whether because of lower cost labor or the need to circumvent local content requirements. But now our alliances have moved increasing toward the beginning of the chain into R and D.

The specific factors leading to this expansion are probably well known to you. ^One is the need to **tap foreign expertise, whehter in basic research, engineering or manufacturing.** Although Japan has the reputaion of being being simply a copier, Japanese firms have made marked progress. For example, the percentage of US patents held by foreign companies, especailly from japan, has grown dramatically in recent years. HItachi received more US patents granted in 1986 than GE, a much larger corporation which has often been the leader in absolute numbers. Indeed, japanese industrial R and D spending levels are at least as high as in the US(Hull and Azumi 1989). A second related factor is increasing **host country pressure for technology transfer and local R and D.** This pressure traditionally came from Asian countries. This was strong in Japan as a result of the government's actually screening foreign investment and only allowing those ventures which helped japanese firms. In a related vein, there is increasing pressure from **customers** for participation in production. This was one of the main reasons Boeing decided to form a partnership with three large japanese firms in production of the new 767. As one Booeing official said, "had the japanese developed a partnership relation with airbus instead of us, they would be flying airbuses today instead of our airliners" (Uchitelle 1989). Third, there is often the desire to **get a foothold in larger domestic and internatnional markets**. Altho this was always an important factor, international joint ventures are increasingly extending distribution beyond the host country market to international markets through exports (Hladick and Linden 199?). Fourth, there is the desire to spread the costs and risks of in-house R and D. As we know, each year the pursuit of technology is more risky and expsnsive. Fifth, many US firms moved into partnerships with Japanese during the 1980s due to shortages of cash

However, there seems to be a major difference in goals between US and Japanese joint venture partners. US firms often enter alliances to avoid investments. Many US joint ventures are little more than fancy outsourcing agreements (Hamel et al 1989).

The results of these alliances have been decidedly mixed. In electronics, partnering has a poor track record. It is felt that western firms in alliances with Japanese give away more than they gain (Hamel et al 1989· see also Rice 1991). But note that the problems are not just between US and Japanese companies. They are also prevalent among US firms. One way to understand the problems is to identify the different assumptions and practices each side brings to joint activities. Here I want to emphasize what japanese firms bring to the relationship.

Differences

1. I have referred to one difference already: **Americans are not used to cooperating**. Indeed, in the opinion of some, we are "just not tempermanetally suited for alliances."[2] Because we are largely sales and market driven, it is often hard for US firms to find an area where all admit what they are giving up and what they expect to gain. **The Japanese, on the other hand, excel in relationships. They are willing to nurture them.** They recognize that these take time and, as a result, the Japanese tend to get more out of technology deals than we do. How have japanese learned to cooeprate so well?

At least part of the answer has to do with the nature of supplier-prime relations, and let me take the auto case as an example. As many of you may know, japanese assemblers like toyota tend to buy rather than make most of their components. But they buy components from suppliers with whom they maintain very close

---

[2] Rice: 32

although often informal ties. In fact, one study characterized the relationships between prime and suppliers as governed not by the invisible hand of Adam Smith that governs the US market, but rather by an **invisible handshake** through which difficulties are ironed out on the basis of **trust.** The relationship is one of partnership rather than arms-length. Moreover, there is no single key contact point beteeen a prime and its supplier, such as a buyer and marketing representative. Instead, there is a product development and procurement process in which many actors have influence over time (Wolf and Taylor 1990).

As a result, Japanese prime contractors have been the principal conduit through which knowledge gleaned from licensed production is diffused to suppliers and vendors. With each new projects, subcontractors typically dispatch teams of engineers to the primes for several weeks of training to master design or manuf. techniques imported from abroad (Friedman and Samuels 1991). Primes will also provide technical guidance on equipment purchases such as new NC machinery or specialty compositve materials technology. Conversely, subcontractors have begun to be critical sources of innovation for the primes. Toyota, for example, gets over 50% of its design modification from its suppliers.

Another part of the answer has to do with the fact that, especially in the development and diffusion of high technology, japanese firms have long been involved in various sorts of **research alliances among competitors. Indeed, much of japan's technological capcities were fostered by novel and borrowed organizational practices - institutions such as research consortia and cartels.** Every gov't program since the 1970s designed to support technology development has provided incentives for additional collaborative research. But this hasn't been the gov't telling firms what to do. Industry associations have been critical players and many gov't efforts have been refused. And let me emphasize that these kinds of alliances do not mean that participants in such allinaces stop competing. They tend to cooperate in early stages of R and D and then move to intense competition the closer they get to the market.

Still another source of experience in cooperation is the R and D lab itself. A recent sutdy concluded that japanese firms are very successful in itnroducing new products because of their **team appraoch** involving horizontal communications across functions. Japanese employees from diverse functions are often teamed to move a product from the idea stage to commercialization as if they were playing **rugby**. As you may know, rugby is a game in which everyone tries to move the balld ownfield togethr. Precisely whether and where such multifunctional teamwork is more beneficial remains open to question (Hull and Azumi 1989).

Finally, note that linkages among firms are often rooted in local, regional and national industrial networks. As a result, firms often see things from a broader perspective and tend not to adopt "cut and run" strategeis more typical of the US. Thus, for example, japanese primes tend not to use their subcontractors as shock absorbers when the economy sours (Friedman and Samuels 1991).

2. A major second difference is that **US firms are not used to or set up for learning or absorbing new technology, whereas technology absorption has been one of the principal strengths of the japanese firm.** Indeed, japanese organizations have often been described precisely as learning organizations. Why and how has this occurred? Let's take the case of japanese military and aerospace firms. This is an area in which the US has clearly dominated and in which, according to many, Japanese efforts have been a failure.[3] And yet, while japan produces few completed airplanes, by many criteria japanese aerospace firms have been a tremdnous success. Indeed, Japan has been especially strong in component exports and in the introduction of new, engineered materials.

One source of this success is diversification: The major japanese defense contractors are diversified manufacturing conglomerate that take special pains to establish mechanisms such as project teams, extensive corporation-wide study groups, and technology focus centers for functional area specialists to share know-how and experience across applications. The result is a cadre of multi functional design and mfg. specialists who understand their application areas comprehensively and who are expected to systematically diffuse their accomplishments throughout the company and even industry. Critical here is the tendency among the japanese to integrate the work of design engineers and process engineers. Also, firms like NEC emphasize the need to

---

[3] This section draws on Friedman and Samuels.

educate R and D managers about the link between markets and generic technologies (Uenohara 1991). As a result, it has been relatively to diffuse new skills and technologies from military to commercial applications.

Also, there seems to be a **premium placed on diversification**. Again, let me address japanese firms in the defense industry: Whereas US primes traditionally isolated defense from commercial production, japanese primes generally have make no distinction between commercial and military production, except at final assembly. At both the prime and supply levels, components and sub assemblies are designed by the same engineers and produced by and tested on the same equipment, regardless of the project for which the equipment was initially obtained.

3. A third major difference that is likely to cause problems is related to the previous two: It has to do with the **relationship between japanese primes and foreign suppliers**. In general, and this draws on my work in East Asia, **non-japanese suppliers are surprised if not shocked by Japanese requests for bottom-line cost information**. That is, japanese primes emphasize quality and price. I'll deal with quality below. With regard to price - the tendency is for japanese primes to expect a certain percentage reduction in production costs each year. If this does not happen, the prime traditionally asks to see the suppliers' books.

4. A fourth difference has to do with the japanese **emphasis on quality**. This is a difficult issue and may be less of a problem in high tech industries than in, say the auto industry or parts of the textile industry. In auto, I am aware of numerous cases in which non japanese suppliers have had a horrendous time trying to sell to japanese assemblers in the US, not to speak of Japan. The common story is that failure rates of prototypes are too high for the Japanese. In some cases, I am convinced that such responses are simply an excuse for the japanese to keep out foreign suppliers. Their preference is to maintain supplier relationships within the existing network. Indeed, one hears many stories of a foreign supplier buying a component produced by a japanese OEM and submitting it to the assembler, only to have the assmebler report that the component failed tests.

But in many other cases the non japanese supplier has simply not grasped the level of consistent quality required by the japanese. And by the way, I am personally aware of numerous cases in the US auto industry in which one source of US weakness had to do with mnagement's refusal to incorporate employee suggestions for quality improement.

5. A further difference has to do with the **japanese emphasis on personal chemistry and relationships**. Now the literatuer on strategic alliances among US firms often emphasizes interpersonal chemistry, whether between CEOs or between technical and maangement staffs (Green et al 199?) But in the Japanese case, the issue of chemistry is more than just getting along with another manger or leader. It has to do with **building trust**. You have undoubtedly heard of what to us is the peculiar architecture of japanese offices: they are wide open. Senior people tend to have larger desks and better chairs, but otherwise everyone is out in the open exposed to each other. The result is constant communication. My feeling is that this reflects not only the tremendous amount of information flow, but also the premium placed on trust and personal relationships. This premium has several practical consequences: Alliances often take longer to establish precisely because it takes time to nurture personal relationships. Second, as you all have heard to some degree, the japanese take a less legalistic approach to agreeents. This is not to say that there are not legal documents. But these documents allow for contingencies. They allow for situations beyond the control of one or both parties. In other words, once the relationship is established, it provides for flexibility and some security for both parties. Finally, this emphasis on chemistry and trust influences the organizational links between primes and suppliers. You may have heard of the japanese auto suppliers associations or "kyoryokukai" through which japanese assemblers work with their vendors to improve efficiency. US automakers have moved to emulate this practice. GM, for example, has created **Supplier Councils** to discuss quality, to disseminate practices such as value engineering, and to encourage suppliers to learn from each other. These are important steps forward, but they seem to lack the **social bonding emphasis** emphasized by the Japanese associations. I have always been amazed by the number and extent of social activities promoted by the japanese groups. Yet they clearly promote a spirit of cooperation among members.

6. Still another differences has to do with the fact that, despite recent efforts to promote basic research in japan, **japanese firms seem to have a harder time engaging in basic research than their US counterparts** (Yamada 199?). There are several reasons for th is, one of which is the fact that traditional standards of

performance for evaluating research in japanese firms have emphasized the speed of development. This leads to promoting R and D researchers than those in basic research. Another reason is that top japanee management has tended to overemphasize matching their rivals in the same industry.

Resulting Problems

Several problems are commonly mentioned with regard to international joint ventures in R and D. As a result of some of the factors noted above, these tend to be all the more serious with japanese firms (see e.g. Hladik and Linden). The first of course involves **the risks of sharing proprietary know-how**. A second related problem involves **issues of control and product design**. If each side wants to control product development, negotiations can easily deadlock. On product design, the problem is often failure to agree on design specifications during negotiations or in some cases after the venture is operational. Third, there are problems of integration and communication with parent firms. Although joint venutres usually require autonomy, they can fail if they are not linked to the parent's goals and objectives and connected by two way communications. This can result in duplication and inefficient use of development resources. The Jpaanese are very good at maintain such integration. Finally, as we all know there are **problems of antitrust and patent regulations**. It is true that R and D partnerships receive special exemptions. But in the US many antitrust restrictions are imposed when the partnerships extend beyond research into mfging. and marketing. Local patents have also been a problem when dealing with the Japanese market, but my impression is that progress has been made on this.

Suggestions

There are major tradeoffs involving sharing propriety knowledge and product design when one forms high tech alliances with japanese firms. The otpion in my view is not to outlaw or refuse participation in such ventures. It is rather to strengthen our own ability to benefit from them so that these become more of a win-win situation. Several suggestions, such as the need to ensure good integration and communication with the parent firm, emerge from the preceeding discussion of differences and problems. Let me mention just a couple of others.

1. First, **it is useful to decide clearly what kinds of information you can share with a japanese partner in advance**. The challenge of protecting proprietary k nowledge is esepcially difficult for US firms since the skills of US firms tend to be more vulnerable to transfer than those of the Japanese. That is, Western firms tend to be strong in discrete, stand-alone technology, such as the design of a semiconductor chip. These types of technologies are easily copied. But the Japanese are traditionally stronger in manufacturing processes. These are competences that are more difficult to transfer because they are part of a complex web. Thus, for example, imitating one part of the web, such as statistical process control or just-in-time, is difficult without knowing the entire complex of processes in which each part is embedded.[4]

So non-Japanese firms have to think about how to limit the transparency of their operations. One way to do this is to establish physical barriers to Japanese firms. In its work with three Japanese firms on the 767, Boeing restricts the movement of Japanese engineers inside its factories, keeping them away from wing design areas and certain computer rooms. IBM has housed one of its collaborative ventures with Fujitsu in an entirely new and separate facility through which IBM can control exactly what Fujitsu sees and what information leaves the facility.

Another approach is to **limit the scope of formal agreements** to cover one technology rather than a whole range. Also, agreements might be structured to specify **performance requirements**. Motorola has taken

---

[4] Unless otherwise noted, this discussion draws on Hamel et al (1989)

an incremental, incentive-based approach to technology transfer with Toshiba. Motorola releases microprocessor technology only as Toshiba delivers on its promise to increase Motorola's penetration of the Japanese market.

It may also be useful to consider **personnel issues** when thinking about technology transfer since the greatest risk of unintended information transfer occurs in day to day interaction of engineers, product developers and marketers. Limiting unintended transfers requires pa ying attention to the roles of **gatekeepers**-those who control information flows to a joint venture partner. Fujitsu, for example, has established a collaboration section through which its various partners request information and help.

2. A second general suggestion is to **learn how to learn from your joint venture partner**. Part of this ability depends on commitment from top management. But real learning obviously takes place at the operations level. One way to enhance your ability to learn is to ensure that operating employees are briefed well on the partner's strengths and weaknesses, and that they understand how acquiring new skills will bolster their own firm's competitive position. A related point is the need to **reconsider the roles of middle managers.** Traditionally, in US firms the power of middle managers is based on control of information. With the need to diffuse newly acquired skills, the power of middle managers should be based on their ability to promote information sharing and learning. Finally, US firms can enhance their learning capacity by using their partners for **competitive benchmarking**. This practice is a strong tradition in Japanese firms.

3. Third and finally, **it's necessary to develop stronger linkages with other US firms.** I say this in part from the perspective of the individual US firm involved in a partnership with a Japanese counterpart: partnering requires experience and it is probably easier to do this with other US firms.

REFERENCES

Friemdan, David, and Richard Samuels. 1991. "How to Succeed without Really Flying: The Japanese Aircraft Industry and Japan's Technology Ideology." Paper presented to NBER Conference on the U.S. and Japan in Pacific Asia." Del Mar, Cal.

Green, John, John Brupbacher and David Goldheim. 199? "Strategic Parntering Aids Technology Transfer." RTM.

Hamel, Gary., Yves L. Doz, and C.K. Prahalad. 1989. "Collaborate with Your Competitors - and Win." Harvard Business Review. (Jan-Feb.).

Hladik, Karen J. and Lawrence H. Linden. 199?. "Is an International Joint Venture in R&D for You?" RTM.

Hull, Frank M. and Koya Azumi. 1989. "Teamwork in japanese and U.S. Labs." Research-Technology Management (RTM) (November-December).

Rice, Valerie. 1991. "Why Teaming Up is so Hard to Do." Electronic Business (April 8): 30-33.

Richardson, Jacques. 199?. "Japan's Techno-Globalism Offers New S/T Vision." RTM.

Uchitelle, Louis. 1989. "A Japanese Strategy for Boeing," New York Times. December 3.

Uenohara, Michiyuki. 1991. "Management View of Japanese Corporate R&D." RTM. (November-December): 17-23.

Yamada, Hideo. 199?. "Obstacles to Basic Research in Japanese Firms." RTM.

CURRENT DISTRIBUTION CONTROL OF CONVERTERS CONNECTED IN PARALLEL *

K. Siri and C.Q. Lee

Department of Electrical Engineering and Computer Sciences
University of Illinois at Chicago
P.O.Box 4348
Chicago, Illinois 60680
Tel.# (312) 996-2664

ABSTRACT - This paper presents two schemes of current distribution control in a parallel connected converters system; master-slave and central-limit controls. In these techniques, we introduce inner control loops to the converters connected in parallel to achieve output current equalization. We use the current distribution error as a criterion for the system performance. Using these control schemes, the current distribution error can be much improved even with non-identical converters in the system. The central-limit technique provides much less transient current overshoot as compared to the response due to the master-slave approach. These distribution techniques are refined so that only a necessary number of converters are active for each load condition. In this case, the central-limit technique can accurately limit the output current of each converter to its maximum rating; however, the master-slave technique creates output current overshoots above its maximum limit.

I INTRODUCTION

In high power applications, dc-to-dc converters are often connected in parallel at their outputs to form a distributive power system. The concept of uniform distribution of power flow among the standard converter modules in the connection is important for the reasons of cost effectiveness, long term maintainability, and future expansion. However, in general, standard converter modules may not have the identical performance characteristics which cause imbalance of currents drawn from their outputs. The modules delivering heavy currents will have their life-time shortened and degrade the system reliability. For these reasons, there are many studies reported recently in this subject matter [3]-[8].

In this paper, two schemes of current distribution control will be analyzed from the system block diagrams so that the steady state distribution errors can be determined. Because of the control approaches used in these schemes, these techniques are called the master-slave and the central-limit controls. The performance characteristics of distributive power systems using these two control techniques will be presented. The comparison between the system performances with and without these distribution controls will also be given. For the purpose of illustration, the system of two buck converters connected in parallel will be analyzed and simulated.

II PRELIMINARY STUDY

In this paper, we deal with the converter system shown in Fig. 1 in which a number of standard converter modules are connected in parallel to deliver a specified power to the output load. Our objective is to devise control techniques to regulate these converters so that their output currents will be equal at all time. To be more specific in our analysis, we use the buck converter as a standard converter module in our system.

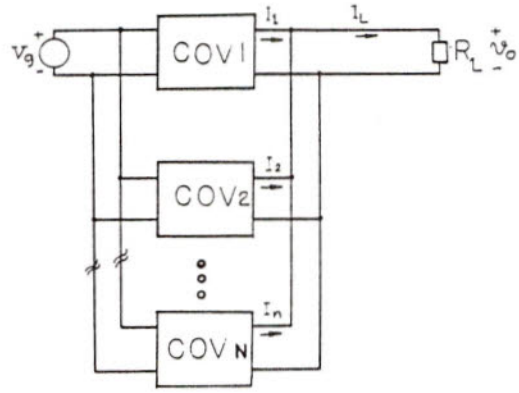

Fig. 1 Parallel input parallel output converters

Consider a set of N buck converters connected in parallel to form a distributive power system with a common feedback control circuit as shown in Fig. 2.

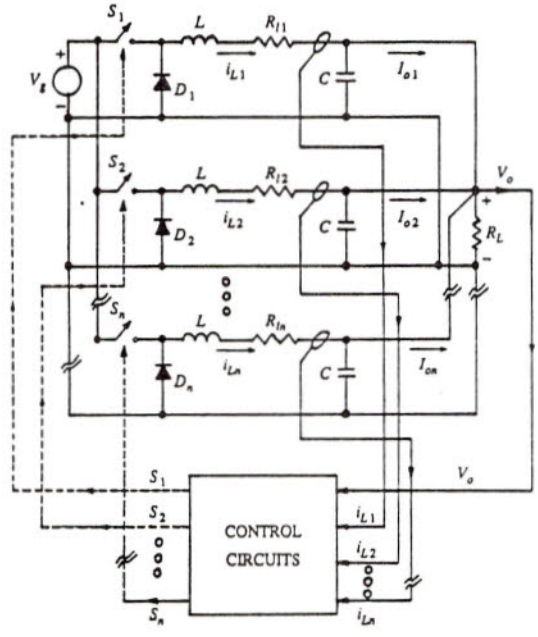

Fig. 2 Multi-loop control of N converters connected in parallel

* This work was supported by Rocketdyne Division, Rockwell International, Canoga Park, CA.

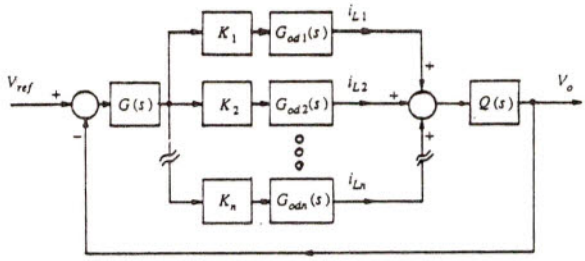

Fig. 3 Block diagram of single loop system of N buck converters

In this figure, the output currents I_{Li}, as well as the output voltage of the parallel connected converter system are fed back to determine the proper switching signals, S_i, to regulate the output current in the power stage of each converter. Consider the conventional approach in which only the output voltage is fed back for the voltage regulation. To determine the current distribution among converters connected in parallel, the overall control block diagram of the system is given in Fig. 3. The transfer functions indicated in the block diagram are defined as follows:

K_i – *PWM gain of the converter i,*

$G_{odi}(s)$ – *Transfer function of the inductor current to duty ratio,*

$G(s)$ – *Transfer function of the compensation circuit,*

$Q(s)$ – *Output impedance function.*

To illustrate the basic problem associated in this traditional approach, we will consider the case when N equals to 2. It can be shown that the transfer functions indicated in the block diagram are given by [10]

$$G_{od1}(s) = \frac{I_{L1}(s)}{d(s)} \tag{1}$$

$$= \frac{(2sC + \frac{1}{R_L})(sL + R_{l2})}{(sL+R_{l1})((2sC+\frac{1}{R_L})(sL+R_{l2}) + 1) + sL + R_{l2}} D V_g$$

$$G_{od2}(s) = \frac{I_{L2}(s)}{d(s)} \tag{2}$$

$$= \frac{(2sC + \frac{1}{R_L})(sL + R_{l1})}{(sL+R_{l2})((2sC+\frac{1}{R_L})(sL+R_{l1}) + 1) + sL + R_{l1}} D V_g$$

$$Q(s) = \frac{V_o(s)}{I_{L1}(s) + I_{L2}(s)} = \frac{R_L}{2sCR_L + 1} \tag{3}$$

Applying Mason gain formula to the block diagram shown in Fig. 3, we obtain the distribution error which is given by

$$I_{L1}(s) - I_{L2}(s) = \frac{KG(s)(G_{od1}(s) - G_{od2}(s))}{1 + KG(s)Q(s)(G_{od1}(s)+G_{od2}(s))} V_{REF}(s) \tag{4}$$

Let $V_{REF}(s)$ be a step function as V_{ref}/s. According to (4), assuming that the function in the denominator has no zero on the right hand side of the complex-plane (RHP), we can calculate the steady state distribution error using the final value theorem. Thus, we have

$$I_{L1}(0) - I_{L2}(0) = \lim_{s \to 0} s(I_{L1}(s) - I_{L2}(s)) \tag{5}$$

where $I_{L1}(0)$ and $I_{L2}(0)$ are the steady state values of $I_{L1}(s)$ and $I_{L2}(s)$. Assume that KG(s) >> 1 as s → 0. The DC current distribution error is then given by

$$|I_{L1}(0) - I_{L2}(0)| \approx \frac{|R_{l2} - R_{l1}|}{R_L (R_{l1} + R_{l2})} \cdot V_{ref} \tag{6}$$

As an example, if V_{ref} = 120 V, R_{l2} = 0.2, R_{l1} = 0.01, and R_L = 2.5 Ω, we obtain

$$|I_{L1}(0) - I_{L2}(0)| = 43.43\ A \tag{7}$$

It can be seen that connecting two non-identical converters in parallel creates the out-of-balance in dc current distribution.

When the converters are controlled by different pulse-width modulators, there exist self-response and cross-response in the output currents. The self-response of a converter is its output current response due to its own pulse-width modulator. The cross-response of a converter is its output current response due to the pulse-width modulator of the other converter. To simplify the analysis, we assume that the cross-responses can be neglected in our derivation. Thus, the transfer functions of the output current to duty ratio can be written as

$$G_{od1}(s) = \frac{I_{L1}(s)}{d_1(s)} \tag{8}$$

$$= \frac{(2sC + \frac{1}{R_L})(sL + R_{l2}) + 1}{(sL+R_{l1})((2sC+\frac{1}{R_L})(sL+R_{l2}) + 1) + sL + R_{l2}} D V_g$$

$$G_{od2}(s) = \frac{I_{L2}(s)}{d_2(s)} \tag{9}$$

$$= \frac{(2sC + \frac{1}{R_L})(sL + R_{l1}) + 1}{(sL+R_{l2})((2sC+\frac{1}{R_L})(sL+R_{l1}) + 1) + sL + R_{l1}} D V_g$$

Equations (8) and (9) will be used again in the following analysis.

III MASTER-SLAVE CONTROL

(III.1) Master-Slave Control of Two Converters

Consider a set of N buck converters connected in parallel with the control scheme as shown in Fig. 4.

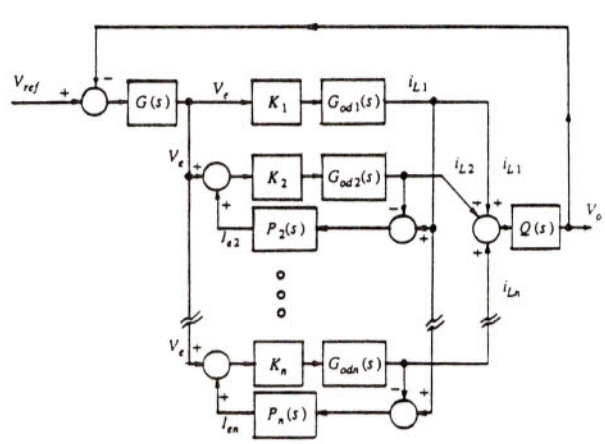

Fig. 4 Master-slave control system of N buck converters

In this converter system, the primary control loops are $G(s)K_i G_{odi}(s)Q(s)$, where i = 1, 2, . . , N, are regulated by the voltage error signal $V_e = G(s)(V_{ref} - V_o)$. Therefore, the output voltage of the system is regulated to $V_o = V_{ref}$. However, with i_{L1} as the reference signal, the inner control loops, $P_i(s)K_i G_{odi}(s)$, where $1 < i \le N$, are used to regulate the inductor current i_{Li} to i_{L1}. For this reason, the converter #1 is called the master converter, and the remaining converters are referred to as slave converters.

In order to make a comparative study of the performance characteristics between different control schemes, we will derive the expression for the current distribution error function for N = 2. From the block diagram given in Fig. 4, for $K_1 = K_2 = K$, it can be shown that such function can be obtained and given by

$$|I_{L1}(0) - I_{L2}(0)| = \frac{V_{ref} KG(0) \times |G_{od1}(0) - G_{od2}(0)|}{\Delta_1(0)} \tag{10}$$

where

$$\Delta_1(0) = 1 + K\ G(0)\ Q(0)\ (G_{od1}(0) + G_{od2}(0)) + K\ G_{od2}(0)P(0) + 2G(0)K^2 G_{od1}(0)G_{od2}(0)P(0)Q(0)$$

In deriving (10), we assume that $\Delta_1(s)$ has no zero on the RHP. From equations (3), (8), (9), and (10), we have

$$|I_{L1}(0) - I_{L2}(0)| = \frac{K\ G(0)\ |R_{l2} - R_{l1}|\ V_g}{\Delta_2(0)} \cdot V_{ref} \tag{11}$$

where $\Delta_2(0) = R_{l1}R_{l2} + (R_{l1}+R_{l2})\ R_L\ (1 + K\ G(0)\ V_g) + 2\ K\ G(0)\ R_L^2\ V_g + K\ V_g\ P(0)\ (R_L + R_{l1}) + \dfrac{2P(0)G(0)K^2(R_L+R_{l2})(R_L+R_{l1})R_L V_g^2}{R_{l1}R_{l2} + R_L(R_{l1} + R_{l2})}$

Given P(0) = 1, Q(0) = 2.5 Ω, K = 4.29 V/s, V_{ref} = 120 V, G(0) = 46.38, R_{l1} = 0.01 Ω, R_{l2} = 0.2 Ω, the current distribution error can be calculated from (11) and is equal to 0.52 mA, which is very small as compared to the error of 43.43 A due to single loop control.

(III.2) Master-Slave Control of Many Converters

When N converters are connected in parallel as shown in Fig. 4, the current distribution error can be defined as $|I_{L1} - I_{Li}|$, where i = 2, 3, . . , N, and I_{L1} is the output current of the master converter. According to the Mason gain formula, the steady state output current of a slave converter, $I_{Li}(0)$, can be written as

$$I_{Li}(0) = \frac{V_{ref} G(0)}{\Delta_N(0)} \left[K_1 G_{od1}(0)A_i(0) + K_i G_{odi}(0)\right] \prod_{\substack{j=2 \\ j\neq i}}^{N} (1 + A_j(0))$$

$$\text{for } 2 \le i \le N \tag{12}$$

where $A_i(s)$ is the inner loop gain of the i-th slave converter, which is equal to $K_i G_{odi}(0)P_i(0)$ where $P_i(s)$ is the compensation amplifier gain for the current error signal, $I_{L1} - I_{Li}$. Similarly, the steady state output current of the master converter, $I_{L1}(0)$, is found to be

$$I_{L1}(0) = \frac{V_{ref} G(0)}{\Delta_N(0)} K_1 G_{od1}(s) \prod_{j=2}^{N} (1 + A_j(0)) \tag{13}$$

Assuming that $A_j(0)$ is much greater than 1, we can make the following approximation;

$$\prod_{\substack{j=2 \\ j\neq i}}^{N} (1 + A_j(0)) \approx A_i(0) \prod_{\substack{k=2 \\ k\neq i}}^{N} A_k(0) \tag{14}$$

Using only the dominating terms, it can be shown that $\Delta_N(0)$ can be simplified as

$$\Delta_N(0) \approx N\ Q(0)\ K_1 G_{od1}(0) \prod_{l=2}^{N} A_l(0) \tag{15}$$

According to (12) to (15), when G(0) is much greater than 1, the distribution error can be approximated as

$$|I_{L1}(0) - I_{Li}(0)| \approx \frac{V_{ref}\ |K_1 G_{od1}(0) - K_i G_{odi}(0)|}{N\ Q(0) K_1 G_{od1}(0) A_i(0)} \tag{16}$$

IV CENTRAL-LIMIT CONTROL

(IV.1) Central-Limit Control of Two Converters

Consider a set of N buck converters connected in parallel in a converter system using the control technique as shown in Fig. 5. In this block diagram, the primary feedback control loops for the output voltage regulation are as same as those in the master-slave approach. But there is one inner feedback control loop, $K_i G_{odi}(s)P_i(s)$, in each converter for the current distribution control. Each inner feedback loop is controlled by the reference current signal, $I_{ref}(s)$, which is the weighted sum of all output currents, $W(s)(I_{L1}(s) + I_{L2}(s) + . . + I_{LN}(s))$, where W(s) is the weighting function. Here W(s) is a constant and is equal to 1/N where N is the number of converters connected in parallel. Consequently, $I_{ref}(s)$ is the central reference signal that every current I_{Li} (s), i = 1, 2, . . , N, will track. To regulate each current to I_{ref} (s), the current error signal I_{ei} is added to the voltage error signal, V_e, in each inner control loop to make a minor adjustment in the duty ratio of each PWM controller.

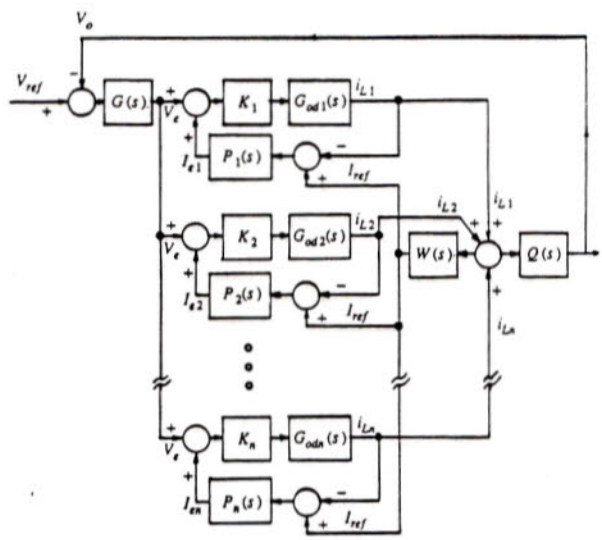

Fig. 5 Central-limit control system of N buck converters

For N equals 2, applying Mason gain formula and the final value theorem to Fig. 5, and assuming $K_1 = K_2 = K$, we obtain the current distribution error as

$$|I_{L1}(0) - I_{L2}(0)|_{DC} = \frac{V_{ref}}{\Delta_3(0)} \left[G(0)\ K\ |(G_{od1}(0) - G_{od2}(0))| + 2\ K\ G_{od1}(0)G_{od2}(0)\ |(P_2(0) - P_1(0))(1-2W(0))|\right] \tag{17}$$

where

$$\Delta_3(0) = 1 + G(0)\ K\ Q(0)\ (G_{od1}(0) + G_{od2}(0)) + (1-W(0))\ K\ (P_1(0)G_{od1}(0) + P_2(0)G_{od2}(0))$$

$$+ G(0)\,K^2 G_{od1}(0)G_{od2}(0)Q(0)(P_1(0)+P_2(0))(\,1 - W(0))$$

$$+ K^2 G_{od1}(0)G_{od2}(0)P_1(0)P_2(0)\,(1 - 2W(0)\,) \qquad (18)$$

We assumed that $\Delta_3(s)$ has no zero on the RHP. Here when W(0) equals 0.5, I_{L1} is approximately equal to I_{L2}. Given G(0) = 46.38, K = 4.29 V/s, Q(0) = 2.5 Ω, $P_1(0) = P_2(0) = 1$, V_{ref} = 120 V, $G_{od1}(0) = 5.123\ V_g$, $G_{od2}(0) = 4.762\ V_g$, and V_g = 160 V, the distribution error can be calculated from (17) and is equal to 1.3 mA, which is negligible as compared to the output currents.

(IV.2) Central-Limit Control of Many Converters

The current distribution error, $|\,I_{Li}(0) - I_{Lj}(0)\,|$ can also be derived for the system of N converters connected in parallel using the central-limit control. According to the Mason gain formula, the output current of the i-th converter, $I_{Li}(0)$, can be found as

$$I_{Li}(0) = \frac{V_{ref}\,G(0)}{\Delta_N(0)} K_i G_{odi}(0)\Big[1 + (1 - W(0)) \sum_{\substack{k=1 \\ k\neq i}}^{N} A_k(0) +$$

$$(1 - 2W(0)\,) \sum_{m\neq n\neq i}^{N} A_m(0)A_n(0) + \ .$$

$$+ \sum_{\substack{l=1 \\ l\neq i}}^{N} K_l G_{odl}(0)A_i(0)W(0)\Delta_l(0)$$

$$+ \ (\,1 - (N - 1)W(0)\,) \prod_{\substack{k=1 \\ k\neq i}}^{N} A_k(0)\Big] \qquad (19)$$

where $A_k(s) = P_k(s)\ K_k G_{odk}(s)$, $\Delta_l(0)$ is the $\Delta(0)$ for that part of the signal flow graph which is nontouching with the forward path $K_l G_{odl}(0)A_i(0)W(0)$. $\Delta(0)$ is given by

$$\Delta(0) = 1 - \sum_m P_{m1} + \sum_m P_{m2} - \sum_m P_{m3} + \ . \ . \ .$$

where P_{mr} is gain product of the mth possible combination of r nontouching loops. For $P_1(0) = P_2(0) = \ . \ . = P_N(0)$, given that W(0) = 1/N and G(0) >> 1, $\Delta_N(0)$ can be derived and approximated from its dominating terms as

$$\Delta_N(0) = \frac{G(0)Q(0)}{P(0)} \prod_{l=1}^{N} A_l(0) \qquad (20)$$

With Mason gain formula and the approximation made to the dominant loop gain products, $|\,I_{Li} - I_{Lj}\,|$ can be derived as

$$|\,I_{Li}(0) - I_{Lj}(0)\,| \simeq \frac{V_{ref}P(0)\ |K_i G_{odi}(0) - K_j G_{odj}(0)|\Gamma(0)}{Q(0)\prod_{i=1}^{N} A_i(0)} \qquad (21)$$

where $\Gamma(0) = 1 + P(0) \sum_{\substack{l=1 \\ l\neq i \\ l\neq j}}^{N} K_l G_{odl}(0)$

V COMPUTER SIMULATION

A FORTRAN program has been written to simulate the responses of two buck converters connected in parallel. Firstly, the system with a single loop for the voltage regulation shown in Fig. 2 is simulated. The output voltage and the output currents are shown in Figs. 6 and 7, respectively.

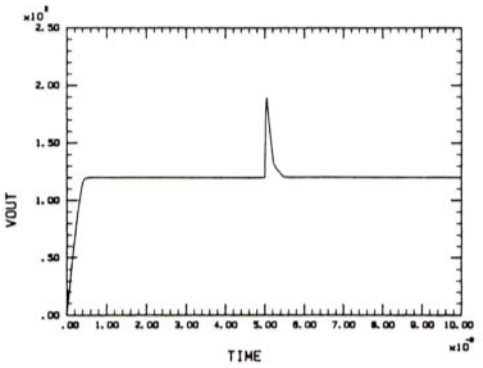

Fig. 6 Output voltage of single loop system of two converters

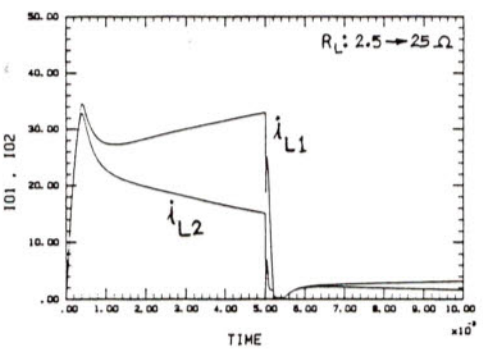

Fig. 7 Output currents of single loop system of two converters

From Fig. 7, we see that the output currents diverge to very different values due to different inductor resistances in the two converters, R_{l1} = 0.01 Ω and R_{l2} = 0.2 Ω. The system with the multiloop feedback using the master-slave current distribution control, shown in Fig. 4, is then simulated. The current distribution is shown in Fig. 8. It can be shown that current I_{L2} closely tracks the master current I_{L1} with some transient overshoot.

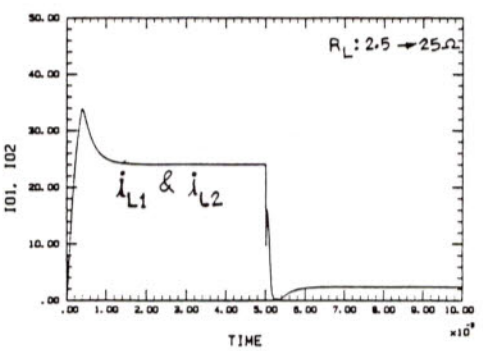

Fig. 8 Output currents of master-slave control system

Finally, the system using the central-limit control shown in Fig. 5 is simulated to obtain their output currents which are shown in Fig. 9.

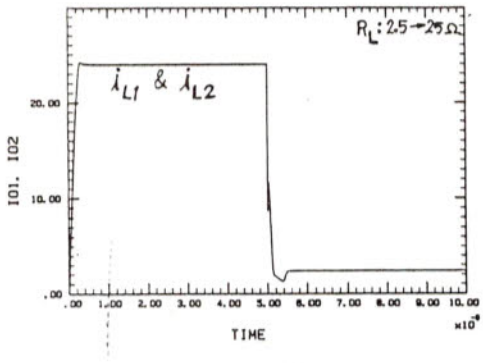

Fig. 9 Output currents of central-limit control system

This figure shows that the output currents I_{L1} and I_{L2} track each other with almost no overshoot. According to these figures, it may be concluded that the current transient responses due to the central-limit control is superior to those due to the master-slave control. Furthermore, the simulated output voltage and the currents in the open loop converter system are shown in Figs. 10 and 11, respectively.

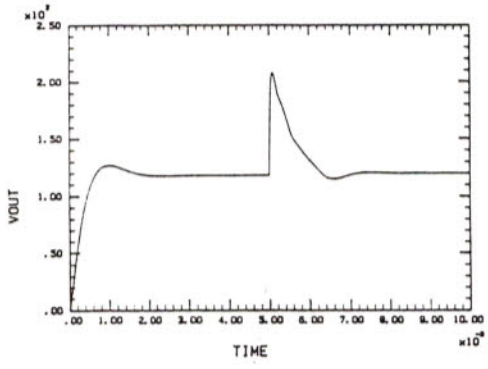

Fig. 10 Output voltage of open loop system of two converters

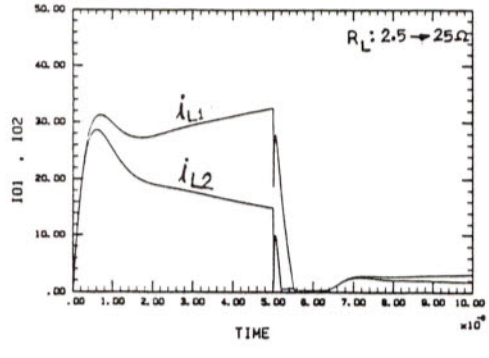

Fig. 11 Output currents of open loop system of two converters

From these figures, it can be seen that the transient times due to the start-up or step-load change are longer than those from the closed loop system.

VI DISTRIBUTION CONTROL FOR MAXIMUM CURRENT LIMIT

With the current distribution control alone, all converters in the system are operating simultaneously even at light load. Thus, the overall efficiency of the system is degraded because the poor efficiency of each converter exists at light load. To alleviate such problem, the converters in the system should be controlled such that some of them will be turned off when the output power drops below a specified minimum level. On the other hand, when the output load increases to a specified maximum value, additional converters should be activated to share the output current. Thus, none of the active converters is operating at more than its power capability. Turning on of an inactive converter, or turning off of an existing active converter is based on a specified output current level which is determined from the number of converters in the active state. The number of these output current levels, called the maximum output current limits, are determined from the number of converters connected in the system. This extra feature of control improves the total efficiency of the system.

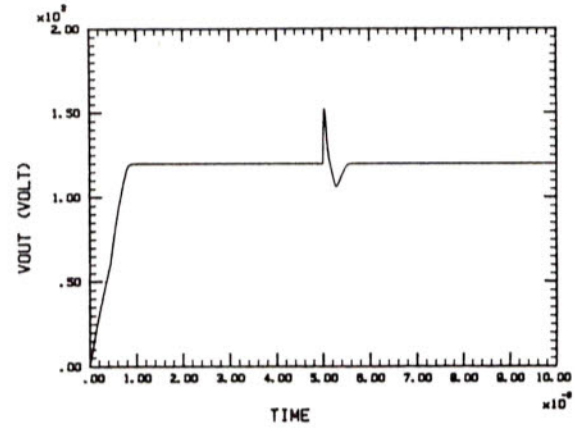

Fig. 12 Output voltage of master-slave system

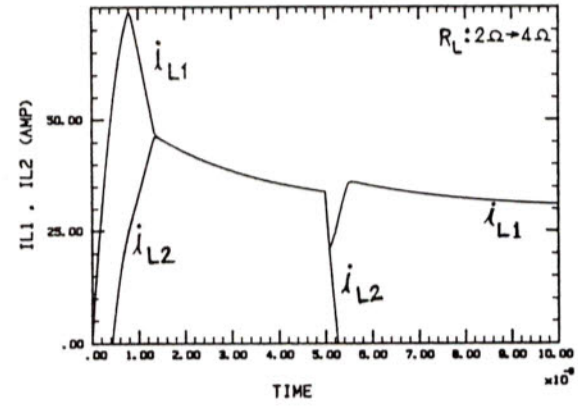

Fig. 13 Output currents of master-slave system

The performance characteristics of the system with these control features can be shown from the simulation results of two buck converters connected in parallel. The simulation of the master-slave current distribution and the maximum current limit control is shown in Figs. 12 and 13. Fig. 12 is the output voltage response for 10 ms with a step load change form 2 to 4 Ω after running the converter for 5 ms. Fig. 13 shows the output inductor currents i_{L1} and i_{L2}. The master current i_{L1} rises from the start. When it reaches the maximum limit of 52.25 A at about

0.4 ms, the slave current i_{L2} begins to rise. However, the master current i_{L1} can have an overshoot above 52.25 A due to the absence of the current control loop in the master converter. At t ≈ 1.4 ms, the slave current i_{L2} tracks the master current i_{L1}. At t = 5 ms, the load changes from 2 to 4 Ω , which causes the current to drop. When the total current decreases below 52.25 A, the slave converter is shut off and only the master converter delivers current to the load.

The simulation results of the central-limit current distribution and the maximum current limit control are shown in Figs. 14 and 15, respectively. Similar to Fig. 12, the output voltage response is given in Fig. 14. Fig. 15 shows the output inductor currents i_{L1} and i_{L2} responses from which it can be seen that current i_{L1} never exceeds the 52.25 A limit. This shows that the central-limit control is superior to the master-slave control.

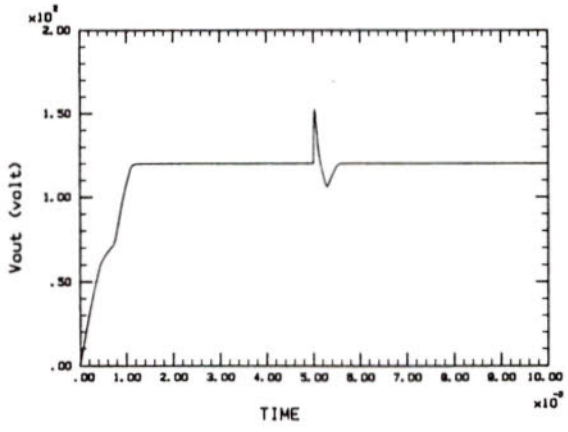

Fig. 14 Output voltage of central-limit system

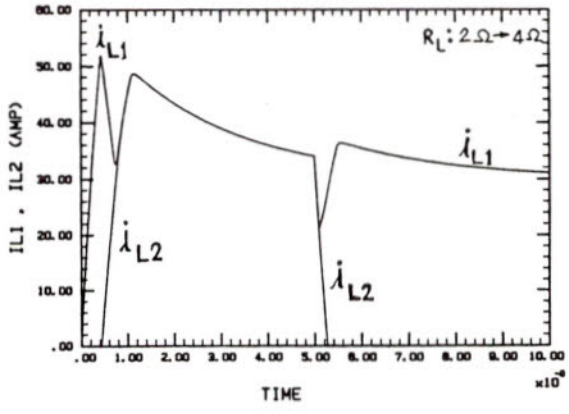

Fig. 15 Output currents of central-limit system

The circuit realization for the maximum current limit control is depicted in Fig. 16 in which ENABLE2 signal is active whenever the total load current, $i_{L1} + i_{L2}$, exceeds the maximum limit, IMAX. This signal enables the driving circuit of the second converter and is used to adjust weighting function W(s).

Since the central-limit technique yields better performance as compared to that of the master-slave technique, three converters connected in parallel for the central-limit control are simulated and their output voltage and currents are shown in Figs. 17 and 18, respectively.

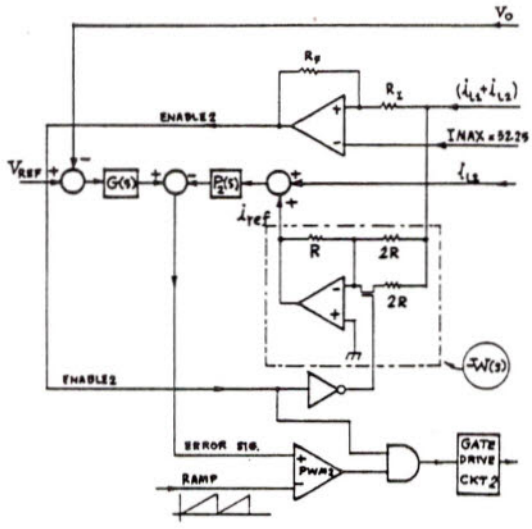

Fig. 16 Maximum current limit control circuit

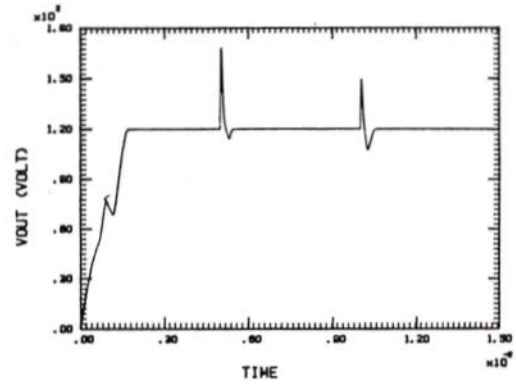

Fig. 17 Output voltage of three converters connected in parallel

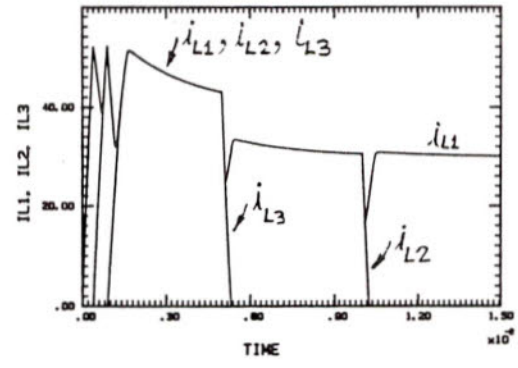

Fig. 18 Output currents of three converters connected in parallel

From Fig. 17, the voltage undershoots always follow the voltage overshoots during the heavy-to-light step load changes. In Fig. 18, the current, I_{L1}, starts from zero while currents I_{L2} and I_{L3} remain zero. When I_{L1} increases to the maximum limit of 52.25 A, I_{L2} starts to build up and causes I_{L1} to decrease below the maximum limit. Later, I_{L1} and I_{L2} track each other and increase together. When the sum of the currents reach the maximum limit of 104.5 A, I_{L3} begins to rise and causes currents I_{L1} and

I_{L2} to decrease. Consequently, at t = 1.2 ms, all three currents track one another. At t = 5 ms, the load changes from 1 to 2 Ω, and all currents start to drop. When the total current drops to 104.5 A, the converter #3 is inhibited, and I_{L3} drops monotonically to zero while the other two currents, I_{L1} and I_{L2}, are still tracking each other. At t = 10 ms, the load changes from 2 to 4 Ω and both currents start to decrease. When the total current falls below 52.25 A, the converter #2 is inhibited and I_{L2} continues to fall until it reaches zero. Thus, only the converter #1 remains active.

VII CONCLUSION

The equalization of currents drawn from dc-to-dc converters connected in parallel is achieved by using additional current control loops. According to the analysis, it is not necessary that the compensation amplifiers within these additional current control loops have high gains because the the dominating loop gain products of the system automatically become high enough to quarantee a good current distribution. The master-slave technique can provide good current distribution. However, it provides no control in the output current overshoots which occur in the output of the master converter. Additionally, the central-limit current distribution control provides tight control to all currents in the converters towards the central-limit reference signal which is the weighted average of the total current to the shared load. Hence, the central-limit technique is superior as compared to those of the master-slave technique.

A technique of distribution control for maximum current limit has been also proposed. By using this technique, converters in the active state are always operating at their optimum loads. Consequently, the overall efficiency of the converter system should remain high even when it operates at high load.

References:

[1] Vatche Vorperian and Slobodan Cuk: "Small Signal Analysis of Resonant Converters", *IEEE Power Electronics Specialists Conference*, June 6 - 9, 1983, Albuquerque, NM

[2] Billy Y. Lau: "The Small_Signal Input-to-Output Frequency Response of Switching Converters', *IEEE Power Electronics Specialists Conference*, vol.2, pp. 1355-1363, April 1988.

[3] John Reed and Naresh Sharma: "Large Parallel UPS Systems Utilizing PWM Technology," *IEEE Power Electronics Specialists Conference*, pp. 282-289, 1984.

[4] Kawabata T. and Higashino: "Parallel Operation of Voltage Source Inverters," *IEEE Transactions on Industry Applications*, pp. 281-287, 1988.

[5] Joseph Perkinson: "UPS Systems - A Review," *IEEE Power Electronics Specialists Conference*, pp. 151-154, 1988.

[6] Holtz Joachim Holtz and Werner Karl-Heinz: "Multi-Inverter UPS System with Redundant Load Sharing Control," *IEEE Power Electronics Specialists Conference*, pp. 159-165, 1989.

[7] T. Suntio, J. Uusitalo and I. Jonsson: "AC-UPS Reliability and Availability Performance: Comparison of Available Solutions," *INTELEC* 14.1 pp. 1-10, 1989.

[8] F. Petruzziello, P.D. Ziogas, and G. Joos: "A Novel Approach To Paralleling of Power Converter Units," *IEEE Power Electronics Specialists Conference*, vol.2, pp. 808-813, 1990.

[9] Benjamin C. Kuo: *Automatic Control System*, fourth edition, PRENTICE-HALL, INC., Englewood Cliffs, NJ 07632, 1982.

[10] Rudolf P. Severns and Gordon E. Bloom: *Modern DC-to-DC Switchmode Power Converter Circuits*, Van Nostrand Reinhold Electrical/Computer Science and Engineering Series, 1985.

Ultra-Low On-Resistance P-channel Lateral DMOS Fabricated on (110)-Oriented Si Substrate

K. Throngnumchai

Nissan Research Center, Nissan Motor Co., Ltd.
1 Natsushima-cho, Yokosuka-shi, Kanagawa-ken, JAPAN 237
Tel. +81-468-67-5183, Fax. +81-468-65-8104
E-mail: kraisorn@nova.lab.nissan.co.jp

This paper presents a p-channel lateral DMOS (LDMOS) featuring improved on-resistance through the use of a (110)-oriented Si substrate. The specific on-resistance of this LDMOS is believed to be the lowest among p-channel power MOSFETs reported to date.

P-channel power MOSFETs are still widely used in such applications as high-side switching and complementary circuits even though their on-resistance, R_{on}, is about three times higher than that of n-channel devices having the same chip-size. While there is a need to reduce the R_{on} value of these devices, conventional (100)-substrates do not have a suitable orientation for this purpose because their hole mobility is lower than that of (110)-substrates.

In this study, we fabricated p-channel LDMOS on both (100)- and (110)-substrates and compared their on-resistance. Both types of samples were fabricated using double metallization and a hexagonal pattern similar to that described in ref. 1. The resistivity of the n-type substrates used in fabricating both sample types was kept constant at 10Ω-cm. To form a p-well on the substrates, a boron dosage of $1.5\times10^{13}/cm^2$ was implanted and diffused at 1120°C in a N_2-atmosphere for 48 hours. The n-body and source were formed using a conventional double diffusion technique. The gate length (L_G), diameter of the source and drain window, and distance from the gate-edge to the drain-edge (L_{off}) were 4μm, 6μm, 6μm, and 1μm respectively. The gate oxides of both types of samples were formed by the same thermal oxidation process at 1050°C in a dry O_2-atmosphere. From the CV characteristics, the thickness of the gate oxides on the (110)- and (100)-substrates was determined to be 62 and 49nm respectively. This difference in thickness is attributed to the dependence of the oxidation rate on the substrate orientation.

The on-resistance of the samples was determined as a function of their effective longitudinal gate field, E_{inv}, defined by $(V_{GS}-V_{th})/t_{ox}$, where V_{GS}, V_{th}, and t_{ox} are the applied gate voltage, threshold voltage, and gate oxide thickness. The measured threshold and breakdown voltages were -3.28 and -51V for the (110)-sample and -2.54 and -46V for the (100)-sample. When E_{inv} was -5MV/cm, the measured specific on-resistance of the (110)-sample was 2.27Ω-cm^2, only 0.64 times as much as the 3.52Ω-cm^2 measured for the (100)-sample.

It was found that the on-resistance ratio between the p-channel LDMOS fabricated on the (110)- and (100)-substrates can be reduced by increasing E_{inv}. This is another advantage of using (110)-substrates for power applications where a high gate field is available. The reduction of the on-resistance ratio between the substrates is thought to be due to the differences in their surface roughness scattering. The relationship between hole mobility, μ_h, and the universal effective longitudinal field, E_{eff}, was found for both substrates using the technique described in ref. 2. A comparison of the measured results indicated that μ_h of the (110)-substrate was reduced at a slower rate than that of the (100)-substrate as E_{eff} increased. This result shows that the on-resistance ratio between the two substrates is dependent on E_{inv}.

[1] M. Hoshi et al., "Low On-Resistance Power MOSFET Using Double metal Process Technology", ISPSD'91, pp. 61-64,1991
[2] S. Takagi et al., "On the Universality of Inversion-layer Mobility in N- and P-channel MOSFETs", IEDM88, pp. 398-401, 1988

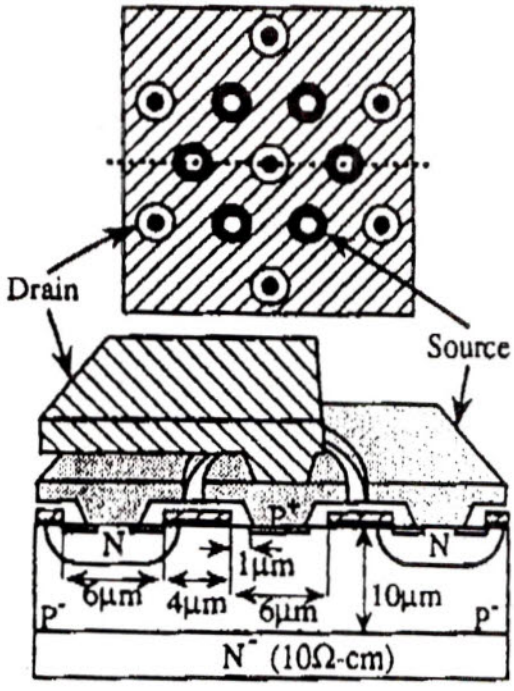

Fig.1 Scheme showed layout pattern and structure of the fabricated LDMOS

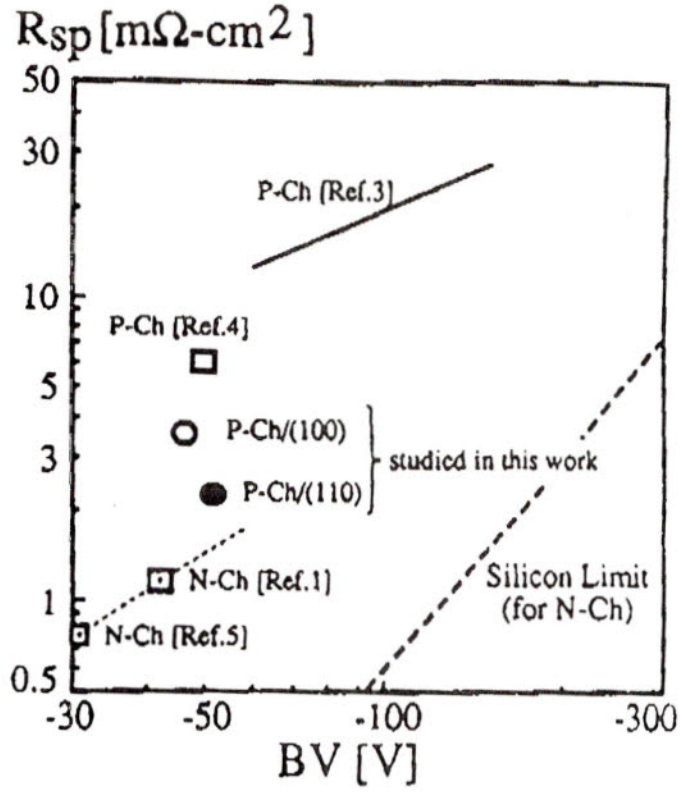

Fig.2 On-resistance vs. breakdown voltage

Ref.3) S. Shugyo et al., NEC-gihou, vol.40, No.5, pp.64-66, 1987 (in Japanese)
Ref.4) A. Cogan et al., Conf. Rec. IEEE Ind. Appl. Soc. Annu. Meet-21st, pp.340-344, 1986
Ref.5) M. Morikawa et al., ISPSD'92, pp.150-154, 1992

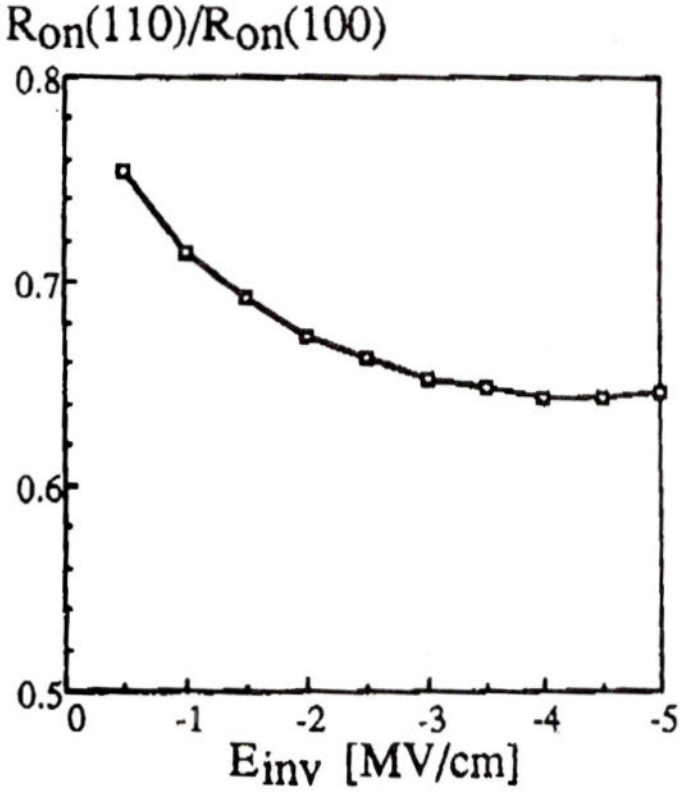

Fig.3 On-resistance ratio between the LDMOS fabricated on the (110)- and (100)-substrates vs. effective gate field. This result can be explained by the dependence of hole mobility on a gate field shown in

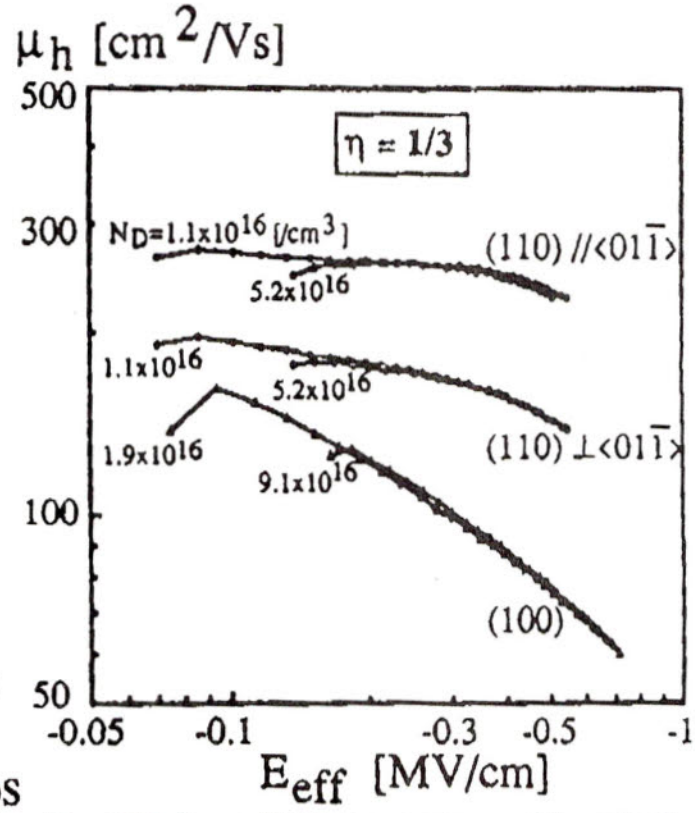

Fig.4 Hole mobility vs. universal longitudinal field. This result shows a different dependence of hole mobility on the longitudinal field between the (110)-

EFFECT OF FRACTIONATED FLY ASH AND SILICA FUME ON HIGH STRENGTH CONCRETE

Chai Jaturapitakkul, Ph.D.
Dept. of Civil Engineering
King Mongkut's Inst. of Tech.
Bangmod, Bangkok, Thailand

Methi Wecharatana, Ph.D.
Dept. of Civil Engineering
New Jersey Inst. of Tech.
Newark, New Jersey 07102,U.S.A.

ABSTRACT

Fly ash is fractionated into different small ranges of particle size distribution. The very fine particle size of fractionated fly ash (smaller than 5 microns) was employed to produce high strength fly ash concrete. Fifteen and twenty five percent of fly ash by weight of cementitious materials were used in the concrete mix as cement replacement. Silica fume in the powder form was also added with the same proportion as fly ash. The compressive strength of fly ash and silica fume concrete was determined and compared to the control high strength concrete. The results show that the compressive strength of fly ash and silica fume concrete achieves a strength of 6000 psi (42 MPa) after 7 days of curing. The rate of strength gain of concrete made from silica fume is very fast at early age but seems to slow down after 7 days. Its strength is almost the same as the control strength at 28 days. High strength concrete made from fractionated fly ash behaves differently that at the early age, the strength of fly ash concrete is lower than those of control and of silica fume concrete. After 14 days, the use of fractionated fly ash in concrete produces the same strength as the control concrete. While at 28 days, the strengths of fly ash concrete are higher than both the control and silica fume concrete. The strengths of these fly ash concretes are in the order of about 8500 psi (58 MPa) whereas the strength for the control and silica fume concretes are about 8000 psi (55 MPa). The compressive strengths of fly ash concrete are in the range of 107% to 115% of the control concrete at the age of 90 days. The results obtained here suggest that fractionated fly ash is a suitable material to produce high strength concrete. The use of fly ash in concrete not only eliminates the cost incurred for the disposal of fly ash but also reduces the cost of high strength concrete.

INTRODUCTION

ACI committee 363 has specified high strength concrete as concrete with a compressive strength of 6000 psi (41 MPa) or greater (ACI 363, 1990). The basic concept to produce high strength concrete is to lower the water/cement ratio as much as possible, usually in the range of 0.25 to 0.30. In achieving this w/c ratio, many high strength concretes incorporate chemical admixtures, such as water reducing agents or high-range water reducing agents or superplasticizers and mineral admixtures such as fly ash or silica fume. The use of a good quality fly ash, meeting specification of ASTM C-618 Class F, is a must in the production of high strength concrete (Task Force Report No. 5, 1977). The fly ash added serves two purposes, one as pozzolanic material to provide additional C-S-H, and the other as filler to reduce voids between cement particles. Optimum amounts are in the range of 10% to 15% by weight of the cement. This may vary considerably in different areas due to the physical and chemical properties of the pozzolan and its reaction with various cements. When silica fume and fly ash were used, the optimum mix is a combination of 10% silica fume with 15% fly ash or slag by volume (Mehta and Aitcin 1990). Silica in the combined mixture provides early strength to concrete while fly ash which is an inert material serves as retarder but provides long term strength. Most high strength concrete mixes presently used contained both silica fume and fly ash.

The use of fly ash in high strength concrete undoubtedly has been demonstrated to be beneficial to the integrity of the composites as well as the economical aspect of the final products. In any event, it should be noted that in such an application, fly ash was often used as generic material. While global performance of high strength fly ash concrete is satisfactory, a clear understanding of how fly ash actually performs in high strength concrete environment remains unknown. This is primarily due to the lack of understanding on the behavior of the fly ash used. The present study uses series of fly ash of known origin, formation, physical and chemical characteristics. With these information, the authors intend to study the role of fly ash in high strength concrete. Of particular interest will be the key parameters of fly ash governing the strength development of the final cement composites.

In this research, testing is made to evaluate the effect of silica fume and fly ash when used as a cement based matrix in concrete. Silica fume in the powder form and the finest fly ash from the dry and wet bottom ashes (3F and 13F) are mixed with concrete as 15% and 25% cement replacements. Superplasticizer is added to lower the water content in the mix. With a high portion of silica fume in the mix, the superplasticizer is used at 10 ml per pound of the cementitious (cement + fly ash or silica fume) materials.

MATERIALS AND TEST PROGRAM

Materials used in this study consist of standard portland cement type I, siliceous sand (river sand) passing sieve No. 4, coarse aggregate with a maximum size of 3/8 inch, fly ash, silica fume, superplasticizer, and water. Two different kinds of fly ash from the utilities in New Jersey were selected for this study. Fly ash of class 13F was obtained from boiler burning coal at a temperature higher than the fusion point of fly ash while class 3F fly ash the temperature in the boiler was lower than the ash fusion temperature. These fly ashes were obtained by separated the original feed fly ash (fly ash received from the utility silo). 3F and 13F fly ashes were very fine with maximum particle size of less than 5 microns and were used to produce high strength fly ash. concrete. Since the particle sizes of fly ash are very fine, they contribute strength to the concrete faster than using the original fly ash that comes directly from the utility. Fifteen and twenty five percent of fly ash by weight of cementitious materials were used in the concrete as cement replacement. Silica fume was also used with the same proportion as fly ash. The compressive strength of high strength fly ash concrete and silica fume concrete were determined and compared. The mix proportions of high strength fly ash and silica fume concrete are shown in Table 1.

Table 1 Mix Proportion of High Strength Fly Ash and Silica Fume Concrete

Ingredient	CSF, Control (lb)	15% Repl. (lb)	25% Repl (lb)
Cement	10	8.5	7.5
Fly Ash or Silica Fume	--	1.5	2.5
River Sand	20	20	20
Aggregate, Basalt 3/8"	30	30	30
Superplasticizer	100 ml	100 ml	100 ml
Water	4.17	4.17	4.17
Water/(Cementitious)	0.417	0.417	0.417

RESULTS AND DISCUSSIONS

Chemical Composition of Fly Ash and Cement

Table 2 shows the chemical composition of fly ash, and cement used in this study. According to ASTM C-618 (1990), both fly ashes (3F and 13F) are classified as Class F fly ash since the oxide of SiO_2 + Al_2O_3 + Fe_2O_3 are higher than 70%. It should also be noted that cement is rich with CaO while the two fly ashes used have only about 3 and 6%. On the other hand, the silica content in cement is only 20% while both ashes have about 40 and 50% of silica content. The loss on ignition (LOI) which is a measure of the carbon content indicates that fly ash consists of about 3-5% of LOI while cement has only 0.73%. Other key variations between cement and fly ash are the alumina and ferrous oxide contents.

Table 2 Chemical Composition of Fractionated Fly Ash and Cement

	Chemical Composition (%)								
Sam	LOI	SO_3	SiO_2	Al_2O_3	Fe_2O_3	CaO	K_2O	MgO	Na_2O
CEM	0.73	2.53	20.07	8.84	1.41	60.14	0.86	2.49	0.28
3F	4.97	1.69	49.89	26.94	5.43	2.99	1.76	0.99	0.33
13F	2.67	3.81	38.93	24.91	12.89	6.85	2.10	1.55	1.31

Particle Size Analysis of Fly Ash

The particle size distributions of fractionated fly ashes are shown in Fig. 1. In case of the 3F fly ash, the finest of dry bottom fly ash, 3F (90%-5 um) means that 90% of the fly ash particles are smaller than 5 microns. The mean diameters of 3F and 13F are 2.11 and 1.84 microns, respectively. When the particle sizes are smaller, they have more spherical particles in the fraction (Hemming and Berry 1986), resulting in the reduction of the water requirement to produce the same workability.

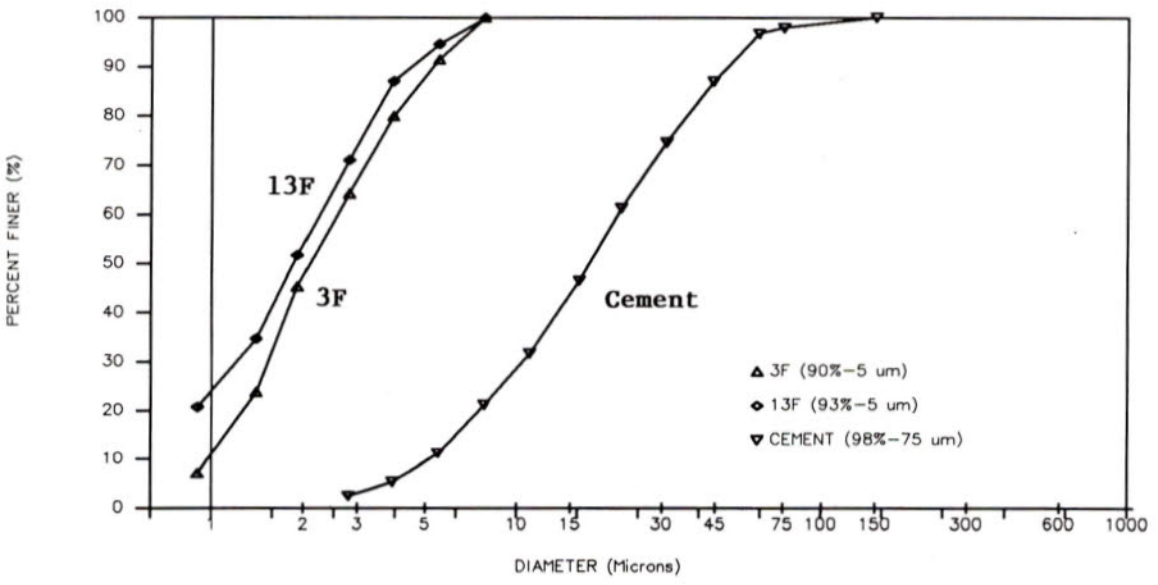

Fig.1 Particle Size Distributions of Fractionated Fly Ash and Cement

Fineness of Fractionated Fly Ash

The fineness of fly ashes both by wet sieve analysis and by the Blaine fineness together with the specific gravity of fly ashes are shown in Table 3. Mean diameter, the diameter of which 50 percent of particles are larger than this size, is also presented in this Table. It should be noted that by using the sieve No. 325 method, the fractionated fly ash samples 3F and 13F have the same fineness since all of them have zero value retained on this sieve.

Table 3 Fineness of Cement and Fractionated Fly Ashes

Sam. No.	Specific Gravity (g/cm^3)	Fineness		Mean Diameter (um)
		Retained 45 um (%)	Blaine (cm^2/g)	
CEM	3.12	-	3815	-
3F	2.54	0	7844	2.11
13F	2.75	0	11241	1.84

Compressive Strength of High Strength Fly Ash and Silica Fume Concrete

Sample CSF represents the control sample, without any fly ash or silica fume. Samples CSF15 and CSF25 are concretes with 15% and 25% of the weight of cementitious materials replaced by silica fume while samples C3F15 and C3F25 are concretes with 15% and 25% replaced by 3F fly ash. And, samples C13F15 and C13F25 are concretes with 15% and 25% of cement replaced by the 13F fly ash. Table 4 shows the compressive strength of high strength fly ash and silica fume concrete. Table 5 is the percentage compressive strength of high strength fly ash and silica fume concrete compared with the control CSF sample. Figs. 2 and 3 are the relationship between the compressive strength of high strength concrete and age when using 15% and 25% replacement of cement by fly ash or silica fume in the mix.

Table 4 Compressive Strength of High Strength Fly Ash and Silica Fume Concrete

Sample No.	Compressive Strength (psi)						Slump (cm)
	1-day	7-day	14-day	28-day	56-day	90-day	
CSF	1912	6352	7346	7881	8645	9322	23
CSF15	2335	7176	7768	8009	8715	9286	1
CSF25	2675	6664	7479	8032	8500	9122	0
C3F15	1216	5855	7056	7820	9031	10023	21
C3F25	1212	5968	7248	8648	9775	10521	20
C13F15	1945	6787	7805	8740	9853	10487	16
C13F25	1782	6091	7240	8561	9814	10748	12

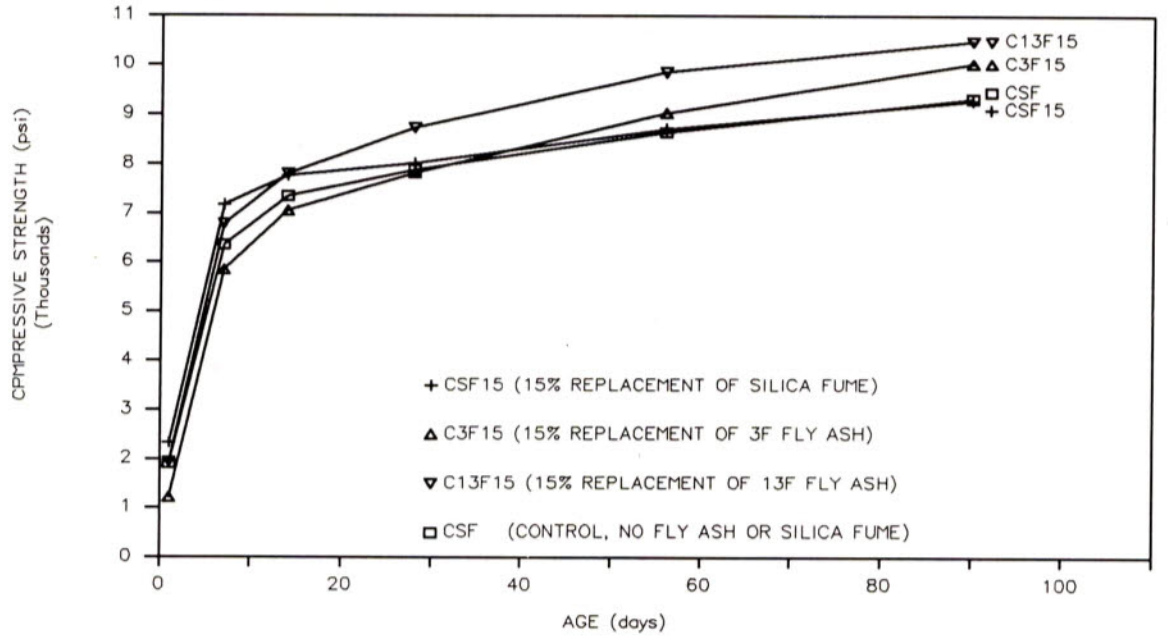

Fig. 2 Relationship between Compressive Strength of High Strength Concrete and Age with 15% Replacement of Fly Ash or Silica Fume

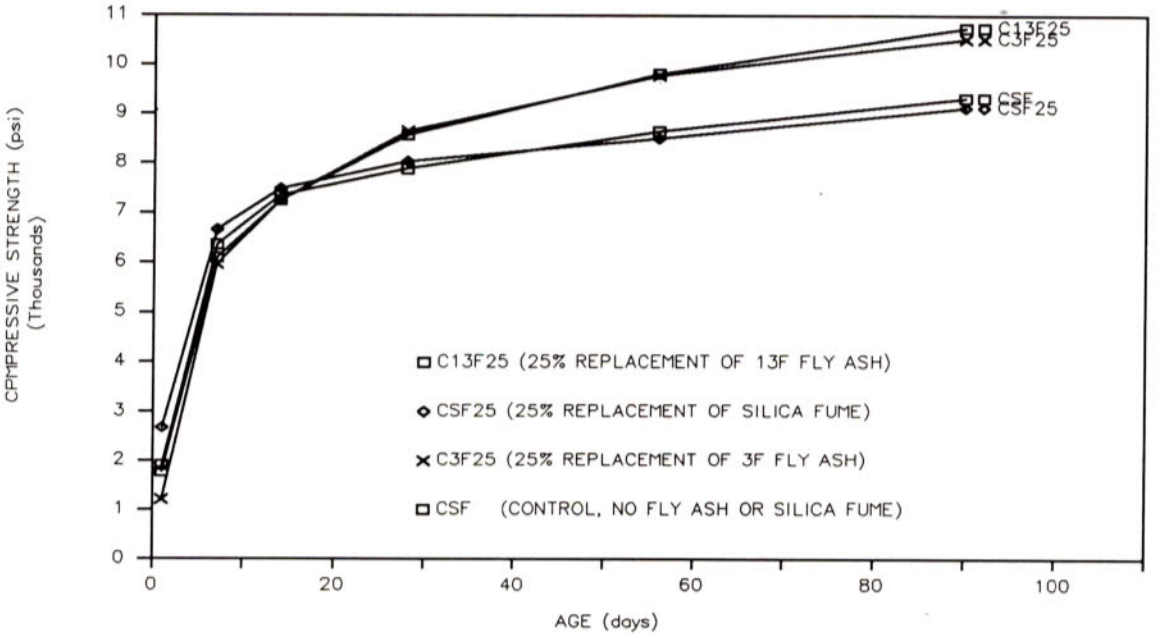

Fig. 3 Relationship between Compressive Strength of High Strength Concrete and Age with 25% Replacement of Fly Ash or Silica Fume

Since the proportions of cementitious materials, sand, coarse aggregate, water, and superplasticizer are constant, the consistency of the fresh concrete depends on the characteristics of cementitious materials. Fresh concrete with 25%

of cement replaced by silica fume had zero slump while the control concrete (CSF) had a 23 cm slump (see Table 4). Because silica fume is a very fine particle material, it has more surface area than cement on an equal weight basis. In general, when the mix proportion of concrete is constant, the mix with silica fume (in powder form) needs more water to maintain the same slump or workability. The slump of concrete with fly ash as cement replacement is lower than that of the control sample. Usually, fly ash of the generic type or original will increase the slump of concrete but, this behavior does not apply to this type of fly ash. 3F and 13F are very fine particle fly ashes, their surface areas as measured by the Blaine method are much higher than that of the cement. The results of this test confirms that very fine particle fly ash will reduce the workability of fresh concrete.

The compressive strength of the control concrete (CSF) varies from 1912 psi (13 MPa) at 1 day to 9322 psi (64 MPa) at 180 days. By the age of 7 days, the compressive strength of CSF reaches 6352 psi (44 MPa), which can be considered as high strength concrete (ACI 363, 1990). The compressive strengths at 1 day of CSF15 and CSF25 are 2335 psi (16 MPa) and 2675 psi (18 MPa), respectively or 22% and 40%, stronger than the control concrete. Concrete with silica fume gains strength very fast at early age. This behavior can be attributed to both the packing and pozzolanic effects. Because particle sizes of silica fume are very small, they fill the voids of the concrete matrix, making concrete denser and more compact after casting. During the curing period, the pozzolanic reaction of silica fume takes place at a faster rate than the fly ash because of its fineness. After 28 days, the strength gain of silica fume concrete slows down and the strength falls below that of the control. The percentage of control strength of high strength silica fume concrete with 25% cement replacement reduces from 140% at 1 day to 98% at 180 days.

High strength concrete made from fly ash behaves in different way. The early strengths of high strength fly ash concrete are usually lower than the control concrete. With 15% cement replacement by the 3F fly ash, the compressive strength of fly ash concrete varies from 1216 psi (8 MPa) at 1 day to 10023 psi (69 MPa) at 180 days or 63% to 108% of the control strength. With 15% replacement of 3F fly ash, the compressive strength at 1 day is expected to be on the order of 80% of the control strength. The lower value observed here may be due to the high dosage of superplasticizer used in this mix. The superplasticizer used in this experiment is about 3 times higher than those recommended by the manufacturer for normal concrete. High dosage of this admixture will generally retard the setting of cement which results in the lower compressive strength at early age. The effect is not as for pronounced in the case of wet bottom fly ash, 13F fly ash. After 7 days, the rate of strength gain of high strength fly ash concrete returns to what would normally be expected. The compressive strength of fly ash concrete is considered to be high strength after 7 days since it exceeds 6000 psi (41 MPa). The strength variation of high strength fly ash concrete with 25% replacement of 13F fly ash varies from 1782 psi (12 MPa) at 1 day to 10748 psi (74 MPa) at 180 days. The greater use of fly ash gives lower compressive strength at the early ages up to 14 days. After 90 days, concrete with higher fly ash content produces higher strength than the concrete with a lower fly ash content. In general, the strength of fly ash concrete using 13F fly ash is higher than those using the 3F fly ash.

Before 7 days, the highest strength found is in the samples with silica fume in the mix. After 14 days, sample CSF15 and C13F15 almost have the same strength of about 7800 psi (54 MPa). At 28 days of curing, high strength concretes using fly ash as cement replacement produced a stronger concrete than for either the control or the silica fume concrete. The strength of samples C13F15, C13F25, and C3F25 are

8740 psi (60 MPa), 8561 psi (59 MPa), and 8648 psi (60 MPa), respectively or 111%, 109%, and 110% as compared with the control strength. As the age increases, the strengths of fly ash concrete also increase. At 90 days, the compressive strengths of fly ash concrete are 107% to 115% of the control concrete.

It is interesting to note that the compressive strength of concrete made with silica fume (both 15% and 25% replacement) have almost the same strength as the control concrete at the age of 90 days. These strengths are in the range of about 9000 psi (62 MPa). It is obvious that silica fume in concrete reacts faster than fly ash and control concrete but the rate becomes slower after 7 days. Figs. 2 and 3 confirm the behavior of high strength silica fume concrete.

CONCLUSIONS

1. Concrete with silica fume has a faster rate of strength gain at early ages than fly ash and control concrete. This behavior can be attributed to the packing and pozzolanic effects. Since the particle sizes of silica fume are very fine, they fill the voids in the fresh concrete and make concrete denser.
2. The early strengths of high strength fly ash concrete are lower than the control and silica fume concrete. But after 28 days of curing, strengths of fly ash concrete are generally higher than those of control high strength concrete.
3. It is obvious that silica fume in concrete reacts faster than fly ash and control concrete but the rate of strength gain becomes slower after 7 days.
4 Fractionated fly ash is a suitable material to produce high strength concrete. The use of fractionated fly ash will lower the cost of concrete.

REFERENCES

ACI Committee 363, 1990, "State-of-the-Art Report on High-Strength Concrete," ACI 363R-84, *ACI Manual of Concrete Practice Part I*, American Concrete Institute, Detroit, 47 pp.

ASTM C 204, 1990, "Test Method for Fineness of Portland Cement by Air Permeability Apparatus," ASTM C 204-89, *Annual Book of ASTM Standards*, Vol. 04.01.

ASTM C 430, 1990, "Test Method for Fineness of Hydraulic Cement by the 45-Micron (No. 325) Sieve," ASTM C 430-89, *Annual Book of ASTM Standards*, Vol. 04.01.

ASTM C 618, 1990, "Specification for Fly Ash and Raw or Calcined Natural Pozzolan for Use as a Mineral Admixture in Portland Cement concrete," ASTM C 618-89a, *Annual Book of ASTM Standards*, Vol. 04.02.

ASTM D 4326, 1990, "Test Method for Major and Minor Elements in Coal and Coke Ash by X-Ray Fluorescence," ASTM D 4326-84, *Annual Book of ASTM Standards*, Vol. 05.05.

Hemming, R.T. and Berry, E.E., 1986, "Speciation in Size and Density Fractionted Fly Ash," *Symposium Proceedings, Fly Ash and Coal Conversion By-Products: Characterization, Utilization and Disposal II*, Material Research Society, Vol. 65, pp. 91-103.

Mehta, P.K. and Aitcin, P.C., 1990, "Principles Underlying Proportion of High-Performance Concrete," *Cement, Concrete, and Aggregates*, Vol. 12, No. 2, pp. 70-78.

Task Force Report No. 5, 1977, "High Strength Concrete in Chicago High-Rise Building," Chicago Committee on High-Rise Building, 66 pp.

MIXED-CONDUCTING OXIDE ELECTRODE FOR SOLID OXIDE FUEL CELL

P. AUNGKAVATTANA AND V.S. STUBICAN

THE PENNSYLVANIA STATE UNIVERSITY
CERAMIC SCIENCE PROGRAM
DEPARTMENT OF MATERIALS SCIENCE AND ENGINEERING
UNIVERSITY PARK, PA 16802

Abstract

The purpose of this research was to study and develop new cathode materials for solid oxide fuel cell. The presently used cathode material $La_{1-x}Sr_xMnO_3$ reacts with YSZ (electrolyte) to form a poorly conductive compound such as $La_2Zr_2O_7$. Materials proposed as the new cathodes were Ca-doped $YFeO_3$ perovskite materials which do not form $La_2Zr_2O_7$ and which were expected to have high electrical conductivity and good thermal expansion match with YSZ. Fine, uniform, dense and crack-free microstructures were developed with $Y_{1-x}Ca_xFeO_3$ (x = 0 to 0.2). Samples were prepared conventionally, from mixed oxides and carbonates or by Pechini process and sintered at 1350°C or 1400°C for 8-16 hours. All specimens were found to be single phase orthorhombic. Thermal expansion coefficients were measured on the samples with x=0, 0.10 and 0.20. The values for all samples were near $10x10^{-6}$ /°C in the temperature range 200° to 900°C. A value of $10.8x10^{-6}$ /°C was measured for the YSZ specimen, indicating an excellent match. The electrical conductivity of doped specimens (except x=0.025) in air was 10^3 S/m at temperature above 500°C, with negligible variations as a function of dopant concentration. This value compares favorably with other perovskites.

Introduction

Solid Oxide Fuel Cells (SOFCs) have been extensively investigated as a highly efficient power generation system. High temperature SOFCs show a great promise for economical, clean and efficient production of electricity in a variety of utility, commercial

and industrial applications (Singhal 1991). This type of fuel cell is suitable not only for cogeneration of heat and electricity because of its high operating temperature, but also for eliminating corrosion or leakage problems by using all solid materials in cell structure. The cells can be operated using a variety of fuels including hydrogen, carbon monoxide and coal-derived gases at temperatures near 1000°C and, therefore do not require any expensive catalysts. Furthermore, because of their high temperature of operation, the cells can be operated directly using natural gas eliminating the need for an expensive external reformer system.

Standard materials used for different components in the state-of-art SOFC are as follows:

1) electrolyte -- yttria stabilized zirconia (YSZ);
2) air electrode -- (La,Sr)MnO_3;
3) fuel electrode -- Ni:YSZ cermet ; and
4) interconnect -- La(Cr,Mg)O_3.

A major research effort has recently been directed towards the development of alternative air- electrode materials for SOFC. The reason for this is (La,Sr)MnO_3 reacts with YSZ, increasing the overpotential at the electrode/electrolyte interface. In this research, Ca-doped Yttrium ferrite was chosen for developing alternative air electrodes. Samples were prepared conventionally, from mixed oxides and carbonates, or by Pechini process Phase investigation, microstructure, electrical conductivity and thermal expansion were studied.

Preparation of $Y_{1-x}Ca_xFeO_3$ Powders

The Pechini process was originally developed to prepare metal oxide powder such as titanates and niobates for capacitors (Pechini 1967). A schematic of the experimental procedure used to synthesize the powder is illustrated in Figure 1. Reagent grade $Y(NO_3)_3.6H_2O$, 99.9% manganese (II) carbonate ($MnCO_3$) and Iron (III) nitrate nonahydrate ($Fe(NO_3)_3.9H_2O$ were used as raw materials. These nitrates and carbonate were mixed and dissolved in a 1:4 molar ratio solution of citric acid and ethylene glycol by heating at 90°C for 4 hours. The resulting clear brown solution was further heated at 140°C for 4 hours while stirring to obtain dry powder. The powder was crushed by mortar and milled by ZrO_2 media in the vibratory mill 8-12 hours and dried in a low temperature oven at 120°C for 24 hours. Dried powder was calcined at 600°C for 1 hour and 1100°C 2 hours. Fine and homogeneous powder was uniaxially dry-pressed at 3000 psi (105.37 MPa) in a stainless steel die. PEG was used as a binder and zinc stearate as a lubricant.

Pellets made from $Y_{1-x}Ca_xFeO_3$ powders were sintered on platinum foil at 1350°C or 1400°C 8 hours for Pechini process and 16 hours for conventional mixed oxide and carbonate method.

Characterization

Qualitative Phase Investigation

The X-Ray diffraction patterns were obtained on calcined powders or surfaces of sintered pellets from an X-Ray diffractometer using CuKα radiation (Rigaku semi-automated X-Ray diffractometers). All operated with a copper x-ray tube target and pyrolytic graphite monochromator. The patterns were scanned at a rate of 4° 2θ /min in the range of 10°- 90° 2θ. Observed patterns were compared to standard patterns taken from the Joint Committee on Powder Diffraction Standards files. Peak positions were determined by applying the peak finder routine from the scintag pad v software package. A piece of SiO_2 was used as an external standard for all measurements. A computer program written by Evans, Appleman and Handwerker (1963) was used to refine the unit cell parameter on the basis of a least square fitting technique. After each calculation, the program reported an accuracy of better than ± 0.0005 nm.

Electrical Conductivity Measurement

Four probe DC conductance

Electrical conductivity of perovskite type materials was measured by the four probe method. The specimens for 4 probe dc conductance were prepared by uniaxial pressing in a rectangular stainless steel die. The dimension of the bar was approximately 4x5x15 mm^3. Platinum wires of 0.2 mm diameter were connected to the bar as electrical probes through pressure contact. To eliminate the effects of surface currents, platinum paste was applied to both edge probes which were used to apply the current. During the conductivity measurement, the specimen was positioned horizontally in a vertical tube furnace.

Microstructural Evaluation

The microstructures of the sintered pellets were examined using a Scanning Electron Microscope. $Y_{1-x}Ca_xFeO_3$ are conducting materials which did not require gold-coating. The voltage used were 20-25 kV and the magnifications were 1.00k, 2.00k and 5.00k.

Thermal Expansion Measurements

A dilatometer was used to determine the thermal expansion coefficient of the samples, $Y_{1-x}Ca_xFeO_3$. The specimens were prepared as the rectangular bars dimension (4x5x15 mm^3) and placed in a tube furface. Heating rate was 2°C / min to 1250°C and cooling rate was the same.

Results and Discussion

The phases present after sintering were determined by x-ray diffraction. Almost all of the samples were found to be orthorhombic similar to $YFeO_3$ compound. The compositions with Ca ≥ 30% were found to exhibit melting and bloating effect at temperature higher than 1350°C.

Electrical conductivity of $Y_{1-x}Ca_xFeO_3$ (x = 0 to 0.20) and $Y_{1-x}CaMnO_3$-based materials (x = 0.1 and 0.2) were measured in air and the temperature range 400-1000°C, using a 4-probe DC technique. The specimen were bar-shaped with the dimensions of approximately 4x4x15 mm^3.

An Arrhenius plot of log σ (S/m) versus 10000/T (1/K) for the 2.5, 5.0, 10.0, 15.0 and 20.0% Ca-doped specimens and also the $YMnO_3$-based compositions, $Y_{0.8}Ca_{0.2}Fe_{0.8}Mn_{0.2}O_3$ and $Y_{0.9}Ca_{0.1}Fe_{0.8}Mn_{0.2}O_3$, is illustrated in Fig.2. The calcium doping shows a strong effect on electrical conductivity which increases for 2 orders of magnitude comparing with pure $YFeO_3$. The linear behavior and similar slopes exhibited by the $Y_{1-x}Ca_xFeO_3$ ($0.025 \leq x \leq 0.2$) suggest that the free energies of formation are relatively constant with Ca dopant (Carini et al. 1991).

The dc electrical conductivity of doped specimens (with the exeption of X = 0.025) in air above 500° C was found to be 10^3 s/m, which compares favorably with other perovskites (Roosmalen et al.1991). These values were also in good agreement with those of Yamamoto et al.(1987). They explained that the absolute values of conductivity were

extremely dependent on the sample preparation method, because of intergrain effects and the amount of oxygen deficiency.

SEM micrographs of samples sintered at various temperatures at different times periods are studied. Fine, uniform, dense, crack-free microstructures were developed in Y_{1-x} Ca_x FeO_3 (x = 0-0.20). The specimens containing x = 0 to 0.15 were found to be single phase orthorhombic and dense while the specimen containing x = 0.20 was appeared to have a few accicular grains. The SEM micrograph of Ca doped - YFeO3-based materials which contain 5% Ca was shown in Fig.3.

Dilatometer was used to measure the percent expansion of the specimens $Y_{1-x}Ca_xFeO_3$ with x=0, 0.1, 0.2 heating to 1250°C and cooling to room temperature at the rate 2°C/ minute. All the specimens were found that the thermal expansion curve had a pronounced hysteresis effect. At first, it was thought that the hysteresis was due to a time-consuming order-disorder phenomenon. According to Buessem et al. (1952), they tested this assumption by heating aluminum titanate samples to a certain temperatures and kept there for several hours. The result was negative: the length of the sample was constant during this time. Eventually, the following conclusions may be drawn:

(1) The hysteresis effect is a reproducible phenomenon (after thermal equilibrium was attained, the length definitely was less than with the usual cooling rate, but returned to the original length within a few hours).

(2) The hysteresis area is a continuous and monotonous temperature function.

(3) The hysteresis effect is connected with a time-consuming process.

A compared graph of percent expansionversus temperature is shown in Fig.4. The values of thermal expansion coefficient for all samples were near 10x10-6 /°C in the temperature range of 200° to 900° C. A value of 10.8x10-6 /°C was measured for YSZ specimen, indicating an excellent match.

Conclusions

Powders of the composition $Y_{1-x}Ca_xFeO_3$ with x= 0.025, 0.05, 0.10, 0.15 and 0.20 were prepared by Pechini process and mixed oxide and carbonate process. Fine, uniform, dense (96-99% of theoretical density) and crack-free microstructures were developed by sintering at 1350-1400°C for 8-16 hours. The total electrical conductivity was measured by four probe dc method at the temperature range 400-1000°C. Total electrical conductivity of investigated specimens $Y_{1-x}Ca_xFeO_3$ (except x=0.025) was approximately 10^3 S/m

above 500°C. Very small variations in electrical conductivity were observed if x was larger than 0.05 atomic%. The obtained values for electrical conductivity compare favorably with those of $La_{1-x}Sr_xMnO_3$ which is presently used as cathode material. Thermal expansion of the ceramic bodies made of $Y_{0.9}Ca_{0.1}FeO_3$ and $Y_{0.8}Ca_{0.2}FeO_3$ were measured and compared with the thermal expansion of the cubic zirconia containing 8 m/o Y_2O_3 (electrolyte material). The obtain results were $9.6x10^{-6}$/°C for $Y_{0.9}Ca_{0.1}FeO_3$, $9.8x10^{-6}$/°C for $Y_{0.8}Ca_{0.2}FeO_3$ and $10.8x10^{-6}$/°C for YSZ. An excellent thermal expansion match was established between Ca-doped $YFeO_3$ (cathode) and YSZ (electrolyte).

References

1. Aungkavattana, P. (1992):"Mixed-Conducting Oxide Electrode for Solid Oxide Fuel Cell", M.S. thesis, The Pennsylvania State University, University Park, PA.

2. Buessem, W. R., N. R. Thielke and R. V. Sarakauskas (1952): "Thermal Expansion Hysteresis of Aluminum Titanate," Ceramic Age, 60, (11), 38-40.

3. Carini, G. F., H. U. Anderson, D. M. Sparlin and M. M. Nasrallah (1991): "Electrical Conductivity, Seebeck Coefficient and Defect Chemistry of Ca-doped $YCrO_3$," Solid State Ionics 49, 233-243.

4. Evans, H. T., D. A. Appleman and D. S. Handwerker (1963): "The Least Squares Refinement of Crystal Unit Cell with Powder Diffraction Data by an Automatic Computer Indexing Method," (abs.) Program, Ann. Meet. Am. Crys. Assoc., Cambridge, MA

5. Pechini, M. P. (1967): U.S. Patent No. 3,330,967.

6. Roosmalen, J. A. M. van, J. P. P. Huijsmans and E. H. P. Cordfunke (1991): "Proceedings of the Second International Symposium on Solid Oxide Fuel Cells, ed. F. Grosz and P. Zegers, S. C. Singhal and O. Yamamoto, Electrochem. Soc. (U.S.A.), The SOFC Soc. Jap., Luxembourg, pp. 507-516.

7. Singhal, S. C. (1991) : Solid Oxide Fuel Cell Development at Westinghouse" in Proceedings of the Second International Symposium on Solid Oxide Fuel Cells, ed. F. Grosz and P. Zegers, S. C. Singhal and O. Yamamoto, Electrochem. Soc. (U.S.A.), The SOFC Soc. Jap., Luxembourg, pp. 25-33.

8. Yamamoto, O, Y. Takeda, R. Kanno and M. Noda (1987): "Perovskite-Type Oxides as Oxygen Electrodes for High Temperature Solid Oxide Fuel Cell," Solid State Ionics, 22, 241-246.

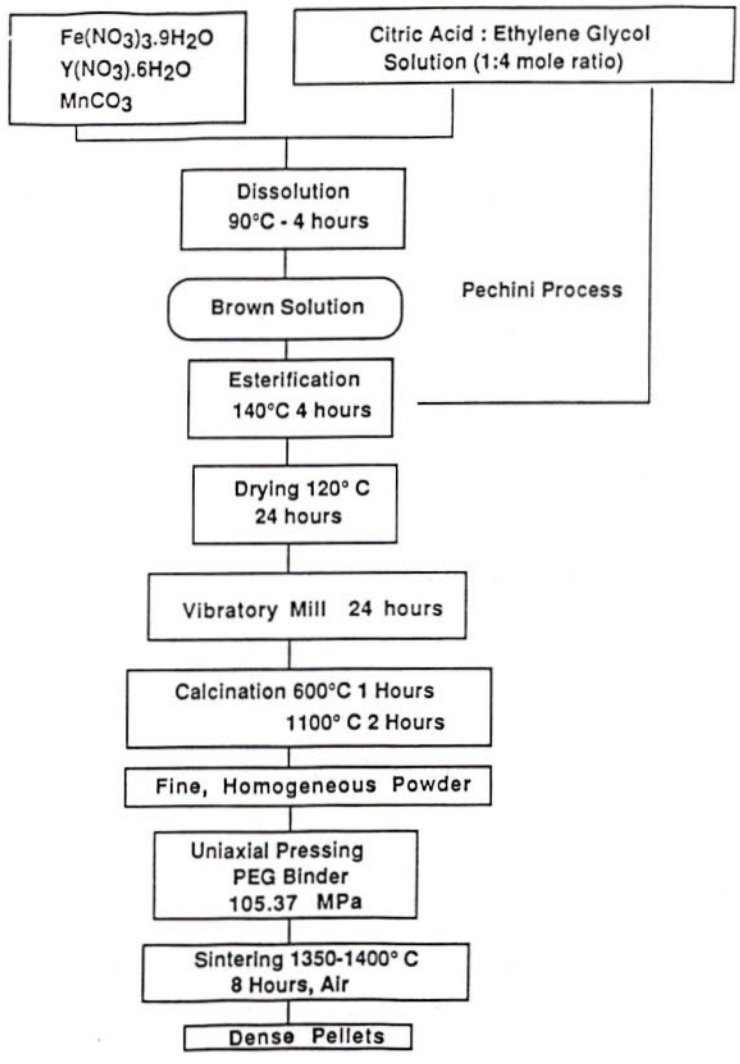

Figure 1 Schematic of the Experimental Procedure

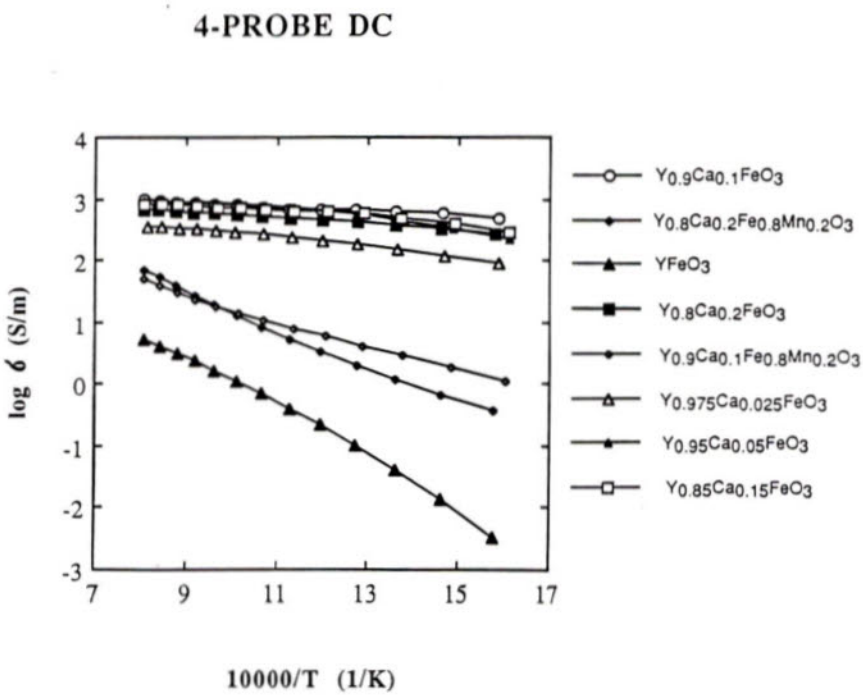

Figure 2 An Arrhenius plot of log σ (S/m) versus 10000/T (1/K) for various compositions

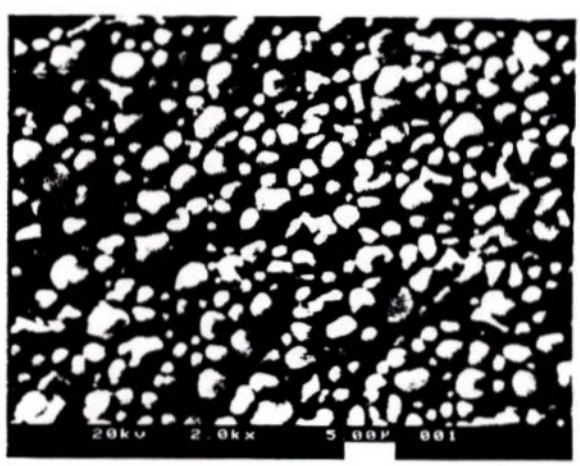

Figure 3 SEM micrograph of $Y_{0.95}Ca_{0.05}FeO_3$ 1400°C 16 hours.

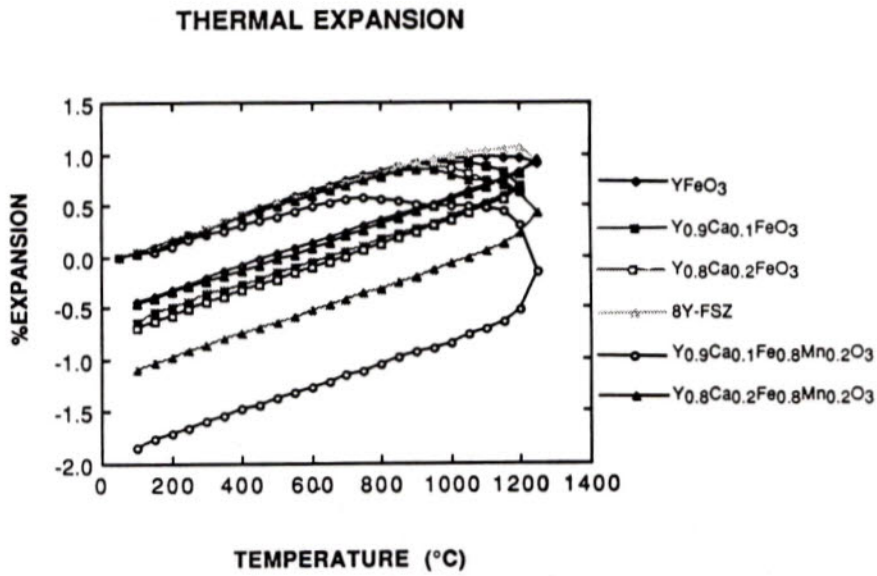

Figure 4 Compared Percent Thermal Expansion versus Temperature of all specimens heating to 1250°C and cooling to room temperature.

Vision-Based Behavioural Modules for Robotic Assembly Systems

Prabhas Chongstitvatana
Department of Artificial Intelligence
University of Edinburgh
5 Forrest Hill, Edinburgh EH1 2QL, UK

Abstract

This work described how to program robots to work reliably in the presence of uncertainty. Some architectural principles are proposed which address the problem of decomposing robotic assembly tasks into modular units such that a robot program can be implemented efficiently, tested easily, and can be maintained or modified without undue complexity. This architecture also provides a framework to integrate sensors into a robotic assembly system.

These modular units are called behavioural modules. They perform their tasks reliably. The problem of uncertainty is dealt with by encapsulating sensing and variation-reducing strategies inside these modules. Experiments are performed with a working robotic assembly system using vision-based behavioural modules.

Programming assembly robots

Reliable assembly with a robot must meet the challenge of dealing with the problem of uncertainty in the real world. Today's assembly robot systems cannot cope with uncertainty nor handle sensing adequately and are in general hard to program. The current generation of industrial robots are primarily position controlled devices and therefore sensing systems, like force sensing or visual sensing, are still difficult to incorporate. The industrial robot can be programmed but the programming is done at a low level; in terms of robot motions. Inevitably, there are variations in the shape or position of the parts. The robot motion has to take into account these uncertainties. Finding a robot motion strategy to achieve a desired part motion is difficult. One way to reduce the uncertainty is to use sensors. To get good results the environment and sensors need to be set up carefully and precisely calibrated. It makes programming with sensors difficult and of very limited use.

The difficulty in programming a robot stems from the fact that, to increase the flexibility of the robot, its sequence of motions must accommodate changes in the real world. Programming at a low abstraction level is a burden and error prone and the program is also sensitive to minor task changes. If a higher abstraction level is to be achieved, an effective way to program the use of sensors must be found. These are problems which have limited the progress of assembly by robots.

Classical approach

The classical approach to assembly robot programming systems typified by RAPT (Popplestone and others; 1980), TWAIN (Lozano-Pérez and Brooks, 1985), Handey (Lozano-Pérez and others, 1987), and Spar (Hutchinson and Kak, 1990), can be characterised as based on the geometry of the objects, relying extensively on the exact knowledge of this geometry to generate robot motions. Sensors are used to update a representation of a world model. Robot motions are planned based on this world model. Because robot motions are

based on planned motions, the uncertainty in the real world is accommodated by sensing and updating the world model. The problem then lies in the quality of the sensing and how accurately the world model reflects the real world.

The problems with the classical approach are that 1) it assumes the world to be perfect, then 2) the uncertainty in the geometry of the parts and their locations are added in and are analysed to determine whether sensing is necessary to reduce uncertainty to an acceptable level. This makes it necessary to do the uncertainty analysis after a plan or partial plan has been created. The results of this analysis are then used to correct or modify the initial plan (Brooks, 1982). Sensing can be introduced to reduce uncertainty at some point in the plan (Lozano-Pérez and Brooks, 1985; Hutchinson and Kak, 1990). This cycle of plan, analyse, and modify is repeated until the analysis uncovers no further problems. This makes the production of each robot program a large task since the problem of uncertainty plagues all aspects of a program.

Behavioural modules

We argued that the classical decomposition of the problem is not correct. Instead of breaking it into functional modules which are controlled by a central system, with perceptual modules as inputs and action modules as outputs, it should be broken into many task-achieving units, where the task is some useful accomplishment in the assembly world in question – such as acquiring a part. Each unit individually connects sensing to action, each unit pursues its specific goal but co-operates with other units to achieve the desired goal. Rather than rely on a world model, the individual unit concentrates on those aspects of the world that are directly relevant to it, i.e. a minimal distributed world model rather than a centralised world model. They may work in parallel and interact with each other.

The difference between this approach and the classical approach is that our planner relies on the execution system to cope with uncertainty. As a consequence it is able to plan in an ideal world, unlike the classical systems which plan from task-level specifications and synthesise sensing and motion strategies down to the manipulator-level. From this ideal world plan the execution system carried out the task using task-achieving units. These modular units are designed, implemented and tested in the real world to perform their intended tasks reliably, and they can be guaranteed to perform their tasks within a certain range of uncertainty. They are called behavioural modules.

Behavioural modules facilitate the use of sensors to cope with uncertainties, therefore increasing the reliability of assembly tasks. It is an abstraction that makes an assembly robot more easily programmed. This is achieved by hiding the specifics of the use of sensors as much as possible from a planner and by avoiding *explicit* reasoning about uncertainty. The planner, therefore, deals with an ideal world in which the robot carries out its operations reliably in the presence of uncertainty. This leaves the planner to deal with the problem of reasoning about the ordering of the assembly and other high level assembly strategies rather than concerning itself with the actual details of robot motions in the assembly cell. Behavioural modules abstract away some of the uncertainty management from the user of a robot such that the module will 'do the right thing' for its task. A user can compose a robot program to do assembly without having to be concerned with the details of the use of sensors to manage uncertainty and the program will work reliably.

We claimed that the decomposition of assembly tasks into behavioural modules should be based on the principles that:

- there is no reliance on a central model of the world for combining sensing and action;
- sensing and action should be tightly coupled within the module;
- prefer to pass control via perception of the world rather than by parameters.

Further discussion of behavioural modules and their characterisation can be found in Chongstitvatana (1992).

Vision-based behavioural modules

The type of vision sensing that is used in systems that employ a world model (Horn and Ikeuchi, 1983; Inoue and Inaba, 1984; Sakane and others, 1987; Heikkila and others, 1988; Andersson, 1988) requires accurate calibration to establish the mapping between the sensor's field of view and a common coordinate system. This type of vision system cannot easily cope with changes in camera parameters, such as changing the position of the camera or changing the view point, zoom, etc. Uncalibrated vision systems avoid problems normally associated with static cameras and also exploit the motion of the observer to derive some useful parameters for the purpose of accomplishing the task in hand (Brooks, Flynn, and Marill, 1987). Visual servo control, which uses image features (i.e. image areas, and centroids) as feedback control signals, eliminates a complex interpretation step, i.e. interpretation of image features to derive world coordinates (Weiss, 1984).

Our principle is to try and replace, as far as is possible, calculations by sensing. This equates to preferring perception over representation. Several techniques are used that contribute to this end. Frequent vision sensing, for example, allows motions in the world to be viewed as linear approximations, and only short term predictions of motion need be made for following an object. The tracking algorithm adopted is similar to that used by others (Jones, 1974; Brown, 1988). The system is purposefully made as calibration free as possible. Relative quantities are used and self-calibration is done while carrying out tasks. This approach is possible because adequate sensing allows self-calibration. The need for calibration to establish the mapping of image data to world coordinates is absent from the system described here. The camera position need not be known. The system does not rely on explicit models of the objects nor does each assembly agent need to know about the other(s). The system does not maintain representations of the Soma pieces, the camera, the robots nor of possible uncertainties due to inaccuracies of the model with respect to the real world.

Experiments

We have done three experiments to validate the concept of behavioural modules. In the first experiment we integrated visual sensing into a robotic assembly system. The experiment is based on an existing system: SOMASS (Malcolm, 1987), which originally did not use sensors, but whose architecture was designed to facilitate their incorporation. This system is extended to incorporate a camera. The task of acquiring a part is implemented using a new behavioural module. This new module uses visual sensing. A camera is used to visually guided the robot hand to pick up a part. By using the motion of the hand tightly coupling with the vision system, this method works without having to rely on any central world model or the knowledge of the camera position.

The second experiment extended the result from the first one. The limitation of the single camera system in the previous experiment is that the sensing gives only two-dimensional data, therefore in order to resolve depth ambiguity along the line of sight some *a priori* knowledge must be available. This experiment introduces the second camera and does not require that knowledge. This two camera system is uncalibrated (don't have to know the cameras positions). We developed an approximation of Jacobian that relates the motion of the hand in the images to the commanded motion. A simple task of stacking blocks is demonstrated. The result showed that the task was performed reliably and the accuracy of the system did not depend on knowing the kinemat-

ics of the robot because the system was self-calibrated.

The third experiment added mobility to the two camera system. This enables it to change its view. This increases the range of assembly tasks that can be performed using visual sensing. New behavioural modules are designed to move the camera head around the object of interest without calibration between the position of the camera head and the object. This experiment demonstrates the use of a mobile camera head to find good views that are suitable for assembly operations. A cameras keeps its fixation point on a target in the image and rotates the camera head to centre its view on the point when the camera head is moved. Visual feedback is also used to perform a part-mating operation which require close range visual sensing. The result shows that moving cameras to view different parts can be achieved without requiring calibration between the robot's and cameras' reference frames, thus preserving the 'no central world model' principle.

The details of these experiments were reported in Chongstitvatana and Conkie (1992a; 1992b) and Conkie and Chongstitvatana (1990).

Conclusion

How to program robots to work reliably in the presence of uncertainty?

The classical approach to this problem is to analyse the uncertainty of the parts' geometry and their locations to determine the sensing and actions that are necessary to reduce the uncertainty to an acceptable level. The problem with the classical approach is that the analysis of uncertainty and the synthesis of sensing and action to reduce the uncertainty are computationally expensive and generally intractable. Presently, this analysis of uncertainty also is only able to represent a subset of the types of uncertainty actually experienced at execution time.

Our approach suggested a different solution: use a competent execution system to deal with the inevitable uncertainty of the real world. This has a profound effect on the architecture of robotic assembly systems. The sensing operations are embedded in the run-time system, which allow the programming (or task planning) to be carried out in an ideal world in which robots perform their tasks reliably.

This work suggested an architecture for the execution system and proposed the criteria for decomposing a task into modular units which are called behavioural modules. Behavioural modules are task-achieving units (the task is in the world, e.g., computational tasks don't count). Programming a robot in terms of behavioural modules leads naturally to task-level programs. Experiments show that behavioural modules can encapsulate the essential information about the world and communicate without relying on a centralised model of the world and without a global coordinate system. An individual module only receives the information that is required to perform its task. The tight coupling of the sensing and action inside individual modules is an important idea in coping with the uncertainty of the real world.

References

Andersson, R.L. (1988). *A robot ping-pong player.* MIT Press.

Brooks, R.A. (1982). Symbolic error analysis and robot planning. *Int. Jour. of Robotic Research*, 1(4):29-68.

Brooks, R.A., A.M. Flynn, and T. Marill. (1987). Self calibration of motion and stereo vision for mobile robot navigation. MIT AI Lab., AI memo 984.

Brown, C.M. (Ed.) (1988). Rochester robot. University of Rochester, Computer Science, technical report 257.

Chongstitvatana, P. (1992). The design and implementation of vision-based behavioural modules for a robotic assembly system, PhD. thesis, Department of Artificial Intelligence, University of Edinburgh.

Chongstitvatana, P., and A. Conkie. (1992a). Behaviour-based assembly experiments using vision sensing. In A. Colin, and E. Emil, (Eds.), *Advances in Machine Vision.* World Scientific Press, Singapore, pp. 329-342, also DAI RP 466.

Chongstitvatana, P., and A. Conkie. (1992b). Active mobile stereo vision for robotic assembly. *Proc. of 23rd Int. Sym. on Industrial Robots*, Barcelona, Spain, pp. 393-397, also DAI RP 590.

Conkie, A., and P. Chongstitvatana. (1990). An uncalibrated stereo visual servo system. *Proc. of the British Machine Vision Conference*, Oxford, pp. 277-280, also DAI RP 475.

Heikkila, T., T. Matsushita, and T. Sato. (1988). Planning of visual feedback with robot-sensor cooperation. *Proc. 1988 IEEE Inter. Workshop on Intelligent Robots and Systems*, Tokyo.

Horn, B.K., and K. Ikeuchi. (1983). Picking parts out of a bin. MIT AI Lab., AI memo 746.

Hutchinson, S.A., and A.C. Kak. (1990). Spar: A planner that satisfies operational and geometric goals in uncertain environments. *AI magazine*, 11(1):31-36.

Inoue, H., and M. Inaba. (1984). Hand-eye coordination in rope handling. In Brady M., and R. Paul (Eds.), *Robotics Research 1*. MIT Press, pp. 163-174.

Jones, V. (1974). Tracking: an approach to dynamic vision and hand-eye coordination. Ph.D. thesis, University of Illinois, Urbana Champaign.

Lozano-Pérez, T., and R.A. Brooks. (1985). An approach to automatic robot programming. MIT AI Lab., AI memo 842.

Lozano-Pérez, T., J.L. Jones, E. Mazer, P.A. O'Donnell, W.E.L Grimson, P. Tournassoud, and A. Lanusse. (1987). Handey: a robot system that recognises, plans, and manipulates. *Proc.of IEEE Int. Conf. on Robotics and Automation*, Vol. 2, pp. 843-849.

Malcolm, C.A. (1987). Planning and performing the robot assembly of SOMA cube constructions. M.Sc. thesis, Department of Artificial Intelligence, University of Edinburgh.

Popplestone, R.J., A.P. Ambler, and I. Bellos. (1980). An interpreter for a language for describing assemblies. *Artificial Intelligence*, 14(1):79-107.

Sakane, S., T. Sato, and M. Kakikura. (1987). Model-based planning of visual sensors using a hand-eye action simulation system: HEAVEN. *Proc. of Int. Conf. Advance Robotics*, pp. 163-174.

Weiss, L.E. (1984). Dynamic visual servo control of robots: an adaptive, image based approach. Ph.D. thesis, Carnegie Mellon University.

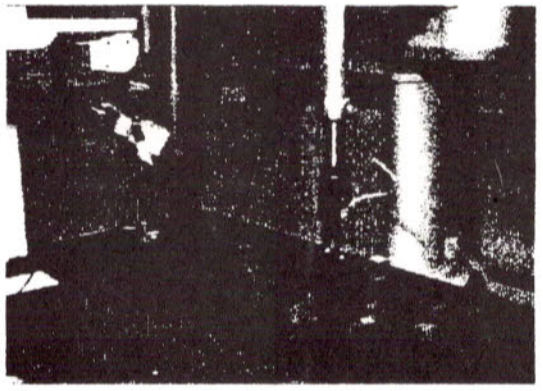

Figure 1: First experiment, one camera system

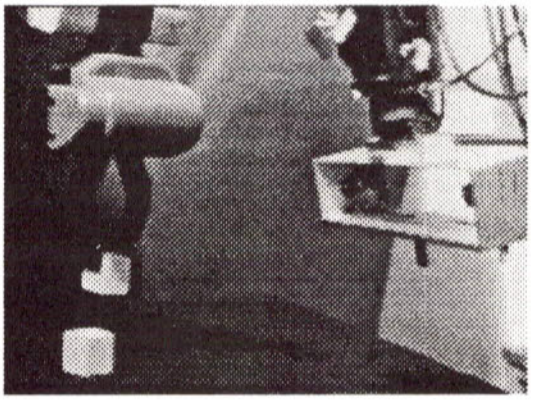

Figure 2: Two cameras system on a mobile head

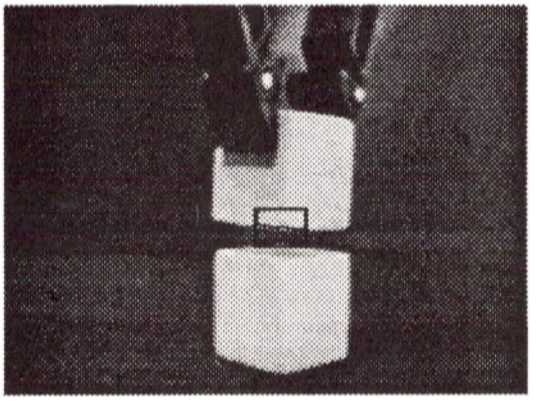

Figure 3: Part-mating using visual feedback

VIRTUAL WEDGING IN THREE DIMENSIONAL PEG INSERTION TASKS

Schitt LAOWATTANA

Department of Mechanical Engineering
Carnegie Mellon University
Pittsburgh, PA 15213

Abstract

Quasi-static wedging of three point contacts is investigated, wherein the concepts of virtual and redundant wedging due to a resultant force falling into a friction cone are proposed. We consider the fully started case of a square peg and hole consisting of two point-surface contacts and one line-line contact. An analysis of the wedging diagram for this highly constrained configuration is carried out and compared to the two dimensional case. An approximate wedging diagram is constructed which shows that wedging of square pegs into square holes is more likely than cylindrical pegs and holes of similar sizes.

1.0 Introduction

Assembly consumes, on average, 50% of a product's in-plant cycle time and direct labor. We believe that Flexible Assembly Systems (FAS) will be highly cost effective where many styles and models of a particular product is required, due to the ease of reprogramming the machines. The various styles and models can be expected to undergo several design changes during the life cycle of the equipment However, a truly flexible assembly environment is, at present, difficult to achieve. A more thorough understanding of Part Mating Analysis is required to be able to program with high repeatability. An example of part mating is the well known "peg-in-hole" problem, which is one of the most ubiquitous assembly operations. Using a pure positional control, the success of peg insertion requires that the part clearance is not smaller than the accuracy and/or the repeatability of the manipulators and manufacturing jigs. In addition, wear of manufacturing machines and imperfect alignment of parts are unavoidable in the manufacturing plant. Dimensions of the same component also differ from one part to another due to practical constraints such as cost and technical shortcomings. The geometrical variations, unfortunately, may cause excessive mating forces, which will then lead to the failure of the insertion process.

Assembly robots in the laboratory which use force control, often operate with inherent instability. When the flexibility of the system induces a vibration within the desired closed-loop bandwidth, instability will often occur. The implementation of high-bandwidth, high-accuracy force control has proven to be difficult. This is especially due to the "contact instability" problem[1], which occurs when contact is made with a rigid environment, such as in the peg insertion process.

Whitney, et. al.[2] established a strategy for inserting a chamfered, round peg into a round hole. This strategy assumes that the peg and hole are rigid and that the peg is mounted with a compliant structure. A special configuration of this compliant structure, Remote Center of Compliance (RCC), gives especially good characteristics in supporting the peg. It reduces the mating forces and the likelihood of jamming and wedging. In this analysis, jamming refers to failure of assembly due to improperly aligned forces; wedging refers to improper geometrical initial conditions. Caine[3] analyzed the insertion of chamferless right rectangular pegs. In this case, there are sets of forces and moments which must be applied to the peg to avoid jamming. Strip[4] extended Caine's approach to include a hybrid force-position strategy using active compliance for convex three-dimensional pegs. This strategy initially tilted the peg and subsequently moved it in contact with the hole. The point of support and the target point were defined such that it would simulate human behavior. The target point was selected based on the shape of both the peg and the hole as well as the point of support on the

peg. Strip also indicated that the reduction of the degrees of freedom leads to an easier interpretation of the forces measured. Strip[5] also invented a passive mechanism for jamming avoidance in three-dimensional insertion. Wedging conditions were not considered.

Three dimensional wedging was studied by Sturges[6], but limited to two opposing contact points. This study also extended the jamming diagram of Whitney, et. al. to the three-dimensional case.

It is essential that both wedging and jamming conditions must be observed for successful peg in hole assembly. Wedging most likely occurs in assembly processes where initial errors cannot be measured, nor guaranteed by the tolerances of mating parts. In this paper, we will investigate conditions for wedging in three dimensions and develop a corresponding wedging diagram.

2.0 Wedging due to three point contacts

There are conditions in which wedging may occur among multiple point contacts, although there is no wedging at any *pair* of contacts between the peg and hole. In the case of multi-point contacts, we classify wedging into three types: two point, virtual and redundant. The two point wedge is described in Whitney, et. al.[2]. Virtual wedging of three point contacts occurs when lines connecting the contact points of each pair *do not* fall within the friction cones of both contacts. However, a combination of two friction cones may form a resultant force which lies within the third friction cone. Such a wedging condition imposes geometric constraints on the forces and the contact points. Redundant wedging is created by multiple instances of two-point wedges and/or virtual wedges.

General conditions for plannar wedging are shown in Figure 1 for a polynomial shaped boundary of a planar hole. Let X_i (i = 1,2,3) be the three contact points on the surface of the hole. Their coordinates $[x_i, y_i]$ are polynomial in C_i with lateral errors, $\varepsilon_i = [c_i^-, c_i^+]$. The notation of Faverjon[7] is particularly useful in developing the constraints for planar wedging. A contact configuration for virtual wedging is a set of C_i for which the following inequalities are satisfied:

$$(X_4 - X_3) \Theta \bar{X}_3 \quad \leq \quad \alpha \qquad (1)$$

where $X_4 = [x_4, y_4]$, the intersection of two friction cones can be determined from:

$$(X_4 - X_2) \Theta \bar{X}_2 \quad \leq \quad \alpha \qquad (2)$$

$$(X_4 - X_1) \Theta \bar{X}_1 \quad \leq \quad \alpha \qquad (3)$$

where X_i : unnormalized normal to contact point i
α : half angle of friction cone

and Θ denotes the angle which associates to two corresponding vectors.

In the case of redundant wedging, a pair virtual wedges is formed with more than one set of contacts. There are three possible pairs [i,j] of contacts: [1,2] [1,3] [2,3] . Six inequalities bound the wedging region of each pair of contacts as follows:

$$(X_i - X_j) \Theta \bar{X}_j \quad \leq \quad \alpha , \qquad (4)$$

$$(X_j - X_i) \Theta \bar{X}_i \quad \leq \quad \alpha . \qquad (5)$$

$$i = 1,2 ; j = i + 1$$

Figure 2 shows how to determine the value θ_{2w} which determines wedging for polygonal contact configurations. Let θ_1 and θ_3 be specified. The contact point 3 is at the origin. The following parameters are given according to the geometry of the hole.

d_2 and d_3 : x-y coordinate of contact point 1
d_1 and d_4 : x-y coordinate of contact point 2

The condition for a virtual wedge exists when point 4 lies within friction cone of point 3. That is , the resultant of the two forces lying on the edge of the first and second friction cones passes through point 3 and therefore lies within the third friction cone.

$$\theta_{2w} = (\frac{\pi}{2} - \alpha) - \tan^{-1}\left(\frac{d_1 - |I_x|}{d_4 - I_y}\right) , \qquad (6)$$

where I_x and I_y are trigonometric functions of d_2 , d_3 , θ_1 and α, shown in the Appendix I.

From Figure 2, the shaded area of the friction cone at point 3 shows a possible region where reaction forces from three contacts(1,2 and 3) are in equilibrium. One boundary of each of the three friction cones intersect at point 4 for $\theta_2 = \theta_{2w}$. Point 4 is a special condition which helps define the upper and lower limits of the wedging space. In general, point 4 does not exist but point 4' and point 4'' show the actual limits of virtual and redundant wedging. The boundaries of the first and the third friction cones also intersect at point 4', whereas those of the first and the second friction cones intersect at point 4". A line 4'-2 connects point 4' and 2. Angle γ is defined as an angle which the line 4'-2 makes with the line 2-4. This angle is the lower limit of θ_2 where the virtual wedging condition is satisfied as θ_2 is rotated counter clockwise. Note that every point along the line 4-4' lies within the third friction cone. We also define β as

an angle between the line 4'-2 and the line 2-1. If the angle θ_2 is decreased by rotating the cone 2 in the counter clockwise direction, a reaction force from the contact point 1 will fall into the friction cone of point 2 and two point wedging occurs. If virtual wedging and two point wedging occur simultaneously, we have redundant wedging. Therefore, in order to have only virtual wedging, γ must be smaller than β.

The value of θ_{2w} is plotted in Figure 3 as a function of d_4 for selected values of θ_1 , θ_3 and d_1, d_2, d_3. The upper bound condition of virtual wedging is determined by adding 2α to θ_{2w}. Its lower bound condition is obtained by subtracting β from θ_{2w}. The upper bound and lower bound conditions of redundant wedging are $(\theta_{2w} - \beta)$ and $(\theta_{2w} - \beta - 2\alpha)$ respectively. To avoid wedging, θ_2 must lie outside the areas of virtual and redundant wedging.

It should be clear from Figure 2 that a sufficient condition for virtual wedging exists if any two friction cones corresponding to two contact points both include the third contact point.

In this section, we introduced the concepts of virtual and redundant wedging in the plane. The extension to three dimensions will be described in the following sections.

3.0 Feature Definitions of a Square Peg and a Hole

Figure 4 shows a square peg and hole. All designations for bounding edges have been attached. A reference frame for the peg is designed with prime(′). The four side edges are described by line segments β'_i (i = 1, ..,4). The four bottom edges are denoted by line segments γ'_i (i = 1, ..,4). O′ is the origin of reference coordinates for the peg which is attached to the first bottom corner, p_1. Let w be the width of the peg. The point-coordinates of the four corner are

$$p'_1 = [\,0 \quad 0 \quad 0 \quad 1\,]^t \tag{7}$$
$$p'_2 = [\,0 \quad w \quad 0 \quad 1\,]^t \tag{8}$$
$$p'_3 = [\,-w \quad w \quad 0 \quad 1\,]^t \tag{9}$$
$$p'_4 = [\,-w \quad 0 \quad 0 \quad 1\,]^t \tag{10}$$

For the square hole, the four top inner edges are described by line segment α_i (i = 1, ..,4). The outer edges of the chamfer are denoted by line segment ε_i (i = 1, ..,4) and the four chamfer corners by line segment δ_i (i = 1, ..,4). It is assumed that the inner edges lie normal to line α. O is the origin of reference coordinates for the hole which is attached to the first inside corner, q_1. If W is the width of the hole, the point-coordinates of the four hole corners will be

$$q_1 = [\,0 \quad 0 \quad 0 \quad 1\,]^t \tag{11}$$
$$q_2 = [\,0 \quad W \quad 0 \quad 1\,]^t \tag{12}$$
$$q_3 = [\,-W \quad W \quad 0 \quad 1\,]^t \tag{13}$$
$$q_4 = [\,-W \quad 0 \quad 0 \quad 1\,]^t \tag{14}$$

In addition, each chamfer surface is defined a point e_i in the plane which contain lines α_i and ε_i .

$$e_1 = [\,c\eta \quad 0 \quad s\eta \quad 1\,]^t \tag{15}$$
$$e_2 = [\,0 \quad c\eta+W \quad s\eta \quad 1\,]^t \tag{16}$$
$$e_3 = [\,-c\eta-W \quad 0 \quad s\eta \quad 1\,]^t \tag{17}$$
$$e_4 = [\,-w \quad -c\eta \quad s\eta \quad 1\,]^t \tag{18}$$

where η is the chamfer angle with the horizontal plane. The symbols c and s represent trigonometric functions for cosine and sine respectively.

4.0 An Approximate Model of Wedging for the Ortho-Configuration

Using the notation for the peg and hole defined in the previous section, we will analyze the onset of wedging with three contacts. Of the many likely contact configurations which are possible after chamfer crossing, the ortho configuration[6] of Figure 5 is typical of three-point constraints. This contact configuration consists of two point-surface contacts and a line-line contact. It is always possible to obtain this configuration during chamfer contact since there is no possibility of planar wedging for the two point contacts. However, as the peg advances to cross the chamfer, the resultant of two contacts might fall into the friction cone of the third contact(point-surface). Eq.(15) , (16), (17) and eq. (18) are shown in the previous section for the purpose of completeness of geometrical description. The chamfer angle (η) is involved in the determination of a lateral error(ε_0) defined in [2]. Since, at the onset of wedging for this configuration, the peg has already passed the chamfer surface, we will consider the contacts made by the geometry of the peg and hole as shown in eq.(7) to eq.(14). The three contacts are pictorially shown in Figure 5 which excludes the chamfer surface. We will develop an approximate wedging diagram for this case taking the x-z plane of the hole as a reference plane and compare it with the two dimensional case of Whitney et. al.[2].

For polygonal pegs and holes, contact configurations such as line-line can be analytically describes by using the Plücker coordinates $[\tilde{N},\tilde{N}_0]$. $\tilde{N}$ is a directional vector which is not necessarily normalized. $\tilde{N}_0$ is a moment of a line l. P is any point on the line l.

$$\tilde{N}_0 = P \times \tilde{N}. \quad (19)$$

The contact states analysis to follow is most conveniently expressed in Plücker coordinates. Let the direction cosines of peg line β' define a unit vector $\tilde{N}'$ at infinity in frame O':

$$\tilde{N}' = [\ \beta'_1 \quad \beta'_2 \quad \beta'_3 \quad 0\ ], \quad (20)$$

which can be transformed to be a unit vector in frame O of the hole by

$$\tilde{N} = D\tilde{N}', \quad (21)$$

where D is the homogeneous transformation matrix which relates the location of the peg with respect to the hole:

$$D = \begin{bmatrix} c\psi c\phi & s\theta c\psi s\phi - s\psi c\theta & s\theta s\psi + c\theta c\psi s\phi & x_o \\ s\psi c\phi & s\theta s\psi s\phi + c\psi c\theta & c\theta s\psi s\phi - s\theta c\psi & y_o \\ -s\phi & c\phi s\theta & c\phi c\theta & z_o \\ 0 & 0 & 0 & 1 \end{bmatrix}, \quad (22)$$

In the analysis below, we will refer to the elements of D as:

$$D = \begin{bmatrix} d_{11} & d_{12} & d_{13} & x_o \\ d_{21} & d_{22} & d_{23} & y_o \\ d_{31} & d_{32} & d_{33} & z_o \\ 0 & 0 & 0 & 1 \end{bmatrix} \quad (23)$$

Contact constraints are readily described by computing the mutual moment between two lines [Hunt (8)]. The mutual moment of two lines is defined as the distance between the lines along their unique common normal multiplied by the sine of the angle between them

$$d \sin\theta = \tilde{N}_1\tilde{N}_{02} + \tilde{N}_2\tilde{N}_{01} \quad (24)$$

If the Plücker coordinates of l_1 and l_2 are:

$$l_1 = \alpha_1 \ \alpha_2 \ \alpha_3 \ , \ \alpha_4 \ \alpha_5 \ \alpha_6 \quad (25)$$
$$l_2 = \beta_1 \ \beta_2 \ \beta_3 \ , \ \beta_4 \ \beta_5 \ \beta_6, \quad (26)$$

then

$$\tilde{N}_1\tilde{N}_{02} = \alpha_1\beta_4 + \alpha_2\beta_5 + \alpha_3\beta_6 \quad (27)$$
$$\tilde{N}_2\tilde{N}_{01} = \beta_1\alpha_4 + \beta_2\alpha_5 + \beta_3\alpha_6. \quad (28)$$

From eq. (26), if p is any point on the line l, the moment part of the Plücker coordinates can be expressed in a matrix form as

$$\tilde{N}_{02} = \Lambda p = \Lambda D p', \quad (29)$$

where is Λ an antisymmetric cross-product matrix:

$$\tilde{N}_{02} = \begin{bmatrix} 0 & \beta_3 & -\beta_2 & 0 \\ -\beta_3 & 0 & \beta_1 & 0 \\ \beta_2 & -\beta_1 & 0 & 0 \\ 0 & 0 & 0 & 1 \end{bmatrix}.$$

At this point, we can use the Plücker coordinates to restate the line segments of the peg and hole, β_2 and α_2, which create the line-line contact at the point 2 of the ortho configuration .

$$\beta'_2 = (0 \ 0 \ 1 \ w \ 0 \ 0) \quad (30)$$
$$\alpha_2 = (0 \ 0 \ 1 \ 0 \ 0 \ -W). \quad (31)$$

These two lines satisfy the line-line contact constraint at point 2 when $z_3 = 0$. By using eq. (24) and (29), we obtain the coordinate of point 2:

$$p_2 = \left[\frac{-\beta_5}{\beta_3} \quad \frac{\beta_4}{\beta_3} \quad 0 \quad 1 \right]^t. \quad (32)$$

From eq. (21), (22), (29),(30) and (31), the coordinate of β_2 in the reference frame of the hole is obtained:

$$\beta_2 = \begin{bmatrix} d_{13} \\ d_{23} \\ d_{33} \\ y_0 d_{33} - z_0 d_{23} + w d_{11} \\ z_0 d_{13} - x_0 d_{33} + w d_{21} \\ x_0 d_{23} - y_0 d_{13} + w d_{31} \end{bmatrix}^t. \quad (33)$$

Setting d = 0 in eq. (24) and substituting with eq. (31) and (33), yields the contact constraint relation:

$$z_0(s\theta c\psi - c\theta s\psi s\phi) + (y_0 - W)c\phi c\theta + w c\phi c\psi = 0. \quad (34)$$

Figure 5 also shows the geometry for onset of wedging (if there is one) as the second point-surface contact (point 1) enters the hole. According to Figure 5, one can see that two point-surface contacts are located at

$$p_1 = (\ 0 \quad y_0 \quad 0 \quad 1\ )^t \quad (35)$$
$$p_3 = (\ x_3 \quad 0 \quad z_3 \quad 1\ )^t \quad (36)$$

We obtain the unknown coordinate of point 1 and point 3 from eq.(9), (22) and (36):

$$y_0 = w\ (\ c\psi c\theta + s\theta s\psi s\phi - s\psi c\theta) \quad (37)$$

$$x_3 = w\,(s\theta c\psi s\phi - c\psi c\phi - s\psi c\theta) \quad (38)$$
$$z_3 = w\,(c\phi s\theta - s\phi). \quad (39)$$

Since virtual wedging can exist if any of two friction cones of two contacts in Figure 5 both include the third contact point, a set of six relationships between contact points can be found. Table I gives the minimum values for friction coefficient, μ, which cause wedging, based on the geometry of Figure 5 and the analysis in section 3 above. To read the table, consider a row number as a friction cone base and a column number as an included contact point. A virtual wedge formed by the friction cones at contact 1 and contact 3 including contact 2 (denoted as *VW(1,2)* and *VW(3,2)*) satisfies relations in row 1 - column 2 and row 3 - column2, viz:

$$\frac{|z_3|}{\sqrt{\left[W^2 + (x_2 - x_3)^2\right]}} \leq \mu \quad (40)$$

$$\left|\frac{(W - y_0)}{x_2}\right| \leq \mu \quad (41)$$

Due to small angle approximation, we assume that the normal to all three contacts is perpendicular to the inner surface of the hole. The inner surface of the hole at point 3 is parallel to one at point 2 but perpendicular to one at point 1. Therefore, *VW(2,3)* and *VW(3,2)* are the same whereas *VW(1,3)* and *VW(2,3)* are reciprocal to *VW(3,1)* and *VW(3,2)* respectively. Replacing inequalities by equalities in eq. (40) and eq. (41) and solving eq.(37) through eq.(41) yield the possible configurations for the onset of wedging, which we now develop into a wedging diagram.

Referring to the wedging diagram for two dimensions (Whitney et.al) in Figure 6, the linear equation of the upper and lower boundary is

$$\theta_0 + s\varepsilon_0 < \theta_w \quad (42)$$

where θ_w , a wedging limit angle, is equal to $\pm c/\mu$.

The parameter s and c represent a slope and clearance ratio between the peg and hole respectively:

$$s = \frac{L_g}{\left(L_g^2 + \frac{K_\theta}{K_x}\right)} \quad (43)$$

$$c = \frac{(W - w)}{W} \quad (44)$$

with

θ_0 : angular error
ε_0 : lateral error
L_g : distance from a rigid support to the peg's tip
K_x : lateral compliance
K_θ^x : angular compliance

A quasi-static analysis, similar to [2], has been carried out relative to the x-axis of the hole for the ortho configuration of the peg. The slope and wedging limit θ_w of eq.(42) is formed using relations given by eq.(37) through (41) and static balances of forces and moments about a compliance center defined in [2]. After doing a bit of algebra and dropping high order terms, we find that:

$$s = \frac{L_g\left[c\theta c\phi c\psi + \mu\left(\frac{W}{w} - \frac{c\psi}{c\theta}\right)\right]}{L_g^2 + \frac{K_\theta}{K_x} - L_g\left[c\theta c\phi s\psi + \mu\left(\frac{W}{w} - \frac{c\psi}{c\theta}\right)\right]} \quad (45)$$

$$\theta_w = \cos^{-1}\left(\frac{-B + \sqrt{B^2 - 4AC}}{2A}\right) \quad (46)$$

with
$$A = W^2 + 2w^2 c\phi s\psi\mu$$
$$B = 2w^2 c\phi^2 c\psi\mu + 2Wwc\phi(1 - \mu^2)$$
$$C = w^2 c\phi^2(2 - \mu^2)$$

Eq. (45) and (46) describe an approximate linear model of wedging which determines the values of θ_w and s . This linear model is valid only if all three angles (θ, ϕ , ψ) are small.($< 5^\circ$) In this case, nonlinear terms are infinitesimal when compared with linear terms. We still need to know the admissible range of lateral error, ε_0 , on the axis of interest so that we can construct a wedging diagram. In addition, the ratio of K_θ / K_x in eq. (45) appears as a value in the reference frame of the hole and will require a transformation from the frame of the peg.

To find ε_0 , let $\tilde{a}$ be the chamfer width. Using the homogeneous transformation matrix, D, in eq.(22) and the geometry of Figure 4, the admissible range of lateral error for avoiding wedging is:

$$\varepsilon_0 = \tilde{a} + W/2 - (w/2)(c\psi c\phi + s\psi c\theta - s\theta c\psi s\phi) \quad (47)$$

Similarly, the compliance supporting the peg, in Figure 7, are transformed to the frame of the hole.

$$K_x = K_x c\psi c\phi + K_y(s\theta c\psi s\phi - s\psi c\theta) \quad (48)$$
$$K_\theta^x = K_\theta^x c\psi c\phi + K_\phi^y(s\theta c\psi s\phi - s\psi c\theta) + K_\psi(s\theta s\psi - c\psi c\theta s\phi)$$

Compliances of the support are denoted by *italic terms*. An approximate wedging diagram shown in Figure 8 is obtained by making small angle approximations and substituting the following parameters into eq.(45) through eq.(48): $\phi=0^{\circ}$, μ = 1.5, L_g = 1 cm, all linear compliances (K_x and K_y) are 1 N/m, all angular compliances (K_{θ}, K_{ϕ} and K_{ψ}) are 50 N-m/rad., w= 9 cm, W=10 cm and ã = .5 cm.

The solid lines and dashed lines represent the wedging diagram in two dimensions and the approximate three dimensional wedging diagram, respectively. The diagram considers the effects of three point contacts. It can be seen that the confined area in the latter case is smaller due to smaller values of θ_w and s. In addition, when the azimuth rotation of the peg, ψ , increases, the admissible range of the lateral error decreases. This means that the wedging space is larger. Therefore, when ψ is small, but non-zero, insertion of square pegs into square holes which leads to the ortho configuration is shown quantitatively to wedge more readily than that of cylindrical pegs and holes of similar support and dimensions.

5.0 Conclusion

Studies of the peg insertion problem have been carried out for over a decade. The Remote Center of Compliance (RCC) which evolved from the early work is successful in facilitating peg insertions with tight tolerance. However, its capability is limited to round pegs and holes with chamfers. It fails to insert polygonal, nonsymmetrically shaped pegs into mating holes. In addition, techniques for using active force control for such mating processes rely on an assumption of predictable initial error due to mating tolerance.

To obtain better understanding of this problem, we have extended the study of the wedging diagram into three dimensions. Possibilities of wedges for fully started contacts , e.g., the ortho configuration between a square peg and hole, reveal virtual wedging among three contracts. The wedging space is now described by the parameters of contact configurations: positions and orientations of the peg relative to the hole. Strategies for initially orienting the peg must avoid this wedging space. It remains to determine wedging conditions for other contact configurations and the constraints between them.

6.0 References

1. Eppinger S. and Seering W. "Introduction to Dynamic Models for Robot Force Control" *IEEE Control Magazine*, Vol.. No. 2, April 1987

2. Whitney, D.E. "Quasi-Static Assembly of Compliantly Supported Rigid Parts." *Journal of Dynamics System, Measurement, and Control*, Vol. 104, pp. 65-77, 1982.

3. Caine, M.E. "Chamferless Assembly of Rectangular Parts in Two and Three Dimensions." Master thesis, Dept. of Mechanical Engineering, Massachusetts Institute of Technology, June 1985.

4. Strip, D.R. "Insertion Using Geometric Analysis and Hybrid Force-Position Control: Method and Analysis." *Proceedings of the IEEE International Conference on Robotics and Automation.* Philadelphia, PA., 1988.

5. Strip, D.R. "A Passive Mechanism for Insertion of Convex Pegs." Sandia National Laboratories, 1988.

6. Sturges, R.H. "A Three Dimension Assembly Task Quantification with Application to Machine Dexterity." *The International Journal of Robotics Research*, Vol. 7, pp. 34-78, 1988.

7. Faverjon B. and Ponce J. "On Computing Two-Finger Force-Closure Grasps of Curved 2D Objects." Proceeding of the 1991 IEEE International Conference on Robotics and Automation, Sacramento, California, pp 424-429, April 1991.

8. Hunt, K.H *Kinematic Geometry of Mechanisms* Oxford University Press, 1978

Appendix I

Geometric relations involving fixed parameters in Figure 2.

Point 4 and 4' have coordinate (I_x,I_y) and(I'_x,I'_y) respectively:

$$I_x = \frac{d_3 - d_3}{\left[\tan\left(\alpha - \frac{\pi}{2}\right) - \tan(\alpha + \theta_1)\right]}$$

$$I_y = \frac{d_3 - d_3}{\left[1 - \frac{\tan(\alpha + \theta_1)}{\tan(\alpha - \frac{\pi}{2})}\right]}$$

$$I_x = \frac{d_3 - d_3'}{\left[\tan\left(\frac{\pi}{2} - \alpha\right) - \tan(\alpha + \theta_1)\right]}$$

$$I_y' = \frac{d_3 - d_3'}{\left[1 - \frac{\tan(\alpha + \theta_1)}{\tan(\frac{\pi}{2} - \alpha)}\right]}$$

Where

$$d_3' = d_2 \tan(\alpha + \theta_1)$$

After knowing these coordinates, θ_{2w} can be determined by using the condition of the normal at the contact point 2:

$$\beta = \theta_{2w} + \tan^{-1}\left(\frac{d_3 - d_4}{d_1 + d_2}\right) - \alpha$$

$$\gamma = \theta_{2w} + \alpha - \tan^{-1}\left(\frac{d_4 - I_y'}{d_1 + I_x'}\right)$$

which leads to eq.(6)

Similarly, we can also obtain the values of β and γ as following.

$$\beta = \theta_{2w} + \tan^{-1}\left(\frac{d_3 - d_4}{d_1 + d_2}\right) - \alpha$$

$$\gamma = \theta_{2w} + \alpha - \tan^{-1}\left(\frac{d_4 - I_y'}{d_1 + I_x'}\right)$$

Note that (θ_{2w} - γ) is the lower bound condition of virtual wedging for the three contact forces along the boundary of friction cones (Also see Figure 2)

Table I. Minimum values of μ sufficient for wedging

		Included Contact Point		
		1	2	3
Friction Cone	1	——	$\left\lvert\frac{(W \cdot y_0)}{x_2}\right\rvert$	$\left\lvert\frac{\sqrt{y_0^2 + z_0^2}}{x_3}\right\rvert$
	2	$\left\lvert\frac{x_2}{(W \cdot y_0)}\right\rvert$	——	$\frac{\lvert z_3 \rvert}{\sqrt{\left[W^2 + (x_2 - x_3)^2\right]}}$
Base	3	$\frac{\lvert x_3 \rvert}{\sqrt{y_0^2 + z_0^2}}$	$\frac{\lvert z_3 \rvert}{\sqrt{\left[W^2 + (x_2 - x_3)^2\right]}}$	——

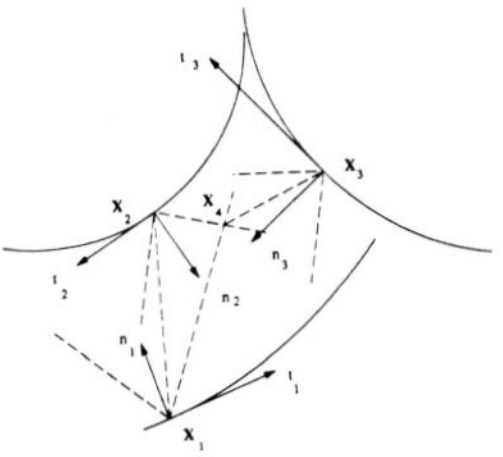

Figure 1. Generalized Three Contact Configuration with Virtual Wedging

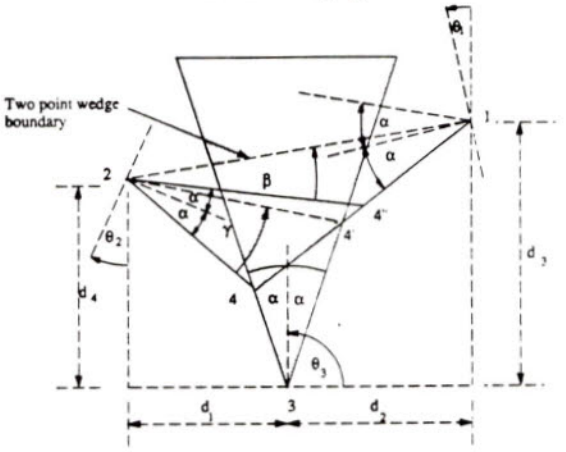

Figure 2. Virtual Wedging in a Polygonal Geometry

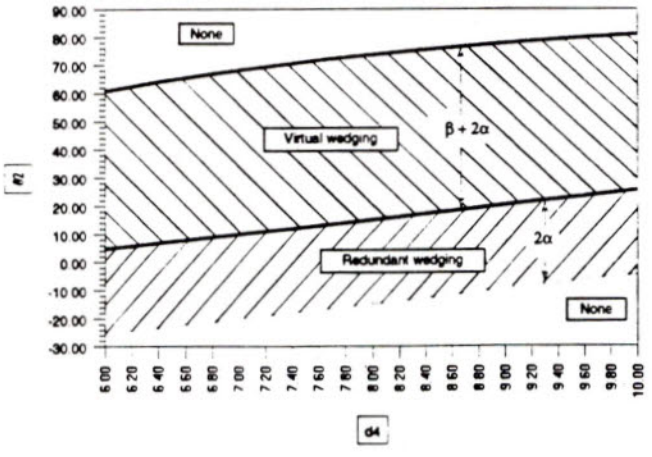

Figure 3. θ_{2w} of virtual and redundant wedging for the contacts in Figure. 2 $\theta_1 = 20^o$, $\theta_3 = 90^o$, $\alpha = 15^o$ and $d_1 = 4.0$ cm, $d_2 = 7.0$ cm, $d_3 = 8.0$ cm

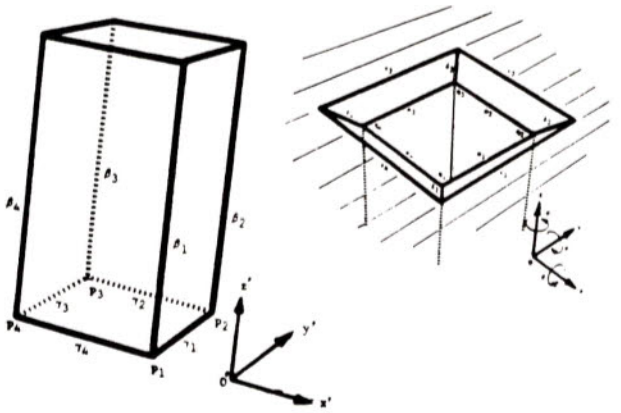

Figure 4. Feature Definitions of a Square Peg and Hole

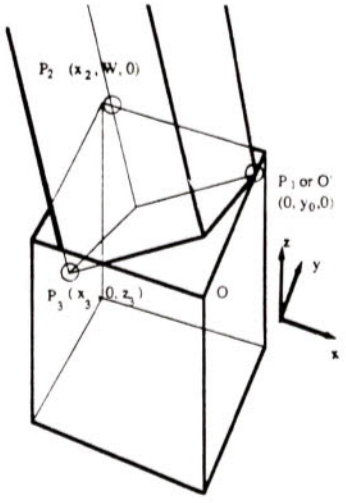

Figure 5. Ortho Configuration at onset of wedging

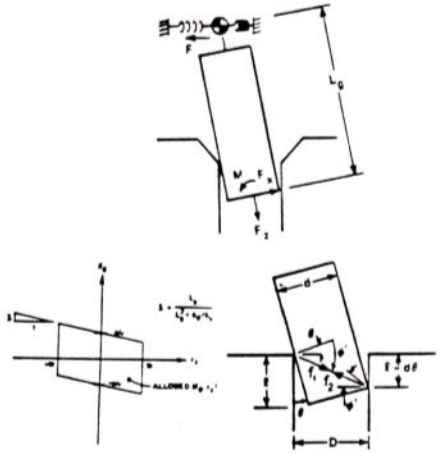

Figure 6. Wedging Diagram for Two-Dimensional Peg Insertion Tasks

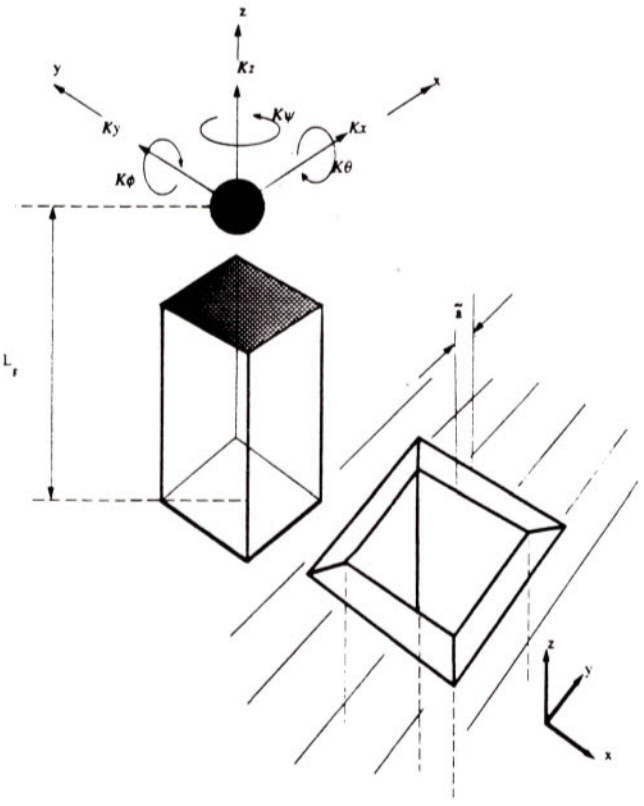

Figure 7. Generalization of Linear and angular compliance of the support

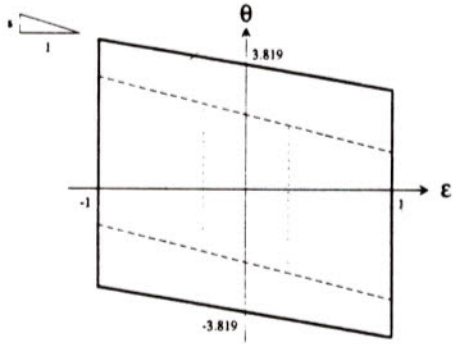

Wedging Diag.	Line symbol	Azimuth angle (ψ) degree	slope	Y- intercept degree	X- intercept cm
Whitney (2D)	———	0	- 0.019	3.819	1
Ortho-Configuration	- - - - -	0	- 0.023	2.457	1
	.....	6			0.55
	. . . . .	10			0.28

Figure 8. Wedging diagram for the Ortho Configuration compared w/ the 2-D Case

REPRESENTATION OF RELATIVE FREEDOM DERIVED FROM GEOMETRIC MODELS

Schitt LAOWATTANA

Department of Mechanical Engineering
Carnegie Mellon University
Pittsburgh, PA 15213

ABSTRACT

Multi-contact constraints representing the assembled state of polygonal solid objects can be represented by screw systems which provide a complete description of rotational and translational freedom. In most cases, the computation of relative freedom does not require consideration of all constraints. We have developed an algorithm to identify redundant constraints, therefore minimizing the complexity of assembly/disassembly planning. We also employ the method to determine relative stability which identifies unstable configurations of assembled parts.

1. INTRODUCTION

One of the major issues in engineering design is how to take concerns from downstream processes into consideration during the preliminary design stages. This issue aims at reducing the cycle times of overall processes while assuming the highest quality levels to products with minimum cost. Downstream processes include testing, manufacturing, quality control , and assembly. It is well known that assembly consumes, on average, 50% of a product's in-plant cycle time and direct labor. Hence, at present, there are many software tools being developed to evaluate and optimize designs before they are passed to production. In particular, tools have been developed for automatic and efficient assembly planning.

T. Yoshikawa et. al [1] proposed the idea of minimizing a criterion function based on the difficulty of a state transition. The optimal path is found among contact-state-networks, introduced by Hirai et al [2]. De Fazio and Whitney [3] developed an interactive method for generating all assembly sequences, in which the order of assembly depends upon which operations are used. This interactive approach allows designers to participate in the assembly planning process so that they can help resolve any ambiguity that arises. Erdman [4] used the AI technique of back projection to search for assembly steps based on the preimage approach.

There is still a need for a relative freedom representation in assembly/disassembly planning since this step is still manual and highly dependent on the planner/designer. Efficient representation must yield the best plans in least time. The seminal work on the kinematic representation of wrenches and twists was done by M.S. Ohwovoriole and B. Roth [5]. The concept of "*reciprocal screw*" was extended to "*repelling and contrary screws*". J. M. Schimmels and M. A. Peshkin [6] recently implemented such concepts to address the design of manipulator admittance for reliable force-guided assembly in two dimensions .R. S. Mattikalli and P. K. Khosla [7] have presented a new method for determining restraints to translational and rotational motion of planar and 3-D objects. R.H. Wilson [8] developed the non-directional blocking graph to indicate the blocking relationships between parts in an assembly. However, this work lacks a clear identification of essential wrenches for the computation of d.o.f of assembled parts. In this paper, we will use concepts similar to [5] to represent the relative freedom of assembled parts. This representation unambiguously finds the possible motions of a part directly from its geometric model under multi-contact

constraints and gives the observer a graphical indicator of these motions.

We introduce our analysis and representation with a simple problem: the assembly of a rectangle in to a corner. Fig. 1 shows the planar assembly/disassembly of a rectangle into a corresponding right angle corner. We define a series of steps in relocating the rectangular from an initial state to a final state as an assembly procedure, and vice versa as a disassembly procedure. In general, the assembly procedure could be planned by reducing the degrees of freedom (d.o.f.) of the rectangle itself until it reaches the final state where the d.o.f. are minimized. The final d.o.f. should be zero so that the assembled parts can maintain their *stability* for any position and orientation. However, in practical circumstances, the final d.o.f. is not always zero and gravity forces on assembled parts may cause them to move. The subject of stability will be treated in section 5.

An example of reducing the d.o.f. of mating parts, is shown in Fig. 2. One possible assembly procedure could start by tilting and moving the rectangle towards one side of the corner until it makes a point-line contact. It is subsequently rotated at the contact point to increase the degree of motion constraint and transform the point-line contact to a line-line contact between the mating parts. Finally, another d.o.f. is eliminated by sliding the rectangle to the corner to make a second line-line contact while maintaining the first one. It should be noted that the disassembly procedure could be obtained by reversing the assembly procedure. However, such a procedure is not always efficient. In this case, it is less complicated to disassemble the rectangle from the final state "5" directly to the initial state "1".

The above example shows the differences between the motion spaces of assembly and disassembly. Neither may be unique. Our interest is to identify the allowable space in the disassembly procedure. Such identification is not only a matter of disassembling parts from each other, but also to find the stability of those mating parts in any assembled configuration. There are two types of allowable motion spaces: Rotational Space ($\mathcal{R}$-Sp) and Translational Space ($\mathcal{T}$-Sp). We will explore the $\mathcal{R}$-Sp in section 2 and ($\mathcal{T}$-Sp) in section 4.

2. DETERMINATION OF $\mathcal{R}$-Sp

Consider the same rectangle that is currently in the final state, as shown in Fig. 3, in which two line-line contacts have been made. There are continuously distributed forces acting on the rectangle directed perpendicularly to both sides adjacent to the corner. These interacting forces could be represented as "zero pitch" wrenches, $\mathcal{W}_i$, in Plücker coordinates. Each of $\mathcal{W}_i$ has six components in the Euclidean space: $[\tilde{w}_i,\ \tilde{w}_{oi}]$, $i = 1, \ldots, \infty$. $\tilde{w}_i$ are directional vectors which are not necessarily normalized. $\tilde{w}_{oi}$ are moments of arbitrary lines ℓ_i. We define $\mathcal{P}_i$ as points on the lines ℓ_i . In this case, ℓ_i and $\mathcal{P}_i$ represent interacting forces and contact points respectively. Formally,

$$\tilde{w}_{oi} = p_i \times \tilde{w}_i. \qquad (1)$$

with the distributed contacts forming two sets:

$$\mathcal{W}_i^x = [\tilde{w}_i, \tilde{w}_{oi}]^x = [\,0\ 1\ 0, 0\ 0\ x_i]^x, \qquad (2)$$

and

$$\mathcal{W}_i^y = [\tilde{w}_i, \tilde{w}_{oi}]^y = [\,1\ 0\ 0, 0\ 0\ -y_i]^x, \qquad (3)$$

$$i = 1 \ldots\ldots \infty.$$

where superscripts refer to the axis about which the wrenches are acting. If "a" and "b" are the width and length of the rectangle, then

$$0 \le x_i \le a, \forall x_i, \text{ and } 0 \le y_i \le b, \forall y_i. \qquad (4)$$

A "zero pitch" twist , $\mathcal{T}$, is defined in terms of angular and linear velocities of the rectangle, as a consequence of the given wrenches. Assume $\mathcal{T}$ and $\mathcal{W}_i$ are in the same coordinate frame.

$$\mathcal{T} = [\tilde{t}, \tilde{t}_o] = [\omega_x\ \omega_y\ \omega_z, \vartheta_x\ \vartheta_y\ \vartheta_z], \qquad (5)$$

where ω and ϑ are angular and linear velocities, respectively.

Disassembly requires separation of mating parts. Ohwovoriole [5] pointed out equivalently that the product of all existing wrenches and the corresponding twist must satisfy the following relation on the repelling screw system:

$$\mathcal{W}_i \cdot \mathcal{T} > 0, \qquad (6)$$

$$\tilde{w}_i \cdot \tilde{t}_o + \tilde{t} \cdot \tilde{w}_{oi} > 0. \qquad (7)$$

A planar motion can be expressed by a twist:

$$\mathcal{T} = [\,0\ 0\ \omega_z, \vartheta_x\ \vartheta_y\ 0], \qquad (8)$$

and if $\omega_z = 0$, we obtain a pure translation of the rectangle. When ω_z is not equal to zero, the rectangle is rotating. Eq.(8) is normalized as:

$$\mathcal{T} = \left[0\ \ 0\ \ 1, \frac{\vartheta_x}{\omega_z}\ \ \frac{\vartheta_y}{\omega_z}\ \ 0\right]. \qquad (9)$$

Substituting Eq.(2), (3) and (9) into the repelling screw system, Eq.(7), we have:

$$\frac{\vartheta_x}{\omega_z} \cdot y_i > 0. \quad (10$$

and

$$\frac{\vartheta_y}{\omega_z} + x_i > 0. \quad (11,$$

Hence, the twists which result from the given wrenches are

$$\mathcal{T}(+) = [0 \ 0 \ 1 \ >y_i \ >\text{-}x_i \ 0], \quad (12,$$

$$\mathcal{T}(\text{-}) = [0 \ 0 \ \text{-}1 \ >\text{-}y_i \ >x_i \ 0]. \quad (13)$$

where $(\pm)$ denotes the direction of the twist.

The region of rotational centers, $\mathcal{R}$, which provide these two twists is obtained from the cross product of $\tilde{t}$ and $\tilde{t}_o$. $\mathcal{R}$ lies in the Euclidean space $[x, y, z]$, and exists as a pair of regions:

$$\mathcal{R}(+) = [<x_i \ >y_i \ 0], \quad (14,$$

$$\mathcal{R}(\text{-}) = [>x_i \ <y_i \ 0]. \quad (15,$$

Intersections of $\mathcal{R}$, for $i = 1.....\infty$, give us:

$$\mathcal{R}(+) = [<0 \ >b \ 0], \quad (16,$$

$$\mathcal{R}(\text{-}) = [>a \ <0 \ 0], \quad (17,$$

As shown in Fig.4. This result is identical to the graphical result of Reuleaux's Kinematics [9]. The rotational space, $\mathcal{R}\text{-}Sp$, can then be obtained by counterclockwise and clockwise rotation of the rectangle about any point in the $\mathcal{R}(+)$ and $\mathcal{R}(\text{-})$ respectively. Notice that the twists which resulted from the array of wrenches due to line-line contact are identical to those resulting from only four essential wrenches: $\mathcal{W}_1$, $\mathcal{W}_3$, $\mathcal{W}_4$ and $\mathcal{W}_6$ (See Fig.4) We define "*Essential Wrenches*" as sufficient and necessary for physical constraint. The locations and directions of such essential wrenches are based on the geometry the mating parts, and derived in the next section.

It must be noted that, in the planar case, $\mathcal{R}$ is generally bounded by at least one screw axis of a wrench. Whenever there is more than one wrench applied to an object in the same direction, but in different locations, some of them may be redundant in terms of finding $\mathcal{R}$ and $\mathcal{R}\text{-}Sp$. The ability to distinguish essential wrenches from redundant wrenches given a solid model is important to efficiently generate assembly plans.

3. ESSENTIAL WRENCHES IN A PLANE

As shown in the previous section, wrenches in a plane can be represented by six parameters in Plücker coordinates. Comparisons of these parameters enable us to identify redundant wrenches and discard them during the initial stage of attachment associated with solid models. Only essential wrenches will be used to find $\mathcal{R}$ and $\mathcal{R}\text{-}Sp$.

3.1 Parallel Wrenches

Let us consider a repelling screw system in which there are many parallel wrenches acting in the same direction. Using the same method described in section 2, namely the intersection of $\mathcal{R}$ resulting from these wrenches, we found that $\mathcal{R}(+)$ is bounded by the far left and top wrenches. Similarly, $\mathcal{R}(\text{-})$ is bounded by the far right and bottom wrenches. Formally:

$$\mathcal{W}^{\mathcal{R}(+)}_{Essential} = \{\mathcal{W}_i \mid (\mathcal{M}_i \cdot \mathcal{M}_k) < 0\}, \ i \neq k, \quad (18,$$

and

$$\mathcal{W}^{\mathcal{R}(\text{-})}_{Essential} = \{\mathcal{W}_j \mid (\mathcal{M}_j \cdot \mathcal{M}_k) > 0\}, \ j \neq k, \quad (19,$$

$$k = 1, \ldots, n,$$

where n is the number of wrenches in the system. Eq.(18) and (19) are applied to the finite subset of Eq.(2) and Eq.(3), with $n = 3$, as shown in Fig. 5. ($\mathcal{W}_1$,$\mathcal{W}_4$) and ($\mathcal{W}_6$,$\mathcal{W}_3$) are found to be essential wrenches for computing $\mathcal{R}(+)$ and $\mathcal{R}(\text{-})$ respectively; the others are redundant. Note that Eq.(18) and (19) can be applied regardless of the origin of the Plücker coordinates.

3.2 Non-Parallel Wrenches

When cross sections of mating parts are polygonal, the contact forces (wrenches) from side to side between mating parts are not parallel (Fig. 6). No side of this polygon is parallel to any other; however, mating forces acting on each side are parallel, and Eq. (18) and (19) can be used to identify the essential wrenches for $\mathcal{R}(+)$ and $\mathcal{R}(\text{-})$. Each essential wrench, shown in Fig. 6, acts perpendicularly at one point on each side. It yields the same effect on $\mathcal{R}(+)$ or $\mathcal{R}(\text{-})$ as several parallel wrenches do. Thus, mapping of wrenches on line-line contacts to point-line contacts is justified. Note that this formulation matches our intuition of assembly/disassembly in both rotational directions, as seen before. The locations of the wrenches , shown in Fig. 6 represent the onset of assembly/disassembly of the polygon into/out of its

socket. Since these wrenches are still not determined to be essential, we call them *equivalent wrenches*. In any assembly of general polygons, one should reduce the computational burden by searching for equivalent wrenches before proceeding with further analysis of essential wrenches. The rest of this section describes an algorithm to identify redundant wrenches from the remaining set of non-parallel wrenches.

"Zero pitch" wrenches can be considered as lines, represented in Plücker coordinates in Eq.(1) is as follows:

$$\mathcal{W}_i = \begin{pmatrix} X & Y & Z & \mathcal{M}_X & \mathcal{M}_y & \mathcal{M}_z \end{pmatrix}_i, \quad (20)$$

where, for any point (x_1,y_1,z_1) on the line $\mathcal{W}_i$,

$$\mathcal{M}_{x_i} = y_1 Z - z_1 Y \quad (21a)$$
$$\mathcal{M}_{y_i} = z_1 X - x_1 Z \quad (21b)$$
$$\mathcal{M}_{z_i} = x_1 Y - y_1 X \quad (21c)$$

In the planar case , Z, $\mathcal{M}_x$ and $\mathcal{M}_y$ are zero.

Since a line/wrench in space depends on four parameters, there is redundancy based on the following relations:

$$X_i^2 + Y_i^2 + Z_i^2 = 1, \quad (22)$$

and

$$X_i \mathcal{M}_{x_i} + Y_i \mathcal{M}_{y_i} + Z_i \mathcal{M}_{z_i} = 0. \quad (23)$$

Consider two non-parallel wrenches intersecting each other in a plane. The angle between these two wrenches, β , can be determined from their direction cosines:

$$\beta_{12} = \arctan\left(\frac{X_1 Y_2 - Y_1 X_2}{X_1 X_2 + Y_1 Y_2}\right) \quad (24)$$

β_{12} denotes the angle made by the first wrench, $\mathcal{W}_1$, to the second wrench, $\mathcal{W}_2$. Referring to the example in Fig. 4, $\mathcal{R}(+)$ may be affected by the addition of another wrench. There may exist a third wrench ,$\mathcal{W}_3$, passing through the intersection point of the first two wrenches, as shown in Fig. 7(a), 7(b) and 7(c). Based on the fact that the intersection of two sets is always less than or equal to the smaller of the two sets, the two essential wrenches for $\mathcal{R}(+)$ and $\mathcal{R}(-)$ are selected as ones with the greatest β, since maximum β yields minimum $\mathcal{R}(+)$ and $\mathcal{R}(-)$.

$$\mathcal{W}_{Essential} = \left\{ \mathcal{W}_i \mathcal{W}_j \mid \left(|\beta_{ij}| \geq |\beta_{mn}|\right) \vee \left(|\beta_{ij}| \leq \pi\right) \right\}, \quad (25)$$
$$i,j,m,n = 1, \ldots, 3 \text{ and } i \neq j,\ m \neq n$$

All possible intersections are given by Fig. 7. Whenever $\mathcal{W}_3$ lies in the region closed by $-\mathcal{W}_1$ and $-\mathcal{W}_2$, $\mathcal{R}(+)$ and $\mathcal{R}(-)$ reduce to a point where all three wrenches intersect. This example extends the notion of a deterministic fixture introduced by Asada et. al.[10], by providing a compact computational procedure. J.M Schimmels and M.A. Peshkin [6] also consider this notion in terms of constraint wrenches and unconstrained twists. A fixture, here, is set up to provide constraining wrenches for a workpiece. The motion of the workpiece is described by the possible twists. The fixture is deterministic iff

$$rank(\overline{\mathcal{W}}) = \mathcal{N} \quad (26)$$
$$where\ \overline{\mathcal{W}} : Constraint\ Matrix = \begin{bmatrix} w_1 & w_2 & \cdots & w_m \end{bmatrix},$$

m is number of wrenches and $\mathcal{N}$ is the number of degrees of freedom of the workpiece. Therefore, $\mathcal{N}$ is three and six for planar and spatial fixtures respectively. When $\overline{\mathcal{W}}$ is full rank, m is equal to $\mathcal{N}$. Any unconstrained motion will cause the workpiece to break contact at least one point.

In the planar case with m = 2, the fixture is always non-deterministic. For $m \geq 3$, the fixture is non-deterministic if and only if the rank of $\overline{\mathcal{W}}$ is not full. In this case, there will always be redundant wrenches which can be discarded in the computation of $\mathcal{R}(+)$ and $\mathcal{R}(-)$. We can use Eq.(25) to identify the essential wrenches since all wrenches in non-deterministic fixtures intersect at one point. This is because any wrench in a non-deterministic fixture is a linear combination of the first two wrenches if the rank is 2.

The general case is when the fixture is deterministic and $m \geq 3$, as shown in Fig. 8. All wrenches in such a case may or may not be essential ones. To distinguish these wrenches from the redundant ones, we have developed an algorithm as follows:

1. The direction of each wrench is determined by the first two parameters in Plücker coordinates. If there are parallel wrenches with opposite directions, $\mathcal{R}(+)$ and $\mathcal{R}(-)$ will not exist.

2. Using Eq.(24), the angle between each pair of wrenches is calculated. The signs of these angles are obtained by the right-hand rule in the order of the wrench in each pair.

3. The pair of wrenches which have highest potential to be essential wrenches is determined by the assumption in Eq.(25). The sign of the angle shows the direction of rotation.

4. All intersecting points , (X_s, Y_s) among wrenches are calculated from direction cosines and moments:

$$X_{ij} = \frac{\mathcal{M}_{z_i} X_j \cdot \mathcal{M}_{z_j} X_i}{X_j Y_i \cdot X_i Y_j}, \qquad (26a)$$

and

$$Y_{ij} = \frac{\mathcal{M}_{z_i} Y_j \cdot \mathcal{M}_{z_j} Y_i}{X_j Y_i \cdot X_i Y_j}, \qquad (26b)$$

$X_{ij} = X_{ji}, Y_{ij} = Y_{ji}$ and $i, j = 1, \cdots m$

Hence, all intersecting points are attached to the wrench numbers as well as their directions.

5. The determination of $\mathcal{R}(+)$ and $\mathcal{R}(-)$ can be done as follows. The boundary of $\mathcal{R}(+)$ loci starts at the tail of the first wrench in the selected pair which has the maximum positive angle. The locus moves along the direction cosine towards the head end. Whenever the locus encounters an intersecting point, it will follow the new wrench if and only if the direction of the new wrench points to the left area of the current wrench. Otherwise, it maintains the current direction. The loci will end either at infinity or repeated values. The latter case gives a closed area for $\mathcal{R}(+)$. In addition, $\mathcal{R}(-)$ will not exist since the intersection for $\mathcal{R}(-)$ is a null set. All wrenches on which the loci pass are essential for computing of $\mathcal{R}(+)$.

Note that the first wrench of the selected pair having maximum negative angle is the second wrench of the the pair having maximum positive angle. $\mathcal{R}(-)$ can be obtained by repeating the above procedure as follows: At intersecting points, the loci of the $\mathcal{R}(-)$ boundary only changes into the direction of the new wrenches if the new direction points towards the right area of the current wrench. $\mathcal{R}(+)$ is a null set if $\mathcal{R}(-)$ is a closed area. A closed area must be checked in both directions to verify the existence of $\mathcal{R}(+)$ and $\mathcal{R}(-)$

When searching for $\mathcal{R}(+)$ and $\mathcal{R}(-)$ is completed, essential wrenches are automatically identified, based on information stored in the geometric model of the part. For example, in Fig. 8, the search algorithm reports that $\mathcal{W}_1$, $\mathcal{W}_2$, $\mathcal{W}_3$, $\mathcal{W}_4$ and $\mathcal{W}_1$, $\mathcal{W}_4$, $\mathcal{W}_5$ are essential wrenches, for $\mathcal{R}(+)$ and $\mathcal{R}(-)$ respectively.

We also implemented this procedure in cases A and B of Fig. 6. The resulting $\mathcal{R}(+)$ and $\mathcal{R}(-)$ are shown in Fig. 9. $\mathcal{W}_1$ and $\mathcal{W}_4$ are found to be essential for $\mathcal{R}(+)$ whereas $\mathcal{W}_1$, $\mathcal{W}_3$, and $\mathcal{W}_4$ are essential wrenches for $\mathcal{R}(-)$.

4. DETERMINATION OF $\mathcal{T}$-sp

In solid modelling, curvature can be represented by a number of consecutive straight lines. Therefore, we can treat convex/concave mating parts as closed or open polygons. Closed polygons usually represent moving parts whereas open polygons are stationary parts, i.e., mating surfaces of closed polygons. We can determine the $\mathcal{T}$-sp directly from the geometry of these mating surfaces.

Each line of an open polygon is described by Plücker coordinates. The direction of each line is either from left to right or vice versa consistently. We can employ Eq.(24) to determine the angle between lines. For the planar case, two lines are required to specify $\mathcal{T}$-sp. We can obtain these two lines from:

$$\ell_{ij} = \left\{ \ell_i, \ell_j \mid \left(|\beta_{ij}| \geq |\beta_{mn}|\right) \vee \left(|\beta_{ij}| \leq \pi\right) \right\}, \qquad (27)$$
$$i, j, m, n = 1, \ldots, k \text{ and}$$
$$i \neq j, \quad m \neq n.$$

where k is number of sides. $\mathcal{T}$-sp is bounded by - ℓ_i and ℓ_j.

An example is shown in Fig. 10 . The direction of each line is assigned arbitrarily from left to right. We find that $i = 1$ and $j = 6$. $\mathcal{T}$-sp is then bounded by - ℓ_1 and ℓ_6. If we assign the direction from right to left, $\mathcal{T}$-sp will be bounded by - ℓ_6 and ℓ_1. The origin of $\mathcal{T}$-sp is point o. Note that point o can be anywhere in space.

This algorithm is robust globally where the geometry of the mating surfaces is a combination of concave and convex segments. Two lines, similar to- ℓ_6 and ℓ_1 are selected to determine $\mathcal{T}$-sp. When β is more than π, $\mathcal{T}$-sp does not exist.

5. CYLINDROID OF $\mathcal{R}$-sp AND $\mathcal{T}$-sp

Fig 11 show $\mathcal{R}(+)$ and $\mathcal{T}$-sp for the part in Fig 6. The boundary of $\mathcal{R}(+)$ is bounded by the first two essential wrenches (Eq. 25). The vectors which are perpendicular to these wrenches are the boundary of $\mathcal{T}$-sp. Both $\mathcal{R}(+)$ and $\mathcal{T}$-sp are considered a "two-system" of twists with minimum (0) and maximum(∞) pitches respectively. They are orthogonal to each other and to the axis of a cylindroid. In the case of disassembly in the (+) direction, the repelling system yields multi solutions in terms of $\mathcal{R}(+)$ and $\mathcal{T}$-sp. All axes of the cylindroid which represent these spaces are in a plane, as shown in Fig. 11. The cylindroid will not exist, if $\mathcal{R}(+)$ is a closed area. In this case, translation(twist with a maximum pitch) is not possible. We can extend this result by adding thickness to the assembled part. The extended model should not be considered as fully three-dimensional one since the geometry of the parts and its

mating surface does not vary in the direction of thickness. We prefer to call it an extruded two-dimensional problem. The part is constrained in the opposite direction of the extrusion. Its $\mathcal{T}$-sp reduces to a line which points towards the direction of extrusion. $\mathcal{R}(+)$ becomes a rectangular wedge with the thickness d (See Fig. 12). d is the width of the top-surface of the mating part. The axes of its cylindroid still lie in a plane.

In the full three dimensional case, such axes exist in space, forming a hypersurface corresponding to variations of pitch $[0, \infty]$ of the resulting twists.

6. THREE DIMENSIONAL $\mathcal{SR}$-Sp AND $\mathcal{ST}$-sp

In sections 2 - 5, we showed how to determine and represent $\mathcal{R}$-sp and $\mathcal{T}$-sp in two dimensions. In this section, we describe an approach to represent relative freedom in assembly and disassembly of a polyhedron in its socket, both in terms of rotational space ($\mathcal{SR}$-sp) and its translational space ($\mathcal{ST}$-sp). The approach uses geometric information from the part itself as well as knowledge of $\mathcal{R}$-sp and $\mathcal{T}$-sp. No new information is required.

We begin with a simple solid model. Fig 13 shows a rectangular block with chamfer sitting in its corresponding socket. The homogeneity and boundedness of the model are assumed. Within these assumptions, a two-dimensional closed polygon is obtained by parallel slices of a cutting plane through the solid model. A closed polygon always exists regardless the orientation (θ, ϕ, ψ) of the cutting plane in the newtonian space(E^3). To illustrate, the cutting plane x'x' is placed parallel to the x-axis of the reference frame. We perform the algorithm in section 3 to obtain $\mathcal{R}(+)$ and $\mathcal{R}(-)$ of each sliced polygon. The direction of the rotational axis is perpendicular and points out from $\mathcal{R}(+)$ and vice versa for $\mathcal{R}(-)$. These $\mathcal{R}(+)$s and $\mathcal{R}(-)$s are multiplied by the equivalent width of the solid model to form the volume of rotational centers. The equivalent width is defined as a line parallel to the rotational axis, measured between boundary of the solid model. Intersection of these volumes yields the space for rotational center, $\mathcal{SR}(\bullet)$. Note that if there exists an $\mathcal{R}(\bullet)$ at infinity (pure translation), the result of the intersection will be at infinity:

$$\mathcal{SR}(+) = \widehat{\mathcal{R}}_i(+) \cdot \ell_k \qquad (28),$$

$$\mathcal{SR}(-) = \widehat{\mathcal{R}}_j(-) \cdot \ell_m \qquad (29)$$

where $\widehat{\mathcal{R}}_i(+)$ and $\widehat{\mathcal{R}}_j(-)$ are the intersecting cross sectional area among the sliced $\mathcal{R}(+)$s and $\mathcal{R}(-)$s respectively. ℓ_m and ℓ_n are the equivalent widths. Both of them lie in the plane orthogonal to the cutting plane.

A given rotational axis for the body must be placed within $\mathcal{SR}(\bullet)$, perpendicular to the cutting plane, where the body is rotated to form the rotational space($\mathcal{SR}$-sp) in the given direction.

It is also possible to perform the operations expressed in Eq.(28) and Eq.(29) for any direction of cutting plane. For simplicity, the y'y' cutting plane is placed perpendicularly to the x'x' cutting plane. Both cutting planes intersect at the corners of the solid model. For example, point O at the top left corner is a projection of the line formed by intersecting of two $\widehat{\mathcal{R}}(\cdot)$ s as a result of slice cutting at point O by two planes. The new space for rotational centers, bounded by the $\widehat{\mathcal{R}}(\cdot)$ s, is formed by a linear combination of them:

$$\widetilde{\mathcal{SR}}(\cdot) = \sum_{k=1}^{m} C_k \, \widehat{\mathcal{R}}_k(\cdot) \qquad (30)$$

$$C_k \neq 0$$

In this example, m is 2. $\widetilde{\mathcal{SR}}(\cdot)$, the new space for rotational centers, can be found at every corner of the solid model. In $\widetilde{\mathcal{SR}}(\cdot)$, there exists infinite rotational axes which lie between those of $\widehat{\mathcal{R}}(\cdot)$ s. This can be seen since the cutting plane is constrained to pass through the line at O. The degree of freedom of rotational centers reduces to three. If the rotational center is located in $\widetilde{\mathcal{SR}}(\cdot)$, the rotational axis is realizable by the following two criteria: (a) the rotational axis contains the rotational point, and (b) the line perpendicular to the axis at the rotational point, must pass through space of the solid model. Note that the space for rotational centers of the overall solid model is not continuous in the case of polygons, as demonstrated by Fig. 13. However, if the number of sides of a polygon approaches infinity, the solid representation of this polygon appears to be a smooth and closed curve. In this case, it is possible to have continuous $\mathcal{SR}(\bullet)$.

The translational space($\mathcal{ST}$-sp), is determined after the rotational axis and $\mathcal{SR}(\bullet)$ are specified. Different sets of $\mathcal{SR}(\bullet)$ give different ($\mathcal{ST}$-sp). The procedure given in section 5, also applies in this case.

7. APPLICATION TO STABILITY ANALYSIS

In this section, we examine the stability of an object from its geometric description. The stability is classified into two types namely rotational and translational stability. We consider first an applied external force thru the c.g of the polygon, as shown in Fig. 14, with the polygon and its mating part placed on an inclined plane. Let θ be the inclination angle, so that at $\theta = 0$, an

additional wrench , $\mathcal{W}_{grav,}$ due to the weight of the assembled part, points vertically downward. Applying the procedure developed in the previous section, we find the new $\widehat{\mathcal{R}}_i(+)$ and $\widehat{\mathcal{R}}_i(-)$ to be the null set. This means that the assembled parts are in a stable configuration where no rotational motion can be assumed. Once we increase the inclination angle (or the angle $\mathcal{W}_{grav}$ makes with the vertical) in either a positive or negative direction, $\mathcal{W}_{grav}$ will intersect the original $\widehat{\mathcal{R}}_i(+)$ and $\widehat{\mathcal{R}}_i(-)$ of Fig. 9, defining a new non-null $\widehat{\mathcal{R}}_i(+)$ and $\widehat{\mathcal{R}}_i(-)$, as in Fig. 14. The assembly has entered a geometrical instability at this point. When the magnitude of $\mathcal{W}_{grav}$ is positive, the polygon can disassemble itself.

Given a geometric model, one may compute values of θ for which the assembled parts are at the onset of the gravitational instability as follows: connect the c.g. point to each intersection point with construction-lines. Let α and γ be the angles each wrench and each construction-line makes with the vertical, respectively. Angles α and γ, as shown in Fig. 14, are found directly from their Plücker coordinate representation. Select the minimum and maximum angle among α and γ to denote the limit of rotational stability ($\theta_{\mathcal{R}(\cdot)}$) for positive and negative direction respectively:

$$\theta_{\mathcal{R}(+)} = \mathcal{M}in(\alpha_m, \gamma_n) \quad (31),$$

$$\theta_{\mathcal{R}(-)} = \mathcal{M}ax(\alpha_m, \gamma_n) \quad (32)$$

m : number of wrenches
n : number of intersection points

Note that by representing $\mathcal{W}_{grav}$ in Plücker coordinates with trigonometric functions [sin(θ), cos(θ)] , the same result expressed by Eq.(31) and Eq.(32) is obtained.

For translational stability, ($\theta_{\mathcal{T}(\cdot)}$), we define λ the angle which each side of $\mathcal{T}$-sp makes with the - x and +x axis for + θ and - θ respectively:

$$\theta_{\mathcal{T}(+)} = \mathcal{M}in(\theta' + \lambda_\epsilon) \quad (33),$$

$$\theta_{\mathcal{T}(-)} = \mathcal{M}ax(\theta' + \lambda_\epsilon) \quad (34),$$

where $\theta' = sgn(\theta)\,|\tan^{-1}\mu|$, and
where μ is the surface coefficient of friction.

It is easy to extend this approach to arbitrary applied forces to determine the stability, for example, of assemblies connected by springs, or to compute disassembly forces by external mechanisms.

8. CONCLUSION

In this paper, we present a method to determine $\mathcal{R}$-sp and $\mathcal{T}$-sp of polygonal objects under multi-contact constraints. This method is based on information from geometric models. Our main contribution is that the proposed algorithm can detect and assign essential wrenches in the screw system and hence, a minimum number of constraints is used in the computation. The method can be attached to any current solid modelling package, as a subroutine to automatically compute the relative freedom of assembled parts. The assembly/disassembly space is thereby obtained efficiently. The result of our study also leads to the determination of stability of assembled parts due to external forces.

9. FUTURE WORK

Application to motion analysis in two dimensions: A shaft and its hole can be modelled as closed polygons, similar to Fig. 6. With given tolerances between the shaft and its hole, we want to find finite motions of the polygonal shaft. The method proposed in this paper would be extended to cover multi $\mathcal{R}$-sp and $\mathcal{T}$-sp as the shaft moves.

REFERENCES

[1] T. Yoshikawa et. al., "Assembly Planning Operation Strategies Based on the Degree of Constraint", Proceeding of 1991 IEEE/ESJ International Workshop on Intelligent Robots and Systems, (1991)

[2] S. Hirai, "Analysis and Planning of manipulation Using the Theory of Polyhedral Convex Cones", Ph.D Thesis, Kyoto University, (1991)

[3] D. Whitney and T. DeFazio, "Simplified Generation of All Mechanical Sequences", IEEE Journal of Robotics and Automation, Vol. RA-3, No. 6, (1987)

[4] M. Erdmann, "Using Backprojection for Fine Motion Planning with Uncertainty", International Journal of Robotics Research, Vol. 5, No. 1, (1986)

[5] M. S. Ohwovoriole and B. Roth, "An Extension of Screw Theory", Journal of Mechanical Design, Vol. 103, (1981)

[6] J. M. Schimmels and M. A. Peshkin, "Admittance Matrix Design for Force-Guided Assembly", IEEE Transactions on Robotics and Automation, Vol. 8, No.2, (1992)

[7] R. S. Mattikalli and P. K. Khosla, "Analysis of Restraints to Translational and Rotational Motion from the Geometry of Contact", 1991 ASME Winter Annual Meeting, (1991)

[8] R.H Wilson, "On Geometric Assembly Planning", Ph.D Thesis, Stanford University, (1992)

[9] F. Reuleaux, *"The Kinematics of Machinery"*, published by Dover, (1963)

[10] H. Asada et. al, "Kinematic Analysis of Workpart Fixturing for Flexible Assembly with Automatically Fixtures", IEEE Journal of Robotics Automation, Vol. RA-1, No.2, (1985)

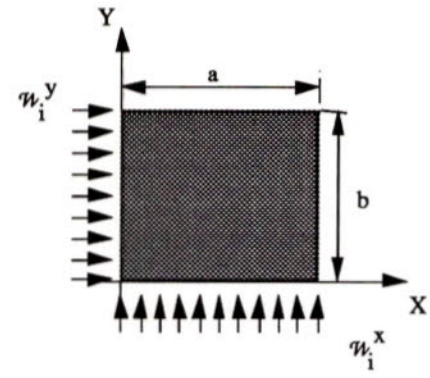

Fig. 3 Force distribution of line-line contacts

FIGURES

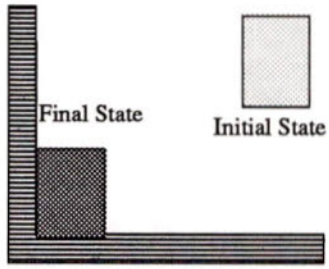

Fig. 1 A rectangle at a corner

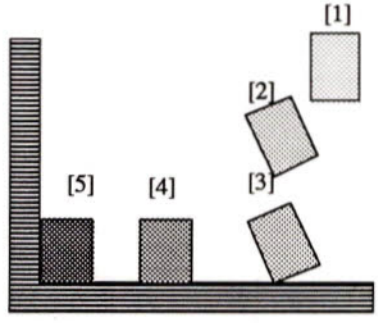

Fig. 2 One possible assembly procedure

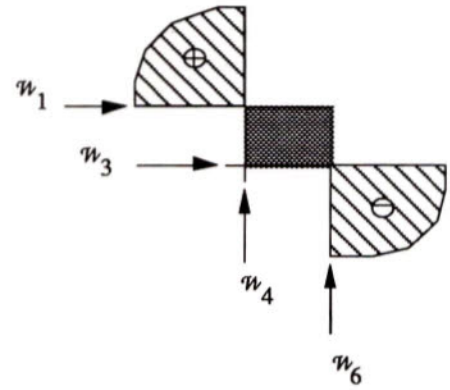

Fig. 4 The region of rotational centers, $\mathcal{R}$

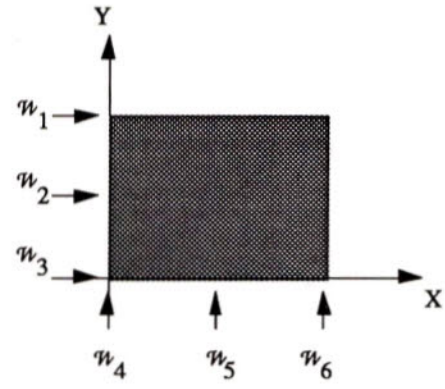

Fig. 5 Parallel wrenches

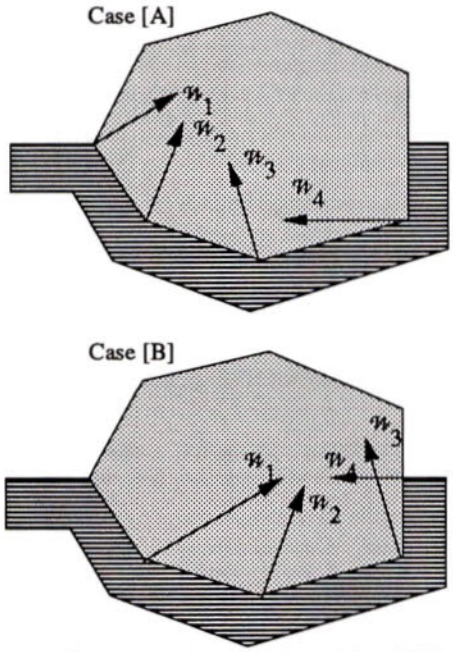

Fig. 6 Equivalent wrenches:[A] for $\mathcal{R}(+)$ and [B] for $\mathcal{R}(-)$

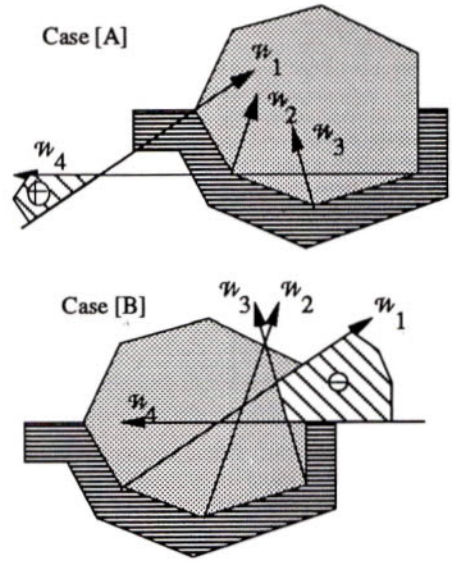

Fig. 9 $\mathcal{R}(+)$ and $\mathcal{R}(-)$ of Fig. 7

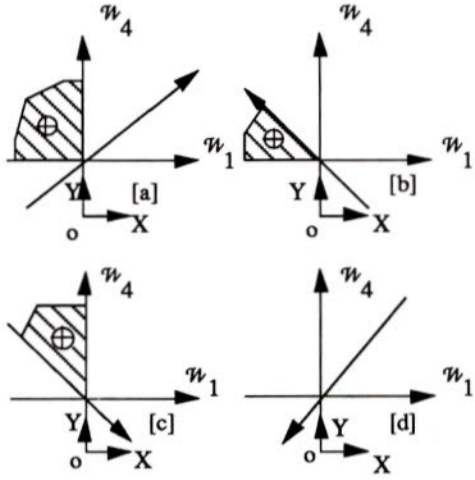

Fig. 7 Three wrench system cases

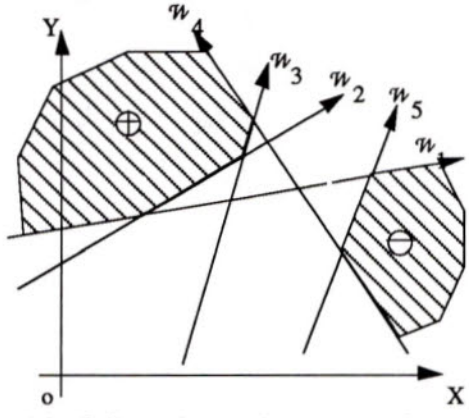

Fig. 8 General case of many wrenches

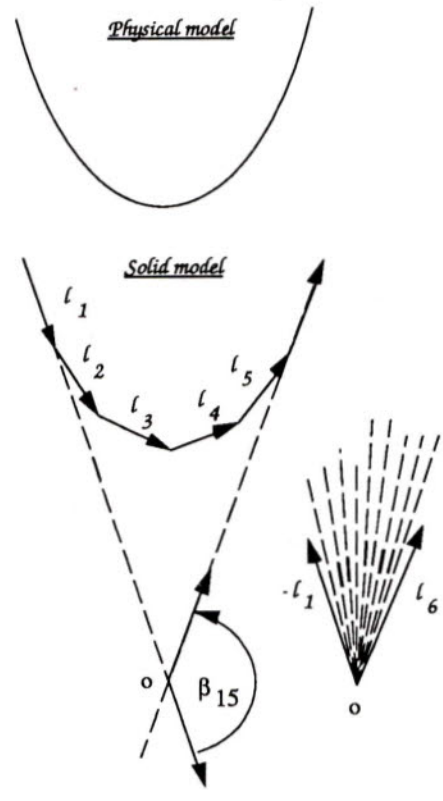

Fig. 10 Solid Model of a curvature and its $\mathcal{T}$-*sp*

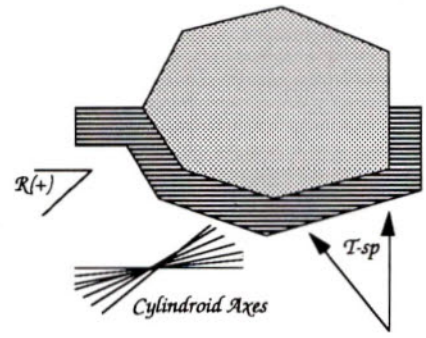

Fig. 11 Cylindroid of $\mathcal{R}(+)$ and $\mathcal{T}$-sp for the assembled part in Fig.6

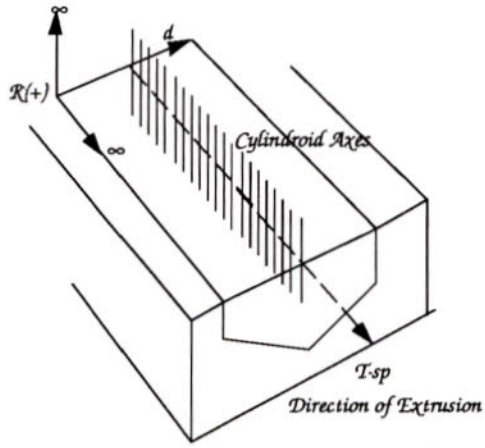

Fig. 12 Extrusion case

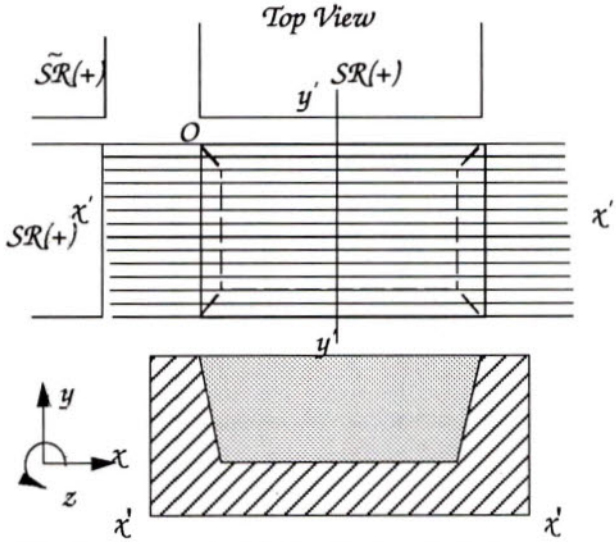

Fig. 13 Rectangular block with chamfer in its socket

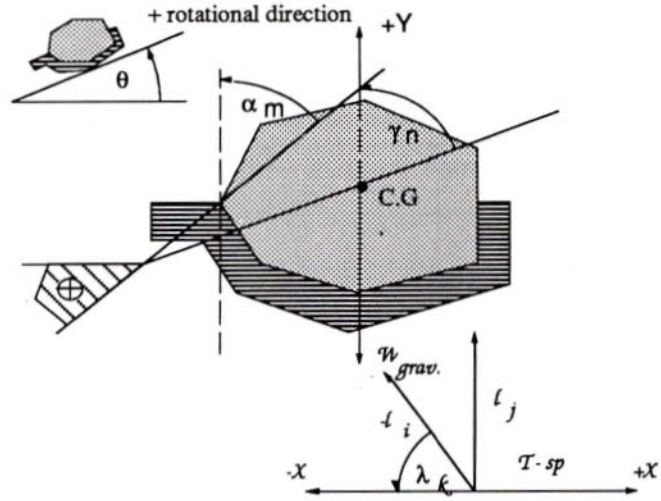

Fig. 14 Stability of assembled parts

FLEXIBLE, TENDON-CONTROLLED DEVICE FOR ENDOSCOPY

Schitt LAOWATTANA

Department of Mechanical Engineering
Carnegie Mellon University
Pittsburgh, PA 15213

Abstract

The high levels of skill required to maneuver present-day, flexible endoscopes which are utilized in esophagoscopy and colonoscopy have prompted us to propose a new class of safer, more easily controlled devices. These devices are based on the familiar bead chain with internal control cables. The study of the physics associated with the flexible control devices is carried out with respect to the design parameters of both the practical system and its environment. The suitable geometries for locking such mechanism are presented herein. We introduce the "Slide Motion" scheme which provides a smooth movement of the endoscope stem with only three continuously controlled degrees of freedom. Such movement is accomplished by implementing a series of relative motions between an outer tube and intermittently stiff spines inside. The strength and stability of the locking mechanism, which exhibits the property of intermittent stiffness, is also discussed.

1. Introduction

Endoscopes have been playing a significant role in reducing invasive surgery for a large number of patients. The field of endoscopy is evolving rapidly. More sophisticated endoscopes with higher performance are being developed and introduced every year. Presently, there are five basic types of endoscopes[1]: conventional structure, rod lens telescope, gradient optic, fiber optic and microchip sensor. The conventional structure is based on the telescopes used for astronomy; by adding a distal prism at the tip, the user can vary the field of view. An object lens and a relay lens form a real inverted image for endoscopists. The rod lens telescope yields better resolution and light transmission through a series of glass rods interspersed with spaces filled with air. External reflection and chromatic aberration are reduced by using a blooming and a flint glass. For very small target areas, the gradient optic can be used since it consists of a single glass element with different refractive indices. However, it has poor light transmission as well as some limitations in viewing angle (45°-60°).

Each of these three endoscopes have a rigid structure, limiting their length of operation. To obtain longer lengths of operation particularly for esophagoscopy and colonoscopy, more flexible endoscopes, such as the fiber optic type, are required. In this type, refraction in a fiber bundle transmits light from a light source to the target area. Images are transmitted back through another fiber bundle which is arranged in a coherent or parallel manner. In the microchip sensor endoscope, another flexible type, the optical elements are completely replaced by microchip sensors and electronic wiring. With adequate light from a non-coherent fiber optic bundle, video images are created for storage as well as for viewing in diagnosis through a monitor. Such a viewing system is called an indirect video system, which has 25% less resolution as compared to a direct video system. However, comparative studies show that flexible endoscopes detect an average of three times as many polyps and cancers than rigid endoscopes.

Although the fiber optic and microchip sensors are more flexible than the previous three, their stems (made of long rubber or plastic tubes) are still positionally uncontrollable over most of their lengths. Figure 1 shows a diagram of the human colon. The colon is comprised of a set of labyrinthine and reverse bends. There are five major parts: the rectum, sigmoid, descending, transverse and ascending colon. The smallest radius of curvature is about 2 to 3 cm, located at the bending portion between the rectum and the sigmoid colon. The transverse colon, 40 to 50 cm long, is the largest and the most mobile part of the colon. Its extends between the right and left colic flexures, forming a loop which is directed downward and forward. Since the transverse colon is suspended posteriorly by the soft living tissue, called the transverse mesocolon, its movements are always affected by the breathing process and other movements in the intestine cavity. Use of a colonoscope is impeded by the presence of peristaltic action of the gut which is continuously attempting to expel the device. Involuntary motions of the gut create difficulties in acquiring a target and in using the array of diagnostic/therapeutic tools which are deployed through a channel in the stem. The gut may also cramp, thus

trapping the device inside the colon. High mechanical flexibility is required for the endoscope to traverse the colon without creating potentially damaging interacting forces. However, this very compliance required in the stem makes maneuvering the endoscope around the bends of the colon extremely difficult. So called "α loops" are often created by the endoscopist to help advance the stem at the reverse bends (e.g., at the sigmoid/descending colon and the descending/traverse colon junctions). Twisting and retracting the stem is required for making such loops. Hence, high interacting forces between the endoscope and the wall of the colon is inevitable. Steering systems at the tip of the endoscope provide two directional controls (up/down and left/right) which are manually operated through two concentric knobs. This manual procedure, which bears no particular relation to the resulting motions, can potentially damage the surrounding tissue. The successful operation and manipulation of these medical devices requires great proficiency as well as a great deal of time. These skills have obviously been mastered by endoscopists all over the world. However, the length of endoscopes is still limited to about 1 meter, which leaves 80% of digestive tract unexplored regardless of which end is entered.

2. Major Objectives for a New Endoscope

As pointed out above, there are many difficulties in operating present endoscopes, which may result in discomfort or risk to the patient. To simplify the endoscopic procedure, we propose a safer, more precisely controllable device. The major objectives of the new device are:

(1) The motion of the endoscope stem must be smooth and should match the labyrinthine paths of the colon. Hence, a highly flexible stem is required.

(2) Integrated with suitable control systems, the endoscope stem is required to minimize the interacting force with the wall of the colon.

Most of the current research on endoscopes is directed toward the enhancement of vision systems and on acquiring wider tip angles. Unfortunately, the fundamental problem of steadily predictable motion has not been completely resolved. This paper focuses on our approach to this problem: a flexible tendon bead chain, which forms a semi-passively controllable spine.

3. Advanced Approaches for Stem Control

For better insertion and retraction, the stem could be actively controllable. The stem would consist of a number of serial rotational joints with a prismatic joint at its base. With the specified positions and orientations of these joints, the stem would traverse the colon easily, avoiding extensive contact with the surrounding tissue. This could be done through the mapping or shifting method which has been implemented in redundant manipulators, by transferring tip trajectories to the following joint and consecutively to the rest of the joints. Tip trajectories would be generated in real time through a manual or automatic steering system which points the tip in the desired direction. While advancing the stem, the succeeding joint then moves toward the position and orientation of the preceding joint in the previous step. This steering strategy is called "*Snake Motion*." We will describe briefly three applications of this approach. The redundant degrees of freedom in snake robots (e.g., Toshiba snake robots [2]-[5]) have been used for obstacle avoidance. Hence, the reachable working space, which may be highly cluttered, could be accessed by their end effectors. However, some of the disadvantages associated with these robots include requiring more, continuous degrees of freedom and operating at slower speeds. Tracking the position and velocity trajectory as well as the position and orientation of the snake tip and stem are computed relative to the joint displacement and the rate of the prismatic joint. Such computations are not trivial, and its difficulty depends upon the current configuration of the snake stem. Trajectory planning also requires a well-modeled environment. Furthermore, miniaturization of the overall system to realize an application in endoscopes is difficult to achieve.

In the Snake Motion scheme, a number of small actuators installed at each joint perform the mapping operation. The complexity of the mechanical arrangements for these mini-actuators and the computation of the mapping operation increase exponentially with the length of the stem for most practical applications. Algorithms employed in planning the trajectory which are based on psudo-inverse Jacobians[6] is proportional to n^3, where n is the number of degrees of freedom. A model of an active endoscope stem utilizing the Snake Motion has been demonstrated using a shape memory alloy (SMA) servo actuator system[7]. SMA[8] is an alloy that can be stretched or deformed rapidly by changing its temperature. The stem of this prototype endoscope consists of five 2-D rotational joints, each of which is 13 mm in diameter and 40 mm in length. These joints are driven by a pair of antagonistic wires of Ti-Ni, a stable type of SMA, through an electrical resistance feedback control system. Changing resistances due to the SMA wire deformation is not completely reversible. This hysteresis between the forward and backward paths is approximately 10%; therefore, position control is inaccurate. Moreover, the speed of advancing and retracting the device is limited by the heating and cooling rates of the SMA. The time, t, which a SMA wire takes

to heat to a temperature, T, above the ambient temperature, T_a, is given by the expression:

$$t = \beta \ln \left[1 - \frac{(T-T_a)}{T_0}\right]^{-1} \quad (1)$$

Where T_0 :Maximum temperature to which the SMA wire would reach when heated by current

β :Time constant = $K\phi^n$

ϕ :Wire diameter

K,n :Function terms depending on which types of alloy are used to make such a SMA wire

The dominant parameters in Eq. (1) for determining the speed of deformation is the time constant, β. For example, a 0.25 mm Ni-Ti wire with 22 N lifting capacity has a β of 3.15. A cluster of smaller wires of the same type and lifting capacity will deform faster than a single wire. However, a larger cross section would be required for such a cluster. Wire spacing, another crucial factor, must be properly allocated in order for an air flow system to remove heat from the wires efficiently. Hence, the trade off between overall size of the SMA actuator system and the deformation time should be carefully considered.

Another type of snake robot called the "ORM"[9] (the Norwegian word for a snake) was developed for the Stanford Artificial Intelligence Project. The positional control of each joint is binary, providing only two states: θ_0 or $-\theta_0$, where θ_0 is a constant. In case of n links, there would be 2^n possible configurations. Consequently, the tip could be placed at 2^n points. Sufficient links are required for the robot to place its tip close to any arbitrary point within its working space. Such a robot would have a high level of difficulty in traversing inside a small, highly labyrinthine and reverse path like the human colon.

One of the more important problems with utilizing the Snake Motion scheme in endoscopy is that the snake tip must glide through the environment while also ensuring that the stem will duplicate the trajectory of the tip. Moreover, the changes in the gut that occur over time must be accommodated for, but there is only a limited knowledge of these changes.

To eliminate the difficulties and limitations found in such Snake Motion schemes, we propose a simpler, semi-passive approach which we call "*Slide Motion.*"

4. Slide Motion Scheme

In this scheme, the stem consists essentially of two major parts: one or two *spines* and an endoscope *conduit*, which is a covering tube for the spine. Using control methods which will be described shortly, the spine can be made temporarily flexible or stiff. The endoscope conduit is an elastomer tube and has a specified degree of passive stiffness so that it can be pushed forward over the stiffened spine without buckling. This outer tube is also radially stiff in order to maintain its circular cross section during bending. A lubricant is supplied at the contacting layer between the spine and the flexible conduit so that the relative sliding motion between them can be realized while minimizing the thrust forces. The distal end is flexed by the endoscopist to observe and point in the desired directions. A typical steering system is driven by two pairs of cables through a series of bent washers. Such a system provides four directions of steering (i.e., up/down and left/right) as shown in Figure 3. However, experienced endoscopists often steer the distal end just in one plane (up/down or left/right) while rotating the endoscope stem to obtain the other degree of freedom. This degree of freedom is considered to be plane redundant, but it aids in achieving the circular steering space more easily. Figure 2 shows a cross section of an endoscope with one spine for controlling the stiffness. In its initial position, the spine is advanced to its maximum limit (about 5 cm) and made rigid. The conduit is then inserted into the colon up to the first substantial curve. While the spine is sufficiently stiff, the flexible conduit moves incrementally relative to the spine, within the predetermined axial travel limits, using the spine as a guide. The flexible conduit is inserted further at the same forward rate that the spine is retracted; thus, the spine is relatively stationary with respect to the patient's gut. The total forward insertion distance of the endoscope is equal to the spine axial travel limits. Such limits would be adjusted to meet the specific requirements for the radius of curvature at each bend of the colon. From Figure 1, the four bends are located at the connections between rectum, sigmoid, descending, transverse and ascending colon. In most patients, the actual configuration of the colon is not completely guaranteed *a priori*. Reverse bends with angles exceeding 360° are found in some patients who have congenital abnormalities.

When the incremental forward motion of the flexible conduit is complete, the spine is relaxed and is pushed forward to its maximum limit. The maximum limit can be obtained because the conduit assumes the shape of the colon through gentle static contact. These motionless contacts form intermittent position constraints which serves as a guide for the relaxed spine. Reaction forces from the gut walls direct toward the center line of the gut, which aid the motion of the spine

inside. The spine is advanced to its maximum limit while the flexible conduit remains stationary with respect to the patient. The spine is then stiffened in its new position. Advancing the conduit and spine are now repeated cyclically; the endoscope is advanced no more than the spine axial travel limit with each cycle.

By reversing the above procedure, the endoscope can be removed from the colon while minimizing the relative motion between the endoscope and the colon. During the removal of a conventional endoscope, the relative motion is quite prominent. This contact causes stress at the curves of the colon along the length of the conduit. The situation becomes worse if a colon wall segment arrests its normal peristaltic action and cramps around the device, resisting removal. Removing the stem against these high interacting forces will significantly increase the risk of trauma. Therefore, minimizing the relative motion and interacting forces is a major advantage.

The stiffened spine inside the flexible conduit resists the involuntary motions of the colon. Thus, the distal end of the endoscope can be positionally supported. This support provides the stable platform required for visual or therapeutic procedures in the colon. From a safety viewpoint, the spine can be relaxed immediately if peristaltic action and/or cramping is observed. Hence, critical damage to tissues is avoided. Moreover, the flexible conduit would not buckle or bend severely and would maintain a more accurate position since it is constrained by the stiffened spine. In some situations, when the stable platform is not required, the spine could be removed and replaced by other therapeutic/diagnostic devices. Such a design for multiple functions of the inside path reduces the dimension of the stem.

In some industrial and space applications, contact with the environment is not possible. For these applications, two spines could be utilized. One spine serves as a spinal cord which mechanically connects the conduit. The other movable spine can then be advanced or retracted to its maximum limit by using the first spine and the case as a guide. Once the second spine has reached its maximum limit, it can be stiffened and the first spine relaxed so that the process can be repeated.

A number of possible design configurations for semi-passively controllable spines will be discussed in the next section.

5. Central Tendon Locking Spine

A central tendon locking spine consists of a set of cylindrical beads strung on a flexible cable. One of the most simple shapes is a cylindrical bead with a hemispheric head and an inverted conical tail. All beads are free to rotate on adjacent beads around their centers. In the presence of a cable tension force, these beads slide axially along the cable until the positional constraints at both ends of the bead chain are satisfied. Consequently, increasing the cable tension force creates friction forces between beads will ultimately increase the apparent stiffness of the entire bead chain. Therefore, pulling the cable stiffens the bead chain, and relaxing the cable tension force loosens it. The bead chain with a continuous cable is shown in Figure 4. While applying a tensile force to the tendon, it is highly desirable that the configuration of the bead chain is not altered, or at least that the reaction forces traverse to the beads are very small.

Frictional losses incurred from bead to bead along the chain reduces the locking strength of the joints near the tip. To improve the locking strength, the surface coefficient of friction, μ, must be as high as possible. Some materials, for example unglazed ceramics and high durometer elastomers, have values of μ approaching 1. The tensile reaction forces encountered in the above geometry preclude the use of these materials. However, it is difficult to make ceramic beads with the above geometry. An equivalent locking chain can be realized by alternating a set of spherical and cylindrical beads which are strung on a flexible cable as shown in Figure 5. These two parts are both axially and end-to-end symmetric. A suitable combination of materials can provide a higher surface coefficient of friction than any single material; for example, a surface coefficient of friction between aluminum and ceramics would be almost 0.5, where it would be 0.2 for aluminum alone.

6. Bead Geometries and Physics of Flexible Bead Chains

In this section, we will examine how bead design affects spine performance requirements which include spine curvatures, diameter, stiffness and stability. As indicated in Figure 6, the effective minimum radius of curvature, R, for the bead chain is the distance from the center of curvature to one side (not the center line). R depends on the rotational displacements available at each joint and the effective bead length, L. The locking strength is also dependent on the geometry and the friction coefficient.

For performance consistency and ease of manufacture, the bead geometry in Figure 4 is selected to be as simple as possible. Standard part shapes with conventional linear and/or circular profiles are desired. Recall that a pull on the tendon should result in locking the chain into position without causing it to move.

Assume that L is the effective length of each bead and that θ is the maximum joint angle at each bead interface. As shown in Figure 6, the minimum bend

radius R, is determined by

$$R = L/2 \cdot \tan(\theta/2). \quad (2)$$

To advance the stem at the reverse bend between the rectum and the sigmoid colon, R must be about 2 cm. L and θ then determine the number of beads, N, at each bend. For example, if the same R and larger L and θ are selected, N will then be reduced. The selection of parameters affects how closely the bead chain can approximate a circular arc, which is a significant factor affecting the clearance between the inside diameter of the endoscope and the bead chain.

A cylindrical bead with a hemispheric head, referred to simply as a Cylindrical Geometry (shown in Figure 7), is bored conically at the tail with a half-angle called "leg angle," θ_L. In order for the bead leg to sit perfectly on the adjacent bead at the maximum rotation, the leg angle must be equal to θ. If the inside and outside diameters (ID and OD, respectively) are large enough, some diagnostic/therapeutic tools could be placed *inside* the bead chain. To prevent interference between such tools and the tendon cables, two cables can be placed *outside* the bead chain. This configuration will be discussed in Section 8.

In case of a single cable, all beads are strung on a flexible cable which is fixed to the bead located at the tip. Analysis of the motion of any pair of beads shows that pulling the inside cable with a tension force, F, will cause one bead to rotate onto the other, resulting in a positive displacement of the cable. This displacement, d, can be calculated as a change in length a-b of Figure 7. The rotational angle, α, varies between 0 and θ_L and can be divided equally among n sub-intervals for the purposes of analysis. Hence,

$$\Delta\alpha = \theta/n \quad \text{(a constant step size)}$$

Cable work for each pair of beads can be obtained as

$$\text{Cable Work}_i(\alpha) = F \cdot \Delta d_i(\alpha) \quad i = 0,..,n \quad (3)$$

where displacement $\Delta d_i(\alpha)$ occurs at α_i for small Δα.

The clockwise torque, $\tau_i(\alpha)$, at each step size (Δα) provides the cable work for a positive displacement as shown in Figure 7:

$$\tau_i(\alpha) = \text{Cable work}_i(\alpha)/\Delta\alpha \quad (4)$$

Cable displacements will not occur if the torque in Eq. (4) does not exceed the threshold torque due to surface friction, such that

$$\text{Resisting Torque}_i(\alpha) = k \cdot \mu_i(\alpha) \cdot F, \quad (5)$$

where k is a geometrical constant which is a function of θ_L,

$$k = \pi.(1 + \cot^2\theta_L)/4,$$

and $\mu_i(\alpha)$ is the static surface coefficient of friction required for locking two beads together at position i.

We equate Eq. (4) and Eq. (5) to obtain the threshold friction coefficient which will just lock the beads together:

$$\mu_i(\alpha) = (1/k)\Delta d_i(\alpha)/\Delta\alpha_i \quad (6)$$

as $n \longrightarrow \infty$

$$\delta d_i(\alpha)/\delta\alpha_i = k.\mu_i(\alpha) \quad (7)$$

Let μ_s be the surface coefficient of friction between the selected materials. The locking position between two beads can then be obtained as a set of angles:

$$\{ \bigcup_{i=1}^{n} \alpha_i \mid \mu_i(\alpha) < \mu_s \} \quad (8)$$

We will see that this set will vary with geometry and material properties. For example, Table 1 shows the computation of $\mu_i(\alpha)$ for a leg angle of 30° and selected values of radius of curvatures, outside diameters and clearance are as follows:

Radius of curvature:	38.10, 25.40, 12.70 and 7.62 mm
Outside diameter :	25.40 and 6.35 mm
Clearance :	14.29 mm (OD = 25.40 mm) and 1.59 mm (OD = 6.35 mm)

The clearance, C, of Figure 7 is the effective indide diameter formed at the maximum rotational angle(α=θ). C is a functionof ID, OD, θ_L,and α. The larger value of clearance makes the placement of some

diagnostic/therapeutic tools inside beads possible. The lower limit on C is restricted by the outer diameter of the cable. Notice that the clearance is always reduced for any bead angle, α. Table 1. shows maximum values of the computed $\mu_i(\alpha)$ for various cases. Case A and B are for the larger values of C. Case C, D, E and F are at the lower limit.

Table 1. $\mu_i(\alpha)$ for the Cylindrical Geometry

C_{min}	Case	R	OD	ID	L	Max. $\mu_i(\alpha)$
14.28	A	25.40	25.40	22.72	12.11	0.62
	B	38.10	25.40	22.72	18.92	0.62
1.59	C	7.62	6.35	3.29	2.29	0.41
	D	12.70	6.35	3.29	5.01	0.41
	E	25.40	6.35	3.29	11.82	0.41
	F	38.10	6.35	3.29	18.62	0.41

Where C_{min} :Minimum clearance, mm
Case :Case used in design analysis
R :Radius of curvature, mm
OD :Outside diameter, mm
ID :Inside diameter, mm
L :Effective length, mm

Plots of D and μ with respect to α are shown in Figure 8. Notice the strong non-linear displacement relation for large beads and the requirement for high coefficients of friction for locking.

As indicated in Figure 8(b), there are some α angles in the interval where $\mu_i(\alpha)$ exceeds, 0.2, the value for aluminum. At these positions, the bead chain cannot lock; consequently, beads having the Cylindrical Geometry are not suitable for use in flexible/stiff spines. In addition, for any $\mu_i(\alpha)$ curve which is not continuous (as depicted in Figure 8(b)), it is impossible to predict the direction of the bead's motion or the resulting chain configuration for certain initial angles (usually between 20° to 30°) when the spine is stiffened.

To improve the locking ability over the entire rotational range, the geometry can be varied to reduce the turning moment. This can be achieved by removing the material from the point where the cable bends from the spherical center. The cable can also be closer to the center line by reducing the inside diameter.

The conical bore aligned with the inside diameter (ID-based) is shown in Figure 9. The conical bore at the head rather than the center of its spherical surface such that its apparent opening is always greater than or equal to the ID of the mating bead. This geometry maximizes the bore throughout the chain. The contact point at α=0°, g, on the spherical surface is determined by θ_L and the bead OD, as shown in Figure 9. t is the actual thickness of the bead wall. To maintain the normal sphere to core contact between the beads, the apparent diameter of the conical bore on the spherical surface must be smaller than the circle described on the core of its mating bead. Thus, the ID of the beads is constrained to be:

$$ID < OD - 2t_m. \quad (9)$$

t_m is the minimum value of the bead wall thickness such that the ID-based Geometry could be realized. By the geometry in Figure 9:

$$t_m = OD.\sin^2\theta_L/2. \quad (10)$$

Figure 10 shows a plot of D and μ versus α of the ID-based Geometry. Parameters used for these calculations, using Eq. (3) - Eq. (7) above, are given in Table 2 .

Table 2. $\mu_i(\alpha)$ for the ID-based Geometry

C_{min}	Case	R	OD	ID	L	Max. $\mu_i(\alpha)$
14.28	A	25.40	ID-based G. cannot be used*			
	B	38.10	ID-based G. cannot be used*			
1.58	C	7.62	6.35	1.69	0.90	0.21
	D	12.70	6.35	1.69	3.62	0.21
	E	25.40	6.35	1.69	10.43	0.21
	F	38.10	6.35	1.69	17.24	0.21

*The condition, $\delta \leq \theta_L$ must be satisfied in order to make the ID-based Geometry. *Please see text.

From Table 2, ID-based Geometry for the large beads cannot be used since Eq. (8) is not satisfied. Figure 10 shows the plot of friction coefficients versus α does not vary. Changing the radius of curvature, R, effects only the effective length, L. There is no relationship between L and the characteristics of the displacement in ID-based Geometry. Moreover, the friction coefficients are almost constant in the region $0 \leq \alpha \leq \theta$.

Smaller beads with such a geometry have also been examined. The results are shown in the Table 3 and Figure 11. The small ID-based Geometry provides the lowest μ, below 0.2. The ID-based Geometries, unlike the Cylindrical Geometry, do not suffer from the problem of discontinuous curves, the bead's motion can

always be predicted. Hence, the small ID-based Geometry can be utilized for the beads in the flexible/stiff spine. Some improvements to enhance its stability will be discussed in the following section.

Table 3. $\mu_i(\alpha)$ for the small ID-based Geometry

R	Case	OD	ID	t	L	Max. $\mu_i(\alpha)$
12.70	A	6.35	0.36	2.99	6.81	0.045
	B	6.35	0.50	2.93	6.81	0.062
	C	6.35	0.61	2.87	6.81	0.076
	D	6.35	0.94	2.71	6.81	0.120
25.40	E	6.35	0.27	3.04	13.62	0.034
	F	6.35	0.42	2.97	13.62	0.053
	G	6.35	0.53	2.91	13.62	0.067
	H	6.35	0.83	2.76	13.62	0.104

7. Tendon Locking Spine Analysis

Arrangements of Spines

The tendon locking spine is constructed by placing a number of small, ID-based Geometry beads over a cable. Two possible arrangements for the single tendon locking spine are shown in Figure 12. Double spines, used where touching the environment is not desired as described in Section 4, are conceptually similar to the single tendon locking spine arrangements.

In the first arrangement, (a), of Figure 12, the locking spine and other diagnostic/ therapeutic tools lie together inside the outer tube. To allow the spine to move easily, another cover sleeve wrapped around the spine is required. The alternative arrangement separates the cover sleeve from the outer tube while maintaining a parallel mechanical connection. This design avoids mechanical interaction between the spine and the medical equipment in the stem.

Joint Strength

From Table 3, the parameter set G (R = 2.5 cm and OD = 0.6 cm) of a ID-based Geometry type is selected based on its μ and small dimensions. A practical endoscope of 1.5 m in length requires approximately 100 beads. When the beads are at relative angles other than 0, the friction at the contacting points reduces the tension force in the cable from the base to the tip of the stem. The iterative equation for computing the cable force at each joint (j) (as indicated in Figure 16) is determined, from geometry, to be:

$$F_j = F_{j-1}(1 - \mu.\tan(\theta_j/2))/(1 + \mu.\tan(\theta_j/2)) \quad (11)$$

Applying Eq. (11) to long chains shows that the cable force decreases along the bead chain. From bench tests, a cable force between two adjacent beads produces a measured turning torque within 1/2% of the predicted value. This reduction is a function of the cumulative angle between each bead and, hence, will vary with stem configuration. Figure 14 shows the predicted reduction in cable tension progressing from the base to the stem where it is flexed into the configuration of the colon shown in Figure 1.

Positional Stability

The stability of the Flexible/Stiff Spine is dependent upon the internal turning torque, which attempts to rotate the beads towards the Axis of Zero Rotational Angle ($\alpha = 0°$) because this is less than the resisting torque due to the frictional force. If the frictional force is not sufficient to prevent relative rotation, the bead will rotate to minimize α. If the bead rotation due to cable tension causes α to increase, the chain would spontaneously develop a kink, with beads alternately rotating. This condition corresponds to the lowest potential energy, which occurs as α tends to θ. As indicated by Figure 11, a positive displacement occurs as the beads are departing from the Axis of Zero Rotational Angle. The surface coefficient of friction, μ, can be expected to decrease due to wear along the contacting surfaces. The entire bead chain could, therefore, become tangled. This unstable configuration may create large displacement between the stem and the colon which obviously could potentially damage the tissue.

To improve the stability of the chain, an offset parameter, ε, is introduced to obtain a negative cable displacement (a change in line a-b) while rotating the bead from 0° to θ. This negative displacement corresponds to the lowest potential energy, which occurs as the rotation tends toward 0°. Therefore, the kinking of the bead chain could be avoided. Larger value of ε would provide a more stable margin; the practical value of ε depends upon the expected rate of wear. Figure 15 shows such an improvement for enhancing positional stability.

9. Discussion

As mentioned in Section 5, one of the limitations on the continuous cable configuration is the loss of cable tension due to the friction between the cable and the beads. To maintain the cable force at a specified level (i.e., sufficient locking strength at each joint), the continuous cable could be replaced by a series of electrical resistance wires as shown in Figure 16. These resistance wires are initially preloaded by stretching them, which causes the bead chain to be normally rigid. When an electrical current is passed through these wires, their longitudinal expansion decreases the original

interacting forces between the beads. Hence, the beads separate from each other, allowing rotational motion at the interfaces; the bead chain then becomes flexible. We are currently investigating the relationships between these parameters for practical operation.

By combining this design with the concept of the alternating bead shape sequential chain, an ideal bead chain could be realized. While stiff, the alternating sequential chain certainly increases the joint rigidity, which is due to the increase in the surface coefficient of friction between the two different materials. A small reduction in the cable force is obtained from the chain which consists of electrical wire segments. Small reductions can be controlled by adjusting the length of the wire segments. The combination of the alternating sequential chain and the electrical wire segments is highly recommended for the Flexible/Stiff Spine.

In some applications where miniaturization is not required, the joint strength and rigidity could be accomplished more easily. For example, high strength hydraulic locking devices could be employed.

In the design of the bead geometry, the most critical design constraint is the reduction of the internal turning torque due to the input work. This work, as a function of α, could be minimized by reducing the cable displacement. Moreover, the lowest potential energy must occur at $\alpha = 0°$; hence, the bead chain which is composed of large, hollow-section beads yielding positive displacements will likely not be stable.

10. Conclusion

Recently, several designs and analyze of multi-degree of freedom robots have been introduced in robotics literature. Such robots have flexible structures which could approximate the morphology and functionality of snakes. However, trajectory planning of snake robots is computationally and mechanically burdensome as the number of degrees of freedom increases. Furthermore, miniaturizing the overall system for some medical applications, as in endoscopy, is difficult to achieve.

We propose a novel semi-passive concept, called the "Slide Motion Scheme," which can produce complicated stem configuration with only a few degrees of freedom. We believe that although the Snake Motion scheme is a viable solution for applications such as obstacle avoidance, the Slide Motion scheme offers certain advantages. With the Slide Motion scheme, no massive computations for mapping positions and orientations are required, and the mechanical arrangements for the actuators are simpler.

We have seen that the ID-based Geometry represents the most advantageous bead design for implementing the Flexible/Stiff Spine, since joint strength and stability are enhanced. This scheme not only provides efficient motion control through simple hardware, but also offers the potential for greater ease of endoscopic procedures. Our on-going research seeks suitable control schemes for semi- and fully-automatic systems. A prototype for this scheme is currently under development.

References

1. Miller R.A., "Endoscopes Instrumentation Evolution, Physical Principles and Clinical Aspects," British Medical Bulletin (1986) Vol. 42, No. 3 , pp. 223-225.

2. T. Tsuchihashi et.al., "A computer Aided Manipulation System for Multijoint Inspection Robot," ICAR'85, pp. 363-369.

3. M. Obama et. al., "A Locomotive Inspection Robot Turbine Building Interior Inspection in Nuclear Power Plants," ICAR'85, pp. 355-362.

4. K. Asano et. al., "Multijoint Inspection Robot," IEEE Transactions on Industrial Electronics. Vol. IE-30, No.3, August 1983, pp. 277-281.

5. K. Asano, "Control System for a Multijoint Inspection Robot," Proceeding of the 1984 National Topical Meeting on Robotics and Remote Handling in Hostile Environments, pp. 375-382.

6. C. Klein an C. Huang, "Review of the Pseudoinverse for Control of Kinematically Redundant Manipulators, " IEEE Transactions on Systems, Man and Cybernetics, March, 1983.

7. K. Ikuta et. al., "Shape Memory Alloy Servo Actuator System with Electric Resistance Feedback and Application For Active Endoscopes," IEEE 1988, pp. 427-430.

8. Schetky L. McD, "Shape Memory Effect Alloys for Robotic Devices," Robotic Age, July 1984, pp. 13-17.

9. Pieper, D.L., "The Kinematics of Manipulators under Computer Control," Memo No. A.I. 72, Stanford University, 1968.

10. Nakano Y., Fujie M., Hosada Y., "Hitachi's Robot Hand," Robotic Age, July 1984, pp. 18-20.

11. Simon M., Kaplow., Salzman E., Freiman P., "A Vena Cava Filter Using Thermal Shape

Memory Alloy," Diagnostic Radiology, October 1977, pp. 89-94.

12. Kalpakjian Serope, "Manufacturing Process for Engineering Material," Addison Wesley, 1985.

13. Keith L. Moore, "Clinically Oriented Anatomy," Williams & Wilkins, 1980.

14. S. Sugano and I. Kato, "WABOT-2: Autonomous Robot with Dextrous Finger-Arm," IEEE International Conference in Robotics and Automation, pp. 90-97. Raleigh North Carolina, 1987.

15. J.K Salisbury and J.J Craig, "Articulated Hands: Force Control and Kinematic Issues, " International Journal of Robotics Research, Vol. 1, No. 1, Spring 1982, MIT Press.

16. S. C. Jacobsen, J. E. Wood, D. F. Knutti and K. B. Biggers, "The Utah/MIT Dextrous Hand Work in Progress," The International Journal of Robotics Research, Vol. 4, No. 3, pp. 21-50, 1984

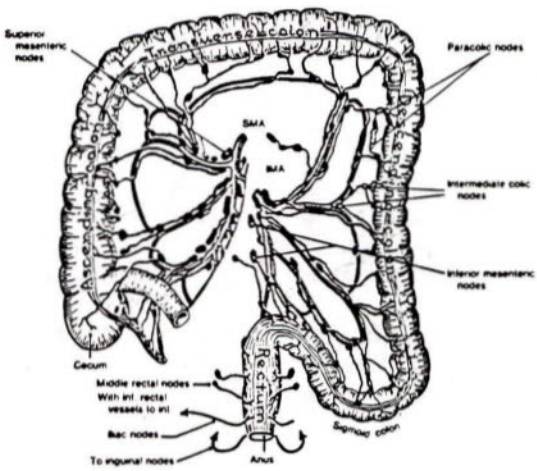

Figure 1. Diagram of Human Colon

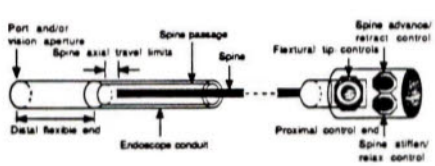

Figure 2. Cross Section of an Endoscope with Controllable Stiffness Spine

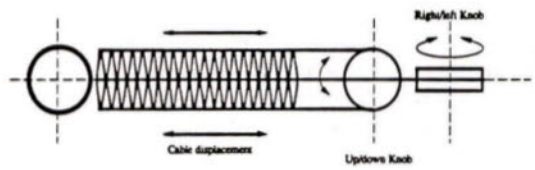

Figure 3. Tip-Steering System

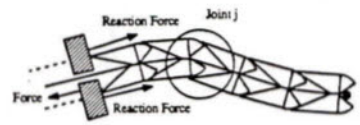

Figure 4. Bead Chain with a Continuous Cable

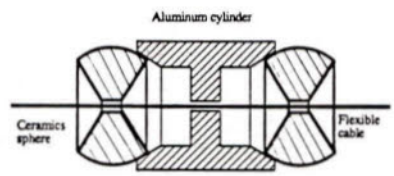

Figure 5. Alternating Bead Shape Sequential Chain

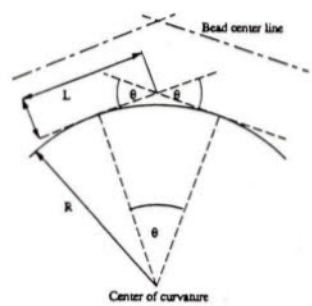

Figure 6. Minimum Radius of Curvature

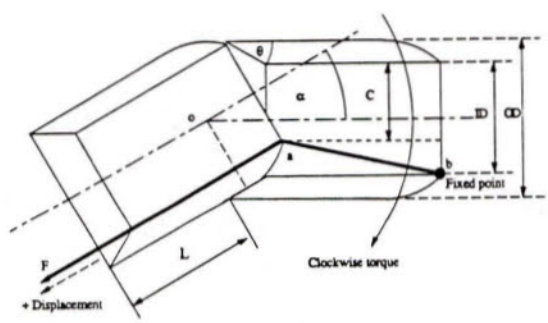

Figure 7. Cylindrical Geometry

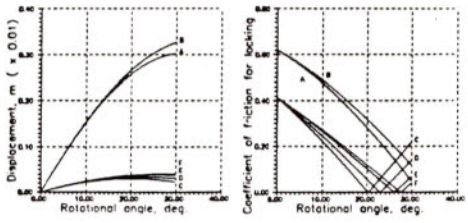

Figure 8. Plots of $D_j(\alpha)$ and $\mu_j(\alpha)$ vs. α for Cylindrical Geometry

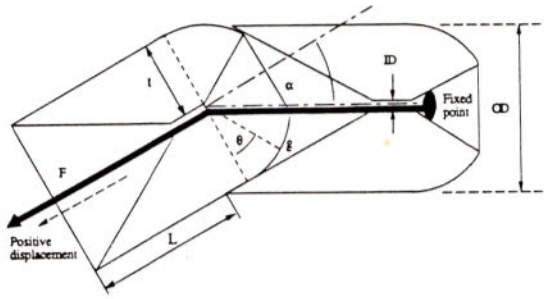

Figure 9. ID-based Geometry

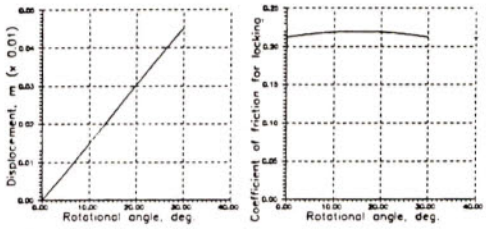

Figure 10. Plots of $D_j(\alpha)$ and $\mu_j(\alpha)$ vs α for the ID-based Geometry

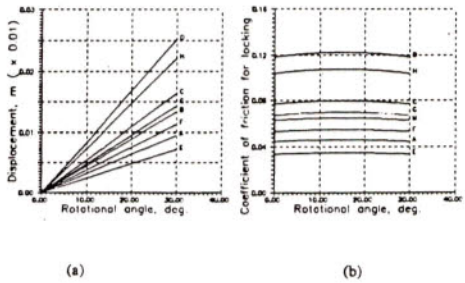

Figure 11. Plots of $D_j(\alpha)$ and $\mu_j(\alpha)$ vs α for the small ID-based Geometry

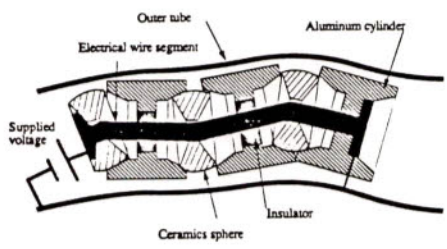

Figure 16. Beads on Electrical Wire Segments

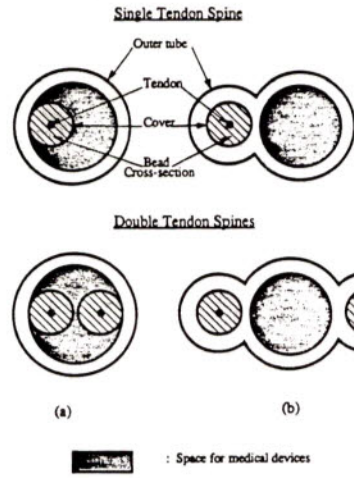

Figure 12. Two arrangements for the single and double spines

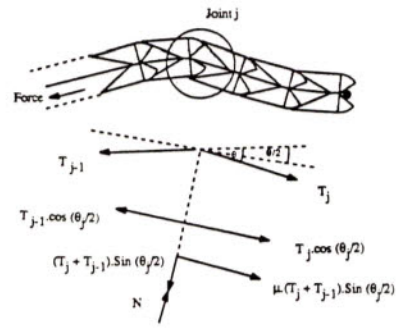

Figure 13. Diagram of force equilibrium at each joint

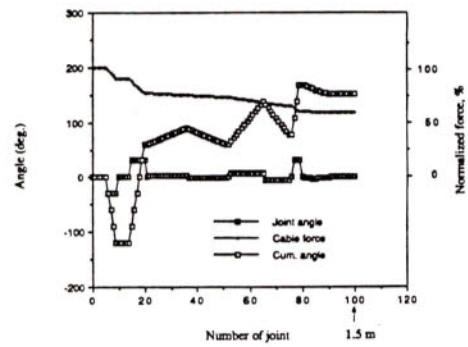

Figure 14. Plot of reduction in cable force for a stem configured as in Figure 1, approximating a normal colon.

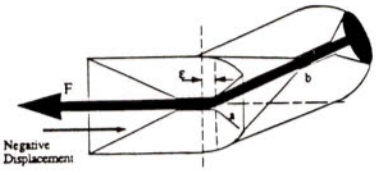

Figure 15. Stability improvement on the small ID-based Geometry

Theoretical Framework of Intelligent Adjustment (IntelAd) System

Suebsak Nanthavanij, Ph.D.
Associate Professor
Department of Industrial Engineering
Engineering (English) Program
Thammasat University
Klongluang, Patumtanee 12121

ABSTRACT

An intelligent adjustment (**IntelAd**) system is a computerized tool developed to help a computer user adjust a workstation by using ergonomic principles. Its purpose is to recommend near-optimal computer workstation settings that help the user maintain correct body posture; thus reducing the risk of developing carpal tunnel syndrome (CTS). **IntelAd** utilizes an algorithm specifically designed to position the computer user and certain hardware units (keyboard and monitor) so that the recommended body posture is obtained. From the user's standing height and sex, **IntelAd** estimates relevant measures such as seat height and depth, lengths of upper and lower arms, eye height, etc. These measures are mapped into the Cartesian coordinate system along with other reference points such as a home row of a keyboard and the center of monitor screen. The resulting set of workstation settings is then compared to ANSI/HFS Standard No. 100-1988 for computer workstations to verify the feasibility of the recommended solution. If one or more conflicts exist, **IntelAd** will search for alternate settings and suggest the best compromise. It is also capable of recommending appropriate settings for workstations with limited adjustment capability (e.g., fixed table height, fixed chair height, etc.)

INTRODUCTION

Recently, a large number of computer users suffering from carpal tunnel syndrome (CTS) has been reported in U.S.A. Some of the job-related factors contributing to this cumulative trauma disorder in the computer users are the use of poorly designed workstation and improper body posture while operating a computer keyboard. During the past few years, many business and industrial corporations in Thailand have intensively utilized microcomputers in their day-to-day operations and on continuous basis. Thus it is of great concern that a large percentage of Thai computer users will be soon affected by CTS if they are not warned about this computer related hazard and properly protected. For a detailed discussion on CTS and other cumulative trauma disorders of upper extremities, see [5].

It has been found that by ergonomically designing a workstation and adjusting it correctly, the risk of developing CTS can be greatly reduced. Researchers have reached a conclusion that a computer workstation should be adjustable to accommodate a wide range of users with different body sizes. Several adjustment ranges for the workstation components (i.e., chair, table, keyboard tray, monitor stand, etc.)have also been recommended. With no surprise, some values are similar while some are significantly different. Virtually all of the above mentioned components can be independently adjusted, meaning adjusting one component has no effects on others. Assuming that the adjustment process is discrete and finite and letting n be the number of adjustable components and m_i be the number of steps that the i^{th} component can be adjusted, the total number of combinations the workstation can be adjusted is

$$\text{Number of combinations} = \prod_{i=1}^{n} m_i$$

It is obvious that the number of combination can become significantly large (or infinite) if the number of steps increases. This presents a major problem when one tries to adjust the workstation in order to obtain ergonomic settings, especially without any assistance or clues.

This paper is organized as follows. Firstly, the design and theoretical framework of **IntelAd** is discussed. The flowchart showing an approximation algorithm of **IntelAd** is given in order to provide readers with an insight to the system's architecture. Assumptions and mathematical formulas used in determining and verifying ergonomic settings are also explained. Finally, an example is given to demonstrate the application of **IntelAd**.

ARCHITECTURE OF THE SYSTEM

IntelAd is designed to be a menu-driven computer program, with several menues linked together so that the users can customize their needs. **IntelAd** utilizes a concept of approximation, thus requiring a

small number of computational steps. The following chart shows the structure of **IntelAd** and the interconnection between its menues.

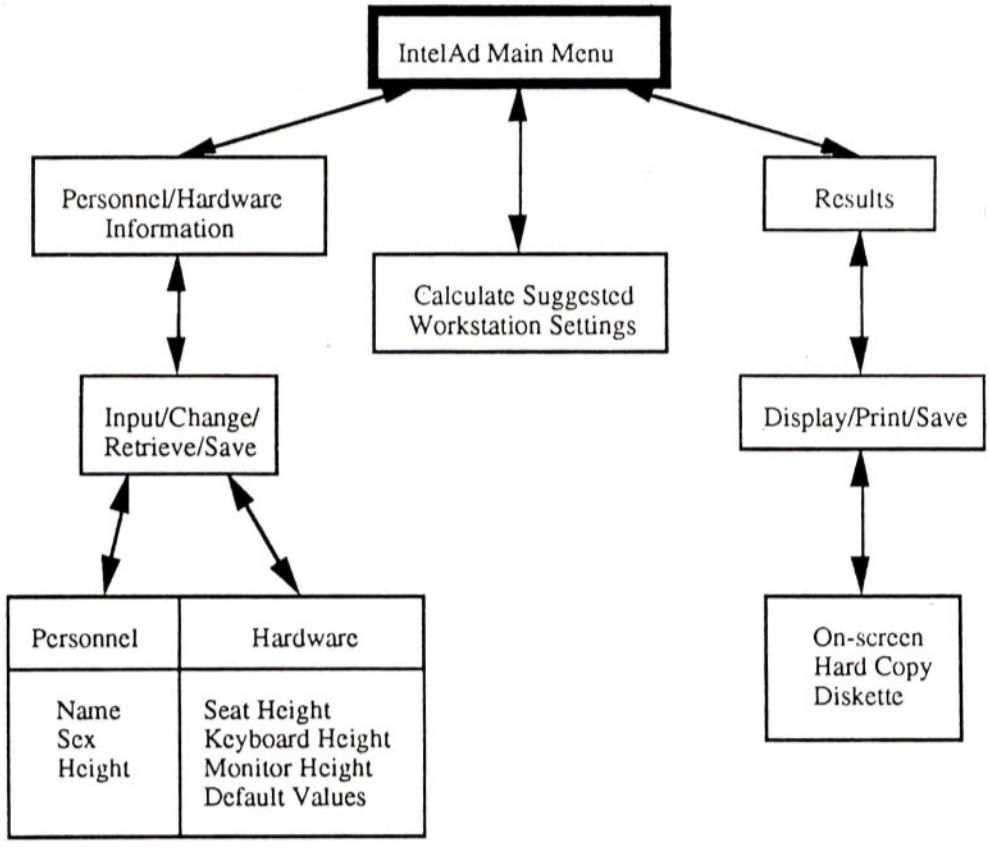

Figure 1: An architectural design of **IntelAd** system

COMPUTATIONAL ALGORITHM

ANSI/HFS Standard No. 100-1988 discusses the recommended ranges of ergonomic workstation components such as computer chair, computer table, keyboard tray, etc. Although it seems that this standard has been developed for the furniture manufacturers not for every day computer users, their values are however useful if we consider them as some starting points for a search of recommended settings. Although the ANSI/HFS standards have been published elsewhere [1], we will once more reprint these adjustable ranges to complete our discussion. For the readers who are interested in knowing different adjustable ranges recommended by other sources, see [4].

Table 1
Adjustable Ranges Recommended by ANSI/HFS Standard No. 100-1988

Component	Lower Value (cm)	Upper Value (cm)
• Seat Height	40.00	49.00
• Elbow Height	46.00	74.00
• Keyboard Height	58.00	71.00
• Keyboard Angle (°)	0	25
• Monitor Height (at center of screen)	74.00	91.00
• Viewing Distance	33.00	71.00
• Viewing Angle	0	60

The lower and upper values shown in Table 1 are used as the default values in **IntelAd**. The user may choose the default ranges or enter the actual values measured from his/her own computer workstation. Other essential information required by **IntelAd** is the user's sex and body height which will be used to determine joint angles necessary to form correct seated posture.

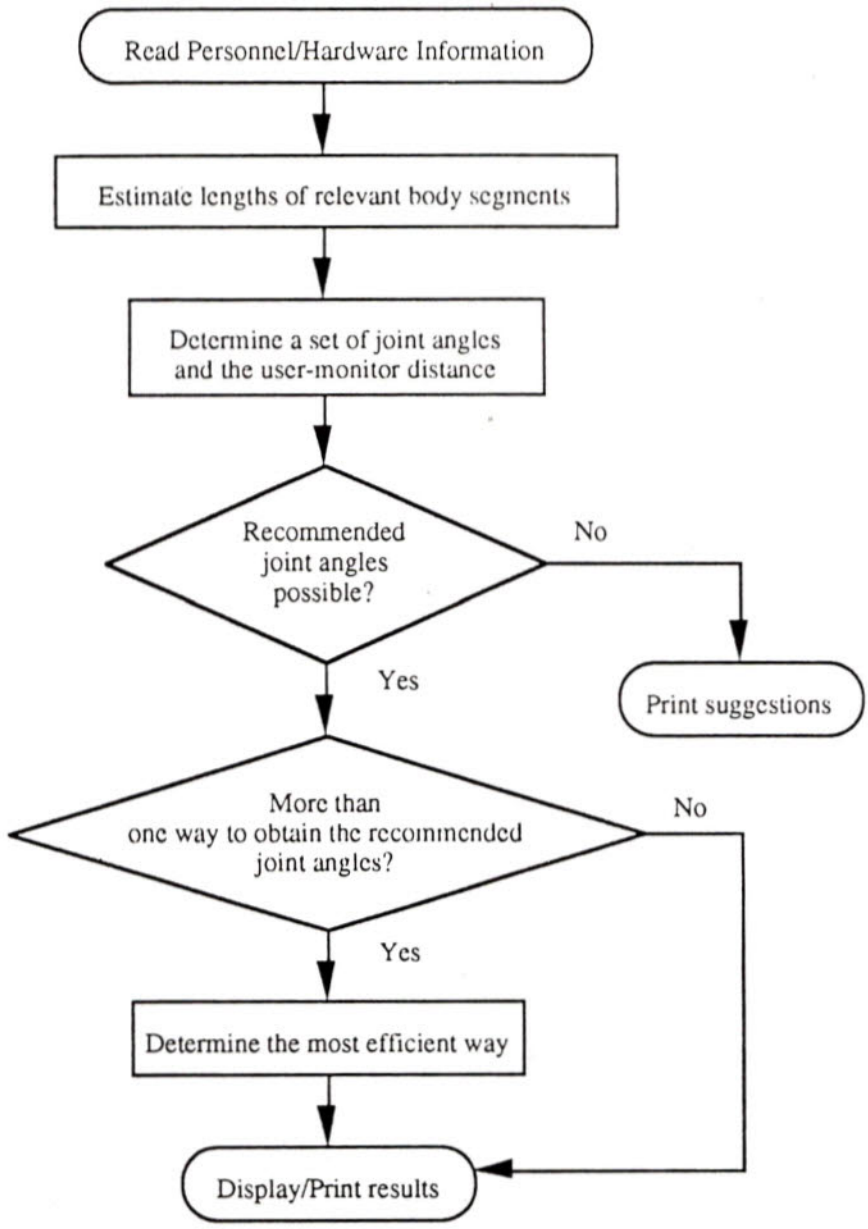

Figure 2: A flow-chart depicting a computational algorithm of **IntelAd**

From a given body height (y), the lengths of all relevant body segments can be estimated by the following formulas (as adapted from [2], [6], [7], and [8]).

Male:	*Seat Height (H)*	=	*0.2533[y]*
	Seat Depth (D)	=	*0.2845[y]*
	Trunk-Shoulder (TS)	=	*0.3368[y]*
	Seated Eye Height (EH)	=	*0.4567[y] - TS*
	Upper-arm Length (UL)	=	*(0.3368-0.1388)[y]*
	Elbow-Fingertip (EF)	=	*0.2746[y]*
	Seated Height (SH)	=	*0.5219[y]*
	Chin-Top of Head (CT)	=	*0.1275[y]*
Female:	*Seat Height (H)*	=	*0.2484[y]*
	Seat Depth (D)	=	*0.2997[y]*
	Trunk-Shoulder (TS)	=	*0.3388[y]*
	Seated Eye Height (EH)	=	*0.4641[y] - TS*
	Upper-arm Length (EL)	=	*(0.3388-0.1444)[y]*
	Elbow-Fingertip (EF)	=	*0.2660[y]*

$$\text{Seated Height (SH)} = 0.5291[y]$$
$$\text{Chin-Top of Head (CT)} = 0.1231[y]$$

The next step is to determine the Cartesian (X,Y) coordinates of the body joints in order to draw a line diagram representing the body figure. We assume that the reference origin (0,0) is the point on the floor where its vertical axis intersects the shoulder joint. Letting *a* be ankle, *t* be toe, *k* be knee, *h* be hip, *s* be shoulder, *el* be elbow, *f* be fingertip, *w* be wrist, *e* be eye, *c* be chin, and *toh* be top-of-head, we obtain

$$X_a = TS \cdot \sin(BA) + \cos(SA) \qquad Y_a = 0$$
$$X_t = 0.1520(y) + X_a \qquad Y_t = 0$$
$$X_k = X_a \qquad Y_k = Y_a + H$$
$$X_h = TS \cdot \sin(BA) \qquad Y_h = Y_k - D \cdot \sin(SA)$$
$$X_s = 0 \qquad Y_s = Y_h + TS \cdot \cos(BA)$$
$$X_{el} = UL \cdot \sin(AA) \qquad Y_{el} = Y_s - UL \cdot \cos(AA)$$
$$X_f = X_{el} + EF \cdot \cos(AA) \qquad Y_f = Y_{el} - EF \cdot \sin(AA)$$
$$X_w = X_f + 0.1080[y] \cdot \cos(AA) \qquad Y_w = Y_f + 0.108[y] \cdot \sin(AA)$$
$$X_e = 5.00 \qquad Y_e = Y_s + EH$$
$$X_{toh} = 0 \qquad Y_{toh} = Y_s + (SH - TS)$$
$$X_c = 0 \qquad Y_c = Y_{toh} - CT$$

where *BA* is back angle, *SA* is seat angle, and *AA* is arm angle.

Based on hardware information entered by the user, **IntelAd** generates a 2-dimensional line diagram of the workstation. The drawing consists of a chair, a table, a keyboard, a desk-top CPU, and a monitor. Letting *mr* be keyboard's median row, *vd* be viewing distance, and *mc* be center of monitor, **IntelAd** determines four side-view corners of the monitor and three side-view corners of the keyboard, with each point in space represented by (X,Y) in the Cartesian coordinate system. The following formulas are necessary for determining recommended workstation settings. Assuming that *VA* = viewing angle and *KA* = keyboard angle,

$$X_{mr} = X_f \qquad Y_{mr} = Y_f$$
$$X_{mc} = X_e + vd \cdot \cos(VA) \qquad Y_{mc} = Y_e - vd \cdot \sin(VA)$$
$$X_{ulc} = X_{mc} + 15 \cdot \sin(VA) \qquad Y_{ulc} = Y_{mc} + 15 \cdot \cos(VA)$$
$$X_{urc} = X_{ulc} + 30 \cdot \cos(VA) \qquad Y_{urc} = Y_{ulc} - 30 \cdot \sin(VA)$$
$$X_{llc} = X_{mc} - 15 \cdot \sin(VA) \qquad Y_{llc} = Y_{mc} - 15 \cdot \cos(VA)$$
$$X_{lrc} = X_{llc} + 30 \cdot \cos(VA) \qquad Y_{lrc} = Y_{llc} - 30 \cdot \sin(VA)$$
$$X_{kb1} = X_f - 8 \cdot \cos(KA) \qquad Y_{kb1} = Y_f - 8 \cdot \sin(KA)$$
$$X_{kb2} = X_f + 8 \cdot \cos(KA) \qquad Y_{kb2} = Y_f - 8 \cdot \sin(KA)$$
$$X_{kb3} = X_{kb1} + 16 \cdot \cos(KA) \qquad Y_{kb3} = Y_{kb1}$$

The image of the computer user is ideally superimposed on that of the computer workstation generated from the above formulas to check if all constraints are satisfied. Should there be even a single constraint violated, **IntelAd** will suggest a corrective solution such as using a footrest, etc.

EXAMPLE

To demonstrate how **IntelAd** works and estimates the workstation setting, an example is given. The personnel information requested by **IntelAd** are the user's name, sex, and body height. Then, **IntelAd** asks about the hardware information such as the adjustable ranges of the chair, keyboard, and monitor height. For simplicity, it is assumed that the chair is adjustable (its range is arbitrarily chosen) but the keyboard and the monitor are not.

The input information are as follows.

Personnel	Name:	Suebsak Nanthavanij	
	Sex:	Male	
	Body Height:	170 cm	
Hardware	Seat Height:	42.00 - 47.00 cm	
	Keyboard Height:	60.00 cm	(fixed)
	Monitor Height:	85.00 cm	(fixed)

Figure 3 shows a printout of the workstation settings recommended by **IntelAd**. It is noted that none of the constraints is violated. However, the elbow angle (the angle between the upper and lower arms) is not 90°.

IntelAd

Intelligent Adjustment System

Personalized Workstation Settings for "**Suebsak Nanthavanij**"

Sex: Male
Height: 170 cm

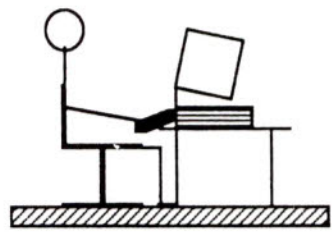

- Height of Seat Pan: 43.10 cm
- Height of Keyboard Home Row: 60.00 cm
- Height of Center of Monitor: 85.00 cm
- Distance Seat Back - Home Row: 46.20 cm

Workstation Constraints:

- Seat height adjustment limits: 42.00 - 47.00 cm
- Keyboard height adjustment limits: 60.00 - 60.00 cm (Fixed)
- Monitor height adjustment limits: 85.00 - 85.00 cm (Fixed)

Figure 3: Computer workstation settings recommended by **IntelAd**

CONCLUSIONS

IntelAd has been developed, tested, and proved that the system work successfully. We are now in the process of improving its verification algorithm by considering the wrist angle is the system's top priority. Furthermore, the next version of **IntelAd** will be more user friendly and more efficient than the current one.

The purpose of the **IntelAd** system is to help computer users adjust the computer workstation according to that recommended by ergonomists. Similar to most expert systems, **IntelAd** suggests the settings which the user may use as a starting point. Due to its approximation algorithm, the results provided by **IntelAd** are usually not the optimal solutions. Nevertheless, the user is led to be within a close proximity of the optimal settings. With its graphical representation of the settings, the user can clearly visualize his/her seated posture if the workstation is adjusted accordingly. The next generation of **IntelAd** is an integrated software-hardware system where the settings will be automatically downloaded to the workstation so that it can adjust itself without human physical involvement.

REFERENCES

[1] ANSI/HFS Standard No. 100-1988. (1988). *American National Standard for Human Factors Engineering of Visual Display Terminal Workstations.* The Human Factors Society, Inc., Santa Monica, California.

[2] Chaffin, D. B. and Andersson, G. B. J. (1991). *Occupational Biomechanics.* 2nd Edition, John Wiley & Sons.

[3] Nanthavanij, S. (1992). "Self-Adjusting Ergonomic Computer Workstation," *Proceedings of the 1992 Engineering Technology Symposium and Exhibition*, pp. 1025-1037.

[4] Nanthavanij, S. (1992). "Ergonomic Computer Workstation: A Tool to Prevent Wrist Motion Injuries," *Safety & Environmental Review*, pp. 44-50.

[5] Nanthavanij, S. (1992). "Computer Workstation Hazard: Wrist Motion Injuries," *Proceedings of the 2nd International Workshop on Advanced Science and Technology Transfer to Thailand*, pp. 411-427.

[6] National Aeronautics and Space Administration. (1978). *Anthropometric Source Book.* U. S. Government.

[7] Winter, D. A. (1990). *Biomechanics and Motor Control of Human Movement.* 2nd Edition, John Wiley & Sons.

[8] Woodson, W. E. (1981). *Human Factors Design Handbook.* McGraw-Hill.

AN ELECTRIC HYBRID BUS DEVELOPMENT PROGRAM

by
Suang Khuwatsamrit, P.E.,Ph.D.

1.0 GENERAL STATEMENT

Electric Vehicles (EVs) do not burn gasoline. EVs also do not use energy when they are caught in the traffic jam in Bangkok. Air quality in Bangkok is beyond crisis proportion. We must electrify our buses, the major source of air pollution. Why should we start with buses? There are several reason behind this selection. First of all, EV is not suitable for long distance traveling, usually less than 150 km which is well within the distance of any bus routes but beyond the vacation traveling in a passenger car. Secondly, passenger cars require both reliability and low cost while public-service buses need reliability over absolute minimum cost. We should start with one goal, making it work good. Then, we can make it inexpensive. The third reason is that Electric bus is the niche product that giant auto manufacturers ignore. But the large size of the traction drive is strategically important for our country to electrify our public transportation system, Electric commuter train and eventually implementing our own intelligent highway Program. Recharging Stations for passenger EV's are considered one of the infrastructure that requires wide-spread political stimulation and huge business investment while they are relatively easy to facilitate for Electric Bus at bus depots. Last but not least, It is impossible to compete with giant auto manufacturers on competitive passenger car market. But, it is quite possible to outdo those giants in this niche market.

Next question is whether we have the technological know how's to do it. There are three technically challenging fields that need real-world design expertise and world-class manufacturing skill. They are human comfort controller which is likely to involve Fuzzy logic, Energy storage and management techniques and high-power PWM Inverter Drive System, likely in the 200-300 kW range. All these are by no mean state of the art technologies. Nor they require multi-million dollar development tools. This product is well within our technical expertise and capital strength to develop. Although, there are a few know-how's to be explored in this program that are not publicly known at this moment. Decades of research in the West and Japan does not translate into decade of catching up for us. Luckily the key technology in this field, namely Static Converter Drive System, changes rapidly in this past five years, most of the old studies need to be re-evaluated in the context of new micro-controller based control strategies, new power semiconductor devices and circuit topologies. We are not that far behind after all.

Now that the technical aspect of the project has been discussed. It is appropriate to address political business issues. What is the return of this investment? The most immediate return will be one less major sources of air pollution. This project also serves as a stepping stone into World-Class Manufacturing and Global OEM Business. Export of Electric Buses from Thailand is quite realistic if we intend to carry this development through second phase and commit to World-Class Manufacturing. The long term benefit will be basis to stimulate the growth of Electronic Manufacturing Industries. This might well be the only mechanism that will transform our industries from agriculture product base to equipment manufacturing base. The know-how's from this project may serve as basis for reverse-engineering of the Light Rail Commuter train system that we are building as part of our infrastructure development in the third phase of this plan.

In summary this plan will directly produce:

- two prototypes of full-size electric bus in three and a half years;
- world-class production of full-size electric bus in five and a half years;
- three prototypes of medium speed commuter trains in seven years.

indirectly, this development plan will support:

- surface-mount contract manufacturing;
- Hybrid electronic component manufacturing;
- Distributed control system design and manufacturing;
- Adjustable speed drive design and manufacturing;
- high efficiency motor manufacturing;
- Industrial process system integrators;
- Industrial Equipment OEM's.

DEVELOPMENT PLAN

PHASE 1 : ELECTRIC BUS DEVELOPMENT

PHASE 2 : ELECTRIC BUS MANUFACTURING

PHASE 3 : ELECTRIC COMMUTER TRAIN REVERSE ENGINEERING

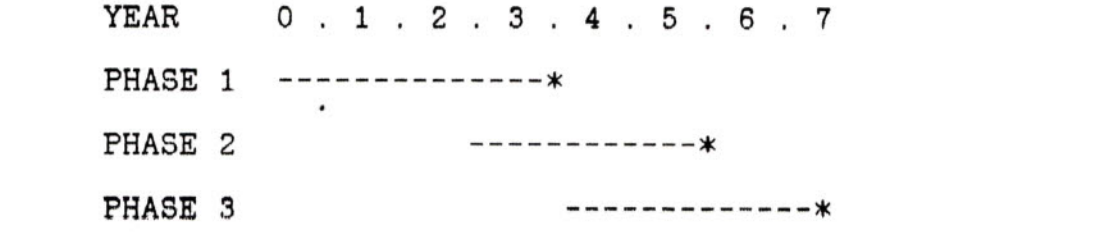

2.0 THE ENVIRONMENTAL IMPACT

Two major differences between Gasoline or Diesel vehicles and Electrically powered buses are:

- Individually maintained Internal Combustion Engines (ICE's) contribute much more air pollutants than well-maintained and centralized Power Plants. Table 1 shows a 1978 study [1]. A recent study by the Electric Power Research Institute (EPRI) also shows similar trend. Results were tabulated in Table 2.

TABLE 1: POLLUTION CONTRIBUTION EV vs. ICV (grams/mile) [1]

EV:	HC	CO	NO2	SO2	Part.
Vehicle	0	0	0	0	0
Power Plant	.128	.024	.696	.752	.080
Refinery	.007	.002	.061	.198	.010
EV Total	.135	.026	.757	.950	.090
ICV:					
Vehicle	.41	9.0	1.50	0.13	0.12
Refinery	.99	.01	.40	.71	.10
ICV Total	1.40	9.01	1.90	0.84	0.22
EV/ICV:	0.09	.003	0.40	1.13	0.41

TABLE 2: EPRI AIR POLLUTION STUDY [2] (grams/km)

	VOC	CO	NO2	SO2	CO2
EV today	.006	.031	.75	1.8	190
EV 1995	.006	.031	.18	.5	200
ICV	.65	6.2	1.5	0.1	400
EV/ICV	0.01	.005	0.50	18.0	0.48

- The second difference is that in traffic jam, EV's do not burn fuel except for auxiliary power such as Air-condition and air-brake compressor and Power Conversion Unit fixed loss which is around 2% at this power range. ICV's keep burning fuel even in idle state. Unfortunately, traffic jam is the way of life in Bangkok.

- Acoustical Noise Pollution is another Bangkok signature that we get used to. A comparison study [3] showed significant improvement in the idle state. Table 3 shows the result of this study.

TABLE 3 : ACOUSTIC NOISE STUDY, EXTERIOR NOISE (dBA) [3]

	Idle	Acceleration	88 km/h
EV	55.4	59.0	67.1
ICV	65.0	68.2	67.6

3.0 SELECTING THE RIGHT TECHNOLOGIES

For successful product development in the developing countries, no state-of-the-art components should be used. The price will not be competitive and the availability will be unpredictable. The winning formula lies in the ability to use basic components in an innovative way that gives us the competitive edge. One good example is the Fuel Cell Technology. It should be reserved as a long term research program rather than an immediate product development project. A good example of a Hybrid Bus was shown in Figure 1. This bus was developed in Italy in 1979 using Diesel Generator/DC Drive Technology. The specifications were: [4]

- 16 hours/day, 300 km/day operation,
- maximum cruising speed of 65 km/hr,
- 0-50 km/hr in 16 seconds,
- 14% climbability,
- 100 passengers loading,
- total weight of 18,000 kg.

The Traction Drive Technologies which include Circuit-Topologies, Power Semiconductor Devices and Control Means have changed drastically since that development. For today Hybrid Bus development, the following Technologies are proposed:

- Optimization of Hybrid energy sources. Repetitive acceleration in Bangkok traffic rules out fully Electric-Powered design even with Regenerative Braking scheme. A relatively small ICE which may be powered by LP gas together with Lead-Acid Batteries should be a good combination.
- A three-phase off-the-shelf induction motor is the power plant of choice. Its ruggedness and minimum maintenance requirement works well in Bangkok road environment. High efficiency can be maintained over 20:1 speed range and light to full load.
- A close-loop vector controlled PWM inverter should be able to provide smooth acceleration and sufficient torque for low speed operation which is the norm of Bangkok traffic. 600 Amp, 1400 Volt IGBT's should serve well as a building block for the PWM Inverter.
- A Human Safety Support and comfort controller is a technically challenging task. Its fully drive-by-wire control should closely imitate its ICE counter-part. It should also include Regenerative and

Mechanical Braking coordination to recover as much Kinetic Energy as possible during the deceleration mode. Fuzzy Logic is well suited for this application.

4.0 THE QUESTIONS OF COST AND PERFORMANCE

- The added initial cost of the Electric Traction Drive System which include Batteries, Inverter, Motor and Controller has been evaluated recently in [5] as follows:
  . Lead-Acid Batteries at $70/kWh
  . Induction Motor at $8-12/kW
  The cost of Inverter plus controller in the 150-200 kW range is around $50-60/kW. All these add up to an estimate of $22,000-26,000. Additional $5,000-7,000 can be expected for Fixed speed ICE supplying auxiliary power and for Regenerative Energy Storage System. This $27,000-33,000 Electric Traction System will be replacing the Diesel Engine, Mechanical Transmission and Water Cooling System.
- Due to the traffic condition in Bangkok, the bus will spent more time idling than cruising. Together with the optimization of the Fixed-Speed ICE and Regenerative Braking, the Depth of Discharge is expected to be kept over 90%. The distributed cost of battery replacement is expected to be $0.10/km.
- With 18,000 gloss vehicle weight, the overall specific energy consumption of the Electric Traction System is estimated at 12.5 kWh/km. At $0.045/kWh of electricity cost, the overall Fuel cost for this Hybrid bus is estimated at $0.56/km. The "Fuel Cost" of the ICE counterpart is expected in the $0.70-0.90/km. A saving of $0.24/km.
  The payback for the extra initial cost of $20,000 is around 83,000 km or 2.5-3.0 years.
- The maintenance and repair cost of the EV was estimated at 30% of its ICE counterpart. [6]
  The modular Design Concept of Electrical Drive design make repair a matter of hours rather than days. Routine maintenance is a matter of once every quarter than once every one or two weeks.
- The Human Riding Comfort Factor of an EV can be designed to be independent of the driver's habit except in the Emergency Brake Slamming situation. The performance and Efficiency of an EV is superior than its ICE Counterparts.

5.0 POTENTIAL MARKET

- This is a golden opportunity for our Government to invest in improving Bangkok air quality with our own effort. Based on the investment analysis presented in previous section, the air quality improvement comes for free. Bonuses could well be catalyzes to transform our $4,000-8,000/worker /year labor intensive assembling industry base to $20,000-30,000/worker/year Industrial Equipment Manufacturing base. The central Government should share good portion of the cost of Prototype Development. While Bangkok Metro. Transit-Authority should procure first production lot to justify the manufacturing investment.
- This Hybrid Bus fits well for Air Port Transit uses. An Electric Hotel Bus can deliver a sense of luxury and good PR.
- Utilities in the United States are investing in EV Developments either through localized consortiums or EPRI. A night-time charging is a good mean for Power System Demand Management. The buses can also be used to transport employee from one facilities to another.
- School Buses in the International Market fits long range strategic plan.
- Each component in the Electric Traction System can be applied to Industrial Equipment. This is a good opportunity for intermediate business diversification.

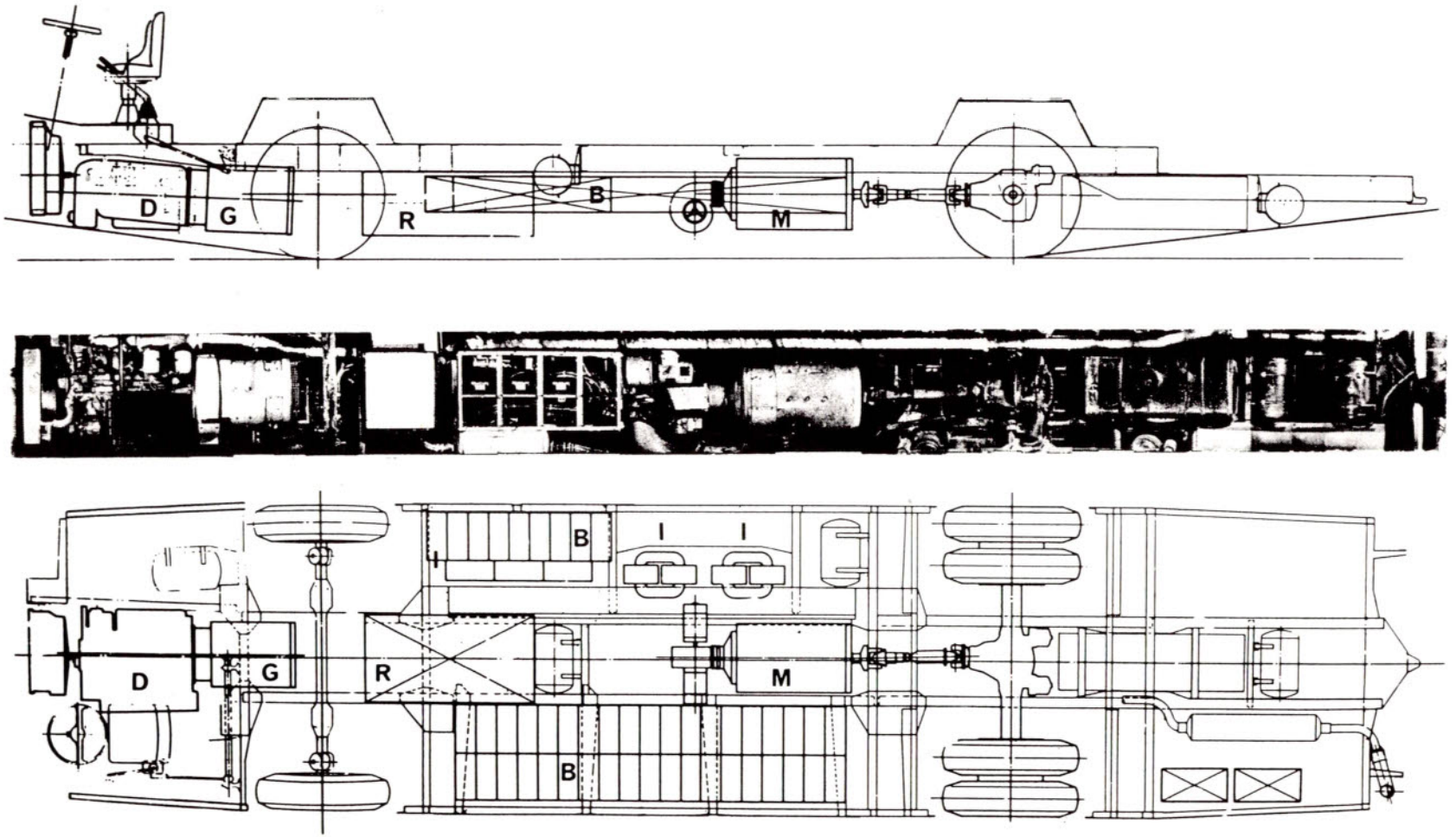

D - Diesel Engine
G - D.C. Generator
M - D.C. Traction motor
B - Lead-acid battery
R - Controller
I - Smoothing inductances

Fig. 1 - Hybrid bus : layout and view from the bottom of electric generation - drive system. [4]

REFERENCES:

[1]: D.L. Harbaugh, "A Comparison of the Overall Air Pollution Contributions of Electric and Gasoline Powered Vehicles in the Los Angeles Area,", The fifth International Electric Vehicle Symposium, Oct. 1978.

[2]: M.J. Riezenman, "Electric Vehicles", IEEE Spectrum, Nov. 1992, pp. 18-21.

[3]: R.D. MacDowall, "Comparative Evaluation of Acoustical Noise Levels of Soleq Evcort EV and ICE Counterpart," Electric Vehicle Technology, Feb. 1990, pp.23-25.

[4]: G. Brusaglino, "Fiat Electric Vehicles Development Process," EVC EXPO 80 Conference Proceedings, May 1980.

[5]: K. Rajashekara and R. Martin, "Present and Future Trends for Electric Vehicles Review of Electrical Propulsion Systems," Proceedings, IEEE Power-Electronics in Transportation, Oct. 1992, pp.7-12.

[6]: J.L. Arias and E.F.Moore, "Operating Cost Comparison of Four EVs vs Their ICE Vehicle Counterparts," EVC EXPO 80 Conference Proceedings, May 1980.

CONSORTIUM OF APPLIED TECHNOLOGIES FOR ENERGY CONSERVATION

Global Energy Conservation is no longer a political buzzword nor a technical jargon but it may determine the well being of human race on this planet. Globally, Billions and Billions of dollars are invested each year for this purpose. It may determines economic well being of a nation in the twenty first century. Energy Conservation can be achieved through:

1. Utilize higher efficiency equipment that deliver same amount of work or comfort with less energy, and

2. Manage our limited energy resources or generation capacity so that more users can take maximum advantage of these resources to produce more goods without sacrifying productivity of any users.

or in more technical words:

1. Kilo-Watt-Hours (kWH) reduction strategy, and

2. on-line cooperative Peak Demand control strategy.

This proposed Consortium will operate in concert with EGAT, MEA and PEA policies to develop and manufacture through its members strategically important products and equipment to replace the present inefficient ones. These products and equipment will also be integrated by the consortium to form a network of on-line Peak Demand control systems. This network is well fit in the development of Industrial zone along the Eastern Seaboard.

Both the Energy Saving and Peak Demand Reduction Plans have been part of the Demand-Side Plans for Utilities in the United States for years. Based on Georgia Power four-year action plan, the Energy and Peak Demand impacts of some of the action programs are shown in the following:

ANNUAL ENERGY SAVING FROM DEMAND-SIDE PROGRAMS
(Gigawatt-hours)

PROGRAM	1993	1994	1995	1996
Lighting	92.6	241.5	385.0	564.2
Motors (no ASD's)	0.4	1.5	3.3	5.8
Interruptible Services	0	0	0	0
TOTAL	93.0	243.0	388.3	570.0
% of Base Forecast	0.1	0.4	0.6	0.9

PEAK DEMAND REDUCTION FROM DEMAND-SIDE PROGRAMS
(Megawatts)

PROGRAM	1993	1994	1995	1996
Lighting	20.4	53.1	84.7	124.1
Motors (no ASD's)	0.1	0.4	0.8	1.4
Interrupt. Services	359.4	408.6	428.9	451.4
TOTAL	379.9	462.1	514.4	576.9
% of Base Forecast	3.2	3.8	4.1	4.4

Based on Georgia Power Plan and our electricity generation plan and rates, the consumer will save

SAVING FOR CONSUMERS

PROGRAM	1993	1994	1995	1996
EGAT Generation Plan (thousand Megawatts)	11.0	11.3	11.7	12.1
Peak Demand Saving (thousand Megawatts)	0.35	0.43	0.48	0.53
Saving @ B237/Kilowatt (Million Bahts)	83	102	114	126
Energy Saving * (Gigawatt-hours)	33	136	211	327
Saving @ B1.1/KWH (Million Bahts)	36	150	232	360
TOTAL SAVING (Million Bahts)	119	252	346	486

* assume 50% utilization @ 6000 Hours annually.

1. STRATEGIC PARTNERSHIPS

In order to realize energy conservation at a national scale, the Consortium must include:

a. Office of the Prime Minister on Energy policies,

b. EGAT, MEA and PEA,

c. NECTEC

d. Participating members from Industrial and Commercial Sectors that will fund all product development programs and will carry those designs through manufacturing with the support of designers from the consortium.

e. Participating colleges and universities through their graduate study programs.

2. THE OBJECTIVES

a. The Consortium will not be in direct competition with NECTEC with the following reasons:
   - it has very narrow focus on applying technologies for energy conservation;
   - it is privately funded by private companies that will manufacture and market the products;
   - it can also serve as a bridge between prototype funded by NECTEC and manufacturable products for commercialization under the consortium focused objective.

b. The Consortium will serve as acting arm to realize National Energy Policies and Economic Development Plans. Government agencies create opportunities for product development for real needs. The Consortium will develop the products. Member companies will manufacture the product to serve those needs and create high-paying jobs in the process. The National needs are served and manufacturing jobs are created.

c. The Consortium will not limit itself to its own product development. Instead, it will
   - adopt and adapt if necessary designs from third parties to be manufactured by its member member companies;
   - provide technical support, within the consortium charters, for the joint venture between member companies and third parties that will result in technology sharing and transfer;
   - reverse engineering, without violating copy right laws, strategic products to be manufactured by member companies.

d. The consortium and its member companies must commit to Global Standard Total Quality Programs as the only avenue for long term prosperity

e. The Consortium must commit to capital investment of modern engineering tools as a mean to shorten time-to-market of a product development program and achieve global competitiveness.

f. The Consortium will nurture and guide our engineers to Internationally accepted design procedures. It will also serve as "landing ground" for our scientists and engineers aboard.

THE STRATEGIC PLAN

a. The consortium will be created by initial funding from member companies and possibly matching fund from government. It will then operate and grow through the royalty payment of its products and services.

b. work with EGAT and PEA tc create an Interruptible Service (IS) Program for the Eastern Seaboard.

c. work with PEA and member companies to define and develop strategic products for the implementation of the IS Program. Product specifications will be open to public. Products may include:
   - Low cost, application specific Energy Management Systems (EMS),
   - General purpose EMS's,
   - Transmission and Distribution System Simulators,
   - IS communication network transceivers
   - PLC's and Distributed Control Systems.

d. work with IS Program participants and PEA as system integrators.

e. work as consultants to third party system integrators for this IS program.

f. work with MEA and member companies to define and develop strategic products for energy efficient programs which may include:
   - high efficiency Lighting equipment, eg. electronic ballasts, Daylighting controls, low-wattage Fluorescent lamps.
   - high efficiency motors and controllers, eg. Adjustable Speed Drives, Reduced Voltage-Starters
   - power line conditioners for non-linear loads, eg. Total Power Factor Controllers, Active Line Harmonic Filters. Tuned Power Factor-Correctors and Static VAR Compensators.
   - Solar energy applications.

   The jointly developed product specifications will be made available to public. However, the product development program will be available only to member companies.

TENSILE AND IMPACT PERFORMANCE OF MODIFIED POLYPROPYLENE/ALUMINUM LAMINATES

BY

W. CHINSIRIKUL AND I. R. HARRISON

THE PENNSYLVANIA STATE UNIVERSITY
POLYMER SCIENCE PROGRAM
DEPARTMENT OF MATERIALS SCIENCE AND ENGINEERING
UNIVERSITY PARK, PA 16802, U.S.A.

INTRODUCTION

Attempts at improving composite materials' properties are largely based on improving adhesion between matrix and reinforcing agent, together with modifying their components' properties. Both polymer-matrix and metal-matrix composites are currently commercially used with an effort to further improve and produce more advanced materials. Polymer/metal laminates were selected as potential materials of interest in this study. However, adhesion of these two dissimilar materials has been considered a crucial problem. This point emphasizes the need for further study of adhesion improvement in polymer-metal combination. In this recent research, the matrix chosen is polypropylene (PP) and the reinforcing element is aluminum (Al); this pair was selected as part of a search for readily available materials with exceptional specific properties.

Our recently published paper (1) has demonstrated a novel successful bonding technique for polypropylene and aluminum surfaces via modification with a newly-developed polypropylene copolymer (2), Poly(propylene-cohexenol) with ≈ 5% OH-groups (PPH). Comparison was made between the PPH copolymer bonding method and a common oxidative treatment involving an acid etching process. It was found that PP/Al laminates bonded by PPH show a remarkable 7 to 10 fold increase in peel strength over acid etched samples.

On peeling Al from the PP layer, failure is principally cohesive. This result is indicative of the excellent bonding between PP and Al, which results in a maximum peel strength of ≈ 700 N/m and ≈ 1200 N/m for unoriented PP/Al and oriented PP/Al laminates, respectively. These bond strength values are greater than those for Epoxy/Al. High modulus, high strength oriented PP films developed by a hot nip drawing technique (3) were used as self reinforced matrices which led to consequent improvement in laminate properties.

In addition to adhesion, enhancement of the laminates' tensile strength, modulus and impact properties were also observed and are reported in this paper. All laminates prepared with the PPH bonding method have superior mechanical properties compared to acid treated samples. However, not only bond strength but also matrix (PP) orientation had a profound effect on the resulting laminates' mechanical performance. The highest modulus and stress-to-break were obtained when the test direction and PP orientation were parallel. Poor transverse properties of this oriented polymer were minimized by designing and constructing cross-ply laminates.

Based upon dropped weight impact data, multilayer laminates of oriented PP and Al showed attractively high total absorbed energy values (≈ 23 J/mm)

which exceed those of the other comparable composites including glass/epoxy, carbon/epoxy and carbon/PEEK. It is important to note that observed improvement in the laminates' tensile strength, modulus and impact properties are thought to be due to both the appreciable increase in adhesive strength of the PP/Al laminates, and enhancement of PP matrices' properties via the orientation process.

EXPERIMENTAL

Materials

The polypropylene (PP) used was a product of Shell Development Co. (denoted 5C08) and extruded as a sheet of thickness 0.9 mm. It has a density of 0.903 g/cc and a melt flow of 2.9. Unoriented PP was prepared by remolding extruded PP at 195°C for 30 min in order to remove any orientation due to extrusion. High modulus and high strength PP was produced via the continuous hot nip drawing technique (1,3). Polymer sheet was drawn at a constant rate, and a neck produced in the hot nip zone. The final draw ratio of oriented PP used in this study was 8, and the resultant material had modulus and tensile strength of ≈4.5 GPa and ≈ 400 MPa, respectively. These values are nearly 5 and 13 times greater, respectively, than those for unoriented PP films. It is apparent that the drawing process produces a self-reinforced polymer, presumably due to the formation of an aligned fibrillar structure, which is responsible for an appreciable increase in both strength and modulus (4-6).

Standard aluminum (Al) foil, 0.0025 cm thick, commercially available, was used as the reinforcing element. Thick Al (0.005 cm), a product of Alcoa, was also utilized in this research. The Al serves both as a reinforcing element and as an adhesive aid between self reinforced drawn PP sheets.

Surface Modification

Pretreatments of Al and PP were carried out using two different approaches.

(1) Acid Etching: Both Al and PP sheets were taken through a three step process following an industry standard developed by Forest Products Laboratory (FPL). In all cases, specimens were degreased in trichloroethylene , cleaned in an alkaline solution and chemically etched in a proprietary dichromate-sulfuric solution (3). All samples were dried in an oven at 30-40°C for 1 hr and then placed in a dessicator for 1-3 hrs, prior to bonding.

(2) PPH Solution Casting: PP sheets were simply degreased in trichloroethylene prior to lamination, whereas Al sheets were treated using the FPL process (degreased and acid etched). A 0.6% solution by weight of PPH copolymer in xylene was applied to treated Al sheets using a draw down rod, based on ASTM Standard 4147-82. This method provides a uniform cast film of thickness ≈ 15 μm. After four hours at room temperature to allow solvent to evaporate, the coated Al sheets were placed in a vacuum oven at 40-50°C for 1 hr, to remove any residual solvent remaining in the polymer, prior to bonding with PP.

Lamination Procedure

PP/Al laminates were prepared in a Carver hot press. Laminates were held at the molding temperature for 20 min and then slow cooled under pressure and vacuum for 5 hrs. Optimum temperature and pressure were found to be 174°C and 4 MPa, respectively. Under these conditions, laminates were able to retain most of the original mechanical properties of drawn PP films and achieve maximum adhesive strength. For oriented PP, parallel and cross-ply laminates had to be aligned prior to bonding.

Tensile Testing

All specimens, including PP, Al and PP/Al laminates, were prepared in accordance with ASTM Standard D882-88. Rectangular samples, with a 2 cm gauge length and 0.5 cm width, were cut with an appropriate knife. In the case of oriented PP samples, cutting at either 0, 90 or 45° to the PP orientation was employed depending upon the desired measurements. Tests were performed on a computer-controlled Instron Model 4201, equipped with a 1 KN load cell. All measurements were conducted at room temperature with a crosshead speed of 1 cm/min. Young' s modulus (E), stress-to-break (σ_b) and strain-to-break (ε_b) were collected for each specimen tested and data calculations performed using Instron software.

Impact Testing

Tests were conducted on 4x4 inch specimens utilizing a Dynatup model 8250 drop tower, equipped with a Dynatup GRC 730-I instrumented impact test data system. A comprehensive description of this apparatus is included in reference 7. The system has capabilities for testing at different impact velocities from 0.61 to 13.41 m/sec, together with varying crosshead weight from 2.5 to 45.5 kg, which allow impact energies in the range of 0.6 to 840 J.

RESULTS AND DISCUSSION

Tensile Properties

Acid Treated Laminates and PPH Bonded Laminates

All mechanical properties of base materials are summarized in Table 1. Table 2 shows tensile performance for acid treated and PPH bonded samples. Mechanical properties of both acid etched and PPH laminates are primarily dependent on the orientation of polypropylene. When the test direction was parallel to PP orientation, the highest mechanical properties were observed. Compared with unoriented PP laminates, these parallel-ply systems show much higher modulus and tensile strength due to the inherent properties of the drawn PP counterpart. However, when PP orientation was perpendicular to the test direction (parallel-ply: 90° test), transverse directional properties were much lower than the quoted values for samples tested in fiber direction (0° test), Table 2. The low values of σ_b and ε_b observed are due to the limited Al contribution because of the low deformability of PP in the transverse direction. Both PP and Al failed simultaneously. This is in contrast to testing in a parallel direction to PP orientation, Al break strain tends to increase, corresponding to an increase in σ_b for parallel-ply laminates.

To minimize the poor transverse properties of drawn material, a cross-ply laminate seems to be an obvious solution. The cross-ply laminates prepared by those two systems (acid etch and PPH solution cast) have properties in between those of parallel plies (0° test) and parallel plies (90° test), Fig.1. Testing a cross-ply laminate, the outer 90° ply of PP first cracked across the specimen length. This transverse ply crack is known to produce local stress concentrations leading to a localized failure of the 0° ply, in fiber composites (8). Since the transverse ply crack was observed in a cross-ply sample, but not in the parallel-ply laminate (0° test), the σ_b of the former appeared to be lower.

As summarized in Table 2, it is evident that PPH bonded laminates exhibit greater properties than those of acid etched laminates. A previously published paper (1) described the excellent bond strength of PPH bonded samples. An increase in adhesive strength has a profound effect on laminate performance. Increasing interfacial adhesion of the material can minimize delamination caused by an applied stress, and allows for higher extension of the Al. In the case of PPH bonded samples, Al is capable of deforming and at the same time it carries the load with PP through to failure. As a result, stress can be transferred throughout the laminate.

Another significant advantage of the PPH bonding method over acid

etching is that the properties of drawn PP are essentially unchanged, since the PP is not acid etched and is only degreased prior to bonding. The principal conclusion to be drawn at this stage is that mutual effects from PP performance, high bond strength due to PPH copolymer and good reinforcement of the Al all play a significant role in producing superior properties for PPH bonded laminates.

Dropped Weight Impact Test Results

Multilayer composites of alternating sheets of drawn PP and PPH cast Al were constructed by compression molding. The laminate is stacked in a systematic cross-ply, $[(0/90/0)/90]_S$. Tests were performed at an impact velocity of 4 m/sec using the instrumented dropped weight impact method and results were analyzed for the following parameters: maximum load, energy to maximum load, total energy absorbed, and deflection. Load and energy are presented on a unit thickness basis. Composites tested were PP/Al multilayer laminates, containing approximately 70% PP by volume, and a glass/epoxy composite (circuit-board type with typically ≈ 60% glass fiber by volume).

To determine whether or not the PP/PPH-Al composite has good energy-absorbing performance, it is essential to compare information from other available materials obtained using the same technique. Based on recent investigations, the falling dart impact method has been applied to many composites such as carbon/epoxy (9), carbon/polyether etherketone (PEEK) (9) and glass fiber reinforced PP composites (10). Data for these materials are compiled in Table 3 for comparison with the PP/Al composite produced in this study.

From Table 3, it is evident that PP/PPH-Al composites exhibit competitive impact characteristics. The PP/Al samples show greater maximum load, total energy absorbed and deflection than those of glass/epoxy, carbon/epoxy and carbon/PEEK composites. However, PP/Al samples yield total energies absorbed which are relatively similar to glass fiber filled PP materials (Fig. 2). As shown in Table 3, PP/Al samples absorb ≈ 23 J/mm where glass fiber/PP composites are slightly higher at ≈ 26 J/mm, which is probably within error bars for the samples. This impact energy for glass fiber/PP composites (and presumably PP/Al composites) was reported to be approximately 3-10 times higher than that for glass fiber reinforced Nylon 6, Nylon 6,6, polyphenylene sulfone and polyester (10). Differences in total energies absorbed in these composites can be attributed to many possible factors. The high energy absorbed in both PP/Al and glass fiber/PP systems may result from the tough PP matrix, coupled with good matrix/reinforcement adhesion. Moreover, differences in ply sequence and fiber content can also

result in changes in total impact energies of composites.

During impact, the energy absorbed by the PP/Al specimen is deemed as that required to create new surfaces. These surfaces are shown by the presence of longitudinal cracking in the PP component and delamination of PP and Al. Failed samples exhibited visible damage around a circular hole; damage is in the form of PP surface cracks and delamination between adjacent layers.

For a material to be tough or to absorb a lot of energy, there must be mechanisms responsible for spreading impact load throughout the sample, such that the entire structure can participate in dissipating the energy. This is accomplished when good adhesion exists between the matrix (polymer) and the reinforcement (usually fibers). With strong interfacial bonding, load can be effectively transferred from matrix to fibers or reinforcement to prevent early local failure. Thus, the considerable energy absorption in PP/Al composites can be considered the result of: (1) a tough PP matrix with viscoelastic behavior which is also self reinforced with fibrillar structures; (2) strong adhesion between PP and Al; and (3) high deformability of the Al.

In conclusion, practical PP/Al multilayer laminates have good energy-absorbing characteristics. The extremely high energy to max load of these materials indicates that large energies are required to initiate cracks, although less energy is necessary to propagate a crack. Consequently impact energy to failure in PP/Al systems exceeds those of other composites including glass/epoxy, carbon/epoxy and carbon/PEEK systems. The impact data presented in Table 3 serves as a demonstration of the applicability of PP/Al composites. Modification of these PP/Al composites with polypropylene copolymer (PPH) has been very successful and demonstrates the feasibility of these new candidate composite materials.

CONCLUSIONS

1. Both bond strength and orientation of matrix (PP) play significant roles in determining mechanical properties of PP/Al laminates. With maximum adhesion, the highest properties were obtained only when oriented PP was used, and the test direction was parallel to the draw direction.

2. Laminates bonded with PPH show an appreciable increase in adhesion with superior mechanical properties compared with acid etched samples.

3. PP/PPH-Al multilayer laminates, with high total energies absorbed of $\approx$ 23 J/mm, demonstrate their potential applicability as an impact-resistant material.

ACKNOWLEDGEMENTS

The authors would like to thank Dr. T. C. Chung and D. Rhubright for providing the copolymer utilized in this study and one of us (W. Chinsirikul) acknowledges support through a Thai government scholarship. Additional thanks go to Alcoa and Shell Development Co., for providing materials used in this research.

REFERENCES

1. W. Chinsirikul, T. C. Chung and I. R. Harrison, *Proceedings of the American Society for Composites (Conference)*, 42 (1992)
2. T. C. Chung and D. Rhubright, *Macromolecules*, 24, 970 (1990)
3. W. Chinsirikul, *M.S. Thesis*, The Pennsylvania State University (1992)
4. M. P. Laughner and I. R. Harrison, *J. Appl. Polym. Sci.*, 36, 899 (1988)
5. M. P. Laughner, *M.S. Thesis*, Pennsylvania State University (1988)
6. K. G. Leewis, T. H. North and M. T. Kortschot, *Antec '90,* 1769 (1990)
7. M. L. Karasek, *Ph. D. Thesis*, The Pennsylvania State University (1992)
8. C.I. Sun and K. C. Jen, *J. Reinf. Plas. Comp.*, 6, 208 (1987)
9. C. K. L. Davies, S. Turner and K. H. Williamson, *Composites*, 16, 279 (1985)
10. D. M. Bigg and E. J. Bradbury, *Polym. Eng. Sci.*, 32, 287 (1992)

Table 1: Mechanical properties of base materials

Material	Angle of test	Modulus (GPa)	σ_b (MPa)	ε_b (%)
Unoriented PP				
PP^A	NA	1.1 ± 0.1	43.5 ± 3.8	15
PP^B	NA	1.3 ± 0.3	42.1 ± 1.7	12
Oriented PP				
PP^A	0	4.8 ± 0.4	414.0 ± 22.0	37
PP^B	0	2.5 ± 0.4	285.5 ± 30.0	55
PP^A	90	1.5 ± 0.1	48.2 ± 0.7	18
PP^B	90	1.4 ± 0.1	45.1 ± 0.6	23
Aluminum				
Al ^{A}	NA	15.5 ± 0.5	70.5 ± 1.1	4
Al B	NA	8.1 ± 0.9	60.8 ± 1.0	2

Note: A: pre-processing samples
B: post-processing samples
NA: no specific angle tested due to isotropic property of material

Table 2: Mechanical properties of acid etched and PPH bonded laminates

Sample	Modulus (GPa)	Tensile Strength (MPa)	ε_b (%)
Undrawn PP laminate			
(PP/Al/PP)acid	1.3 ± 0.4	35.0 ± 2.6	10
(PP/Al/PP)PPH	1.5 ± 0.3	36.3 ± 2.3	16
Drawn PP laminate			
(Parallel-Ply: 0° test)acid	1.6 ± 0.2	166.2 ± 3.6	40
(Parallel-Ply: 0° test)PPH	2.9 ± 0.6	205.4 ± 16.0	43
(Cross-Ply)acid	1.2 ± 0.1	110.6 ± 8.1	42
(Cross-Ply)PPH	2.4 ± 0.3	179.3 ± 12.2	65
(Parallel-Ply: 90° test)acid	0.9 ± 0.1	37.2 ± 1.7	11
(Parallel-Ply: 90° test)PPH	1.4 ± 0.2	40.3 ± 1.6	11

Table 3: Comparison of composite impact properties

Parameters	PP/PPH-Al	Glass/Epoxy	Carbon/Epoxy *	Carbon/PEEK **	Glass/PP ***
Ave. thickness (mm)	**1.20**	1.59	2.00	2.10	2.90
Max Load (kN/mm)	**2.61 ± 0.38**	0.70 ± 0.10	2.10 ± 0.30	3.24 ± 0.43	1.34
Energy to Max Load (J/mm)	**20.07 ± 4.20**	1.21 ± 0.25	3.00 ± 0.50	4.76 ± 0.95	-
Energy after Max Load (J/mm)	**2.58 ± 0.50**	4.40 ± 0.68	9.50 ± 1.50	14.29 ± 2.46	-
Total energy absorbed (J/mm)	**22.65 ± 4.00**	5.60 ± 0.88	12.50 ± 1.25	19.05 ± 2.86	25.79
Deflection to Max Load (mm)	**15.26 ± 1.90**	3.49 ± 0.45	≈ 3.00	≈ 4.00	-
Deflection to Failure (mm)	**17.90 ± 1.30**	17.50 ± 1.14	≈ 10.00	≈ 15.00	-
Impact velocity (m/sec)	**4.00**	4.00	3.00	3.00	6.00

Note: Impact properties of composites reported in literature

* : Carbon/Epoxy (60% vol. of carbon fiber)

** : Carbon/PEEK (60% vol. of carbon fiber)

*** : Glass fiber filled PP composite (30 % vol. of glass fiber)

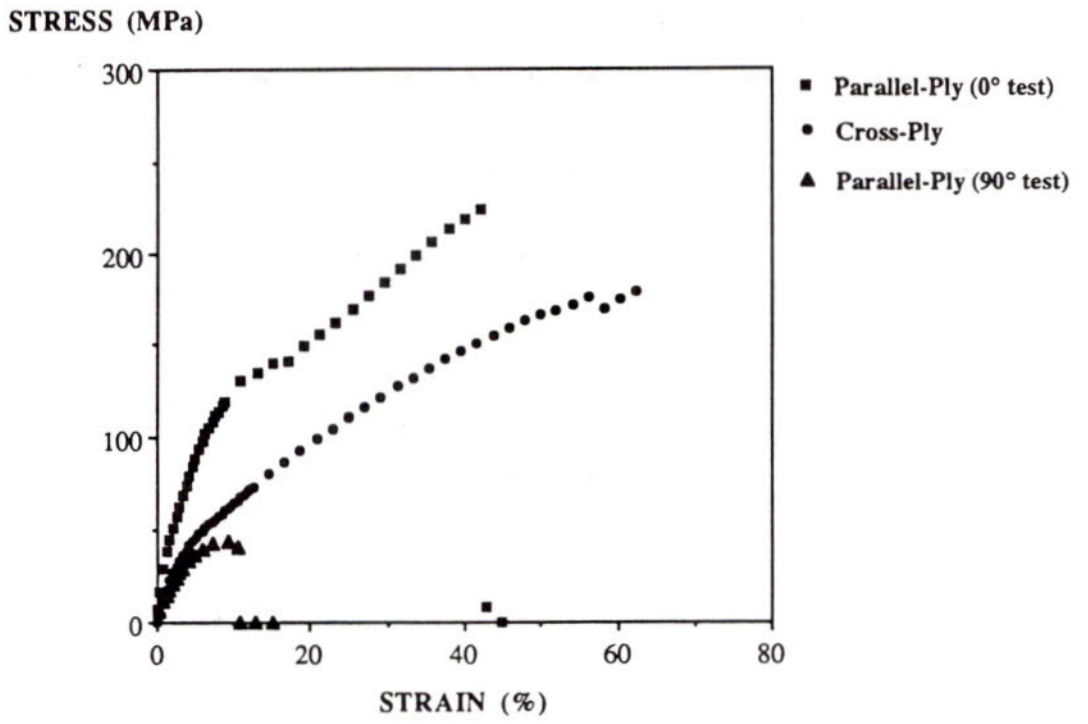

Figure 1: Stress-strain curve for various test orientations of PPH bonded laminates

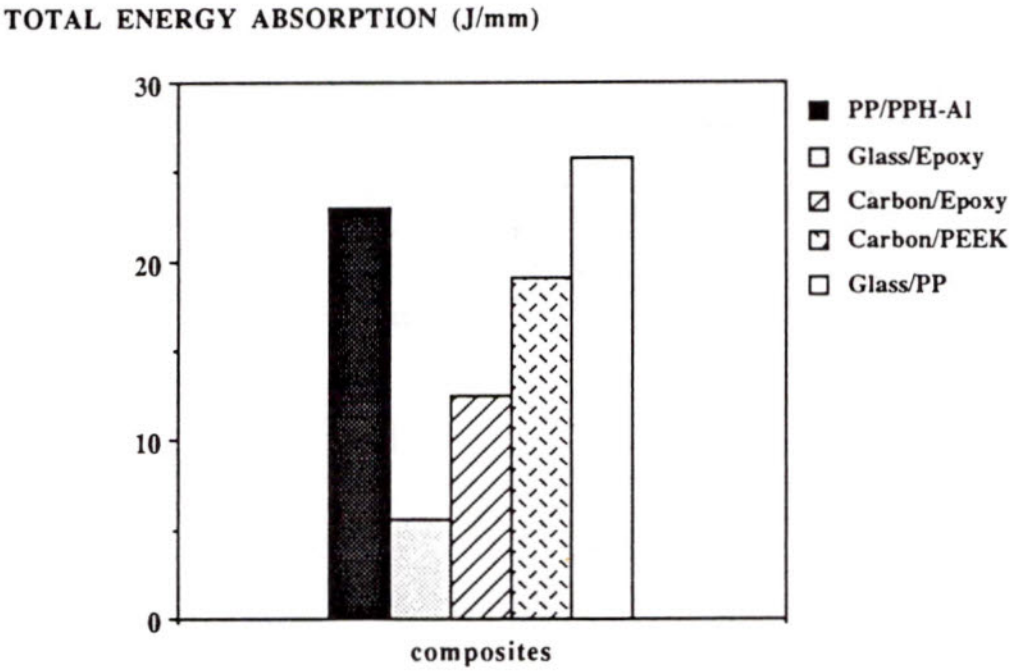

Figure 2: Comparison of composite impact properties

ขอขอบคุณ

คณะกรรมการจัดการประชุม The Third International Conference on Advanced Science & Technology Transfer to Thailand ขอขอบคุณ หน่วยงาน ส่วนราชการ และบริษัทเอกชน ที่ได้สนับสนุนการประชุมครั้งนี้ ดังรายนามต่อไปนี้ :

1. กลุ่มบริษัทพรีเมียร์
2. กลุ่มบริษัทชินวัตรคอมพิวเตอร์แอนด์คอมมิวนิเคชั่นส์
3. เครือเจริญโภคภัณฑ์
4. สำนักงานพัฒนาวิทยาศาสตร์และเทคโนโลยีแห่งชาติ
5. สภาอุตสาหกรรมแห่งประเทศไทย
6. บริษัท โตโยต้า มอเตอร์ (ประเทศไทย) จำกัด
7. กลุ่มบริษัทล็อกเล่ย์
8. International Organization of Migration
9. Thai Airways International
10. United Airlines
11. Northwest Airlines
12. Scandinavian Airlines System
13. American Airlines
14. Japan Airlines